THE UNIVERSITY
of EDINBURGH

Functional Analysis of Ovine Herpesvirus 2 Encoded microRNAs.

Aayesha Riaz

Thesis presented for the degree of Doctor of Philosophy

The University of Edinburgh

2014

Declaration

I hereby declare that this thesis is of my own composition, and that it contains no material previously submitted for the award of any other degree. The work reported in this thesis has been executed by myself, except where due acknowledgement is made in the text.

Aayesha Riaz
2014

Division of Infection and Immunity
The Roslin Institute and R(D)SVS
University of Edinburgh
Easter Bush
Edinburgh
EH25 9RG

Acknowledgements

I am thankful to Almighty Allah, most Gracious, who in His infinite mercy has guided me to complete this PhD work. May Peace and Blessings of Allah be upon His Prophet Muhammad (peace be upon him).

I want to pay deep felt gratitude to my supervisors Dr. Bob Dalziel and Prof. John Hopkins for their continuous and sustained guidance, mentoring and supervision. Truly, it was an honour and a matter of great pride to work with such dedicated people.

It was Dr. Dalziel who found me raw and set the tone for this long and arduous journey. He helped me through the tough initial phases of this lengthy journey. He understood my limitations and was always there to extend a helping hand whenever I needed it. I can vividly recall those moments of anguish and desperation when my project hit difficulties and he would come up with innovative ideas or guide me towards other professionals who could help me out. He also appreciated my family constraints and also those related to my work when I was not able to be present in Edinburgh.

Prof. Hopkins was never less helpful. His always open door and reassuring attitude kept my spirits high to reach this goal. I never found him to be less than encouraging and he never lost patience with my stutters.

I am also appreciative to Dr. Finn Grey who never raised an eyebrow when I approached him to discuss intriguing and complex issues that either related to the lab work and / or any other technical matters related to my project.

Dr. George Russell, Dr. Amy Buck and Mrs. Liz Thornton were kind enough to give cells and psi-M23-2 construct for use in this study. I would also like to thank Mr. Mick Watson, Miss Alison Downing and Miss Frances Turner for helping me carry out the bioinformatics analysis. I would also like to thank Dr. Bernadette Dutia and Mrs. Liz Archibald for their kind help and support whenever I needed.

I was so lucky to find the other members of Dalziel group; Claire Levy, Pete Wasson, Suzanne Esper, Katie Nightingale and particularly Inga Dry who worked with me not only as colleagues but as friends. Also, I would like to thank the members of Finn's group; Natalie Reynolds, Jon Pavelin and particularly Stephen Chiwashe. They worked with me for long hours to ease me through many complex situations.

Special thanks to Shoko for both moral and physical support, particularly when she was so kind to share her flat with me when I needed it the most. I also consider myself lucky to have friends like Gigi, Shuo, Xuan, Yoshi, Meng Meng and Aya. The laughs and moments of sorrow that we shared together were so unforgettable. I am also thankful to Ian, Anton, Yvonne, Marlynne, Karen, Dung, and Amr for their time to time support in and out of the lab.

I would also like to thank the Higher Education Commission of Pakistan for giving me the opportunity to come to the University of Edinburgh for PhD and for funding my work.

Last but not the least I am thankful to my family, especially my husband Zubair for his endless support, my kids Abdullah and Tehreem and my parents for their continued support and unending prayers.

Abstract

Ovine herpesvirus 2 (OvHV-2) is a gamma herpesvirus and is the causative agent of lymphoproliferative disease – sheep-associated malignant catarrhal fever in susceptible ruminants, including cattle. Sheep become persistently infected but do not show apparent clinical infection. MCF is characterized by marked T cell hyperplasia and proliferation of unrestricted cytotoxic large granular lymphocytes (LGLs) which leads to necrosis of infiltrated tissues and generally causes death of the host. Little is known about the underlying molecular basis of MCF pathogenesis or what controls the differences in clinical outcome of infection in two closely-related host species.

MicroRNAs (miRNAs) constitute a large family of small, ~22nt, noncoding RNA molecules that regulate gene expression by targeting messenger RNAs post-transcriptianally in eukaryotes and viruses. Herpesvirus encoded miRNAs have been shown to play a role in regulating viral and cellular processes including cell cycle and may have a role in pathogenesis. OvHV-2 has also been found to encode for at least 46 OvHV-2 miRNAs in an immortalized bovine LGL cell line. 23 of these miRNAs have also been validated by northern blot analysis and RT qPCR. It was hypothesised that these OvHV-2 miRNAs may regulate viral and cellular genes expression and may play a role in MCF pathogenesis. The aim of this project was to determine if OvHV-2 miRNAs have functional targets within viral and host cell genes.

Bio-informatic analysis has predicted several targets for these OvHV2 miRNAs in the 5' and 3' UTRs of several virus genes. Luciferase inhibition assay confirmed that

out of 13 selected predicted targets, three (two targets ORF73 and one within ORF50) were positive and functional. A fourth predicted target was also found functional (ORF20), but its functionality could not be confirmed by knocking out the target site. A newly developed technique Crosslinking, Ligation And Sequencing of Hybrids (CLASH) was also used to identify miRNAs bound targets within cattle and sheep genome. High throughput sequencing and analysis of the hybrid data revealed many target genes. Four of those targeted genes, were validated by luciferase inhibition assays and three were found to be targeted by OvHV-2 miRNAs.

This study gives the first evidence of viral miRNAs bound to their targets in cattle and sheep cells, by a highly sensitive technique-CLASH and provides a tool for studying differences in pathogenesis of two closely-related host species.

LAY SUMMARY

Malignant catarrhal fever (MCF) is a fatal disease of cattle and deer caused by infection with the virus ovine herpesvirus 2 (OvHV-2). Sheep are infected soon after birth, carry the infection for life but never show signs of any disease. If cattle catch this virus from sheep they develop MCF and usually die. This disease is economically important not only in the UK but also in Sub-Saharan Africa and other areas of the developing world where it places a major burden on food production. In sheep the virus infects, and then lies dormant for the life of the animal, in cells of the immune system, these cells continue to function normally. In cattle the same type of cell is infected but they change such that they now become aggressive and attack and kill other cells in the body, resulting in disease and death. A major question in understanding how OvHV-2 causes disease is: why, given that sheep and cattle are closely related species, do sheep survive and cattle die? Herpesviruses normally only infect one species and have co-existed and evolved with that species for millions of years. A previous study in the group identified molecules, termed microRNAs (miRNAs), produced by the virus that have the potential to control the way the infected immune cell functions. miRNAs work by affecting how much of a particular protein is produced in a cell and they do this by binding very specifically with the mRNA ("blueprint") for this protein and targeting it for destruction. The hypothesis is that the virus miRNAs have evolved to work in sheep immune cells and allow the virus to colonise these cells and survive long term. In order to investigate this hypothesis it is necessary to identify the viral and cellular proteins targeted by these miRNAs, this formed the basis of this thesis. Herpesviruses can either grow in a cell and produce new virus or remain dormant for long periods of time. I first showed that virus miRNAs can affect the production of three virus proteins , important in controlling whether the virus is dormant or growing. The control of this step may differ in sheep in cattle and may influence disease. I then investigated which cellular mRNAs (and so proteins) are targeted by virus miRNAs in sheep and cattle. I used a novel method which allows the purification of miRNAs bound to their target mRNAs. The mRNAs are then analysed and the protein they produce identified. This complex technique identified a number of cellular mRNAs (proteins) which are potentially targeted by the virus miRNAs. Using bioinformatics I analysed which targeted proteins would be predicted to play a role in disease and went show that two of these were in fact targeted by the virus miRNAs.

Table of Contents

List of Figures

List of Tables

Abbreviations

3’	Three prime
5’	Five prime
32P	Radioactive phosphorus isotope
α	Alpha
β	Beta
γ	Gamma
µg	Microgram
µl	Microlitre
µM	Micromolar
µm	Micrometre
~	Approximately
°C	Celsius
>	Greater than
>	Greater than or equal to
<	Less than
%	Percent
*	Asteric
4-Oct	Octamer-binding protein 4
TM6SF1	Transmembrane 6 superfamily member 1
A	Adenine
ABR	Active breakpoint cluster region-related protein
ADAMTS1	A disintegrin and metalloproteinase with thrombospondin type 1 motif
ADAMTSL4	A disintegrin and metalloproteinase with thrombospondin motifs 1-like protein 4
ADAT3	tRNA-specific adenosine deaminase-like protein 3
Ago	Argonaute/eukaryotic translation initiation factor 2C (eIF2C)
AGTPBP1	Cytosolic carboxypeptidase 1
AIDS	Acquired immune deficiency syndrome
Akt	V-akt murine thymomo viral oncogene homologue
AlHV-1	Alcelaphine herpesvirus 1
ALMS1	Alstrom syndrome protein 1
AMP	Ampicillin
ANK1	Ankyrin 1
Ankrd26	Ankyrin repeat domain containing protein26
ANOVA	Analysis of variance
APBB1IP	Amyloid beta A4 precursor protein-binding family B member 1-interacting protein
ARE	Antioxidant response element
ARHGAP20	Rho GTPase-activating protein 20
ATP	Adenosine triphosphate
ATP5B	Adenosine triphosphate synthase subuit B
ATP6V1B1	ATPase, H+ transporting, lysosomal 56/58kDa, V1 subunit B1
ATX	Autotaxin
BALF-1	BamHI A leftward reading frame 1 of Epstein-Barr virus
BALF-2	BamHI A leftward reading frame 2 of Epstein-Barr virus
BALF-5	BamHI A leftward reading frame 5 of Epstein-Barr virus

BART	BamHI A rightward transcript of Epstein-Barr virus
bcl	B cell lymphoma
BCL2L13	B cell lymphoma 2-like 13
BCLAF-1	B cell lymphoma-associated transcription factor 1
BCLF-1	BamHI C leftward reading frame 1 of Epstein-Barr virus
BD	Bacto agar
BDLF-1	BamHI D leftward reading frame 1 of Epstein-Barr virus
BDRF-1	BamHI D rightward reading frame 1 of Epstein-Barr virus
BFRF-3	BamHI F rightward reading frame 3 of Epstein-Barr virus
BGLF-4	BamHI G leftward reading frame 4 of Epstein-Barr virus
BHK	Baby hamster kidney
BIC	B Cell integration cluster
BILF-1	BamHI I leftward reading frame 1 of Epstein-Barr virus
Bim	B cell lymphoma 2-like 11
BLAST	Basic local alignment search tool
blastn	Basic local alignment search tool for nucleic acids
BoHV-1	Bovine herpesvirus 1
BORF-1	BamHI O rightward reading frame 1 of Epstein-Barr virus
BORF-2	BamHI O rightward reading frame 2 of Epstein-Barr virus
bp	Base-pair
BRLF-1	BamHI R leftward reading frame 1 of Epstein-Barr virus
BXLF1	BamHI X leftward reading frame 1 of Epstein-Barr virus
BZLF-1	BamHI Z leftward reading frame 1 of Epstein-Barr virus
C1	Cluster-1
C2	Cluster-2
C3	Cluster-3
Ca	Calcium
CA12	Carbonic anhydrase 12
cAMP	Cyclic Adenosine mono phosphate
CATSPERB	Catsper channel auxiliary subunit beta
CCDC88B	Coiled-coil domain-containing protein 88B
CDC25C	Cell division cycle 25 homologue C
Cdk	Cyclin-dependent kinase
CDKN1A	Cyclin-dependent kinase inhibitor 1A
cDNA	Complementary deoxyribonucleic acid
CDS	Coding sequence
CEBPβ	CCAAT/enhancer binding protein beta
CEP152	Centrosomal protein 152kDa
CEP350	Centrosomal protein
Cl	Chloride
CLIP	Crosslinking and immunoprecipitation
CLASH	Cross linking, ligation and sequencing of hybrids
CMV	Cytomegalovirus
CO2	Carbon dioxide
ConA	Concanavalin A
CPNE2	Calcium-dependent membrane-binding protein
CPSF	Cleavage and polyadenylation specificity factor
CR2	Complement receptor type 2

CRAC	Crosslinking and analysis of cDNA
CREB	Cyclic adenosine monophosphate responsive element binding protein
CREM	Cyclic adenosine monophosphate responsive element modulator
CRK	v-crk avian sarcoma virus CT10 oncogene homolog
CSDE1	Cold shock domain-containing protein E1
CSTF	Cleavage stimulation factor
CSTF3	Cleavage stimulation factor subunit 3
CXCL11/	Chemokine (C-X-C motif) ligand 11
CYP4F22	Cytochrome P450 4F22
DC	Dentritic cells
DCP	Decappig complex protein
DEG	Differentially expressed genes
DEnG	Differentially enriched genes
DEPC	Diethylpyrocarbonate
DES	Desmin
DGCR8	DiGeorge syndrome critical region gene 8
DHX57	Putative ATP-dependent RNA helicase
DLL1	Delta-like protein 1
DMEM	Dulbecco's modified Eagle's medium
DMSO	Dimethyl sulfoxide
DNA	Deoxyribonucleic acid
dNTP	Deoxyribonucleotide triphosphate
dsDNA	Double-stranded deoxyribonucleic acid
dUTP	Deoxyuridine triphosphate
e.g.	Exempli gratia; for example
E2F1	E2F transcription factor 1/retinoblastoma-associated/binding protein
EBER	Epstein-Barr virus encoded ribonucleic acid
EBNA	Epstein-Barr virus nuclear antigen
EBV	Epstein-Barr virus/human herpesvirus 4
EDTA	Ethylenediaminetetraacetic acid
EEHV-1	Elephant endotheliotropic herpesvirus 1
EGFP	Enhanced green fluorescent protein
EHV-2	Equid herpesvirus 2
ENPP2	Ectonucleotide pyrophosphatase/phosphodiesterase family member 2
EPAS1	Endothelial PAS domain-containing protein 1
et al.	*Et al*ii; and others
Exp-5	Exportin 5
FAM71F1	Protein FAM71F1
FBXL21	F-box/LRR-repeat protein 21
FCS	Foetal calf serum
FDR	False discovery rate
FGARAT	Formylglycinamide ribotide amidotransferase
FGF19	Fibroblast growth factor 19
FHOD1	Formin homology 2 domain containing 1

FT	Flow through
FLUC	Firefly luciferase
FOXRED2	FAD-dependent oxidoreductase domain-containing protein 2
FTH1	Ferritin heavy chain subunit 1
FXRI	Fragile X-related protein
g	Gram
g/gp	Glycoprotein
GAG	Glycosamioglycan
GATM	Glycine amidinotransferase; mitochondrial
GFP	Green fluorescent protein
GLI2	Zinc finger protein
GMEM	Glasgow-modified Eagle's medium
GTP	Guanosine triphosphate
GUCY1A1	Guanylate cyclase soluble subunit alpha
HCF-1	Host cell factor 1
HCMV	Human cytomegalovirus/human herpesvirus 5
HCV	Hepatitis C virus
HEK-293T	Human embryonic kidney cells
HHV-6A	Human herpesvirus 6A
HHV-6B	Human herpesvirus 6B
HIC1	Hypermethylated in cancer 1 protein
HITS-CLIP	High throughput sequencing of RNA-CLIP
HIVEP2	Human immunodeficiency virus type I enhancer binding protein 2
HL	Hodgkin lymphoma
HLAII	Human leukocyte antigen class II
hr(s)	Hour(s)
HSV-1	Herpes simplex virus 1/human herpesvirus 1
HSV-2	Herpes simplex virus 2/human herpesvirus 2
HTLV-1	Human T cell lymphotropic virus 1
hTREX	Human transcription and export complex
i.e.	Id est; that is
IAP	inhibitor of apoptosis
ICP	Infected-cell polypeptide
IE	Immediate-early
IFN γ	Interferon gamma
IL	Interleukin
ILTV	Infectious laryngotracheitis virus/gallid herpesvirus 1
IM	Infectious mononucleosis
IP	Immunoprecipitation
IPA	Ingenuity Pathway analysis
IRES	Internal ribosome entry site
ISLR2	Imunoglobulin superfamily containing leucine-rich repeat protein 2
ITGA8	Integrin alpha-8
JAK	Janus kinase
Jun	Jun proto-oncogene
JNK	Jun N-terminal kinase

K	Potassium
Kb	Kilobase
KCl	Potassium chloride
KHDRBS3	KH domain-containing; RNA-binding; signal transduction-associated protein 3
KLHL2	Kelch-like 2
km	Kilometre
KSHV	Kaposi's sarcoma-associated herpesvirus
L	Litre
LAMB2	Laminin protein family of extracellular matrix glycoproteins
LANA	Latency-associated nuclear antigen
LAPTM4B	Lysosomal-associated transmembrane protein 4B
LARII	Luciferase assay reagent II
LAT	Latecy associated transcripts
LB	Luria Bertani
LGL	Large granular lymphocyte
lin	Abnormal cell lineage
LIX1L	LIX1-like protein
LMP	Latent membrane protein
LPA	lysophosphatidic acid
LPHN3	Latrophilin-3
LRRC30	Leucine-rich repeat-containing protein 30
LUC7L2	Putative RNA-binding protein Luc7-like 2
M	Molar
MAGI3	membrane associated guanylate kinase, WW and PDZ domain containing 3
MAP3K2	mitogen-activated protein kinase kinase kinase 2
MARK4	MAP/microtubule affinity-regulating kinase 4
MCD	Multicentric Castleman's disease
MCF	Malignant catarrhal fever
MCF2L	MCF.2 cell line derived transforming sequence-like
mCi	Millicurie
MCMV	Murine cytomegalovirus/murid herpesvirus 1
MDBK	Madin-Darby bovine kidney cells
MDV-1	Marek's disease virus 1/gallid herpesvirus 2
MFE	Minimal folding free energy
Mg	Magnesium
mg	Milligram
MgCl2	Magnesium chloride
MgSO4	Magnesium sulfate
MHC	Major histocompatibility complex
MHV-68	Murine herpesvirus 68/murid herpesvirus 4
MICB	Major histocompatibility complex class I polypeptide-related sequence B
min	Minute
miRNA/miR	Micro ribonucleic acid
miRNP	Micro ribonucleoprotein
ml	Millilitre

MLL5	Myeloid/lymphoid or mixed-lineage leukemia 5
mM	Millimolar
mmol	Millimole
mRNA	Messenger ribonucleic acid
myosin-3	MYHC-Embryonic
Na	Sodium
Na2H2PO4	Sodium dihydrogen phosphate
NaCl	Sodium chloride
NaOH	Sodium hydroxide
NAV2	Neuron navigator 2
NCBI	National centre for biotechnology information
NEB	New England Biolabs
NF-kB	Nuclear factor of kappa light polypeptide gene enhancer in B cells
ng	Nanogram
NH4	Ammonium
NIPAL2	NIPA-like protein 2
nM	Nanomolar
nm	Nanometre
NPC	Nasopharyngeal carcinoma
NRF2	Nuclear factor like 2
NRXN1	Neurexin-1-alpha
NRXN1	Neurexin-1-alpha
nt	Nucleotide
OD	Optical density
oligo(dT)	Oligodeoxythymidylic acid
oncomiR	Oncogenic micro ribonucleic acid
OR10K1	Olfactory receptor family 10 subfamily K member 1
ORF	Open reading frame or transcript derived from the designated open reading frame
orf	Protein translated from the designated open reading frame
Ov	Unique ovine herpesvirus 2 open reading frame
OvHV-2	Ovine herpesvirus 2
PACT	Protein activator of PKR
PAK7	p21 protein (Cdc42/Rac)-activated kinase 7
PAR-CLIP	Photoactivable riboucleoside enhaced-CLIP
PARD3B	Par-3 partitioning defective 3 homolog B
PAZ	PIWI, Argoaute and Zewile
P-bodies	Processing bodies
PBS	Phosphate buffer solution
PCR	Polymerase chain reaction
PDCD6	Programmed cell death 6
PDCL3	Phosducin-like 3 Calcium/calmodulin-dependent 3'; 5'-cyclic nucleotide phosphodiesterase 1A
PDE1A	Cyclic nucleotide phosphodiesterase 1A
PFKFB3	6-phosphofructo-2-kinase/fructose-2; 6-biphosphatase 3
PITRM1	Pitrilysin metallopeptidase 1
PKA	Protein kinase A

pmol	Picomole
POLN	DNA polymerase theta subunit
polyA	Polyadenylation
pre-miRNA	Preliminary micro ribonucleic acid
pre-mRNA	Preliminary messenger ribonucleic acid
pri-miRNA	Primary micro ribonucleic acid
PRPF39	PRP39 pre-mRNA processing factor 39 homolog (S. cerevisiae)
PRSS35	Inactive serine protease 35
pSILAC	Pulsed stable isotope labelling with amiacid I cell culture
PTEN	Phosphatase and tensin homologue
PTLD	Post transplant lymphoproliferative disease
PVDF	Polyvinylidene fluoride
RGS17	Regulator of G-protein signaling 17
RISC	Ribonucleic acid-induced silencing complex
RLC	RISC loading complex
RLUC	Renilla luciferase
RNA	Ribonucleic acid
rpm	Rotations per minute
RPMI-1640	MDBK were grown in Roswell Park Memorial Institute 1640 medium
RPS6KL1	Ribosomal protein S6 kinase-like 1
rRNA	Ribosomal ribonucleic acid
Rta	R transactivator
RXFP3	Relaxin-3 receptor 1
SA-MCF	Sheep-associated malignant catarrhal fever
SCFD1	Sec1 family domain-containing protein 1
SCMH1	Polycomb protein SCMH1
SDS	Sodium dodecyl sulfate
Sec	Second
SEC13	SEC13 homolog
SEF	Sheep emryo fibroblasts
SEMA3A	Semaphorin-3A
SEMA3D	Semaphorin-3D
SEMA7A	Semaphorin 7A
SHH	Sonic hedgehog signalling
SLC25A16	Solute carrier family 25
SLC9A5	Solute carrier family 9, member 3
Smad5	Sma/mothers against decapentaplegic homologue 2
snoRNA	Small nucleolar ribonucleic acid
snRNAs	Spliceosomal ribonucleic acids
SNRNP25	U11/U12 small nuclear ribonucleoprotein 25KDa
SOBP	Sine oculis-binding protein homolog
SOC	Super optimal broth with catabolite repression
SRR	Serine racemase
ssDNA	Single-stranded deoxyribonucleic acid
STAT	Signal transducer and activator of transcription
TAE	Tris-acetate-ethylenediaminetetraacetic acid

TBC1D9	TBC1 domain family member 9
TBE	Tris-borate-ethylenediaminetetraacetic acid
TCR	T cell receptors
TCTP	Translationally-controlled tumor protein (TPT1)
TDRD12	Tudor domain containing 12,
TE	Tris-ethylenediaminetetraacetic acid
TEMED	Tetramethylethylenediamine
TGFR1	Transforming growth factor receptor 1
TGFβ	Transforming growth factor beta
THBS1	Thrombospondin 1
TLR	Toll-like receptor
TNFα	Tumour necrosis factor alpha
TPT1	Translationally controlled tumor protein
TRAF6	TNF receptor asspciated factor 6
TRBP	Trans-activation-responsive ribonucleic acid binding protein
TRIM27	tripartite motif containing 27
tRNA	Transfer ribonucleic acid
TSAP	Thermo sensitive alkalie phosphatase
TWEAKR	Tumour necrosis factor-related weak inducer of apoptosis receptor
™	Trademark
U	Unit
UBN1	Ubinuclein-1
UL	Unique long open reading frame or transcript derived from the designated unique long open reading frame
UPK1B	Uroplakin-1b
US	Unique short open reading frame or transcript derived from the designated unique short open reading frame
UTR	Untranslated region
UV	Ultraviolet
V	Volt
v/v	Volume per volume
VEGF	Vascular endothelial growth factor
VLDLR	Very low-density lipoprotein receptor
vols	Volumes
VPS33B	Vacuolar protein sorting-associated protein 33B
VWA5B2	von Willebrand factor A domain-containing protein 5B2
VZV	Varicella-zoster virus/human herpesvirus 3
w/t	Weight per volume
WA-MCF	Wildebeest-associated malignant catarrhal fever
WBC	White buffy coat
WDR60	WD repeat domain 60
x g	G force, relative centrifugal force
Ybx1	Y box binding protein 1
ZBED5	Zinc finger, BED-type containing 5
ZBTB7C	Zinc finger and BTB domain-containing protein 7C
ZNF3	Zinc finger protein3
ZNF608	Zinc finger protein 608

Chapter 1: Introduction

1.1 Herpesviruses

Herpesviruses are widely distributed in nature. Most animal species have been shown to be infected with at least one, and sometimes several distinct, herpesviruses (Pellet and Roizman, 2007, McGeoch and Davison, 1999). The number of the herpesviruses that have been isolated exceeds 200 (Pellet and Roizman, 2007). Despite this knowledge, the majority of potential animal hosts for herpesviruses have so far not been investigated (Wibbelt *et al*., 2007). Herpesviruses have co-evolved with their hosts for millions of years. This notion is supported by the understanding that they have diversified from a common ancestor, in a manner mediating co-speciation of herpesviruses with host species, through species-specific latent infections (Umene and Sakaoka, 1999, Fossum *et al*., 2009).

Herpesviruses share a number of biological properties including shared expression of a large number of enzymes involved in nucleic acid metabolism (e.g. thymidine kinase), DNA synthesis (e.g. DNA helicase/primase) and processing of proteins (e.g. protein kinase). Herpesvirus genomic synthesis and the assembly of capsids occurs in the nucleus. All known herpesviruses are able to establish and maintain a latent state in their host. In the infected cell, the viral genome is present in an episomal and circular form during latency and only a small subset of viral genes is expressed (Pellet and Roizman, 2007). Latent virus is able to reactivate following cellular stress, and resumes viral replication and new infectious virion production.

1.1.1 Herpesvirus structure

A typical herpesvirus particle consists of a core containing genomic linear double stranded DNA which is wrapped in an icosahedral capsid of T=16 symmetry and has an approximate diameter of 100 to 110 nanaometres (nm) (Figure 1.1). The viral capsid is surrounded by a loosely organised protein structure termed the tegument. The tegument contains many viral proteins which play important roles in initiating host cell infection, regulating viral gene expression, assisting transport of viral proteins across the nuclear membrane and controlling the packaging of viral DNA (Penkert and Kalejta, 2011, Yu *et al*., 2011).

A lipid bilayer envelope derived from patches of altered host cellular membrane, surrounds the tegument. The viral envelope also contains embedded virally encoded glycoproteins which vary in number and relative amount, for example herpes simplex virus-1 (HSV-1) encodes at least 11 glycoproteins (Roizman and Knipe, 2001). The size of the virion increases from 120nm to approximately 300nm after the inclusion of the tegument and envelope (Roizman & Pellett., 2001).

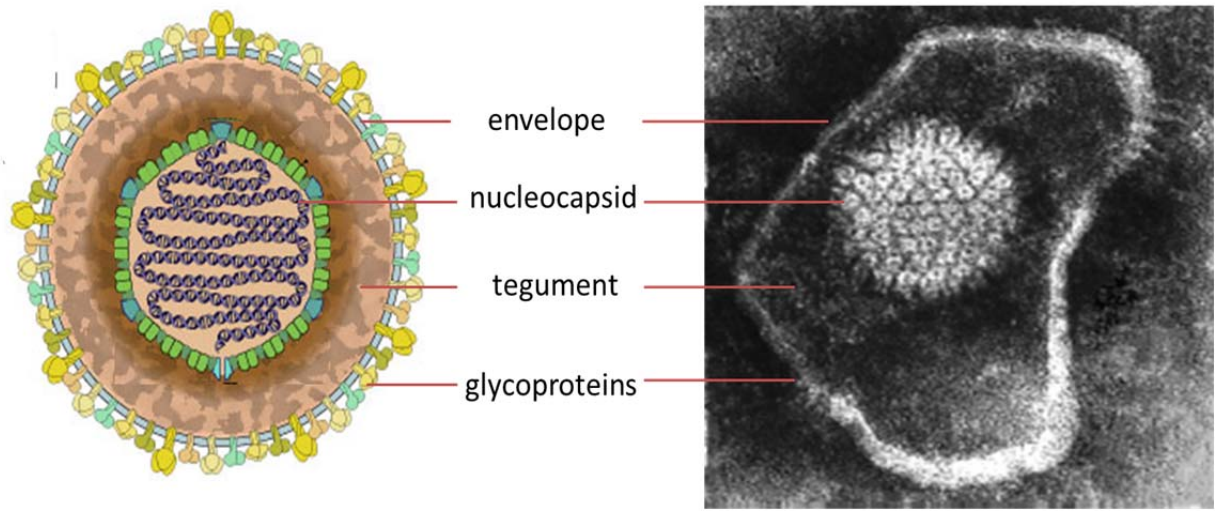

A B

Figure 1.1: A typical herpesvirus virion

A. Diagrammatical representation showing the major structural components (image adapted from http://viralzone.expasy.org/all_by_species/526.html)
B. Electrom micrograph of herpes simplex virus (taken from http://pathmicro.med.sc.edu/mhunt/dna1.htm).

1.1.2 Herpesvirus genome

Herpesvirus genomes vary in length from 120 to 250 kilobase pairs (kb) and encode between 70-220 open reading frames (ORFs) (Roizmann *et al*., 1992, Cha *et al*., 1996) although recent characterization of clinical human cytomegalovirus (HCMV) strain suggests that the viral genome has 252 ORFs that may encode potential proteins (Murphy *et al*., 2003). The current estimate is that 43 ORFs are core genes and are conserved throughout the herpesvirus family. The core genes include capsid proteins, tegument proteins and components involved in DNA replication (McGeoch and Davison, 1999). The remaining ORFs are unique and vary between sub-families (alpha, beta & gamma) species and genus. In addition to protein coding regions, there are several regions within herpesvirus genomes which either do not encode for any protein or encode non-coding RNAs (Stevens., 1981, Hart *et al*., 2009). Furthermore microRNAs (miRNA) have also been identified in most of the herpesviruses (Cai *et al*., 2006b, Grey *et al*., 2005, Levy *et al*., 2012, Pfeffer *et al*., 2004). miRNAs will be discussed in greater detail in Section 1.4.

Herpesvirus genomes contain internal and terminal repetitive (reiterated) sequences through extensive regions. The genome length can vary depending on the copy number of these repeat sequences. Herpesviruses are grouped into six categories A – F, on the basis of the presence and location of reiterations of terminal sequences greater than 100 base pairs (bp) (Pellet and Roizman). A diagrammatic representation of the sequence arrangements of each group is shown in Figure 1.2. In the viruses in group A (e.g channel catfish herpesvirus) a large sequence from one terminus is directly repeated at the other terminus of the genome. These regions are

named as left terminal repeat (LTR) and right terminal repeat (RTR). In group B viruses (e.g herpesvirus saimiri (HVS), the genomes possess a variable number of directly repeated sequences at either of the termini. The grouping of Group C virus (e.g Epstein-Barr virus (EBV) genomes is similar to that of group B with the exception that the direct repeat sequences are fewer in number in comparison with group B. Additionally group C unique genome sequences are further divided by other directly repeated, though unrelated, genome sequences of more than 100 bp. In the group D virus genomes (e.g varicella-zoster virus (VZV), the unique sequences are grouped into unique long (UL) and unique short (US) regions. In this group, the repeat sequence present on one terminus is also present in an inverted orientation internally. The US domain is flanked by those inverted repeat sequences. The genomes of group E viruses (e.g herpes simplex virus (HSV) and human cytomegalovirus (HCMV) are also divided into UL and US domains. However, the difference is the presence of its own inverted repeat sequence on the flanks of each domain. These sequences are called RL (long or large) and RS (short or small) repeat. Quite similar to US domains of group D viruses, in the viruses of group E, UL and US domains can invert to each other resulting in four possible isomers. The genomes of group F (e.g tupaia herpesvirus) do not contain any repeat sequences (Figure 1.2) (Roizman *et al*., 1992).

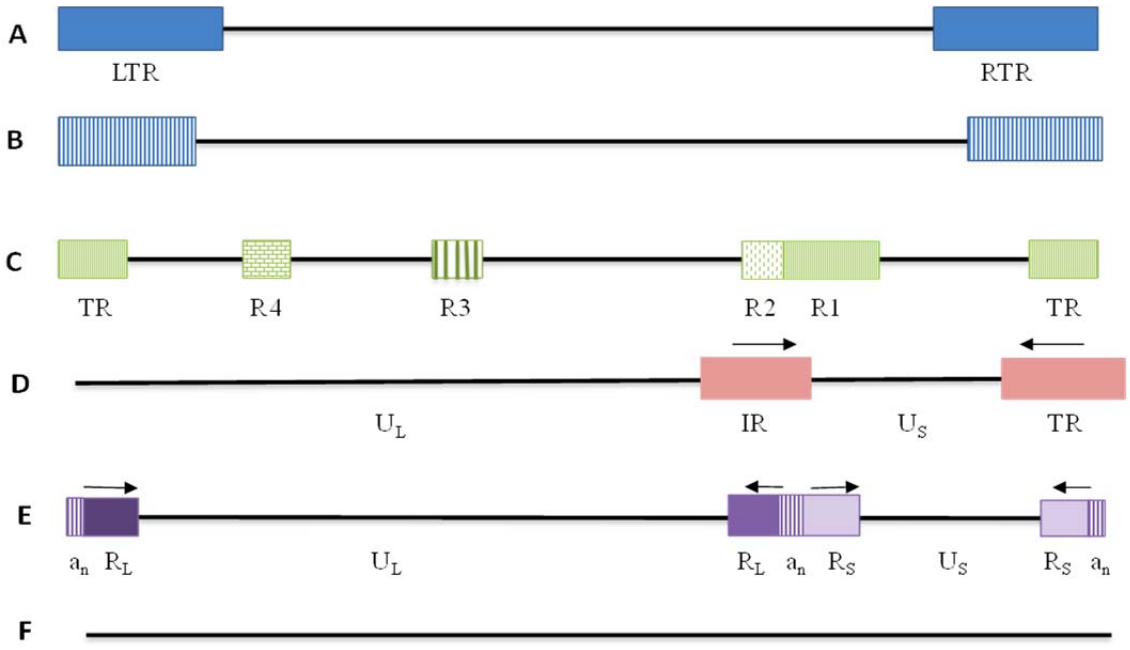

Figure 1.2: Schematic diagram depicting the sequence arrangement of six classes (A-F) of viral genome of herpesvirus family.

The genomes A, B, C, D, E and F are exemplified by the channel catfish herpesvirus, herpesvirus siamiri, Epstein-Barr virus, varicella zoster virus, herpes simplex viruses, and tupaia herpesvirus, respectively. The relative orientations of repeat sequences are indicated with arrows. The genomes of group A viruses contain a large sequence from one terminus directly repeated at the other terminus. The genomes of group B viruses contain a variable number of directly repeated sequences at both termini. The genomes of group C viruses contain both terminal repeats and other unrelated repeat sequences that subdivide the unique sequence. The unique regions of the genomes of group D viruses are divided into two segments separated by an inverted repeat of the terminal region from the short (U_S) segment. The unique regions of the genomes of group E viruses are similarly divided with inverted repeats flanking both the long U_L and U_S regions. On one terminus there are n copies of sequence 'a' next to a larger sequence designated as 'R_L'. The other terminus has one directly repeated 'a' sequence next to a sequence designated as 'R_S'. The terminal repeat 'R_La' and 'R_Sa' sequences are inserted in an inverted orientation. Terminal reiterations in the genome of group F have not been described. (Figure adapted from Roizman *et al*., 1992).

1.2 Herpesvirus classification

The members of *Herpesviridae* family are divided into three sub families: *Alphaherpesvirinae*, *Betaherpesvirinae* and *Gammaherpesvirinae*. Herpesvirus classification is based on; biological properties, DNA sequence homology, similarities in the genome sequence arrangements and relatedness of important viral proteins (Roizman & Pellett., 2001).

1.2.1 Alphaherpesviruses

Alphaherpesviruses have a broad host range, efficient and short reproductive cycles and establish latency primarily but not exclusively, in sensory neuronal cells (Roizman & Pellett., 2001). This sub-family is divided in four genera: *Simplexvirus* (including HSV-1), *Varicellovirus* (including VZV), *Mardivirus* (including Marek's disease virus (MDV) and *Iltovirus* (including infectious laryngotracheitis virus).

HSV-1 (human herpesvirus 1, HHV-1) and HSV-2 (human herpesvirus 2, HHV-2) were the first of the human herpesviruses to be discovered and are among the most intensively investigated of all viruses (Roizman & Knipe., 2001; Hunt., 2011). HSV generally causes genital or oral infections which can result in a wide range of clinical conditions, from mild cutaneous lesions to fatal encephalitis. Primary infection of HSV is generally asymptomatic. After transmission through the epithelial mucosa of mouth or genitals, virus establishes latency in the sensory ganglia which are innervating the site of infection. Reactivation of the virus may occur as a result of stress. Symptoms related to HSV reactivation (typically cold sores) include small, grouped vesicles or blisters on the epithelial surfaces which then pustulate, ulcerate

and later form a crust. Vesicles are filled with newly produced infectious virions. HSV-1 can also cause more severe clinical symptoms including vision loss, serious complications of atopic eczema, erythema multiforme, Stevens-Johnson syndrome, neurological impairment and death in neonates (Ferrante *et al*., 2000)

Varicella Zoster virus (VZV, human herpesvirus 3) is another widespread, human pathogen. It is efficiently transmissible, usually during childhood, through skin to skin contact and inhalation of infected droplets. VZV causes chicken pox (varicella) which is characterized by the appearance of widespread skin lesions (Arvin, 1996, Asano *et al*., 1990, Ito *et al*., 2001). VZV establishes latency in sensory ganglia and its reactivation remains limited, generally once in a lifetime resulting in a localized vesicular rash (herpes zoster). Reactivation can be frequent in immune suppressed systems. VZV can also cause serious infections such as pneumonia, liver failure, varicella encephalitis, cerebellar ataxia and thrombocytopenia in immunosuppressed individuals (Rawson *et al*., 2001).

Marek's disease virus (MDV or gallid herpesvirus 2) is a member of *Mardivirus* genus and is the cause of Marek's Disease (MD). In poultry, MDV initially infects B lymphocytes although latency is established in CD4+ T cells (Mwangi *et al*., 2011). It was reclassified as an alphaherpesvirus due to its sequence homology and gene organization as against its classic classification as a gammaherpesvirus (Buckmaster *et al*., 1988, Roizmann *et al*., 1992). It is highly contagious and has identical early stages of replication to other members of the *Alphaherpesvirinae* (Schumacher *et al*., 2005). MDV does not release detectable free enveloped virus into the supernatant of cultured cells (Calnek *et al*., 1970, Tischer *et al*., 2005)

1.2.2 Betaherpesviruses

Unlike alphaherpesviruses, betaherpesviruses have a restricted host range and a long reproduction cycle. Betaherpesvirus infection progresses slowly in cell culture and the infected cells become enlarged rather than lyse (Roizmann *et al*., 1992). Latent infection is established predominantly in monocytes or macrophages. The viruses in this sub-family are subdivided into 4 genera (*Cytomegalovirus*, *Muromegalovirus*, *Roseolovirus*, and *Proboscivirus*) comprising 14 species (AJ *et al*., 2009, Davison *et al*., 2009).

Human *Cytomegalovirus* HCMV (human herpesvirus 5 or HHV-5) is a pathogen in immunocompromised individuals. Primary infection typically starts with replication of the virus in the mucosal epithelium as a result of direct contact with infectious secretions from an infected individual. Primary infection is generally asymptomatic but occasionally can lead to the development of prolonged fever and mild hepatitis (similar to gammaherpesvirus EBV mononucleosis) (Crough and Khanna, 2009). In a natural infection, HCMV establishes latency in monocytes, macrophages and their progenitors while reactivation may occur with shedding of the virus from mucosal sites (Mocarski, 2004). Severe clinical conditions of HCMV virus are usually only observed in neonates and immunosuppressed individuals. Congenital HCMV infection can result in jaundice, purpura, hepatosplenomegaly, microcephaly and sensorineural hearing loss in neonates (Pass *et al*., 2006). HCMV more rarely presents with multisystem manifestations, in immunocompetent individuals, with symptoms ranging from fever, rash, anemia and thrombocytopenia to retinitis, encephalitis, pneumonitis, hepatitis and pancreatitis (Rafailidis *et al*., 2008). Organ

and stem cell transplantation may involve complications including HCMV infection leading to fatal pneumonitis (Gandhi *et al*., 2003, Green *et al*., 2012).

1.2.3 Gammaherpesviruses

The members of the sub family *Gammaherpesvirinae* have a limited host range. The experimental host range of the gammaherpesviruses is limited to the family or order to which the natural host belongs (Roizman & Pellett., 2001). Gammaherpesviruses replicate in lymphoblastoid cells and some also cause lytic infections in epithelioid and fibroblastic cells, *in vitro*. Unlike alpha- and betaherpesviruses, gammahepesviruses establish and maintain latency in either T or B lymphocytes (Ackermann, 2006). In addition to the genes conserved between herpesviruses, each gammaherpesvirus also contains a set of unique genes which are usually located at the terminal regions of the genome and which are important for viral pathogenesis. In addition, gammaherpesviruses have more cellular homologue genes than the members of the other two sub-families. The viruses in this sub-family are sub divided into 4 genera (*Lymphocryptovirus, Rhadinovirus, Macavirus, and Percavirus)* comprising 34 species (AJ *et al*., 2009, Davison *et al*., 2009)

EBV is the most studied virus in the genus *Lymphocryptovirus*. EBV is found in the vast majority of adults worldwide. EBV is a strictly human pathogen and in most cases transmitted through saliva (Ascherio and Munger, 2010). Primary infection occurs usually in infants and has an asymptomatic course. In contrast, in adolescents it leads to infectious mononucleosis (IM), a lymphoproliferative disease characterised by lymphadenopathy, tonsillitis, pharyngolaryngitis and skin eruptions (Henle *et al*., 1968). Primary infection occurs in epithelial cells of the oropharynx

and after replication at the infected site latency is established by targeting the naïve B cells in such a manner that the immune response of the host is not activated (Babcock *et al*., 1998, Thompson and Kurzrock, 2004). EBV has also been linked to numerous lymphomas in immunodeficient individuals; Burkitt's lymphoma (BL), Hodgkin lymphoma (HD), nasopharyngeal carcinoma (NPC) and post-transplant lymphoproliferative disease (PTLD) (Henle and Henle, 1970, Haque *et al*., 1996). Immunocompetent individuals may develop EBV associated cancers due to the host genetic background/ contributing environmental factors in the growth of EBV, in certain geographical locations.

Human herpesvirus 8 (HHV-8, Kaposi's sarcoma-associated herpesvirus (KSHV) is a *Rhadinovirus* and humans are the only known hosts of the virus. There are currently three proliferative diseases associated with KSHV infection; Kaposi's sarcoma (KS) (a tumor of endothelial cells origin), primary effusion lymphoma (PEL) (a B-cell lymphoma) and multicentric Castleman's disease (MCD) (B-cell lymphoproliferative disorder). These lymphomas are most frequently identified in immunosuppressed individuals, particularly patients with acquired immunodeficiency syndrome (AIDS) (Chang *et al*., 1994, Moore and Chang, 2001). KSHV transmission occurs mostly through saliva. The principal site of KSHV lytic replication is the oropharynx, most likely in B cells of tonsillar or other pharyngeal lymphoid tissue (Duus *et al*., 2004). Latency is established in B-cells and in latent infection the linear viral genome circularizes in the nucleus and is maintained as an episome autonomously there. Because most viral genes are not expressed, viral gene

expression is sharply restricted in latency and there is no cytotoxicity and no virus particles are produced (Ganem, 2010).

Murine gammaherpesvirus 68 (MHV-68) or murid herpesvirus 4 (MHV-4) is another member of the genus *Rhadinovirus*. MHV-68 was originally isolated from the bank vole (*Cletrinomys glariolus*) in Slovakia (Blaskovic *et al*., 1980). MHV-68 appears to be widespread among rodent populations and MHV-68 infection of laboratory mice also represents an amenable model system for investigating gammaherpesvirus pathogenesis (Simas and Efstathiou, 1998). Transmission of MHV-68 occurs through the intranasal route. Lytic infection occurs in the alveolar epithelial cells in the lungs followed by virus dissemination and latent infection of B lymphocytes as well as macrophages (Sunil-Chandra *et al*., 1992). Latently infected B lymphocytes reside and maintain latency in spleen. Initially, those cells undergo expansion which results in splenomegaly, followed by an infectious mononucleosis-like syndrome, and lymphoproliferative disease (Sunil-Chandra *et al*., 1992, Nash *et al*., 2001, Flano *et al*., 2002).

Herpesvirus saimiri (HVS) a T lymphotropic virus, is the classical prototype of the genus *Rhadinoviruses*. The natural host for HVS is squirrel monkeys (*saimiri sciureus*) and these are found to be persistently infected with this virus. Squirrel monkeys are usually infected by HVS via saliva within the first two years of life (Melendez *et al*., 1968). HVS is apathogenic in its natural host, but causes acute peripheral T cell lymphomas in other monkey species after experimental infection (Fickenscher and Fleckenstein, 2001). Certain strains of HVS e.g C488 have the ability to transform human T-lymphocytes to continuous growth without the need of

re-stimulation by an antigen or a mitogen, providing for the first time a means of human T-lymphocyte immortalization in cell culture (Fleckenstein and Ensser, 2004).

Ovine herpesvirus 2 (OvHV-2) and Alcelaphine herpesvirus 1 (AlHV-1) are members of genus *Macavirus*. Both viruses have been shown to cause a fatal lymphoproliferative disease (malignant catarrhal fever (MCF) in cloven-hoofed animals (Russell *et al*., 2009, O'Toole and Li, 2014) and will be discussed in detail in Section 1.4.

1.3 Herpesvirus life cycle

The life cycle of herpesviruses is divided into two different stages in the host; the lytic stage and the latent stage. The lytic stage involves virus replication and release of infectious virus particles from the infected cell. In the latent stage, virus genome persists in the infected cell as an episome with very little virus gene expression and no infectious progeny is produced. The latent virus is able to reactivate following a number of stimuli including cellular stress, UV, immunosuppression or tissue damage and resumes viral replication and new infectious virion production.

1.3.1 Attachment and entry

Viral entry into the host cell is first step in the typical lifecycle of the herpesviruses. Most of the herpesviruses enter into the host cell by fusion but some also use the endocytic pathway for viral entry (Nicola *et al*., 2003, Nicola and Straus, 2004). The glycoproteins present in the viral envelope interact with the target molecules present on the host cell membrane and allow the entry of viral capsid and tegument proteins

into the host cell cytoplasm. The process of HSV virion attachment involves the interaction of five glycoproteins (gB, gC, gD, gH-gL heterodimer) with the surface of host cells (Akhtar and Shukla, 2009). Initial interactions occur between gC and gB (to a lesser extent) with the glycosaminoglycan (GAG) molecules present on the host cell membrane. This interaction brings the cellular and viral membranes into close apposition. Heparin sulphate proteoglycan is the predominant GAG molecule involved in this interaction (Shieh *et al*., 1992) though other molecules like chondroitin sulphate can also be used in its absence. After initial attachment to the cell membrane, the process of penetration begins which depends on the host cell type and mode of entry (Campadelli-Fiume *et al*., 2007). Viral entry may require fusion of the virion envelope with the plasma membrane or with the membrane of an intracellular vesicle (Clement *et al*., 2006). In HSV, gD interacts with one of several specific cell membrane receptors; nectin-1, nectin-2 herpesvirus entry mediator (HVEM) or 3-O sulfated heparin sulphate (3-O HS) (Spear, 2004, Shukla *et al*., 1999). The binding of gD to one of its cognate receptors induces conformational changes in gD that cause the formation of a multi-glycoprotein complex involving gB, gD, gH-gL (Atanasiu *et al*., 2007, Subramanian and Geraghty, 2007). Nectins (Warner *et al*., 1998, Geraghty *et al*., 1998) and 3-O HS (Shukla *et al*., 1999) have a wide tissue distribution and can mediate entry of all HSV-1 strains tested. Soluble forms of gD and its receptors can trigger fusion of HSV with the host cell membrane which indicates that the interaction of gD with its receptors has a role in the attachment and fusion for entry of HSV (Tsvitov *et al*., 2007).

EBV interacts with the B lymphocytes through the interaction of EBV envelope glycoprotein gp350/220 with the cellular complement receptor type 2 (CR2 or CD21) (Carel *et al*., 1990, Connolly *et al*., 2011, Fingeroth *et al*., 1984). K8.1 of KSHV and gp150 of MHV-68, are thought to be the homologues of gp350/220 and carry out the initial attachment of these viruses (Stewart *et al*., 2004, Sun *et al*., 1999). It has also been shown that a complex of three glycoproteins gp85 (homologue of gH), gp25 (homologue of gL) and gp42 are essential for virus penetration into host cells. Attachment of EBV to host cells is not sufficient to trigger fusion; instead a complex formed of gp25-gp42-gp85 (three-part complex) mediates the interaction by binding gp42 to the human leukocyte antigen class II (HLA class II) on target B cells (Li *et al*., 1997), whereas entry into epithelial cells which lack HLA class II, requires a glycoprotein complex without gp42 (two-part complex) (Borza and Hutt-Fletcher, 2002). To accommodate infection of both epithelial and B cells EBV virions carry both two and three part complexes and the ratio of the two on the virus particle also influences the cell tropism of the virus (Shannon-Lowe *et al*., 2006). Deletion of gp42 or addition of gp42 can produce virus that can infect only epithelial cells or only B lymphocytes respectively (Borza and Hutt-Fletcher, 2002).

The HSV and EBV receptor-binding activities described above can trigger fusion but are not sufficient for the completion of this process. To initiate the core fusion machinery, a glycoprotein complex in HSV (gB and gH-gL) and EBV (gB and gp85-gp25) is required (Haddad and Hutt-Fletcher, 1989, Miller and Hutt-Fletcher, 1988). gB is a conserved herpesvirus fusion protein and has been shown to have a key role in virus attachment to host cells and fusion of the envelope with the host cell

membrane (Backovic and Jardetzky, 2011, Heldwein et al., 2006). Viral fusion proteins are thought to be inserted into the host cell membrane and undergo large conformational changes by refolding, which draw viral and host cell together (Connolly *et al*., 2011). As a result a fusion pore is formed that allows mixing of the cytoplasmic contents with viral contents. This step delivers the viral tegument and nucleocapsid into the cytoplasm (Akhtar and Shukla, 2009). Fusion at the plasma membrane is a pH-independent process (Spear, 2004) whereas low pH is required for HSV-1 entry through an endocytic route for certain cell types (Nicola *et al*., 2003, Nicola and Straus, 2004). EBV also uses endocytosis to enter into the normal B cells (Miller and Hutt-Fletcher, 1992). The low pH of the endosome effects major conformational changes in the fusion proteins and leads to the fusion of the HSV-1 envelope with the plasma membrane of the vesicle releasing the nucleocapsid and tegument into the host cell cytoplasm (Stampfer *et al*., 2010). In HSV-1, dissociation of the outer tegument from the nucleocapsid occurs during entry into the cytoplasm and is mediated by UL13 (viral tegument protein) through phosphorylation (Kelly *et al*., 2009). Inner tegument proteins; UL36 and UL37 remain associated with the capsid and are transported along with the nucleocapsid to the nucleus. UL36 assists in the transfer of the viral genome into the nucleus through the nuclear pore (Kelly *et al*., 2009, Sodeik *et al*., 1997). Upon entry into nucleus the genome circularizes without prior viral protein synthesis and lytic replication (Garber *et al*., 1993).

1.3.2 Lytic replication

Transcription of herpesviruses genes occurs via a highly regulated expression cascade (Honess and Roizman, 1975). Soon after HSV infection (about 2 to 4 hours post-infection) the viral immediate early (IE) genes (also referred to as alpha or α) are expressed. The peak expression of the next set of genes; early (E) genes (also referred to as beta or β) occurs between about 4 to 8 hours post-infection. The third set of genes are late (L) genes (also referred to as gamma or γ), whose peak expression occurs between about 7-15 hours post-infection (Alwine *et al*., 1974, Boehmer and Lehman, 1997, Honess and Roizman, 1975).

The transcription of IE genes does not require *de novo* protein synthesis (Moriuchi *et al*., 1993). VP16 a HSV-1 tegument protein plays a key role in promoting the expression of IE genes. VP16 is synthesized during the late phase of HSV-1 replication and is packaged into the tegument during virion assembly. During infection of host cells, this protein is released and stimulates transcription of HSV-1 IE genes (Batterson and Roizman, 1983). It acts in complex with the cellular proteins; Octamer binding protein Oct-1 (Oct-1) and host cell factor-1 (HCF-1) to activate RNA polymerase II-dependent transcription from the viral IE genes (ICP0, ICP4, ICP22, ICP27 and ICP47) promoters through their TAATGARAT motifs (Gerster and Roeder, 1988, Grondin and DeLuca, 2000, Kristie *et al*., 1989, Xiao and Capone, 1990). It has been reported that HCF-1 carries VP16 to the nucleus where the VP16-HCF-1 complex binds to Oct-1 bound to IE genes promoters leading to the transcription of the IE genes to initiate the viral gene cascade (Roizman & Knipe., 2001).

In EBV, the proteins encoded by IE genes BZLF-1 (Zta) and BRLF-1 (replication and transcription activator (Rta) have been shown to play key roles in inducing lytic gene expression (Westphal *et al*., 1999). In B cells, the expression of BZLF-1 and in epithelial cells, the expression of BZLF-1 or BRLF-1 is sufficient to trigger induction of EBV lytic infection (Hardwick *et al*., 1988, Rooney *et al*., 1989, Wen *et al*., 2007, Zalani *et al*., 1996). The Rta protein is analogous to other gammaherpesvirus transactivators; ORF50 of HVS, KSHV and MHV-68 (Lukac *et al*., 1999, Whitehouse *et al*., 1997) which are also capable of driving lytic replication in latently infected cells (Gradoville *et al*., 2000, Goodwin *et al*., 2001, Wu *et al*., 2000a). EBV Rta, has been shown to activate its own expression as well as the transcription of a number of viral IE genes including other transactivators such as Zta and BMLF-1 also referred as Mta. In the gammaherpesviruses, Mta and its homologues encoded by ORF57 are capable of both post-transcriptional activation and repression of a number of viral genes and the shuttling of intronless viral mRNAs (Chen *et al*., 2002, Goodwin *et al*., 2000, Whitehouse *et al*., 1998, Williams *et al*., 2005). KSHV ORF50 and HVS ORF50a have also been shown to induce ORF57 gene expression (Lukac *et al*., 1999, Nicholas *et al*., 1991, Walters *et al*., 2005, Whitehouse *et al*., 1997).

The products of IE genes initiate the transcription of E genes. Many E genes are involved in viral DNA replication such as DNA polymerase (e.g EBV BALF-5, OvHV-2 ORF9), ss-DNA binding proteins (e.g EBV BALF-2), ribonucleotide reductase (e.g EBV BORF-2 and BORF-1, OvHV-2 ORF60 and ORF61) and thymidine kinase (e.g EBV: BXLF-1, OvHV-2 ORF21) (Roizman and Knipe, 2001). The products of some of the E genes cluster at the origin of replication of viral

genome. It has been proposed that herpesvirus DNA synthesis is initiated by a theta mechanism and at some point and by an as yet undefined mechanism, theta replication switches to the rolling circle mode, which is the predominant mode of herpesvirus DNA replication (Lehman and Boehmer, 1999) and results in the formation of long head to tail concatamers of viral genomic DNA being produced (Ben-Porat *et al*., 1976).

Newly synthesized viral DNA genomes are used as templates for L gene transcription, and the late mRNAs produce viral structural proteins necessary for the assembly of progeny virions inside the nucleus (Johnson and Baines, 2011). Cleavage and packaging of concatemeric DNA occurs in newly formed capsids. It is a tightly coupled process in which the cleavage of the genome concatemers occurs at the terminus of one unit length as they are packaged into the capsid (Boehmer and Lehman, 1997). Before the insertion of viral DNA, a protein scaffold is formed to support the capsid. EBV BDRF1 acts as a scaffold on which other late structural capsid proteins BCLF1, BFRF3, BORF1 and BDLF1 form a spherical procapsid (Henson *et al*., 2009). BVRF2 cleaves the BDRF1 scaffolding as the newly replicated viral DNA is packed inside, resulting in the formation of a mature icosahedral nucleocapsid (Dasgupta and Wilson, 1999, Paulus *et al*., 2010).

The completed nucleocapsids are released from the nucleus through a two stage enveloping process. The first envelope is made through budding at the inner nuclear membrane into the perinuclear space. De-envelopement of the first envelope occurs by fusion with the outer nuclear membrane (Mettenleiter, 2002) and de-enveloped nucleocapsids are delivered to the cytoplasm for association with tegument proteins.

The second envelope is acquired during rebudding into the trans-Golgi network. The newly formed virions are then transported to the cell surface and are released by exocytosis (Kelly *et al*., 2009, Mettenleiter, 2002).

In HSV-1, two of the herpesvirus conserved proteins UL31 and UL34 are involved in embedding the nucleocapsid into the inner nuclear surface. The UL13 protein is involved in the destabilization of the nuclear surface for the entrance of the nucleocapsid into the perinuclear space. In the Golgi, the proteins UL36 and UL37 have been shown to make the first layer of the tegument and proteins UL11, UL16, and UL21 make the outer tegument layer (Johnson and Baines, 2011, Mettenleiter *et al*., 2013).

In EBV gB is thought to have a role in the initial envelopement of the nucleocapsid due to higher levels of gB being present in the nuclear membrane of cells producing virus than in the mature enveloped virions (Kelly *et al*., 2009). In addition, gB also plays a role in nuclear egress (Herrold *et al*., 1996). EBV gH and gp350/220 are found in the Golgi and on the plasma membrane of infected cells. gp350/220 is the most abundant virus protein in the lytically infected cell membrane and virus envelope, whereas only a small amount of the protein accumulates in the infected cell nuclear membrane. It is thought that during the re-envelopment process at the plasma membrane level, the virus receives envelope rich in gp350/220 (Gong and Kieff, 1990). Mature progeny virions reach to the surface by vesicular movement through the Golgi apparatus and are released into the extracellular space by exocytosis.

1.3.3 Herpesvirus latency

In latency, the virus enters a state where there is limited gene expression and no replication occurs (Ackermann, 2006). In this stage of the herpesvirus life cycle the nucleosomes become relatively more stable and dense (Nevels *et al*., 2011, Paulus *et al*., 2010). The expression of genes during latency varies considerably among herpesviruses. Consistent with the previous section, in this section the strategies of HSV-1 and EBV will be discussed.

The latency associated transcripts (LATs) are the only viral transcripts which are detected frequently in HSV-1 latency (Stevens, 1987, Nicoll *et al*., 2012). No protein product has been attributed to the LAT gene. LAT is complementary to an α gene, ICP0 and overlaps the ICP0 transcript and it has been suggested that LAT inhibits ICP0 expression by an antisense mechanism (Gordon *et al*., 1988, Jones, 2003, Perng and Jones, 2010, Wagner *et al*., 1988). There have been various reports regarding the role of LAT expression in the establishment of latency or reactivation of virus from latency (Leib *et al*., 1989, Bergstrom and Lycke, 1990, Hill *et al*., 1990, Nicoll *et al*., 2012, Trousdale *et al*., 1991, Thompson and Sawtell, 1997). Ahmad *et al* reported that 2.0-kb region of the LAT intron and the exon 1 region of the LAT were important in protection from apoptosis (Ahmed *et al*., 2002). LAT inhibits apoptosis and maintains latency by promoting the survival of infected neurons (Perng *et al*., 2000, Perng *et al*., 2002) possibly by down-regulation of the transcripts of α genes involved in lytic replication such as ICP0 (Chen *et al*., 1997, Garber *et al*., 1997). It has also been shown that repression of lytic gene expression during latency was achieved by HSV encoded miRNAs in latently infected cells (Jurak *et al*., 2010,

Tang *et al*., 2009, Tang *et al*., 2008, Umbach *et al*., 2008, Umbach *et al*., 2010). LAT region encodes for more than 50% of HSV-1 miRNAs which are expressed abundantly during latency (Jurak *et al*., 2010, Cui *et al*., 2006, Sun and Li, 2012). In transient transfection assays, HSV-1 LAT region encoded miRNA, miR-H2, can repress expression of ICP0 (Umbach *et al*., 2008) (Section 1.5.6.1).

In gammaherpesviruses homologues of EBV EBNA-1 or KSHV LANA are considered to play a key role in the maintenance of latency. During latency as many as eleven EBV genes are expressed; six EBV nuclear antigens (EBNA1, EBNA2, EBNA3A, EBNA3B, EBNA3C and EBNALP), three latent membrane proteins (LMP1, 2A and 2B); transcripts from the *Bam*HIA region (BART) of the viral genome and small, non-polyadenylated, non-coding RNAs, EBER1 and EBER2 (Rickinson and Kieff, 2001, Young and Rickinson, 2004). It has been shown that there are three types of latency (I, II, III) that can occur in EBV virus on the basis of viral transcripts present (Rowe *et al*., 1992, Thorley-Lawson and Babcock, 1999). By using different transcription programs latent EBV genomes can multiply in dividing memory cells (latency type I), induce B-cell differentiation (latency type II) and activate naïve B cells (latency type III) (Odumade *et al*., 2011). Latency type I is seen in Burkitt's lymphoma and during this EBNA-1 viral transcripts, BARTs, EBER1 and EBER2 are found. Activation of a Qp promoter initiates the transcription of EBNA-1 and it is the only virus protein expressed in type I latency. Latency type II can be seen in Hodgkin's lymphoma, T cell lymphomas and nasopharyngeal carcinoma. In latency type II, LMP-1, LMP-2A and LMP-2B along with other latency I associated viral transcripts are expressed. Activation of one or more LMP

promoters leads to the expression of LMPs. LMP-1 has been shown to have a role in preventing apoptosis by inducing the expression of bcl-2 (Kaye *et al*., 1993), while LMP-2A and LMP-2B proteins inhibit the B cell activation required for lytic replication (Longnecker, 2000). In addition to the viral transcripts expressed in latency type II, latency type III cells express five more EBNA transcripts: EBNA2, EBNA3A, EBNA3B, EBNA3C and EBNALP. They perform various functions in both up and down regulation of viral gene expression. This state of EBV latency has been seen in cultured human EBV infected B cells and cells derived from B cell lymphomas. It has been reported that EBV encoded miRNAs played important role EBV latency. Three of the EBV miRNAs which flank the BHRF1 ORF are found exclusively in B cells with latency III. Remaining EBV miRNAs are located within the introns of the BART region and are consequently called the BART miRNAs and are located in two clusters. Yang *et al* reported that miR-BHRF1 and miR-BART families were expressed differentially in a tissue- and latency type-dependent manner. In NPC tissues and the EBV-positive cell line C666-1, 10% of all the detected miRNAs were expressed from the BART region, suggesting that these miRNAs have important roles in maintaining latent EBV infections and in driving NPC tumorigenesis. In addition, EBV miRNA-based clustering analysis clearly distinguished between the three distinct EBV latency types (Yang *et al*., 2013).

Latently infected B cells can occasionally be stimulated to reactivate and produce new virions, which can infect new B cells and epithelial cells (Odumade *et al*., 2011). The precise stimuli which trigger the reactivation *in vivo* is not clearly understood. The presumption is that the reactivation occurs as a result of B cells

response to foreign or unrelated infections because in B-cell lines, B-cell receptor stimulation can trigger reactivation (Amon and Farrell, 2005, Odumade *et al*., 2011).

1.4 Malignant Catarrhal Fever

1.4.1 Occurrence and significance

Malignant catarrhal fever (MCF) is a sporadic, mostly fatal disease of cattle and other cloven-hoofed species including deer, water buffalo, bison and swine (Loken *et al*., 1998, Martucciello *et al*., 2006, Reid *et al*., 1984, Schultheiss *et al*., 2000). MCF is characterised by acute lymphoproliferation and marked necrosis in susceptible species. MCF is mainly caused by one of the two gammaherpesviruses from genus *Macavirus*; ovine herpesvirus 2 (OvHV-2) and alcelaphine herpesvirus 1 (AlHV-1). OvHV-2 is naturally present in sheep and causes sheep associated MCF (SA-MCF) while AlHV-l is naturally present in wildebeest and causes wildebeest associated MCF (WA-MCF). These viruses do not produce any clinical disease in their natural hosts but cause MCF in susceptible species some of which are closely phylogenetically related to the reservoir hosts (Bridgen and Reid, 1991, Plowright *et al*., 1960). In susceptible species MCF is traditionally regarded as a disease with a short clinical course, low morbidity and high case fatality rate, though there have been some cases where recovery and chronic disease was observed (O'Toole *et al*., 1997).

MCF was first discovered in 1923 in Africa in cattle that were in close contact with wildebeest herds and in 1930 in Europe in cattle that were kept in intimate contact with apparently healthy sheep (Mushi and Rurangirwa, 1981), referring to (Mettam,

1924). WA-MCF has also been reported in Eastern and Southern Africa where wildebeest are found (Plowright, 1965a, Bedelian *et al*., 2007, Straver and van Bekkum, 1979). WA-MCF has also been identified as a problem in zoological parks and game farms where wildebeest are kept (Meteyer *et al*., 1989, Whitaker *et al*., 2007). SA-MCF was initially observed in Europe however it is found worldwide wherever sheep or cattle or other MCF susceptible species are kept together (Russell *et al*., 2009). SA-MCF has been reported in Europe (Collery and Foley, 1996, Desmecht *et al*., 1999, Frolich *et al*., 1998, Yus *et al*., 1999), America (Reid and Robinson, 1987), Africa (Rossiter, 1981), the Middle East (Abu Elzein *et al*., 2003), and Southeast Asia (Wiyono *et al*., 1994).

Several members of the order Artiodactyla are highly susceptible to MCF including species classified within the subfamily *Bovinae* e.g cattle, water buffalo and bison (Dettwiler *et al*., 2011, Li *et al*., 2006, Martucciello *et al*., 2006, Reid *et al*., 1984, Schultheiss *et al*., 2000). The members of family *Cervidae* e.g deer, reindeer and moose have also been shown to be susceptible hosts (Crawford *et al*., 2002, Denholm and Westbury, 1982, Li *et al*., 1999, Neimanis *et al*., 2009, Reid *et al*., 1979). Pigs (family *Suidae*) are also among the affected species (Albini *et al*., 2003, Alcaraz *et al*., 2009, Loken *et al*., 1998).

1.4.2 MCF viruses

The MCF virus (MCFV) group include ten members which belongs to the genus *macavirus* of the *Gammaherpesvirinae*; AlHV-1, OvHV-2, AlHV-2 caprine herpesvirus 2 (CpHV-2) (naturally infects goat), Ibex-MCFV (naturally infects Nubian ibex), hippotragine herpesvirus 1 (HipHV-1) (naturally infects roan

antelopes), Muskox-MCFV (naturally infects musk ox), Aoudad-MCFV (naturally infects aoudad) and MCFV-WTD causing the classic MCF in white-tailed deer (may infect domestic goats naturally) (O'Toole and Li, 2014, Davison *et al*., 2009, Russell *et al*., 2009, Li *et al*., 2000, Li *et al*., 2005, Li *et al*., 2014).

1.4.2.1 AlHV-1 and OvHV-2

AlHV-1 and OvHV-2 are the two best characterized causative agents of MCF (Russell *et al*., 2009).

Primary infection caused by AlHV-1 is asymptomatic in its natural host (blue wildebeests) and most wildebeest calves before three months of age are infected with the virus and excrete the virus in their nasal and lachrymal secretions. Perinatal calves are thought to be the main source of AlHV-1, however wildebeest cows may also excrete virus in late pregnancy or when in stress (Plowright, 1967, Mushi, 1980, Rweyemamu *et al*., 1974).

OvHV-2, the causative agent of SA-MCF is closely related to AlHV-1. Sera from adult sheep showed cross reactivity to AlHV-1 however sheep sera were not virus neutralizing (Rossiter, 1981). It has also been shown that sera from cattle infected with non-WA-MCF (NWA-MCF) could cross react with AlHV-1 but not neutralize it (Rossiter, 1983). These studies suggested that virus associated with sheep was antigenically related to AlHV-1 (Rossiter, 1981, Rossiter, 1983, Reid *et al*., 1989b). Attempts to culture the virus *in vitro* from tissues of SA-MCF affected animals, have not been successful. However, it is possible to derive lymphoblastoid cell lines (LCL) from the tissues of SA-MCF affected animals (Reid *et al*., 1989a, Reid *et al*.,

1983). These cell lines were found to contain viral DNA with homology to AlHV-1 (Bridgen and Reid, 1991) and this finding led to the proposal that SA-MCF was caused by a herpesvirus and named as ovine herpesvirus-2 (OvHV-2). In 1993, a polymerase chain reaction (PCR) test was developed using OvHV-2 DNA isolated from OvHV-2 infected LCL (Baxter *et al*., 1993). This test has subsequently been used for the diagnosis of SA-MCF and for the presence of OvHV-2 in natural host and in the cases of suspected SA-MCF in susceptible species (Baxter *et al*., 1993, Li *et al*., 1995, Loken *et al*., 1998, Muller-Doblies *et al*., 1998). The genomes of AlHV-1 and OvHV-2 have been sequenced and compared (Dewals *et al*., 2006, Ensser *et al*., 1997, Hart *et al*., 2007). The sequencing of the OvHV-2 genome from a large granular lymphocyte (LGL) cell line derived from a SA-MCF affected cow has shown that its genome is co-linear with the other rhadinoviruses (Hart *et al*., 2007). It is also somewhat similar to AlHV-1 genome and shows 40-90% of similarities across the genome including the majority of unique ORFs (Hart *et al*., 2007, Ensser *et al*., 1997).

1.4.3 Clinical forms of MCF

MCF-susceptible species are considered as dead-end hosts. This disease is characterized by the sudden onset of fever as well as ocular and nasal discharge, corneal opacity, generalized lymphadenopathy, lymphoid cell infiltration, degenerative lesions in the mucosa of the upper respiratory tract and the gastrointestinal tract (Russell *et al*., 2009, Li *et al*., 2014, O'Toole and Li, 2014). The natural incubation period for cattle is generally 2 to 10 weeks but can be as long as 9 months (Plowright, 1990). In an outbreak following exposure of cattle to sheep in an

enclosed space, the mean number of days between apparent exposure and death due to MCF was 71 with a range of between 46 to 139 days (Moore *et al*., 2010). The disease course is three times shorter when cattle are inoculated with infected blood from acutely infected animals (Pierson *et al*., 1979).

There can be five overlapping clinical forms of MCF; head and eye form, peracute, alimentary, neurological, and cutaneous (Russell *et al*., 2009, O'Toole and Li, 2014).

The head and eye form of the disease is the most common and characteristic. In this form symptoms are predominantly seen in head and neck regions of the animal. Discharge from eyes and nose is a classic feature of this form (Figure 1.3). Other signs include fever, inappetence, lesions from buccal cavity and muzzle, diarrhoea and depression. Due to the lesions in the buccal cavity slight to marked drooling can be observed. Initially the nasal discharge is serous but may progress to mucopurulent and purulent. Mucopurulent discharge from ocular mucosa is also common. Ocular swelling, corneal opacity, photophobia, enlargement of lymph nodes in the head and neck region, hyperventilation, and/or death are the additional presentations which can be seen in affected animals (Costa *et al*., 2009).

Peracute MCF is the most severe form of the disease. It is characterised by pyrexia, depression, diarrhoea, dysentery, occasional oral and nasal mucosa inflammation and death within 24-72 hours (Smith, 2002). Severe hemorrhagic gastroenteritis is prominent in all affected animals.

Intestinal MCF is similar to the peracute form. Pyrexia, diarrhoea, hyperaemia of oral and nasal mucosa with accompanying discharges, and lymphadenopathy is

descriptive of this form. The symptoms become more prominent with the progress in the disease which leads to death of the animal within 4-9 days.

Cutaneous MCF is rare and appears more often in wild ruminants than in cattle. Cutaneous lesions may present in the form of circular alopecia that secreted clear yellow exudates in the regions sometimes at the base of the horns, the dewclaws and the interdigital space (David *et al*., 2005).

Neurological MCF is also a rare form of the disease. Nervous signs such as hyperaesthesia, incoordination, head shaking and pressing, nystagmus and muscle tremors may be present in the absence of other clinical signs or as part of a broader more characteristic syndrome (OIE, 2013).

1.4.4 Gross pathology

Widespread post-mortem (PM) lesions can be recognized in MCF affected cases however the severity of PM findings can vary between animals. PM lesions include extensive inflammation, ulcerations and petechial haemorrhages of the systemic mucosal membranes, necrotic lesions of mucosa and enlarged lymph nodes (Metzler, 1991, Russell *et al*., 2009). Peracute MCF fatalities show lesser lesions other than hemorrhagic enterocolitis, whereas animals which died of the head and eye form can present lesions in several tissues and organs including liver, brain, joints, kidneys and urinary and respiratory tracts.

Lesions in the upper respiratory track involve hyperaemia of the nasal passage, nasal turbinates, larynx and trachea with the presence of mucopurulent exudates. Erosions

Figure 1.3: A cow exhibiting clinical signs of head and eye form malignant catarrhal fever.

(Picture courtesy of Dr Bob Dalziel).

.

and ulcerations of the pharyngeal and tracheobronchial mucosa are also found (Liggitt *et al*., 1978, O'Toole *et al*., 2007, Reid *et al*., 1984, Selman *et al*., 1974). Erosions and haemorrhages are seen throughout the gastrointestinal tract predominantly in the oesophagus, tongue and occasionally the forestomachs and intestine. In general, lymph nodes are enlarged and oedematous, although the extent of lymph node involvement varies within an animal. The liver and spleen are congested and enlarged. Ocular lesions consist of synechiae formation where the iris adheres to either the cornea (i.e. anterior synechia) or lens (i.e. posterior synechia) and fibrosis is seen in the corneal substantia propria. Ulcers causing corneal perforations result in the entrapment of the iris in the cornea (O'Toole and Li, 2014). Within the urinary tract, hemorrhagic infarcts in the kidney and characteristic echymotic haemorrhages of the epithelial lining of the bladder are often present (OIE, 2013).

1.4.5 Microscopic pathology

The microscopic findings of MCF include epithelial degeneration, vasculitis, hyperplasia and necrosis of lymphoid organs as well as mononuclear cell infiltration in the affected tissues (Simon *et al*., 2003, Liggitt *et al*., 1978, Selman *et al*., 1974). Mostly lymphocytes and lymphoblasts with fewer monocytes and macrophages are present in these infiltrates. Lymphocytic infiltration is found as major histopathological finding in the affected tissues. Another significant finding is epithelial necrosis and sloughing due to the infiltration. These lesions are usually found in the oral and nasal mucosa, epithelia of the gastrointestinal tract, biliary epithelium, conjunctiva, ducts of endocrine glands, urinary tract, respiratory tract and

brain. Vasculitis may also found in the small and medium blood vessels of these tissues (Costa *et al*., 2009, Liggitt and DeMartini, 1980b, Metzler, 1991, Russell *et al*., 2009, Sanford and Little, 1977). Lymph node hyperplasia is characterised by an expansion of lymphoblastoid cells in the paracortical region, whereas degenerative lesions in the severely affected lymph nodes are generally associated with the presence of foci. Interstitial accumulation of lymphoid cells in non-lymphoid organs can be found, in particular the renal cortex and periportal areas of the liver. In the kidney development of multiple raised white foci of lymphoid cells may be very extensive (OIE, 2013).

1.4.6 Transmission of AlHV-1 and OvHV-2

The transmission of both AlHV-1 and OvHV-2 from wildebeest calves and lambs, respectively, appears to occur by contact or aerosol transmission routes, under 1-year of age (Mushi *et al*., 1981, Russell *et al*., 2009, Li *et al*., 1998). Shedding of the virus from the natural host is associated with lambing or calving (wildebeest) (Li *et al*., 2004). Under natural conditions, most lambs acquire OvHV-2 by about three months of age and produce cell-free infectious virus from oral and nasal secretions, until 6 to 9 months of age (Collery and Foley, 1996). However, no conclusive evidence has been found that viral shedding is increased in dams at parturition (Li *et al*., 2004).

There have been reports of transmission over distances of five kilometres between lambs and bison without any physical contact (Li *et al*., 2008). Infected lambs can transmit OvHV-2, through nasal secretions to susceptible species without direct contact (Moore *et al*., 2010). Similarly, the oral and nasal discharges by wildebeest calves living in a closed area may initiate the transmission (Plowright, 1965b),

however, how the infectious virus travel over long physical distances in the open without any direct contact is yet to be discovered. The viruses can also be transmitted between individuals of the natural hosts and from natural to susceptible species, by the horizontal route through liquid discharges from the noses and the eyes of the infected lambs/wildebeest calves. It has also been shown that wild boars can transmit OvHV-2 through semen to sows which develop MCF at a later stage (Costa *et al*., 2010). Susceptible species are dead end hosts and cannot transmit OvHV-2 or AlHV-1 (Kim *et al*., 2003, Muller-Doblies *et al*., 2001). The possible reason for this might be that the virus replicates in a cell-associated manner in susceptible species and cell-free virus, required for transmission, is not produced (Russell *et al*., 2009).

Experimental induction of WA-MCF in cattle can be achieved using wildebeest nasal secretions containing AlHV-1 or via the transfer of intact blood cells or crude cell suspensions derived from the affected tissues of infected animals (Plowright, 1964, Plowright, 1965b, Plowright, 1965a). It has recently been shown that SA-MCF can be transmitted to bovine calves via nebulizations with OvHV-2 positive nasal secretions (Taus *et al*., 2005, Taus *et al*., 2006). Transmission of SA-MCF from affected to healthy cattle can also be achieved via transfer of large volumes of blood or lymph node cell suspensions (Liggitt and DeMartini, 1980b, Liggitt and DeMartini, 1980a, Reid *et al*., 1986), however this is not a natural route.

1.4.7 Immunization

Due to short clinical course of the disease, MCF affected animals can die within a few days after the presentation of initial symptoms and the treatment is not viable. Serological testing has been used as an important diagnostic tool for both natural and

susceptible species. AlHV-1 and OvHV-2 are serologically related (Li *et al*., 1994, Loken *et al*., 2009, O'Toole *et al*., 1997) and antibodies from carrier sheep and MCF affected cattle are able to recognise AlHV-1 antigen (Rossiter, 1981, Rossiter, 1983). Due to the lack of an OvHV-2 permissive cell culture system, attenuated AlHV-1 vaccines were used to try and provide protection against OvHV-2, however all the efforts proved unsuccessful (Edington and Plowright, 1980, Plowright *et al*., 1975).

Unlike OvHV-2, cell-free attenuated and virulent AlHV-1 can be obtained from tissue culture. Recent immunization studies using AlHV-1 demonstrated that immunity to MCF can be induced by the use of an attenuated AlHV-1, adjuvant containing vaccine, administered by intramuscular injection (Haig *et al*., 2008, Russell *et al*., 2012). The vaccine protected the cattle from fatal intranasal challenge with pathogenic AlHV-1 at both three and six months post-vaccination and high titres of virus neutralizing antibodies could be detected in the nasal secretions of the protected animals (Haig *et al*., 2008, Russell *et al*., 2012).

Efforts are underway to develop systems which could help in the production of OvHV-2 vaccines. In a study in sheep, Li *et al* described the development of an *in vivo* system that mimics a neutralization test to measure antibody's ability to block OvHV-2 at the entry site. The test was based on the mixing of virus and anti-OvHV-2 serum before challenge by intranasal nebulization. The sheep who had received the OvHV-2 positive showed approximately 1000 fold reduction in infectivity, based on delayed seroconversion and delayed detection of viral DNA, compared to the sheep that had received OvHV-2 negative serum (Li *et al*., 2013a).

The other reliable control measure for MCF is to keep susceptible species separated from potential natural hosts (Traul *et al*., 2005). A distance of one kilometre is regarded as the minimum distance of separation to limit the risk of virus transmission (Barnard, 1990).

1.4.8 Large granular lymphocyte cell lines

Lymphoblastoid cell lines can be derived from various tissues of MCFV infected animals (Cook and Splitter, 1988, Russell *et al*., 2009). These cells contain electron dense granules within their cytoplasm and have the morphology of large granular lymphocytes (LGL). The LGLs exhibited indiscriminately cytotoxicity characteristic of natural killer cells and can kill various target tissues in a major histocompatibility complex (MHC) unrestricted manner (Herberman and Ortaldo, 1981). These cell lines can be maintained *in vitro*, by the addition of exogenous interleukin-2 (IL-2).

LGL cell lines established from the lymph nodes of OvHV-2 infected cattle have been shown to contain OvHV-2 DNA; e.g BJ1004, BJ1044, BJ1104, BJ971 and BJ1035 (Schock *et al*., 1998). These cell lines were unable to transfer disease to rabbits, deer and other cattle. Uninfected T lymphocytes proliferated on the exposure of concanavalin A (ConA) whereas LGL cell lines were found to be unresponsive to ConA stimulated proliferation. Studies on the surface phenotype of the five LGL cell lines showed that three (BJ1004, BJ1035 and BJ1104) were $CD4^+/CD8^-$ T cells, one (BJ971) was $CD4^-/CD8^+$ T cells and one (BJ1044) was a mixture of $CD4^+/CD8^-$ and $CD4^-/CD8^+$ T cells. In addition these cell lines constitutively express; tumour necrosis factor-α (TNF-α), interferon- γ (IFN-γ) and IL-10 (Schock *et al*., 1998).

LGL cell lines from OvHV-2 infected cattle had viral genomes that were mainly circular in form, which is suggestive of latency (Rosbottom *et al*., 2002). In another study Thonur *et al*., 2006 showed that these cell lines contained a mixture of circular and linear genome configurations, which indicated that LGLs may be comprised of a mixture of latently and productively infected cells (Thonur *et al*., 2006).

1.4.9 Proposed model for MCF pathogenesis

OvHV-2 DNA can be detected in most organs as well as in buffy coat cells of cattle with MCF. However, demonstration of viral antigen in MCF affected tissues has largely been unsuccessful and it has been hypothesized that direct viral cytotoxicity is not involved in MCF pathogenesis (Ackermann, 2006). The vasculitis and necrosis in a variety of MCF affected tissues is mainly due to the infiltration and accumulation of large number of LGLs (Liggitt and DeMartini, 1980a, Muller-Doblies *et al*., 2001, Taus *et al*., 2006). LGLs derived from tissues of MCF infected animals showed a variable expression of CD2, CD4 and CD8 (Meier-Trummer *et al*., 2010, Schock *et al*., 1998, Swa *et al*., 2001). Proliferating LGLs have a natural killer cell phenotype, and these cells are activated by cytokines released from other lymphocytes and kill other cells in an un-restricted MHC class I, manner (Cook and Splitter, 1988).

Significant, but low, levels of IL-2 have also been detected in lymph nodes of MCF affected animals (Meier-Trummer *et al*., 2009). IL-2 has been shown to play a key role in the propagation of T-cells *in vitro* (Smith and Johnson, 1988). It has been reported in various studies that a lack of IL-2 leads to T lymphocytes establishing an abnormal growth rate (Sharfe *et al*., 1997) which might be mediated through

interactions of IL-2 with regulatory T-cells (Almeida *et al*., 2002, Kramer *et al*., 1995). The critical role of IL-2 in the development and expansion of regulatory T lymphocytes in lymph nodes helps in supressing the autoreactivity and replication of T lymphocytes (Nelson, 2004). It is possible that accumulation and autoreactivity of the T lymphocytes in MCF-affected animals is due to the low abundance of IL-2 in the lymph nodes (Meier-Trummer *et al*., 2009).

A mixture of $CD8^+$ cytotoxic γ/δ T cells, $CD4^+$/perforin- αβ T regulatory or helper cells, B cells and macrophages has been found in the inflammatory infiltrates from MCF infected bison. It has been hypothesized that γ/δ T cells latently infected with OvHV-2 might be the cause of necrotic lesions in the vasculature (Nelson *et al*., 2010, O'Toole and Li, 2014). It has also been suggested that only a small number of OvHV-2 infected lymphocytes are infiltrating in MCF lesions and most of the cells are uninfected, multiplying T lymphocytes. This may also suggest that MCF has an autoimmune like pathology (Reid *et al*., 1984, Meier-Trummer *et al*., 2010, Russell *et al*., 2009, Schock and Reid, 1996).

1.5 MicroRNAs

1.5.1 History

MicroRNAs (miRNAs) are small (21-24 nucleotide (nt) in length) non-coding RNAs, which are able to regulate gene expression at the post transcriptional level (Bartel, 2004). The first miRNA; lin-4 (22 nt long) was identified in a nematode; *Caenorhabditisis elegans* (*C. elegans*) in 1993 by the Ambros and Ruvkun laboratories simultaneously (Lee *et al*., 1993, Wightman *et al*., 1993). It was found to negatively regulate the expression of the lin-14 protein product by targeting complementary sites in the 3' untranslated region (3'UTR) of the lin-14 mRNA via an antisense RNA-RNA interaction (Wightman *et al*., 1991, Wightman *et al*., 1993). Mutation in the lin-4 ORF did not affect its function, suggesting that lin-4 did not encode for a protein (Lee *et al*., 1993). This discovery remained unrealized for almost seven years when Reinhart *et al,* identified a second miRNA; let-7 in *C. elegans* (Reinhart *et al*., 2000). let-7 was found to interact with the 3'UTRs of lin-41 and lin57 mRNAs and inhibit their translation (Abrahante *et al*., 2003, Vella *et al*., 2004). These discoveries unveiled a new family of RNAs which later became known as microRNAs (miRNAs) (Lee and Ambros, 2001). It has since been shown miRNAs are expressed in large numbers and present in a diverse range of different species (including algae, arthropods, nematodes, protozoa, vertebrates, plants, and viruses) (Bartel, 2004, Lee *et al*., 2004b, Grundhoff and Sullivan, 2011). The latest miRBase release (v20, June 2013), contains 24521 miRNA loci, processed to produce 30424 mature miRNAs from 206 species (Kozomara and Griffiths-Jones, 2014) (http://www.mirbase.org/). The regulatory roles of miRNAs have been

identified in various biological processes including cell fate determination, proliferation, cell death, immune response and tumorigenesis (Bhatt *et al*., 2011, Dong *et al*., 2013, Tuddenham and Pfeffer, 2013).

1.5.2 miRNA biogenesis

The biogenesis of miRNAs is a multistep process. It involves sequential processing and editing of transcribed miRNA genes (Figure 1.4). Then majority of miRNAs are derived from large RNA polymerase (pol) II transcripts, while a small proportion of miRNAs is derived from pol III transcripts (Lee *et al*., 2002, Monteys *et al*., 2010). These primary transcripts (pri-miRNAs) are 5'end capped and 3' end polyadenylated and range from hundreds to thousands of nucleotides in length (Cai *et al*., 2004, Aparicio *et al*., 2006). Pri-miRNAs are transcribed from introns, exons, intergenic regions or in an antisense direction of annotated genes (Cai *et al*., 2004, Kim, 2005, Lee *et al*., 2004a). A single pri-miRNA transcript can either generate monocistronic miRNA or polycistronic clusters of miRNAs, under the influence of a single promoter or different promoters for individual miRNAs (Cai *et al*., 2004, Lee *et al*., 2002, Song and Wang, 2008). Approximately 40% of human miRNAs are cotranscribed as clusters encoding more than one miRNA sequences in a single pri-miRNA transcript (Altuvia *et al*., 2005, Hertel *et al*., 2006). A pri-miRNA contains an imperfect double-stranded (ds) stem-loop structure flanked by single-stranded (ss) RNA. One arm of the stem-loop structure includes the mature miRNA (Zeng *et al*., 2005).

The stem-loop structure and the flanking region of the pri-miRNAs direct the pri-miRNAs to a multiprotein complex called the microprocessor complex (Beezhold *et*

al., 2010, Davis-Dusenbery and Hata, 2010, Landthaler *et al*., 2004, Lee *et al*., 2003). The microprocessor complex contains an RNase III enzyme called Drosha and its cofactor protein DiGeorge syndrome critical region gene 8 (DGCR8). DGCR8 interacts with the stem-loop structure and recruits Drosha, which then cleaves the pri-miRNAs precisely at the stem-loop structure and liberates a 60-110 nt long RNA product called the precursor miRNA (pre-miRNA) with a 5' phosphate and a 2 nt overhang at the 3' end (Kim *et al*., 2009, Zeng *et al*., 2005, Zeng and Cullen, 2005) (Figure 1.4). The 3' overhang and adjacent stem of pre-miRNA is recognized by a heterodimer made up of Exportin 5 and Ran-GTP cofactor (Exportin/Ran complex). The Pre-miRNA interacts with the Exportin/Ran complex and is exported from the nucleus into the cytoplasm (Bohnsack *et al*., 2004, Leisegang *et al*., 2012).

In the cytoplasm the hydrolysis of Ran-GTP to RanGDP causes the release of the pre-miRNA from the Exportin/Ran complex (Wang *et al*., 2011). The pre-miRNA is then taken up by the RISC loading complex (RLC) made up of an RNase III enzyme called Dicer, its cofactors; TAR RNA‑binding protein (TRBP) and protein activator of PKR (PACT) and the argonaute-2 (Ago-2) protein (Gregory *et al*., 2005, Haase *et al*., 2005, Lee *et al*., 2006, MacRae *et al*., 2008). TRBP and PACT are not absolutely required for pre-miRNA processing but they seem to help in stabilizing Dicer, recruiting Ago-2 and in RLC formation (Chendrimada *et al*., 2005, Kok *et al*., 2007, Lee *et al*., 2006). Once in the RLC, the exported pre-miRNA is recognized by the PAZ (piwi-argonaute-zwille) and two RNase III domains (RNase IIIa and RNase IIIb) of Dicer (Lingel *et al*., 2003, MacRae *et al*., 2007, MacRae and Doudna, 2007,

Yan *et al*., 2003). Once bound, Dicer cleaves the pre-miRNA at the base of the stem-loop, leaving an ~22 nt miRNA duplex with a 5' phosphate and a 3' OH with 2 nt overhang (Zhang *et al*., 2004).

Once pre-miRNA has been cleaved by Dicer, the resultant miRNA duplex directly interacts with an Ago protein (also called as elF2C2) to generate the effector complex; RNA induced silencing complex (RISC) (Gregory *et al*., 2005, Hutvagner and Zamore, 2002, Mourelatos *et al*., 2002). The Ago family proteins are the key effector molecules of RISC (Maniataki *et al*., 2005) and are composed of PAZ, MID and PIWI domains. The PAZ domain recognizes and interacts with the 2 nt overhang at 3' end of the miRNA, whereas the MID domain anchors the 5' end of the miRNA (Lingel *et al*., 2004, Jinek and Doudna, 2009, Ma *et al*., 2004). The PIWI domain structure is similar to RNase H and is thought to play a role in cleaving of the target mRNA bound to the miRNA (also called slicer activity) (Kim *et al*., 2009, Ma *et al*., 2005, Parker *et al*., 2005). In mammals four Ago proteins (Ago1-4) are associated with the miRNA but among those only Ago2 has been found to have an enzymatically competent PIWI domain with slicer activity to cleave the target mRNA strand that are perfectly complementary to the mature miRNA (Liu *et al*., 2004, Meister *et al*., 2004).

After loading onto Ago proteins the miRNA duplex is unwound by helicases. One strand of the duplex remains in Ago and acts as a mature miRNA (the guide strand or miRNA), whereas the other strand (the passenger stand or miRNA*) is released for degradation or to be incorporate into another RISC as another mature miRNA (Ghildiyal *et al*., 2010, Hutvagner and Zamore, 2002, Kim *et al*., 2009, Okamura *et*

al., 2008). Relative thermodynamic stability of the two strands in the duplex, determines which strand is to be selected as the guide strand (Khvorova *et al*., 2003). The strand with the less stable base pairing at the 5' end is incorporated into RISC and becomes the mature miRNA. If both strands of the duplex are used as mature miRNAs with similar frequency then 5p or 3p is added at the end of their names to denote which arm of the duplex, the mature sequence comes from (Griffiths-Jones *et al*., 2006). Once the mature miRNA has become associated into RISC, the miRNA is used to guide and bind the complex to their complementary target sites located in the mRNA transcripts.

1.5.3 Mode of action of miRNAs

1.5.3.1 miRNA target recognition

miRNAs generally regulate gene expression by binding to target mRNAs, at a post transcriptional level. Plants show perfect or near perfect complimentarity between miRNA and their target mRNA and induce translational repression through degradation of their target transcripts (Brodersen *et al*., 2008) whereas in animals, miRNAs generally use a 6-8 nt sequence (seed region) out of ~21 nt of miRNA sequence to recognize the target mRNA (Lewis *et al*., 2003). The miRNAs seed region is located at nucleotide position 2-7 or 2-8 at the 5' end of the mature miRNA (Gottwein and Cullen, 2007) and it is this region which is most conserved across metazoan miRNAs (Lewis *et al*., 2005, Lim *et al*., 2005). The binding of most miRNAs includes the 5' seed region however the presence of non-seed interactions have also been reported e.g. at the 3' end of miRNAs and a site in the centre of miRNAs (Helwak *et al*., 2013, Lee *et al*., 2009, Shin *et al*., 2010).

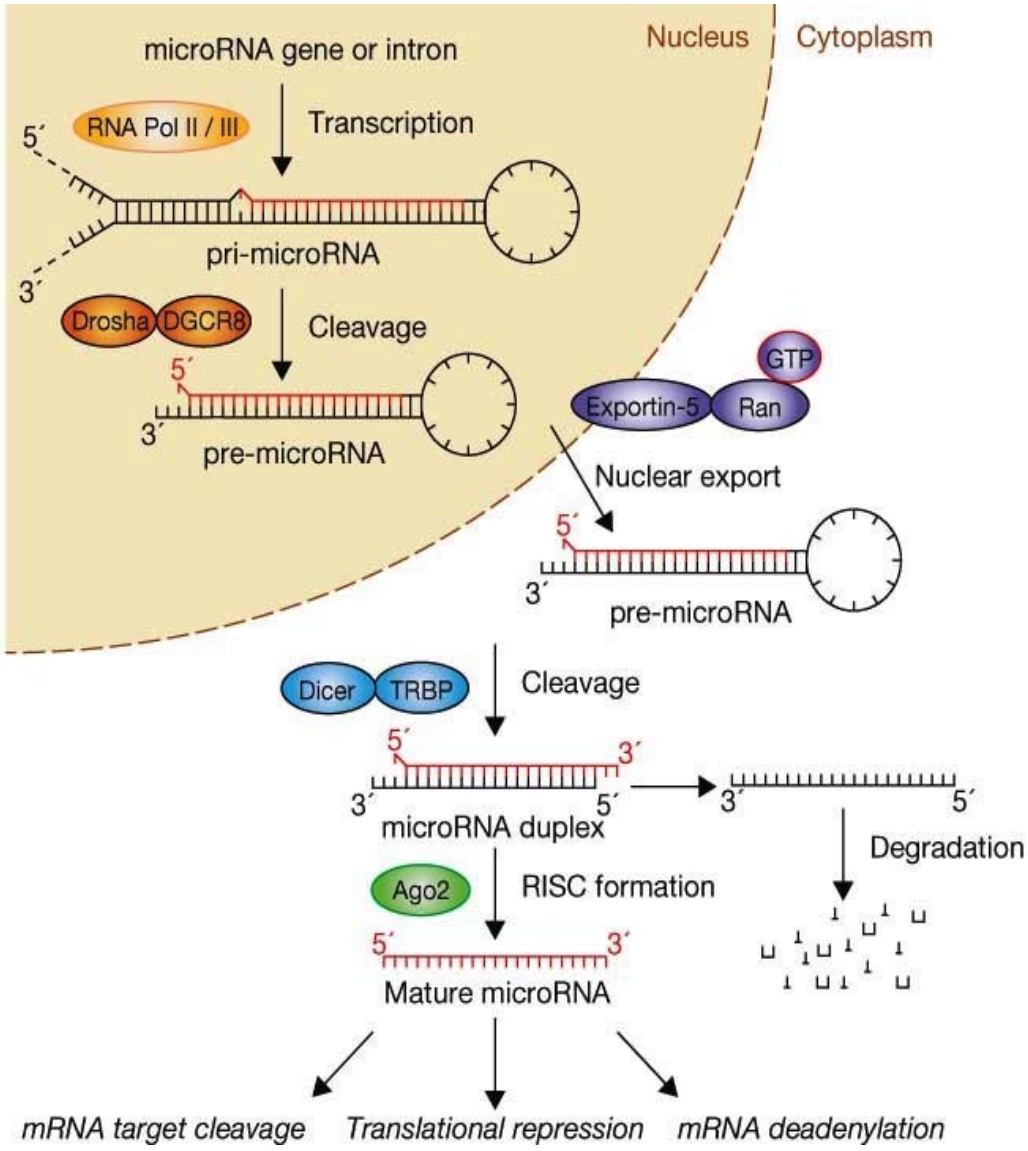

Figure 1.4: Schematic diagram of miRNA biogenesis.

(Adapted from (Winter *et al*., 2009)).

Helwak *et al* mapped human miRNAs and mRNAs interactions using a biochemical approach combined with bioinformatic analysis; "Cross linking, Ligation And Sequencing of Hybrids (CLASH) and identified that approximately 60% of the interactions between the seed region and target sites in mRNAs were non-canonical containing bulged and mismatched nucleotides. Eighteen percent of the total miRNA-mRNA interactions, in this study, involved the 3′ end of miRNAs, with little evidence for 5′ end contact (Helwak *et al*., 2013). In addition to seed region match, base pairing with target mRNA at the 3'end of miRNA is also possible and is called supplementary pairing (Grimson *et al*., 2007). The presence of mismatches or G:U pairing (refers to the pairing of a G with a U instead of a C) in the seed region is also acceptable, however target repression can be affected in this type of pairing (Doench and Sharp, 2004, Brennecke *et al*., 2005, Didiano and Hobert, 2006).

A miRNA can target several mRNAs by hybridizing to the target site/s (complementary to the miRNA seed region) located in the 5'UTRs, coding regions and/or 3'UTRs leading to translational inhibition or mRNA degradation (Brennecke *et al*., 2005, Grey *et al*., 2010, Lee *et al*., 2009, Lytle *et al*., 2007). miRNA-mediated mRNA cleavage, mediated most likely by Ago2 RNase H activity, is based on perfect complimentarity between the miRNA and its target mRNA (Bushati and Cohen, 2007, Davis *et al*., 2005, Doench *et al*., 2003, Hutvagner and Zamore, 2002). However an imperfect complementarity between miRNA and its target mRNA might lead to the initiation of the other mechanisms of miRNA mediated gene silencing; translational repression and mRNA degradation.

1.5.3.2 Translational repression

The process of mRNA translation initiates with the recognition of the 5' cap by eukaryotic translation initiation factor (eIF) 4E, along with other eIFs (eIF4G, eIF4A and eIF3). This interaction facilitates the recruitment of ribosomes to the 5′ end of mRNA and thus initiates translation.

It has been suggested in various studies that miRNA mediated translational repression can occur at the translational initiation stage or at the translational post-initiation stage (Chekulaeva and Filipowicz, 2009, Filipowicz *et al*., 2008, Huntzinger and Izaurralde, 2011, Hussain, 2012).

mRNAs whose translation is not dependent on the presence of 5' cap i.e mRNAs containing an internal ribosome entry sites (IRES) and mRNA which has a non-functional 5' cap, have been found to show resistance to miRNA-mediated repression (Humphreys *et al*., 2005, Mathonnet *et al*., 2007, Meijer *et al*., 2013, Pillai *et al*., 2005, Wakiyama *et al*., 2007). These studies suggest that miRNA-mediated silencing interferes with eIF4E function or the cap recognition process during the initiation of translation. Moreover, evidence also suggests that repression of cap-dependent translation can be mediated by inhibiting the formation of the mature ribosomal complex i.e. by inhibiting the recruitment of the 40S subunit and 80S initiation complex formation (Thermann and Hentze, 2007) or by inhibiting the joining of the 60S ribosomal subunit with the 40S subunit (Chendrimada *et al*., 2007, Hussain, 2012). In another study, Mathonnet *et al,* discussed the possibility that Ago2, as a part of the RISC, interacts with the 5'cap of the mRNA and interferes

with the binding of eIF4E, which leads to the inhibition of translation initiation (Mathonnet *et al*., 2007).

miRNA-mediated inhibition of translation at the post-initiation stage has also been proposed as another mechanism to target mRNAs. It was found that the lin-4 miRNA did not change the abundance of the target mRNA lin-14 in polysomal fractions, suggesting that translation was initiated normally and that miRNAs might act after translational initiation (Olsen and Ambros, 1999). Various other studies also supported this mechanism of inhibition and provided evidence that repressed mRNAs were associated with actively translating polysomes (Maroney *et al*., 2006, Nottrott *et al*., 2006, Petersen *et al*., 2006). miRNAs can also interfere with the elongation phase of translation either by causing degradation of the nascent polypeptide chain (Nottrott *et al*., 2006) or by initiating premature ribosome drop-off from the target mRNA (Petersen *et al*., 2006).

1.5.3.3 miRNA mediated degradation of target mRNA

Although, previous studies suggested that miRNA mediated silencing results in the repression of translation of the target mRNA without changing the mRNA levels (Olsen and Ambros, 1999), recent studies have indicated that miRNA-mediated translational repression is associated with the destabilization and degradation of the target mRNA (Behm-Ansmant *et al*., 2006b, Eulalio *et al*., 2009).

Degradation of target mRNA by an miRNA, requires deadenylation and/or 5'decapping of the target mRNA (Behm-Ansmant *et al*., 2006b, Humphreys *et al*., 2005). The degradation of the target mRNA is thought to occur in the cytoplasmic P-

bodies (Eulalio *et al*., 2007, Liu *et al*., 2005, Parker and Sheth, 2007). The Ago proteins, the poly(A) binding proteins (PABP) and the P-body protein GW182, are all involved in the deadenylation of the target mRNA (Braun *et al*., 2011, Fabian *et al*., 2009, Fabian *et al*., 2011, Zekri *et al*., 2009). GW182 protein recruits the deadenylase complexes; CCR4-CAF1-NOT1 and PAN2-PAN3 through direct interaction with NOT1 and direct or indirect interaction with PAN3 and PABP respectively. These interactions are considered important for the deadenylation and degradation of the target mRNA in a 3'-to-5' direction. However, the exact mechanisms involved in the recruitment of the deadenylase complex to the RISC and subsequent deadenylation of the poly(A) tail are still not well understood (Braun *et al*., 2011, Fabian *et al*., 2011, Hussain, 2012, Yamashita *et al*., 2005, Zekri *et al*., 2009).

The next step in miRNA-mediated degradation involves the 5' decapping of the target mRNA by the decapping-complex proteins DCP1 and DCP2 (Rehwinkel *et al*., 2005). Knockdown of the decapping-complex proteins has been shown to lead to an accumulation of deadenylated mRNAs (Behm-Ansmant *et al*., 2006a, Eulalio *et al*., 2007). A decapped mRNA is then degraded by the exonuclease activity of the major cytoplasmic 5'– 3' exonuclease XRN1 (Cougot *et al*., 2004, Rehwinkel *et al*., 2005).

1.5.3.4 miRNA mediated translational activation

Several miRNAs have been reported to induce translational activation instead of repression under certain conditions or in specific cells (Lin *et al*., 2011a, Vasudevan *et al*., 2007, Vasudevan, 2012). Translational up-regulation by miRNAs could be achieved in two ways; activation by direct action of the miRNA or by the relief of

repression where the action of a repressive miRNA is abrogated (Vasudevan, 2012). The translation of the CAT1 mRNA is repressed by a liver specific miRNA miR-122, in the P-bodies in human hepatoma cells. However following amino acid starvation the CAT1 mRNA is released from the P-bodies and interacts with the polysomes. This process depends on the binding of HuR, an AU rich-element binding protein, to the 3'UTR of the CAT1 mRNA and it is this binding that inhibits the repression by miR-122 (Bhattacharyya *et al*., 2006). Another miRNA miR-369-3 has been shown to target the 3'UTR of TNFα mRNA and repress its translation in proliferating cells, however in G1/G0 arrested cells translation of TNFα mRNA has been found to be up-regulated. It has been reported that under serum starvation conditions miR-369-3 in RISC, bound to TNFα mRNA could recruit the fragile X–related protein 1 (FXR1) and stimulate mRNA translation (Vasudevan *et al*., 2007, Vasudevan and Steitz, 2007). Another miRNA, miR-10a which can interact with the 5′-terminal oligopyrimidine tract (5′-TOP) motif in the 5'UTR of many ribosomal proteins' mRNAs, has also been shown to up-regulate translation of these mRNAs under stress conditions or nutrient shortage (Orom *et al*., 2008).

1.5.4 Biological function of miRNAs

miRNAs play important roles in the regulation of most biological processes. The biological processes involved include cellular differentiation (Chen *et al*., 2004), proliferation (Pickering *et al*., 2009), apoptosis (Cimmino *et al*., 2005), regulation of immune response (O'Connell *et al*., 2010, Rodriguez *et al*., 2007, Taganov *et al*., 2006), embryonic development (Johnston and Hobert, 2003), cell migration (Chen *et al*., 2011), the cell cycle (Petrocca *et al*., 2008), angiogenesis (Fish *et al*., 2008),

tumorigenesis (Xia *et al*., 2008a) and virus replication (Zheng *et al*., 2011). A detailed discussion of regulatory roles and functions of miRNAs is not possible in this thesis, however, a few examples of the miRNAs involved in the regulation of immune system, cellular differentiation, cell proliferation and cell development are described as follows.

Disruption in the expression of miRNAs by interfering with the miRNA processing or miRNA processing components, has been shown to cause differentiation and developmental defects in variety of cell types (Chen *et al*., 2004, Esau *et al*., 2004, Makeyev *et al*., 2007, Luo *et al*., 2013, Yi *et al*., 2008). Embryonic stem (ES) cells from dicer deficient mouse have been found to be defective in differentiation as well as in the generation of miRNAs (Kanellopoulou *et al*., 2005). Similarly, Ago2 deficient mice are embryonic lethal and defective in siRNA responses (Liu *et al*., 2004). miRNAs miR-124 and miR-9 are considered important in the regulation of mammalian neural development. The overexpression and knock down of miR-124 triggers and prevents neural development respectively (Gao, 2010).

miRNAs also have been shown to have roles in B and T cell lineage differentiation. miR-181a was the first miRNA reported to have a role in B cell differentiation in bone marrow. Overexpression of miR-181a facilitated B cell development which resulted in a two to threefold elevation of the B cell number and a twofold reduction in the circulating T cell number (Chen *et al*., 2004, de Yebenes *et al*., 2013). Recent studies have suggested that miR-181a can control the strength of T cell receptor (TCR) signaling, during T cell development in the thymus. It has also been suggested in that study that increasing miR-181a expression in mature T cells increases their

sensitivity to peptide antigen whereas inhibiting miR-181a expression in immature T cells reduces sensitivity (Li *et al*., 2007). It has been reported that two miRNAs miR-17-92 and miR-34a also play major roles in B cell differentiation and deletion of these miRNAs blocks the transition of pro-B cells to pre-B cells, a vital step in the development of the B cells (Rao *et al*., 2010, Ventura *et al*., 2008). In Dicer deficient animals, the expression of two of the predicted targets of miR-17-92; the pro-apoptotic gene Bim and tumor suppressor PTEN are strongly up-regulated (Koralov *et al*., 2008). miR-34a is up-regulated by p53 and the ectopic expression of miR-34 induces cell cycle arrest. Furthermore, it has also been reported that the expression of miR-34a is altered in various cancers (Hermeking, 2010, Raver-Shapira *et al*., 2007). These pieces of evidence suggest a role for this miRNA in cell cycle regulation.

Various miRNAs have been found to be important in the regulation of the immune system. miR-146a is expressed in various immune cell types including dendritic cells (DC), monocytes and macrophages and its expression has been shown to be deregulated in various cancers (Montagner *et al*., 2013, de Yebenes *et al*., 2013). miR-146a and –b were found to be induced after toll-like receptor (TLR) signaling. miR-146a has been shown to be a negative regulator of inflammation. Its expression is increased by to the response of lipopolysaccahrides (LPS) in monocytes (Taganov *et al*., 2006). It targets and suppresses the expression of two proteins; TNF receptor-associated factor 6 (TRAF6) and IL-1 receptor-associated kinase 1 (IRAK1) that are important in NF-kB activation by mediating TLR and interleukin-1β (IL1-β) signaling (Taganov *et al*., 2006). It has been shown that a chronic inflammatory

response developed in miR-146a deficient mice, which lead to B cell malignancies (Zhao *et al*., 2011a).

miR-155 is the most studied miRNA in mature B cells. Activation of B and T lymphocytes leads to the induction of miR-155 which suggests that it might play a role in regulation of immune system (Babar *et al*., 2012, Haasch *et al*., 2002, Tili *et al*., 2007). Increased expression of miR-155 has been observed during the DC activating and maturation (Turner *et al*., 2011). miR-155 deficient mice failed to activate T cells efficiently and showed defective antigen presentation function in these cells which contributed in the overall reduced immune response (Rodriguez *et al*., 2007). miR-155 was however also the first miRNA described as oncogenic (Tam and Dahlberg, 2006). The primary transcript of miR-155 is encoded in a non-protein coding region, the B cell integration cluster (BIC). Over expression of BIC and miR-155 has been observed in lymphomas of activated B-cell origin including Hodgkin's lymphoma (Kluiver *et al*., 2005, van den Berg *et al*., 2003). Transgenic mice over expressing miR-155 develop pre-B cell proliferation and lymphoblastic leukemia/high grade lymphomas (Costinean *et al*., 2006). The functional orthologues of miR-155 (MDV-miR-M4 and KSHV-miR-K12-11) have been found in herpesviruses (will be discussed in Section 1.5.6.1).

miRNAs are also involved in the regulation of the host response upon different infections. miR-122 has been shown to up-regulate the translation of hepatitis C virus (HCV). miR-122 binds to two target sites located in the 5'UTR of HCV RNA. This interaction stops the activity of the 5'exonuclease Xrn1, preventing the decay of HCV RNA and hence stimulating translation (Li *et al*., 2013c). It has also been

reported that both of the target sites, within the HCV genome, involve extensive base pairing outside of the miR-122 seed region and form a stable tertiary complex (Mortimer and Doudna, 2013). In contrast, another miRNA miR-101 has been shown to suppress HSV-1 replication by targeting the 3'UTR of a mitochondrial ATP synthase subunit beta (ATP5B) suggesting that ATP5B might function as a pro-viral factor (Zheng *et al*., 2011).

1.5.5 Approaches for miRNAs target identification

Since the discovery of miRNAs, an extensive amount of work has been done on miRNA target identification and regulation of those target mRNAs at the translational stage. However, to identify and validate miRNA targets to allow understanding of the functions of miRNAs, proved to be the most challenging aspect of miRNAs studies. Several approaches have been successfully applied for miRNA target identification, however, a combination of computational and experimental approaches has been found to be the most useful.

1.5.5.1 Bioinformatic approaches

A number of computational programs have been developed to identify/predict putative miRNA targets. Those programs include miRanda (John *et al*., 2004), Pictar (Lall *et al*., 2006), TargetScan (Ruby *et al*., 2007), PITA (Kertesz *et al*., 2007), DIANA-microT (Kiriakidou *et al*., 2004), rna22 (Miranda *et al*., 2006) and RNAhybrid (Rehmsmeier *et al*., 2004). These algorithms all work on the basis of basic miRNA-mRNA interaction rules i.e sequence complementarity between the seed region at the 5'end of the miRNA and the target site in the mRNA,

thermodynamic stability of the duplex (miRNA-mRNA) and conservation of the target site between orthologous genes (Yu *et al*;., 2009). All of these algorithms set different parameters such as scoring and threshold, to predict or identify the targets and makes it difficult to get common sets of target genes by these methods. Most of these programs predict target sites within the 3'UTR of mRNA, however many studies have shown the presence of putative miRNA target sites within the 5'UTR and CDS of the mRNAs (Liu *et al*., 2013, Thomson *et al*., 2011, Zhou *et al*., 2009). As discussed above, these algorithms use sequence complementarity to predict the targets, due to which a significant proportion of false positive targets are generated (Didiano and Hobert, 2006). To overcome this problem, targets predicted by these algorithms are generally validated by experimental approaches.

1.5.5.2 Experimental approaches

Currently three main experimental approaches have been developed for identification of the miRNA targets: whole transcriptome based analysis, biochemical approaches such as crosslinking and immunoprecipitation technique (CLIP) of isolated RNAs and proteomic analysis.

Transcriptome analysis

Transcriptome analysis is based on the measurement of gene expression in cells in the presence or absence of specific miRNA.

Microarray is used to analyse the effect of miRNAs on the transcripts and also to compare the global gene expression profile of the test sample vs a control sample (Lim *et al*., 2005). Lim *et al* used a microarray approach to examine changes in

transcript levels upon over expression of miR-124 and miR-1 in Hela cells. Approximately 100 genes were found to be significantly down-regulated in each case and all genes identified also had target sites complementary to the seed region of each miRNA used (Lim *et al*., 2005).

Microarrays for the identification of miRNAs targets have limitations; Firstly, it is possible that some of the observed changes in gene expression are not produced by direct targeting of miRNAs. Secondly, this method cannot detect miRNAs that cause minor or no change in the mRNA levels e.g miRNAs that cause translation repressions not mRNA degradation. Deep sequencing techniques such as RNA-seq can be used as an alternate to microarray. RNA-seq does not require complementary probes and is capable of measuring the expressed transcripts accurately, hence provides more in depth analysis of the data. It also allows the analysis in species for which a full transcript map is not available.

The targets identified using these methods and bioinformatics approaches (Section 1.5.6.1) can be validated using luciferase based reporter assay. The dual luciferase assay has and continues to be widely used in miRNAs studies. A description of the dual luciferase assay is presented in chapter 3 (Section 3.2).

Biochemical approaches

These approaches are based on the identification of the direct physical interactions between miRNA-mRNA target pairs and the Ago2 protein in the RISC. Purification of mRNAs bound to miRNAs can be achieved through immunoprecipitation (IP) of Ago2 in the RISC also called a Co-IP or RISC-IP (Beitzinger *et al*., 2007, Chi *et al*.,

2009, Grey *et al*., 2010). The immunoprecipitated, or "pulled down" mRNAs can then be identified through expression profiling approaches such as microarray analysis or deep sequencing. However this method has some limitations; the interaction between miRNA and mRNA might be disrupted by the multi-step experimental conditions used in the Co-IP or RISC-IP approach, low stringency of IP might also purify indirect targets and this method can only give information regarding the targeted genes but not on the specific interaction sites.

To overcome these issues an improved method, high throughput sequencing of RNAs isolated by UV crosslinking and immunoprecipitation (HITS-CLIP), was introduced (Chi *et al*., 2009, Zisoulis *et al*., 2010). This method uses UV irradiation which covalently crosslinks the Ago2 protein with the miRNA-mRNA complex with which it is in direct contact within the cells (Chi *et al*., 2009). Crosslinking of proteins with nucleic acids is an irreversible process and crosslinked complexes can withstand the stringent purification conditions in the CLIP techniques. HITS-CLIP has been successfully used to identify cellular targets of KSHV (Haecker *et al*., 2012) and EBV (Riley *et al*., 2012) encoded miRNAs.

To overcome the problem of low efficiency crosslinking due to the short wavelength radiation (254 nm) used in HITS-CLIP, Hafner *et al,* introduced a new method called photoactivable-ribonucleoside-enhanced-CLIP (PAR-CLIP) (Hafner *et al*., 2010). In this technique cells are incubated with a photoactivable nucleoside, 4-thiouridine (^{4S}U) to be incorporated into the transcripts in the cells. After that a UV crosslinking is performed at 365 nm wavelength and Hafner *et al,* reported that mRNA recovery was 100 to 1000fold better when compared to other CLIP methods using short

wavelength and without ^{4S}U (Hafner *et al*., 2010). ^{4S}U has a preference to bind with guanine instead of adenine. During cDNA synthesis ^{4S}U binds to guanine and during PCR-amplification these turn thymidine to cytosine respectively in the PCR product, that will be deep sequenced. This method also has an advantage of mapping the exact crosslinking sites (Corcoran *et al*., 2011, Hafner *et al*., 2010, Spitzer *et al*., 2014). Gottwein *et al* and Skalsky *et al* successfully used PAR-CLIP to identify the miRNA targets in KSHV and EBV respectively (Gottwein *et al*., 2011, Skalsky *et al*., 2012) Skalsky *et al*., 2012). Nevertheless HITS-CLIP and PAR-CLIP techniques do not provide a definitive target identification.

Recently a new technique called crosslinking ligation and sequencing of hybrids (CLASH) has been developed to overcome the limitation inherent to previous CLIP techniques (Helwak *et al*., 2013). Using CLASH, miRNAs and their targeted transcripts can be identified together due to an intramolecular ligation step. An RNA ligase is used to covalently link a small proportion of the purified mRNA molecules to their targeting miRNAs. This allows the identification of miRNAs linked to their target genes and their specific interaction sites through chimeric miRNA-mRNA target sequences. The CLASH technique has been shown to be highly specific. Sequencing of the chimeric reads also revealed large number of non-canonical interactions between miRNAs and target mRNA pairs (Umbach *et al*., 2010). More detail on the CLASH technique is presented in Chapter 4.

Proteomic approaches

Proteomic methods are useful to identify miRNAs targets when miRNAs cause very little or undetectable changes in the levels of target mRNAs. The difference, in the

levels of newly synthesized protein in the presence and absence of specific miRNA can be measured using a pulsed stable isotope labelling with aminoacids in cell culture (pSILAC) (Baek *et al*., 2008, Selbach *et al*., 2008, Vinther *et al*., 2006). In this method different amino acids are labelled with different heavy isotopes in the growth medium of cultivated cells, with or without specific miRNAs. Cells are harvested, samples pooled, digested and analysed by mass spectrophotometry. The ratio of isotopes quantitatively determines the relative expression of protein. Vinther *et al* used pSILAC to examine the targets of miR-1 in Hela cells. A total of 504 proteins were identified, however 12 of those proteins were repressed after miR-1 induction, and 6 of the 12 proteins were validated (Vinther *et al*., 2006).

1.5.6 Viral miRNAs

Viruses are well known for controlling the host cell regulatory system for their survival and propagation and it was hypothesized that virus encoded miRNAs could help viruses to evade the immune response as a result of regulating both cellular systems and viral gene expression (Tuddenham and Pfeffer, 2013, Sullivan, 2008). Because miRNAs are non-immunogenic and occupy little genomic space, virus encoded miRNAs can be a powerful mechanism for viruses to modulate host gene expression (Sarnow *et al*., 2006).

Viral miRNAs were first identified in EBV, by Pfeffer and co-workers in 2004, after small RNA profiling of infected cells. Those viral miRNAs were differentially expressed depending on the stage of the viral life cycle (Pfeffer *et al*., 2004). Since that discovery, over 400 viral miRNAs have been identified from genomes of different viruses including herpesviruses, polyomaviruses, retroviruses, adenoviruses

and Iridoviruses (Cai *et al*., 2006a, Jurak *et al*., 2010, Kincaid *et al*., 2012, Rosewick *et al*., 2013, Pfeffer *et al*., 2005, Samols *et al*., 2007). DNA viruses which replicate in the nucleus have been shown to encode most of the viral encoded miRNAs. Herpesviruses encoded miRNAs represent the majority of viral encoded miRNAs identified and herpesviruses also have the highest average number of miRNAs encoded per virus i.e typically >10 per genome (Kincaid and Sullivan, 2012). In the nucleus, DNA viruses have full access to the miRNA biogenesis initiating machinery (Kincaid and Sullivan, 2012, Tuddenham and Pfeffer, 2013). Those viruses which replicate in the cytoplasm (e.g Pox, HCV) might not have evolved to encode miRNAs possible due to their lack of contact with Drosha (Cullen, 2010). Some studies have shown that human immunodeficiency virus type 1 (HIV-1) also encodes for miRNAs (Bennasser *et al*., 2004, Omoto *et al*., 2004), however more recent studies reported that HIV-1 neither encodes for any miRNAs nor represses the RNA interference machinery in infected cells (Lin and Cullen, 2007, Pfeffer *et al*., 2005). There is very little reported evidence that RNA viruses might encode miRNAs. Kincaid *et al* showed that a retrovirus; bovine leukemia virus (BLV) clearly encodes numerous miRNAs (Kincaid *et al*., 2012, Rosewick *et al*., 2013). BLV encodes a conserved cluster of miRNAs that are transcribed by RNA polymerase III. The transcribed hairpin structures directly serve as Dicer substrates thus avoiding the cleavage of its RNA genome and mRNA by Drosha (Kincaid *et al*., 2012).

1.5.6.1 Herpesviruses encoded miRNAs

Herpesviruses encoded miRNAs constitute more than 90% of the viral encoded miRNAs so far identified (Grundhoff and Sullivan, 2011, Tuddenham and Pfeffer,

2011, Tuddenham *et al*., 2012). The functions and functional targets of the majority of these miRNAs however, remain unknown. A few targets of herpesvirus encoded miRNAs have been found to play a role in the regulation of viral and cellular gene expression, maintainance of latency, immune evasion and viral pathogenesis (Table 1.2 and 1.3). It is out of the scope of this thesis to give a description of all the known targets for herpesvirus encoded miRNAs. However, some of the miRNAs which have viral targets involve in viral replication and pathogenicity and cellular targets involve in immune evasion, apoptosis resistance and support latency, will be discussed.

Viral targets of herpesvirus encoded miRNAs

It has been reported that miRNA targeting of lytic or IE and late genes to regulate the viral life cycle, is used by many of the herpesviruses (Table 1.2).

HSV-1-miR-H2-3p is antisense to ICP0 and its expression causes a translational repression of ICP0 (an immediate early transcriptional activator), which might be expected to promote or maintain viral latency (Umbach *et al*., 2008). HSV-1-miR-H6 targets the IE transcription factor ICP4 which is required for maximal expression of most HSV genes (Umbach *et al*., 2008, Watson *et al*., 1980). HSV-2-miR-H2, -H3 and -H4 have been shown to target ICP0 and ICP34.5 (a viral neurovirulence factor) (Tang *et al*., 2009). ICP34.5 is involved in virus replication and down regulation of this viral protein might result in the establishment and maintenance of latency.

Table 1.1: Current number of virus encoded miRNAs

Family	Subfamily	Virus	Current number of viral encoded miRNAs
Herpesviridae	*α-Herpesviridae*	Bovine herpesvirus 1	12
		Herpes B Virus	15
		Herpes Simplex Virus 1	27
		Herpes Simplex Virus 1	24
		Marek's disease virus	26
		Marek's disease virus type 2	36
	β- Herpesviridae	Human cytomegalovirus	26
		Mouse cytomegalovirus	29
		Human herpesvirus 6	8
	γ- Herpesviridae	Epstein Barr Virus	44
		Kaposi's Sarcoma-associated herpesvirus	25
		Murine Herpesvirus 68	28
		Rhesus lymphocryptovirus	68
		Rhesis monkey rhadinovirus	11
		Herpesvirus saimiri	6
Polyomavirus		BK polyomavirus	2
		JC polyomavirus	2
		Merkel cell polyomavirus	2
		Simian virus 40	2
Polyomavirus-like		Bandicoot papillomatosis carcinomatosis viruses	2
Retrovirus		Bovine leukemia virus	10

Foot notes: Adapted from miRBase release (v20, June 2013) (http://www.mirbase.org/).

MDV1-miR-M7-5p, targets two MDV IE genes, ICP4 and ICP27 which suggests that this miRNA may play an important role in establishing and maintaining viral latency (Strassheim *et al*., 2012). In addition, MDV also encodes a functional viral ortholog (MDV1-miR-M4) of the cellular miRNA miR-155 which targets UL28 and UL32 proteins involved in the cleavage and packaging of viral DNA (Muylkens *et al*., 2010).

HCMV-miR-UL112-1 targets the viral immediate early gene IE72 (also known as UL123 or IE1) and can modulate viral replication and can lead to viral latency (Grey *et al*., 2007, Murphy *et al*., 2008).

Several studies on KSHV miRNAs reported that the KSHV transactivator RTA/ORF50, can be targeted by different miRNAs (miR-K-12-1, miR-K-12-5, miR-K-12-7, miR-k-12-9*, miR-k-12-9) directly or indirectly (Bellare and Ganem, 2009, Lei *et al*., 2010, Lin *et al*., 2011b, Lu *et al*., 2010). EBV-miR-BART2 targets the viral DNA polymerase BALF5 and it has been shown that regulation of BALF5 by miR-BART2 is important for the correct control of the switch from latent to lytic life cycle (Barth *et al*., 2008). EBV-miRs originating from the BART cluster 1 are reported to regulate the expression of the viral LMP1 protein (Lo *et al*., 2007). LMP1 is produced during EBV latency and is required to induce cell growth and transformation for the development of nasopharygeal carcinoma (NPC) (Izumi *et al*., 1997). However, over expression of LMP1 can result in growth inhibition and increase apoptosis (Eliopoulos *et al*., 1996). It is proposed that EBV miRNAs tightly regulate LMP1 expression for EBV pathogenesis.

Cellular targets of herpesvirus encoded miRNAs

Herpesvirus miRNAs with known cellular targets may play a significant role in cell survival, proliferation and immune evasion, which helps in viral persistence and pathogenesis (Table 1.3). HCMV-miR-UL112-1, EBV-miR-BART2-5p and KSHV-miR-K12-7 have a common target, a NK receptor ligand: major histocompatibility complex class I related chain B (MICB) (Nachmani *et al*., 2009, Stern-Ginossar *et al*., 2007). Binding of one of these miRNAs to the MICB transcripts results in a decrease in MICB binding to the natural killer activating receptor (NKG2D) resulting in inhibition of NK cell recognition of virally infected cells, suggesting the role of these miRNAs is immune evasion (Nachmani *et al*., 2009, Stern-Ginossar *et al*., 2007). HCMV-miR-UL112-1 also targets Bcl-2 associated factor, BclAF1, which is a nuclear protein important in apoptosis, transcriptional regulation and export of RNA from the nucleus (Sarras *et al*., 2010). It has been reported that the BclAF1 protein is also targeted by viral proteins, p71 and UL35 at the start of HCMV infection. An increase in the expression of BclAF1 inhibits viral replication and a reduction in BclAF1 levels enhances HCMV gene expression. These findings suggest that cellular genes important for viral persistence can be targeted by viruses using more than one strategy (Lee *et al*., 2012). HCMV-miR-US25-1 targets a number of cellular genes involved in the regulation of the cell cycle and results in the arrest of the G1/S phase of the cell cycle (Grey *et al*., 2010).

MDV-1 encodes a miRNA, miR-M4 which is an ortholog of cellular miR-155. miR-155 plays an important role in the lymphocyte differentiation (Section 1.5.4). Zhao *et al,* found a significant role for miR-M4 in lymphomagenesis in chickens infected

with a virulent strain of MDV-1. A miR-M4 deleted virus failed to induce lymphomas in the chickens after infection (Zhao *et al*., 2011b). KSHV-miR-K12-11, was also identified as an orthologue of miR-155 and they have nearly identical sets of target mRNAs (Skalsky *et al*., 2007). It has been reported that ectopic expression of either miRNA can inhibit BACH-1, a transcriptional repressor. Furthermore the mRNA levels of BACH-1 are down regulated in latently infected KSHV-infected endothelial cells (An *et al*., 2006) which might be due to miR-K12-11 targeting. miR-K-12-11 and miR-155 have also been found to target CCAAT enhancer binding protein β (C/EBPβ) which is a negative regulator of IL-6 and is involved in B cell lymphomagenesis (Boss *et al*., 2011) and Jarid2 which plays an important role during embryonic development and cell differentiation and functions as a tumor suppressor (Dahlke *et al*., 2012).

KSHV-miR-K-12-6-3p targets thrombospondin 1 (THBS1) which encodes a protein involved in cell to cell adhesion, and has anti-proliferative and anti-angiogenesesis activity. It has been observed that the translation of THSB1 mRNA was inhibited by miR-K-12-6-3p (Samols *et al*., 2007). Lu *et al* found that KSHV miR-K12-4-5p can target the Rbl2 3′ UTR and down regulate Rbl2 protein levels. Rbl2 is a member of the Rb family and has global effects on the control of the cell cycle and cellular-differentiation (Lu *et al*., 2010). KSHV-miR-12-1 targets a cellular cyclin-dependent kinase inhibitor, p21 and strongly attenuates the cell cycle arrest which normally occurs in response to p53 activation (Gottwein and Cullen, 2010). KSHV miRNAs; miR-K12-10a, K12-9 and K12-5 target TWEAKR, IRAK1 and MYD88 respectively and reduce inflammatory-cytokine expression (Abend *et al*., 2012, Abend *et al*.,

2010). EBV-miR-BHRF1-3 have been shown to help immune evasion of the virus by targeting CTL chemoattractant CXCL11 leading to a reduction in the recognition of EBV infected cells by CTLs (cytotoxic T lymphocytes) (Xia *et al*., 2008b). As a means of protecting cells from apoptosis, EBV-miR-BART5 targets the pro-apoptotic protein, p53 up-regulated modulator of apoptosis (PUMA) in nasopharyngeal carcinoma (Choy *et al*., 2008).

1.5.7 OvHV-2 encoded miRNAs

Like other herpesviruses OvHV-2 also encodes miRNAs (Levy *et al*., 2012). Using high throughput sequencing and bioinformatics, 46 OvHV-2 encoded miRNAs were predicted(Levy PhD thesis, 2012), eight of those were validated by northern hybridization as putative miRNAs expressed in the BJ1035 cell line and named as ovhv2-miR-1 – miR-8 (Levy *et al*., 2012).

The discovery of OvHV-2 miRNAs was the first report of the expression of virally encoded miRNAs in the *Macavirus* genus of the *Herpesviridae*. OvHV-2 encoded miRNAs are located throughout the genome in three clusters, in regions of the genome which were not encoded for any protein (Figure 1.5). Cluster 1 is located at the left hand end of the OvHV-2 genome and encodes five miRNAs. Cluster 2 and -3 are located between ORF11 and ORF17/17.5, in a 9.3 kb region of the genome which does not encode for any functional protein. Both of these clusters are approximately 4 kb apart from each other. Cluster 2 and -3 encode twenty seven and three miRNAs respectively (Figure 1.5).

Since the work described in this thesis was carried out, a further study has validated the expression of a total of 35 OvHV-2 encoded miRNAs (Nightingale *et al*., 2014) (Table 1.4). A new nomenclature for OvHV-2 encoded miRNAs was also introduced in that study. However I will use the previous nomenclature as described in Table 1.4.

1.5.8 Aims of the study

The identification and validation of viral and cellular targets of OvHV-2 miRNAs is an important step in understanding the role of those miRNAs in virus biology. Bioinformatic analysis predicts a large number of possible OvHV-2 miRNAs targets in host (cattle or sheep) and viral transcripts. Experimental approaches to validate selected targets would be a realistic approach. So the overall aim of this thesis work was to identify and functionally validate the OvHV-2 miRNAs targets in virus and host transcripts. Specifically, we aimed to:

- Validate the predicted OvHV-2 ORFs as targets of OvHV-2 miRNAs using dual luciferase assays.
- Identify mRNAs targeted by OvHV-2 miRNAs in the cattle and sheep cells and validate those predicted targets by CLASH technique.

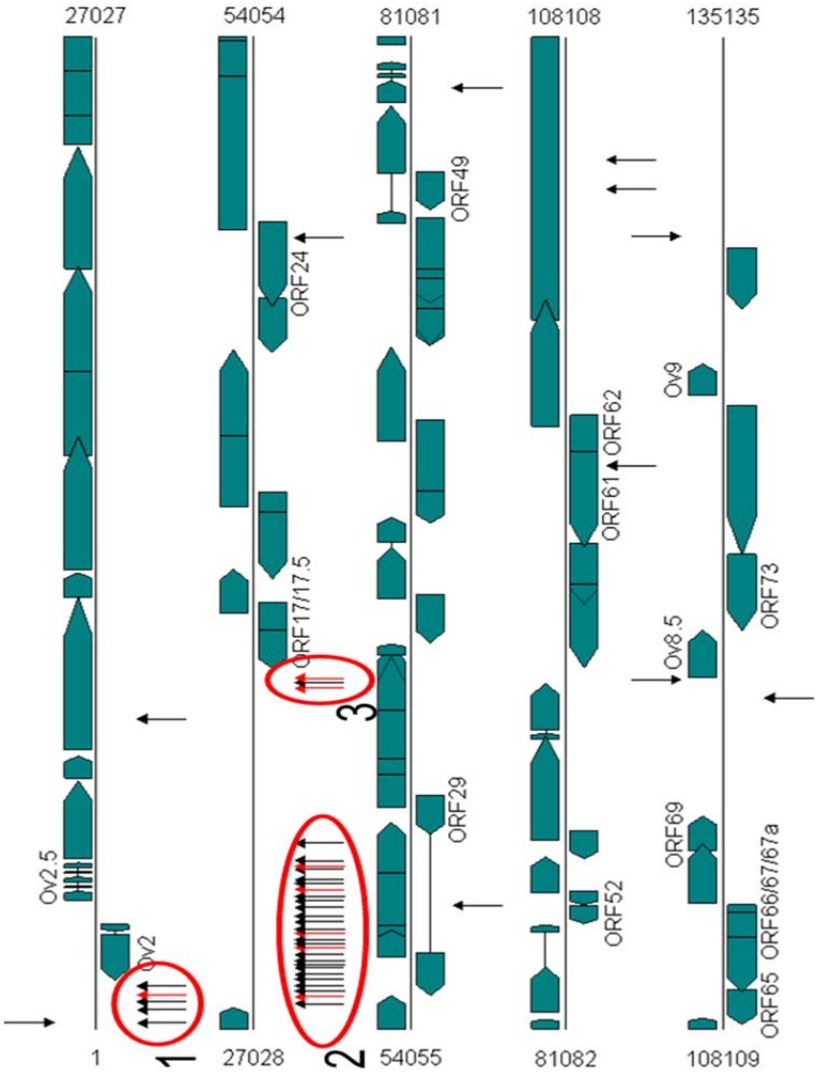

Figure 1.5: Schematic diagram of OvHV-2 genome showing validated and predicted ovhv2-miRs.

Sites of miRNAs are shown in red and black arrows. Red arrows indicated the miRNAs validated by northern blot analysis (Levy *et al*., 2012). Red circles around miRNAs are indicating three major cluster regions of ovhv2-miRs (cluster 1, 2 and 3). OvHV-2 predicted ORFs are shown with closed boxes and arrows indicating the direction of transcription.

Table 1.2: Viral targets of herpesvirus encoded miRNAs

Sub-family	Virus/miRNA	Target	Function
α-Herpesviridae	HSV-1/miR-H2-3p, HSV-2/miR-H2	ICP0	Viral Immediate early transactivator
	HSV-1/miR-H6, MDV-1/miR-M7-5p, ILTV/miR-15	ICP4	Viral Immediate early transactivator
	HSV-2/miR-H3, HSV-2/miR-H4	ICP34.5	Establishment and maintainance of latency
	MDV-1/miR-M4	UL28, UL32	Cleavage/packaging of viral DNA
β-Herpesviridae	HCMV/miR-UL112-1	IE72/UL123/IE1	Immediate early gene
γ-Herpesviridae	KSHV/miR-K12-5, KSHV/miR-K12-7-5p, KSHV/miR-K12-9*, EBV/miR-BART6-5p	RTA/ORF20	Viral transactivator
	EBV/miR-BART2	BALF5	Viral DNA polymerase
	EBV/miR-BART6-5p	EBNA2	Viral transactivator
	EBV/miR-miR-BART9, EBV/miR-BHRF1-1	LMP1	Latent viral protein, oncogene

Table 1.3: Cellular targets of herpesvirus encoded miRNAs

Sub-family	Virus/miRNA	Target	Function
α-Herpesviridae	MDV-1/miR-M3	SMAD2	Anti-apopototic
	MDV-1/miR-M4	HIVEP2, CEBPβ, PU.1, BCL2l13, PDCD6	Viral pathogenesis
β-Herpesviridae	HCMV/miR-UL112-1	MICB	Role in immune evasion
	HCMV/miR-UL-148D	RANTES	Chemokine
	HCMV/miR-UL-112-1	BclAF1	transcriptional regulation
	HCMV/miR-US25-1	Cyclin E2	Cell cycle inhibition
	MCMV/miR-M23-2	CXCL-16	Chemokine
γ-Herpesviridae	EBV/miR-BART2-5p, KSHV/miR-K12-7	MICB	Role in immune evasion
	EBV/miR-BHRF1-3	CXCL-11	Chemokine
	KSHV/miR-K12-1, KSHV/miR-K12-9	IRAK1	TLR signalling
	KSHV/miR-K12-5, KSHV/miR-K12-11	MYD88	TLR signalling
	KSHV/miR-K12-1	p21	Cell cycle inhibotor
	KSHV/miR-K12-11	SMAD5	TGFβ signalling
	KSHV/miR-K12-1, KSHV/miR-K12-3-3p, KSHV/miR-K12-6-3p, KSHV/miR-K12-11	THBS1	Tumor suppressor, anti agiogenic
	KSHV/miR-K12-11	BACH1	Transcription regulation
	EBV/miR-BART3, EBV/miR-BART9, EBV/miR-BART17-5p		Transcription regulation
	KSHV/miR-K12-11	TWEAKR	Role in immune evasion
	EBV/miR-BART5	PUMA	Pro-apoptotic factor
	KSHV/miR-K12-4-5p	Rbl2	Cell cycle regulation

Table 1.4: Recent and previous nomenclature for OvHV-2 encoded miRNAs

Recent nomenclature (Nightingale *et al*., 2014) Ovhv2-miR-	**Previous nomenclature** (Levy *et al*., 2012; Riaz *et al*., 2014) Ovhv2-
Ov2-2	miR-1
Ov2-1	-miR-6
17-30	-miR-34
17-29	miR-2
17-28	miR-36
17-27	miR-37
17-26	miR-38
17-25	miR-39
17-24	miR-40
17-23	miR-41
17-22	miR-42
17-21	miR-43
17-20	miR-3
17-19	miR-45
17-18	miR-46
17-17	miR-4
17-16	miR-48
17-15	miR-49
17-14	miR-50
17-13	miR-51
17-12	miR-53
17-11	miR-54
17-10	miR-5
17-9	miR-57
17-8	miR-58
17-7	miR-60
17-6	miR-6
17-5	miR-62
17-4	miR-63
17-3	miR-7
17-2	miR-67
17-1	miR-8
24-1	miR-83
61-1	miR-163
73-1	miR-217

Foot notes: The eight OvHV-2 miRNAs validated by northern hybridization (Levy *et al*., 2012) are indicated in blue.

Chapter 2: Material & Methods

2.1 Molecular techniques

2.1.1 Isolation of DNA

DNA was extracted from eukaryotic cells using the Qiagen DNeasy Kit according to the manufacturer's protocol. Cells were pelleted at 300 x g for 5 min at room temperature and resuspended in sterile phosphate buffer solution (SPBS). The cells were lysed with sodium dodecyl sulphate (SDS) followed by treatment with proteinase K. RNA was degraded with RNase A. The lysate was combined with a chaotropic salt buffer to optimize DNA binding to the column membrane. Bound DNA was washed in two steps and eluted in the provided buffer. After purification all DNA samples were stored at either 4^{o}C or at -20^{o}C for long term storage.

2.1.2 Polymerase chain reaction

Pfu Turbo DNA polymerase (Stratagene) was used according to the manufacturer's protocol. All samples were made up to a final volume of 50 µl in 0.2 ml thin walled PCR tubes. Each reaction mix contained 1× cloned Pfu DNA polymerase reaction buffer with $MgSO_4$, 10-100ng of DNA template, 10-25mM each dNTP, 100-125 ng of both the forward and reverse primers (Eurofins MWG Operon) (Appendix-3), 1 I.U. of Pfu DNA polymerase and nuclease free water. The reaction conditions consisted of one cycle of denaturation at 95^{o}C for 5min, 35 cycles of 30sec denaturing at 95^{o}C, 30 sec annealing at 55-60^{o}C, and extension at the rate of 1 min per kb at 72^{o}C, with a final extension cycle of 7 min at 72^{o}C in a PCR Sprint Thermal Cycler, (Thermo Scientific). During the last cycle (extension) Taq DNA polymerase (Biolabs) (1µl) was added to each reaction mixture.

2.1.3 PCR product purification

PCR products were purified using a QIAquick PCR Purification Kit (Qiagen) or MinElute PCR Purification Kit (Qiagen) according to the manufacturer's protocol. 5volumes of Buffer PB was added to 1 volume of the PCR product and applied to the supplied spin column. The columns were centrifuged at 12,000 x g for 30-60 sec, washed with Buffer PE (supplied with the kit) and the DNA eluted with 10-30 µl buffer EB (10mM Tris-Cl, pH 8.5) or water.

2.1.4 Agarose gel electrophoresis

PCR products or plasmid DNA were analysed by electrophoresis in 1-1.5% agarose (Invitrogen) or 3% intermediate melting temperature agarose (MetaPhor, Lonza) containing 0.05 mg ethidium bromide (Sigma) in 1x TAE (Tris-acetate-EDTA) buffer (Appendix-1). An appropriate volume of 6x loading dye was added to each sample and electrophoresis was carried out in horizontal gel tanks at 80V for 45 min to 1 hr. Samples were compared with 1 kb, 100bp, 25bp, and 10bp DNA ladders (New England Biolabs) for size estimation.

2.1.5 Restriction enzyme digestion of DNA

Restriction enzyme (New England Biolabs) digestion was carried according to the manufacturer's instructions using the recommended buffer at 37^{o}C for 1-2 hr. Digests were carried out in a total volume of 10-20 µl using 10U of each restriction enzyme with 1 µg of plasmid DNA. Digested DNA samples were analysed by agarose gel electrophoresis (Section 2.1.4).

2.1.6 Extraction of DNA from agarose gels

DNA fragments were extracted from agarose gels using the QIAquick Gel Extraction Kit or MinElute Gel Extraction Kit (Qiagen) according to the manufacturer's protocol. The gel slice with the DNA fragment of interest was excised from the gel, dissolved in the buffer QG at 55^{o}C (for high melting temperature agarose) or 37^{o}C (intermediate melting temperature agarose). Isopropanol was added to the dissolved gel and the mixture was applied to a QIAquick gel extraction column or a MinElute gel extraction column. Elution of DNA from column was as described in section 2.1.3.

2.1.7 DNA ligation

For cloning PCR products the PCR 4-TOPO vector (Appendix-2 for vector map) (Invitrogen) was used according to the manufacturer's protocol. 2 µl of the PCR product, 1 µl of salt solution (1.2M NaCl, 0.06M MgCl2) and 1 µl of the TOPO TA vector were mixed and incubated for 5 min at room temperature.

Ligation of the restriction digested DNA insert with a digested and dephosphorylated vector was carried out at a molar ratio of 2 (insert):1 (vector). Each ligation mixture also contained 1 µl of T4 DNA ligase (New England Biolabs), 1 µl of 10x Ligase Buffer and water to a final volume of 10 µl. Ligation reactions were incubated overnight at 16^{o}C.

2.1.8 Quantification of nucleic acid by spectrophotometry

Nucleic acid concentration was determined using a NanoDrop ND1000 Spectrophotometer (Thermo Fisher Scientific, UK) at an absorbance reading of OD_{260}nm and OD_{280}nm. A pure DNA or RNA had at a 260/280 ratio of ~1.8 or ~2.0 respectively. Using the formula $OD_{260}$of 1= 50 µgml^{-1} DNA or 40 µg ml^{-1} RNA, absorbance of concentration of nucleic acid was calculated.

2.1.9 Sequencing of plasmid DNA

Plasmid DNA was sequenced using the Big Dye® Terminator v3.1 Cycle Sequencing Kit (Applied Biosystems). Plasmid DNA (300-500 ng) was added to sequencing primers (3.2 pmol/µl) (for list of sequencing primers see Appendix-3), 1.5 µl of 5 x Big Dye Buffer and 1 µl Terminator Ready Reaction Mix. The sequencing reaction was performed on a PCR Sprint Thermal Cycler, (Thermo Scientific) using the following reaction conditions for 30 cycles.

96^{o}C	10 sec	denaturation of plasmid DNA
50^{o}C	5 sec	annealing
60^{o}C	2 min	elongation
4^{o}C	hold	

Plasmids were sequenced by the Gene Pool, Ashworth Laboratory, Kings Building, University of Edinburgh or by the GATC Biotech, Germany. DNA sequences were analysed using NCBI nucleotide-nucleotide BLAST (http://blast.ncbi.nlm.nih.gov/Blast.cgi).

2.1.10 Isolation of RNA

RNA was isolated from cultured cells using TRIzol® (Invitrogen) according to the manufacturer's protocol. Briefly 0.75 ml of TRIzol® Reagent was added to 0.25 ml of cells in suspension (5–10 × 10^6 cells) or for adherent cells lines 1 ml TRIzol® Reagent was added directly to the cells in the culture dish per 10 cm^2 area. Cells were lysed by pipetting up and down several times. The sample was incubated for 5 min at 23°C. 0.2 ml of chloroform was added to the reaction mixture and the tube was shaken vigorously for 15 seconds, incubated for 2–3 min at room temperature and centrifuged at 12,000 × g for 15 min at 4°C. The upper transparent aqueous phase of the sample was removed and 0.5 ml of 100% isopropanol was added to it. The sample was incubated at room temperature for 10 min and centrifuged at 12,000 × g for 10 min at 4°C. The supernatant was removed and the pellet washed twice with 75% ethanol. After each wash the sample was vortexed briefly, and centrifuged at 7500 × g for 5 min at 4°C. The RNA pellet was air dried for 5–10 min on ice, and re-suspended in 15-30 µl of nuclease free water. The RNA sample was then incubated in a water bath at 55–60°C for 10 min. The concentration of the RNA was determined as described in section 2.1.8 and stored at -80°C.

2.1.11 Reverse transcription of miRNAs

Reverse transcription of miRNAs for cDNA synthesis was performed using the miScript Reverse transcription Kit (Qiagen) according to the manufacturer's protocol. Template RNA (section 2.1.9) (200 ng) was added to the reaction mix containing 4µl of the 5 x miScript RT buffer, 1 µl of the miScript Transcriptase mix,

0.5 µl of RNaseOUT (Invitrogen) (40 U/µl) and nuclease free water to a final volume of 20 µl. The reaction was incubated for 60 min at 37°C and then for 5 min at 95°C.

2.1.12 Quantitative real time PCR

Real time quantitative PCR (RT-qPCR) for the detection of miRNAs was performed using the miScript SYBR Green PCR Kit. RT-qPCR was carried out in 0.2ml strip tubes in a Rotor-Gene Q (Qiagen). Template cDNA (0.1-10ng) was added to a reaction mix containing 10µl of 2x SYBR Green PCR master mix, 2µl of 10 x Universal Primer, 2µl of the miRNA specific forward primer (Invitrogen) (Appendix-3) and nuclease free water to a final volume of 20µl. RT-qPCR was performed using the following cycling conditions

PCR initial activation step	15 min at 95°C
3 step cycling for 40 cycles:	
Denaturation	15 sec at 94°C
Annealing	30 sec at 55°C
Extension	30 sec at 70°C

2.2 Bacterial techniques

2.2.1 Bacterial culture

7.5 g Bacto agar (BD) was added to 500 ml Luria-Bertani (LB) broth (Merck) (Appendix-1) and autoclaved. The culture media was supplemented with ampicillin (100 µg/µl) (Sigma) at 45°C-50°C. The gel was gently swirled and then poured into petri dishes (Sterilin) aseptically and allowed to solidify. For liquid culture, agar was not added to LB broth.

2.2.2 Transformation of chemical competent cells

One Shot® TOP10 Chemically Competent E. coli (Invitrogen) were transformed according to the manufacturer's protocol. A vial of 50µl of the competent cells was thawed on ice. 1-5µl of the ligation reaction (section 2.1.7) or plasmid was added to the vial and incubated on ice for 30min. The cells were heat-shocked for 30sec at 42^{o}C without shaking and immediately placed on ice for 2 min. 250 µl of pre-warmed SOC medium was added to the cells and cells were shaken in an orbital incubator at 225 rpm for 1 hr at 37^{o}C. The transformation reaction was spread on to pre-warmed LB agar plate (supplemented with ampicillin) and incubated at 37^{o}C overnight.

2.2.3 Small scale isolation of plasmid DNA from bacteria

Isolation of plasmid DNA from transformed bacteria was carried out using a QIAprep Spin Miniprep Kit (Qiagen) according to the manufacturer's instruction. A single colony was picked from the freshly streaked LB agar plate, inoculated in 1-5 ml of LB broth supplemented with 100 µg/µl of ampicillin and incubated at 37^{o}C in an orbital shaker at 225 rpm for 24 hr. Bacterial cells were harvested by centrifugation at 3,000 x g in a bench top centrifuge for 5min at room temperature. The supernatant was removed and the bacterial pellet re-suspended in 250 µl of the buffer P1 containing RNase A, when there were no visible cell clumps, 250 µl of buffer P2 was added, followed by 350 µl of buffer N3. The lysate was centrifuged at 18,000 x g for 10 min. The supernatant was carefully applied to the spin column and centrifuged at 18,000 x g for 30-60 sec. The flow through was discarded and the sample in the column was washed with 500 µl of buffer PB by centrifugation at

18,000 x g for 30-60 sec. The column was washed by adding 750 µl of ethanol containing buffer PE and centrifuged at 18,000 x g for 30-60 sec. To completely remove the residual ethanol the column was centrifuged at 18,000 x g for 1 min. The plasmid DNA was eluted into a 1.5 ml microcentrifuge tube by applying 50 µl of buffer EB (10mM Tris, PH8.5) and the column was then centrifuged for 1 min at 18,000 x g.

2.2.4 Large scale isolation of plasmid DNA from bacteria

Isolation of plasmid DNA on large scale from transformed bacteria was carried out using a QIAGEN Plasmid Maxi Kit (Qiagen) according to the manufacturer's instruction. A single colony was picked from a freshly streaked LB agar plate, inoculated into 1-5 ml of LB broth supplemented with 100 µg/µl of ampicillin and incubated at 37^{o}C in an orbital shaker at 225 rpm for approximately 8 hr. 300-500 µl of this starter culture was inoculated into 200-500 ml of LB broth supplemented with 100 µg/µl of ampicillin and incubated for 12-16 hr at 37^{o}C in an orbital shaker at 225 rpm. Bacterial cells were harvested by centrifugation at 6000 x g for 15 min at 4^{o}C. The bacterial pellet was re-suspended in 10 ml of the supplied RNase containing buffer P1, 10 ml of buffer P2 was then added to the sample. The sample was incubated at room temperature for 5 min and 10 ml of buffer N3 was added. The sample was incubated on ice for 20 min and centrifuged at 20,000 x g for 30 min. The QIAGEN-tip 500 column was equilibrated with 10 ml of buffer QBT. The supernatant was carefully applied to the column and allowed to enter the resin by gravity flow. The column was washed with 30 ml of Buffer QC twice and plasmid DNA was eluted with 15 ml of Buffer QF and collected in a clean 30 ml glass Corex

tube. 10.5ml of isopropanol was added and the sample centrifuged at 15,000 x g for 30 min at 4°C. The DNA pellet was washed with 5ml of 70% ethanol and allowed to air dry it for 5-10 min. The pellet was re-dissolved in 300-500µl of buffer TE (10mM Tris-Cl, pH 8.5).

2.2.5 Preparation of bacterial stocks for long term storage

150 µl of sterile glycerol was added to 850 µl of the bacterial culture, The mixture was vortexed to ensure the proper mixing and stored at -80°C.

2.3 Protein techniques

2.3.1 Isolation of protein from cultured cells

Cells were detached as described in section 2.5.1 and were pelleted by centrifugation at 1500 x g for 5 min at room temperature. Cells in suspension culture were pelleted by centrifugation at 1500 x g for 5 min at room temperature. Cell pellets were washed twice in phosphate buffer saline (PBS) (Appendix-1) and 5 x 10^4 cells were re-suspended in 250ul 1 x protein sample buffer (Appendix-1) The samples were denatured by heating at 95-100°C for 5 min.

2.3.2 SDS-Polyacrylamide gel electrophoresis (SDS-PAGE)

10% acrylamide gels (Appendix-1) were used for SDS-PAGE. The resolving gel (Appendix-1) was poured between the plates. The resolving gel was allowed to polymerize for 20-30 min and stacking gel (Appendix-1) was poured over it and a comb was placed in it. The gel was allowed to polymerize for 30 min and placed in a Mini-Protean II apparatus (Bio-Rad) according to manufacturer's instruction in 1 x

SDS running buffer (Appendix-1). After removing comb the wells were washed with 1 x SDS running buffer to remove any un-polymerised acrylamide. Denatured protein samples were loaded onto the gel. One well was loaded with ColourPlus Prestained Protein marker (New England BioLabs) for protein size estimation. The gel was run at 150-200 Volts (V) for 1-1.5 hr or until the dye front reached the end of the gel.

2.3.3 Western blotting

Separated proteins in the gel were then transferred to polyvinylidene fluoride (PVDF) membrane (Millipore). The transfer was performed using a Semi Dry Electroblotter A (Acro). PVDF membrane and 6 pieces of 3MM Chr chromatography paper (Whatmann) were cut to the size of gel. The membrane and the blotting papers were soaked in methanol and the semidry transfer buffer (Appendix-1) respectively prior to use. Three sheets of blotting paper were placed in the centre of the anode of electroblotter. The membrane was placed on top of these followed by the gel. The remaining three sheets of blotting papers were placed on top of the gel and any trapped air bubbles were carefully squeezed out by gently rolling a pipette over the top blotting paper. The transfer was performed at 0.4mA/cm2 or 20-25 V for 30 min.

The membrane was carefully removed after transfer and rinsed in 1x Tris buffered saline (TBS) (Appendix-1). The membrane was transferred to blocking buffer (Appendix-1) at 4^{o}C for 1-2 hr and then incubated overnight at 4^{o}C in appropriate primary antibody diluted in blocking buffer. The membrane was washed four times in TBST for 20 min each. Bound primary antibody conjugated with horseradish

peroxidase (HRP), was detected by incubating the membrane in equal amounts of ECL solutions A and B (ECL Plus Western Blotting Detection Kit, GE Healthcare). For bound primary antibodies which were not conjugated with HRP, the membrane was incubated with an appropriate secondary HRP conjugated antibody in blocking for 1 hr. The membrane was washed four times in TBST for 20 min each and bound antibody was detected as described above.

2.4 Tissue culture

2.4.1 Culture of adherent cell lines and primary cell lines

Adherent cell lines baby hamster kidney cell (BHK-21), human embryonic kidney cells (HEK-293T), Madin-Darby bovine kidney cells (MDBK) and primary sheep embryo fibroblasts (SEF) were cultured in polystyrene cell culture flasks or dishes. BHK-21 were grown in Glasgow-modified Eagle's medium (GMEM) (Gibco) supplemented with 10% new born calf serum (NBCS), 1% v/v penicillin/streptomycin, 1% (v/v) L-glutamine (Sigma) and 10% (v/v) tryptose phosphate broth. HEK-293T and SEF were grown in Dulbecco's modified Eagle's medium (DMEM) supplemented with 10-12% foetal calf serum (FCS) and 1% penicillin/streptomycin. Media for SEF was also supplemented with 1% (v/v) L-glutamine. MDBK were grown in Roswell Park Memorial Institute 1640 medium (RPMI-1640) supplemented with 5% FCS and 1% penicillin/streptomycin. Cells were cultured at 37^{o}C with 5% CO_2.

Cells were passaged when they reached a cell density of approximately 90%. Confluent cells were washed first with phosphate buffered saline (PBS) and then

incubated with 0.05% (w/v) trypsin-EDTA (Gibco) for 2-5 min at room temperature or 37^{o}C until the cells detached from the bottom of the flask. Cells were then re-suspended in 5-10 ml of complete media containing FCS. The cells were pelleted by centrifugation at 1500 x g for 5 min at room temperature. The supernatant was removed and the cell pellet was re-suspended in fresh media. To count the viable cells, a sample of the cell suspension was diluted in Trypan Blue Solution (Sigma) and unstained live cells were counted in a haemocytometer. Cells were re-seeded at approximately 5 x 10^6 cells/ T175cm^2 (Nunc).

2.4.2 Culture of suspension cell lines

BJ1035 cell were grown in suspension in Iscove's Modified Dulbecco's Medium (IMDM) (Invitrogen) (Hart *et al*; 2007) supplemented with 10% (v/v) FCS, 1% (v/v) penicillin/streptomycin and 350 U per ml Proleukin (IL-2) (Novartis Pharmaceutical). Cells were incubated at 37^{o}C in 5% CO_2. The growth of the cells was indicated by the formation of clumps in the suspension. When many large clumps were observed, the cells were passaged by pipetting up and down to break the clumps and 1/2 of that volume was transferred to a new flask with an equal volume of fresh complete medium. Viable cell counting was as described in the section 2.4.1.

2.4.3 Preparation of cell Lines for long term storage

For long term storage cells which were 70-80% were removed from the flask (section 2.5.1) and re-suspended at a concentration of 5 x 10^6 cells per 1 ml of freezing medium containing 90% FCS and 10% v/v dimethylsulphoxide (DMSO). 1 ml of suspension was aliquoted in a cryovial, wrapped in cotton wool and slowly frozen

overnight at -80^{o}C. The vials were then transferred to liquid nitrogen for long term storage.

2.4.4 Growing cell lines from frozen stock

Frozen cells were removed from liquid nitrogen and immediately thawed at 37^{o}C. The thawed sample was transferred to 10 ml of pre-warmed complete medium. Cells were pelleted at 1500 x g for 5 min, re-suspended in 8-10 ml of the pre-warmed complete medium and added to a T25 cm^2 flask. Cells were then placed in an incubator at 37^{o}C with 5% CO_2.

2.4.5 Transfection of cell lines with plasmid DNA using Lipofectamine 2000

BHK-21 cells and SEF were transfected using Lipofectamine 2000 (Invitrogen) with miRNA mimics (miScript miRNA Mimics, Qiagen) or plasmid DNA. The amounts and concentrations of Lipofectamine 2000, plasmid DNA/DNAs, miRNA mimics and Opti-MEM® used with cells seeding densities are described as in Table 2.1. Cells were plated onto appropriate plates either on the day of transfection (BHK-21) or 24hr before transfection (SEF). The appropriate amounts of plasmid DNA with or without miRNA mimics and Lipofectamine 2000 were diluted in OptiMEM® as described in Table 2.1. The Lipofectamine 2000 reaction mix was incubated at room temperature for 5min prior to addition of pre-mixed plasmid DNA or miRNA mimics in OptiMEM®. Samples were mixed and incubated for a further 20min at room temperature and added to cells in each well in a drop wise manner. The plates were gently swirled for proper mixing and the cells were incubated for 24 hr at 37^{o}C with 5% CO_2.

Table 2.1: Detail of the quantities of ingredients used in the transfection of cell lines.

Dish size	6 well plate	96 well plate	96 well plate	24 well plate
Cell density/well	5 x 10^5	1 x 10^4	1 x 10^4	1 x 10^5
Plasmid 1 amount (µg)	4	0.32	0.160	0.4-0.5
Plasmid2 amount (µg)	-	-	0.160	-
Dilution volume for Plasmid DNA (µl)	50	25	25	30
Lipofectamine 2000 (µl)	10	0.5	0.5	3
dilution volume for Lipofectamine 2000 (µl)	50	25	25	30
miRNA mimic concentration (nM)	-	50 /100	50 /100	25 / 50
Transfection volume (µl)	3000	150	150	560

2.4.6 Production of lentivirus particles

Lentivirus particles were generated by transient transfection of HEK293-T cells. 150cm^2 tissue culture dishes were seeded with 2 x 10^7 cells 24 hr before transfection. 15µg of transfer vector [tagged AGO2 lentivector (AGO2-PTH) (a generous gift from Dr. Finn Grey) or pLenti CMV Blast lenti vector (AddGene) (Appendix-2) were used as transfer lentivectors in transfections along with 13.5µg of packaging plasmid psPAX2 and 2.5µg of envelop plasmid pMD2.G (generous gifts from Dr. Finn Grey). Plasmid DNA and 160µl FuGene® HD were diluted separately in 1650ul of OptiMEM® and incubated for 5 min at room temperature. Both mixtures were then mixed together and further incubated at room temperature for 15-20 min. The mixture was then added drop wise to the cells containing fresh medium with

supplements. The plate was rocked back and forth to mix and incbubated at 37^{o}C with 5% CO_2 for 24 hr. The supernatant containing lentivirus was collected after 24 hr and then after 48hr. Both collections were pooled, filtered through 0.45µm filters (Sartorius) and stored at -80^{o}C.

2.4.7 Determination of antibiotic resistance in lentivirus transduced cells (Kill curve)

To determine the minimum concentration of the antibiotic which causes complete cell death, cells were plated in 8 wells of three 24 well plates at a cell density of 1 x10^4 per well. Puromycin (Sigma) and Blasticidin (Sigma) was used as a selection marker for the AGO2-PTH lentivirus and pLenti CMV Blast lentivirus respectively. Plates were seeded with cells on the same day and cells were added with dilutions of antibiotic ranging from 0µg/ml to 7µg/ml. The medium was replaced every 48 hr with complete medium containing appropriate antibiotic. The viability of cells was examined for 10-14 days (every 24 hr). The minimum concentration of antibiotic that caused complete cell death within 4-6 days was used for subsequent selection of lentivirus transduced cells.

2.4.8 Transduction with lentivirus particles and selection of transduced cells

Cells were seeded in 24 well plates at a cell density of 1 x 10^4 per well, in 500µl of the medium with supplements, 24 hr before transduction at 37^{o}C and 5% CO_2. Cells were transduced with appropriate lentivirus (Section 2.5.6).

Polybrene (Millipore) was used to enhance the efficiency of the lentivirus infection and 8µg per ml was diluted in 500µl of the medium with supplements. The original

medium was replaced with polybrene containing medium. For suspension cells old medium was removed by pelleting the cells by centrifugation at 1500 x g for 3-5 min. The supernatant was removed and pellet was re-suspended in 500µl of polybrene containing media. The lentivirus stock (section 2.4.6) was thawed at 37^{o}C. 2 fold dilutions of lentiviruses were prepared and the cells were infected by adding each dilution in to a separate well. The plates were rocked back and forth to mix and incubated at 37^{o}C with 5% CO_2. After 24 hr virus containing medium was removed and fresh medium with supplements was added to cells. The cells were incubated for further 24 hr at 37^{o}C with 5% CO_2. The cells were split 48 hr post transduction in the medium containing the appropriate concentration of appropriate antibiotic, for selection of successfully transduced cells. The medium was replaced with fresh antibiotic containing media every 3-4 days until all the un-transduced and control cells (un-transduced cells) died. The dilution of virus at which most of the cells remained viable after 4-6 days of selection, was used to infect cells in future transductions. Antibiotic selection was stopped after 10-14 days and successfully transduced cells were transferred into T25 cm^2 and then after a 1-2 passages into T75 cm^2 tissue culture flasks for generation of lentivirus expressing stable cell lines.

2.5 Site directed mutagenesis

For site directed mutagenesis the Quick Change Site-Directed Mutagenesis (Stratagene) protocol was followed.

2.5.1 Mutagenic primers design

Primers for mutagenesis (HPLC purified) (Eurofins MWG Operon, Germany) were designed in such a way that each primer was 42-45 bases in length, with a melting temperature (Tm) of $\geq 78^{o}C$. To estimate the primer Tm following formula was used:

$$Tm = 81.5 + 0.41(\%GC) - 675/ \text{primer length (nt)} - \% \text{ mismatch}$$

The desired mutation sites included 6 bp sequences (See Appendix-3 for mutagenic primers and mutation sites) in the middle of the primer with ~10-15 bases of correct sequence on both sides and desired mutation sites were replaced by restriction enzyme site sequence in the primers. Both primers (reverse and forward) in each pair annealed to the same region on opposite strands of the plasmid during amplification.

2.5.2 Amplification of the mutated plasmid

To amplify the mutated plasmid 50µl reaction mixture was prepared as follows:

Template DNA	= 20 ng
10x P*fu* DNA polymerase buffer	= 5.0 µl
Forward primer	= 125 ng
Reverse primer	=125 ng
dNTPs (10mM)	= 10mM
ddH2O	= up to 50µl
then add	
Pfu-Turbo (2.5 units)	= 1.0µl

PCR conditions

1st cycle = 95° for 30 seconds

and then 18 cycles of:

95°C for 30 sec

55°C for 1 min

68°C for 1 min per kb of template DNA

After PCR amplification of the mutated DNA, the parental DNA (template DNA) in the reaction mixture was degraded by enzyme Dpn-I (New England BioLabs). 1-2 µl Dpn I was added to the PCR product and incubated at 37°C for 1 hr. The DpnI digested DNA was transformed into TOP10 chemically competent cells (section 2.2.3). Plasmid DNA was purified as described in 2.2.4. Successful mutation was later confirmed by treating the sample with restriction enzymes (section 2.1.4) and by sequencing (section 2.1.8) (Appendix-3 for sequencing primers). Successfully mutated DNA templates were used for transfecting the BHK 21 cells (section 2.4.5) and for performing luciferase assays (section 2.6)

2.6 Dual luciferase assays

Luciferase reporter activity assays were performed using the Dual-Luciferase Reporter Assay System (Promega) according to manufacturer's instruction. Transfections were performed in BHK21 cells in triplicate in 24 well plates and in six replicates in 96 well plates as described in section 2.4.5.

The 3'UTRs/regions of genes of interest with predicted binding sites of OvHV-2 miRNAs were cloned downstream of a renilla luciferase reporter gene (into the multiple cloning sites) in the psiCHECK™-2 Vector (Promega) (Appendix-2 for

vector map). The psiCHECK^{TM}-2 vector also possessed a secondary firefly luciferase reporter gene which acts as a normalization control for renilla luciferase. Cells were co-transfected with reporter vectors with or without the 3'UTR of interest and with mimic miRNAs in varying concentrations as described in section 2.4.5 and incubated for 24 hr at 37^{o}C with 5% CO_2. Medium from transfected cells was carefully removed and cells rinsed in PBS. The PBS was carefully removed, and 100µl of 1x Passive Lysis Buffer (PLB) was dispensed into each well. The plate was slowly shaken for 15 min at room temperature and 20µl of the lysate from each well of a 24 well plate was transferred to a 1.5 ml tube. 100µl of the lyophilized Luciferase assay reagent II (LAR II) was added to the tube and mixed by pipetting. Firefly luciferase activity was recorded for 10 sec in DLR-0-INJ Promega GloMax 20/20 Luminometer (Promega). To the same tube 100µl of 1xStop & Glo reagent was added and Renilla luciferase activity was recorded as above. The procedure was repeated for all samples.

For samples in 96 well plates cells were lysed in 20 µl of the PLB in each well by slow shaking for 15 min at room temperature and 10µl lysate from each well was transferred to flat bottom opaque 96 well plates. A GloMax® 96 Luminometer (Promega) with double injectors was used to measure the luminescence according to manufacturer's instruction. Injector 1 of the luminometer was set to dispense 50µl LARII. For measurement, a 1-2sec delay and a 5-10sec read for firefly luciferase activity were selected. Injector 2 was then set to dispense 50µl Stop & Glo® Reagent, followed by a 1-2sec delay and 5-10sec read time for Renilla luciferase activity.

For dual luciferase assays for the validation of predicted OvHV-2 miRNA binding sites in the 5'UTRs of the genes of interest, 5'UTRs were cloned immediately upstream to firefly luciferase reporter gene into the multiple cloning sites in plasmid pGL4.10 (Promega). pGL4.10 was co-transfected into BHK-21 cells with mimic miRNAs in various concentrations as described in section 2.4.5 and another reporter vector PRL (Promega) encoding renilla luciferase gene to normalize the firefly luciferase expression. Dual luciferase assays were performed in 96 wells plates as described above.

For luciferase assays to validate the predicted target genes obtained from CLASH analysis (Section 4.4.2 and 4.4.4) custom oligonucleotides were created. Oligonucleotides were designed in such a way that each primer was 85-90 bases in length with the miRNA target site in the middle of the primer. Both primers (reverse and forward) were complementary to each other. Restriction sites were put on 5' and 3' ends of each primer. The primer pair was annealed using annealing buffer (Appendix-1). To anneal the primers pair 50 µl reaction mixture was prepared as follows:

Primer 1(100 µM): 5 µl

Primer 2(100 µM): 5 µl

Annealing buffer: 5 µl

ddH_20: up to 50 µl

The above reaction mix was incubated to 95^{o}C for 1-2 min and incubated room temperature for overnight. The annealed primers and psiCHECK vector were the digested with appropriate restriction enzymes, analysed by agarose gel electrophoresis, extracted from the gel, cloned and sequenced as described in section 2.1.5-2.1.9. Successfully cloned vectors were used to carry out luciferase assays as described above in this section.

2.7 Crosslinking , Ligation And Sequnecing of Hybrids (CLASH)

CLASH (previously called as CRAC) was performed using protocols previously described (Granneman et al., 2009, Kudla et al., 2011, Helwak and Tollervey, 2014).

2.7.1 Crosslinking of RNA and lysate preparation

3 x 10^7 AGO2 expressing BJ1035 cells (BJ1035-AGO2) were suspended in 1 ml of PBS and spread evenly in a 10cm petri plate on ice (4 plates were used per sample). Crosslinking was performed in a Stratalinker® UV Crosslinker (Stratagene) at 400mj/cm^2. Cells were then transferred to 1.5 ml tube and centrifuged at 1500 x g for 5 min at 4^{o}C. To the cell pellet was added 2.5 ml of ice cold lysis buffer with protease inhibitor (appendix-1). Tubes were incubated on ice for 10 min and then centrifuged at 14,000 x g for 10 min at 4^{o}C. Supernatant was then stored at -80^{o}C in sterile vials.

AGO2 expressing SEF (SEF-Cluster-3) with or without OvHV-2 miRNAs expression were seeded in 15 cm cell culture dishes at a cell density of 1.2 x 10^7 per plate (10 plates were used per sample). Plates were incubated for 24 hr at 37^{o}C with 5% CO_2. Media was then removed from each plate and cells were washed with cold

PBS. Plates were placed on ice and crosslinking carried out as above. After crosslinking 1ml of cold lysis buffer with protease inhibitor was added to the cells and the cells were removed with a sterile cell scrapper. The lysed cells were transferred to 15ml tubes and incubated on ice for 10 min. The tubes were then centrifuged at 14,000 x g for 10 min at 4^{o}C and supernatant was stored at -80^{o}C in sterile vials.

2.7.2 Conjugation of Dynabeads with rabbit IgG

60mg of Dynabeads (Invitrogen) were re-suspended in 16ml of 0.1M sodium phosphate buffer pH7.4 (Appendix-1). Beads were washed with slow agitation on a rocking platform for 10min. The tube containing the bead suspension was then placed onto a magnetic holder (Dyna MPC-6 Magnetic Particle concentrator) and when all the beads were attached to the magnet, the buffer was aspirated. 20µg of Rabbit IgG (Sigma) in 0.1M sodium phosphate buffer pH7.4, 3M ammonium sulphate (Appendix-1)) was added per mg of washed Dynabeads, and incubated at 30^{o}C with slow tilt rotation for 16-24 hr. Dynabeads coated with IgG were washed on the magnetic holder, once with 100mM glycine HCl pH2.5, once with 10mM Tris pH 8.8, once with 100mM triethylamine, 4 x with PBS and once with PBS 0.5% Triton X-100 (Appendix-1 for recipes). Finally the IgG coated Dynabeads were re-suspended in PBS/0.02% sodium azide (Appendix-1) and stored at 4^{o}C.

2.7.3 Small scale RISC immunoprecipitation on Dynabeads

The lysate (section 2.7.1) was added to the IgG coated Dynabeads (200µg beads /100µl sample) and incubated for 45min at 4^{o}C with slow rotation to bind the cross-

linked complex. The tube with beads was placed in the magnetic holder and when all the beads were attached to the magnet the flow through was aspirated and stored at -20^{o}C. The beads were washed with 5ml of low salt (LS-IgG-WB), 5ml of high salt (HS-IgG-WB) washing buffers and 1 x PNK_5 (Tris HCl and 5mM 2-mercaptoethanol containing buffer) (Appendix-1 for buffers recipes) to remove non-specific interaction. All washings were performed on magnetic holder as described in section 2.7.2. The Dynabeads were then re-suspended in 100µl 1 x protein sample buffer (Appendix-1). 20-25µl of the lysate (section 2.7.2) and the flow through (above) were also diluted in 3-5µl of 10 x protein sample buffer. Western blot analysis was performed on the Dynabeads sample, the flow through sample and the lysate as described in section 2.3.

2.7.4 Large scale RISC immunoprecipitation on Dynabeads

The lysate (section 2.7.1) was added to the IgG coated Dynabeads (20mg beads /one sample) and incubated for 45min at 4^{o}C with slow rotation to bind the RNA in the cross-linked complex. The beads were washed with 5ml of low salt (LS-IgG-WB), 5ml of high salt (HS-IgG-WB) washing buffers and 1 x PNK_5 (Tris HCl and 5mM 2-mercaptoethanol containing buffer) (Appendix-1) to remove non-specific interaction. All the washings of Dynabeads were performed on magnetic holder as described in section 2.7.2. To reduce the size of cross-linked RNAs Dynabeads were re-suspended in pre-warmed 500µl PNK_5 buffer, 0.5 unit RNAseA+T1 mix (1µl of 1:20 dilution in H_2O of RNase-IT cocktail) (Agilent) and incubated it for 3min at 20^{o}C. The tube was snap cooled on ice for 1 min and then placed on to the magnetic holder.

When all the beads were attached to the magnet, the RNase mix was aspirated off and then discarded.

Cross-linked complexes bound to Dyna-beads were then eluted by washing in a 3 x 250µl of 6M Guanidine-HCl containing buffer (Ni-WB-I) using the magnetic holder as described above. Before each elution beads were shaken for 10min at 20^{o}C.

2.7.5 Affinity purification of RISC complex on nickel-charged resin

Nickel-charged resin (Ni-NTA superflow, Qiagen) was used for affinity purification of 6 x His-tagged protein in the cross-linked complexes in the eluate (section 2.7.4). 50µl of the resin were washed twice with Ni-WB-I buffer by centrifugation at 1000 x g for 20-30 sec. 750µl of the eluate was then transferred to the resin and incubated at 4^{o}C for 2hr on a rotating platform. The resin was loaded onto a snap cap polyethylene spin column (Pierce) and washed, on the column, once with Ni-WB-I, once with buffer without Guanidine-HCl (Ni-WB-II) and once with 1 x PNK_5 buffer (Appendix-1). The cap from the bottom of the column was removed after each wash to remove the washing buffers by gravity flow and the cap replaced back on the column for the subsequent steps.

2.7.6 Phosphorylation, dephosphorylation and ligation of resin bound RNA in cross-linked complexes

To phosphorylate the RNAs in RISC complexes bound to resins in the column (section 2.7.5) the following reaction mix was made in a 1.5 ml tube.

ATP (stock 100mM, final 1mM(New England Biolabs)	0.8 µl
RNAsin (20U/µl stock) (New England Biolabs)	2 µl
T4 PNK (5µ/µl stock) (New England Biolabs)	4 µl
5 x PNK_{10} buffer (Appendix-2)	16 µl
Nuclease free water	57.2 µl

The above reaction mix was added to the resin in the column and incubated at 20^{o}C for 2-3 hr on a thermo-shaker at 500 rpm. In the column a ligation reaction was then performed to ligate bound miRNAs to target mRNA in the cross-linked complexes. The following reaction mix was prepared in a separate 1.5 ml tube and added to the above reaction mix in the column.

ATP (stock 100mM, final 1mM)	0.8 µl
RNAsin (20U/µl stock)	2 µl
T4 RNA ligase I (New England Biolabs)	4 µl
5 x PNK_{10} buffer	16 µl
Nuclease free water	57.2 µl

The column was then incubated at 16^{o}C overnight on a thermoshaker at 500 rpm. The ligation reaction mix was discarded by gravity flow by removing the cap from the bottom of the column. The resin in the column was washed as described in section 2.7.4. RNAs in RISC complexes bound to resin in the column were dephosphorylated using Thermosensitive Alkaline Phosphatase (TSAP) (Promega). The following reaction mix was prepared in a 1.5 ml tube and then added to the column:

TSAP	8 µl
RNAsin (20U/µl stock)	2 µl
5 x PNK_{10} buffer	16 µl
Nuclease free water	54 µl

The resin was then incubated at 20^{o}C for 45min on a thermo-shaker at 500 rpm The dephosphorylation mix was discarded and the resin in the column were washed as described in section 2.7.4. After dephosphorylation RNA in the cross-linked complexes was ligated to 3´linkers (miRCat-33, Integrated DNA Technologies) (3´ linker sequence- Appendix-3) using truncated T4 RNA Ligase II (New England Biolabs). The following reaction mix was prepared in a 1.5 ml tube and then added to the column.

3' linker (10µM)	8 µl
T4 RNA Ligase II, truncated	4 µl
RNAsin (20u/ul stock)	2 µl
PEG 8000 (stock 25%, final 10%) (New England Biolabs)	32 µl
5 x PNK_{10} buffer	16 µl
Nuclease free water	18 µl

The above reaction mix was incubated at 16^{o}C, overnight on a thermoshaker at 500 rpm. The column was then washed as described in section 2.7.4. RNA in the cross-linked complexes in the column was then radiolabeled with T4 polynucleotide kinase (New England Biolabs) and ATP [γ-^{32}P] (6000Ci/mmol, 10mCi/ml EasyTide,

250µCi, Perkin Elmer) for visualization. The following reaction mix was prepared in a 1.5 ml tube and then added to the column.

32P-γ-ATP	3 µl
RNAsin (20U/µl stock)	2 µl
T4 PNK (5U/µl stock)	4 µl
5 x PNK_{10} buffer	16 µl
Nuclease Free Water	55 µl

Columns were incubated at 37°C, for 40min on a thermoshaker at 500 rpm and then washed as described in section 2.7.3.

2.7.7 Elution of RNA bound to cross-linked complexes from the nickel resin

Elution of the RNA bound to cross-linked complexes from the nickel resin (section 2.7.6) was performed with 1ml of imidazole containing elution buffer (Ni-EB-200) (Appendix-1) at room temperature. The resin in the column was re-suspended in 200 µl Ni-EB-200 and incubated in a thermoshaker at room temperature for 5 min. The elution was performed by removing the cap at the bottom of the column and eluate was collected in a 1.5 ml tube by gravity flow. The elution step was repeated twice with 200 µl and 600 µl of Ni-EB-200 respectively in the same 1.5 ml tube as described above.

2.7.8 Trichloroacetic acid (TCA) precipitation of RNA bound to cross-linked complexes

200µl of 100% TCA (Appendix-1) was mixed with 1ml of the eluate (section 2.7.7) and 2µg of bovine serum albumin (BSA) and the sample was centrifuged for 20min at 4^{o}C at 14,000 x g. The pellet was washed twice by centrifugation at 14,000 x g for 10min with 1 ml of ice cold acetone to remove any remaining TCA and vortexed before each centrifugation. The pellet was air dried and re-suspended in 10µl of nuclease free water and 10µl of 2 x Sample Buffer (NuPAGE). The sample was heated for 10min at 65^{o}C and the RNA bound to cross-linked complexes was resolved on a 4–12% BisTris NuPAGE precast gel (Invitrogen) in NuPAGE 1 x MOPS SDS running buffer (Invitrogen) in Mini-PROTEAN electrophoresis system (BIO-RAD). ColourPlus Prestained Protein marker (BioLabs) was loaded into one well for protein size estimation. The gel was run at 150 V for 40min-1 hr or until the xylene cyanol reached the end of the gel. The separated proteins were then transferred to a Polyvinylidene fluoride (PVDF) membrane (Millipore). The transfer was performed using the wet transfer method using NuPAGE Transfer Buffer (Invitrogen) with methanol (20% v/v). PVDF, 6 pieces of 3MM Chr chromatography paper (Whatmann) and 2 sponges were cut to the size of gel. The membrane was soaked in methanol and the blotting papers and sponges were soaked in the transfer buffer prior to use. The membrane was then sandwiched between 3 sheets of soaked blotting papers and sponges. Trapped air bubbles were carefully squeezed out by gently rolling a pipette over the top of blotting papers. The transfer was performed at 100V for 2hr on ice, in a vertical tank filled with transfer buffer. After transfer the

membrane was carefully removed, wrapped in a cling film and exposed to film (Kodak BioMax MS-1) for 24 hr at -80^{o}C along with a fluorescent ruler. The film was put over the membrane and with a needle the film and the membrane was pierced in correspondence to an approximately 100Kd band. Using the holes as reference remove the membrane slice out with a sterile blade and transferred into a 1.5 ml tube.

2.7.9 Extraction of the RNA bound to cross-linked complexes from the PVDF Membrane

100µg of proteinase K mixed with 400µl of proteinase K mix (Appendix-1) was added to the membrane slice (section 2.7.8) to digest the proteins associated with the cross-linked complexes and was incubated for 2hr at 55^{o}C on thermoshaker at 500 rpm. The membrane was then removed from the sample and proteinase K treated mix was used in the subsequent steps.

2.7.10 Phenol: Chloroform: Iso-amylalcohol (PCI) extraction and ethanol precipitation

RNA was subsequently extracted by adding 50µl 3M sodium acetate pH5.5 and 500µl PCI to the proteinase K treated mix (section 2.7.9) and centrifuged at a 14,000 x g at 4^{o}C for 30 min. The upper phase of the sample was collected and 1ml 100% ethanol and 20 µg of glycoblue (Invitrogen) added. The reaction mix was then incubated at -80^{o}C for 30min and centrifuged at a 14,000 x g at 4^{o}C for 30min. The pellet was washed twice with 1 ml of 70% ethanol by centrifugation at 14,000 x g for 5min, air dried and re-suspended in 12.5 µl of nuclease free water.

2.7.11 Phosphorylation and ligation 5´ linkers to the cross-linked RNA

12.5 µl recovered cross-linked RNA (section 2.7.10) was phosphorylated by adding 1µl polynucleotide kinase, 1.5µl 10 x RNA ligase buffer I and 1mM ATP to make up total volume up to 15µl. The reaction mix was incubated for 30min at 37°C on a thermoshaker at 500 rpm. The RNA in the reaction mix was then ligated to 1µl barcoded 5′ linkers (Appendix-3) (a generous gift from Dr. Finn Grey) with 0.5µl T4 RNA ligase I (New England Biolabs) and 2.5 µl of nuclease free water at 16 °C overnight on a thermoshaker at 500 rpm. For each sample a different 5' linker was used. After 5′ linker ligation another PCI extraction and ethanol precipitation was performed as described in section 2.7.10. The RNA pellet was re-suspended in 8µl of nuclease free water.

2.7.12 Reverse transcription (RT) and PCR amplification of cDNA

Cross-linked RNA (section 2.7.11) was used as a template for reverse transcription using the miRCat-33 primer (Integrated DNA Technologies IDT) for the production of cDNA. The following reaction mix was added to the 8µl of cross-linked RNA.

dNTPs (2.5mM)	4 µl
3'miRCat RT Primer (10µM)	1 µl

The sample was incubated at 80^{o}C for 3 min and on ice for 5 min. 6µl of the following reaction mix was then added to sample:

First Strand Buffer (Invitrogen)	4 µl
0.1 M Dithiothreitol (DTT)	1 µl
RNasin (20U/µl stock)	1 µl

The sample was incubated at 50^{o}C for 3min. 1µl of Superscript III (Invitrogen) was added to the sample and further incubated at 50^{o}C for 1 hr. To inactivate the Superscript the sample was heated at 65^{o}C for 15min and to degrade template RNA 2µl RNase H (New England BioLabs) was added to the sample at 37^{o}C for 30 min. The sample (cDNA) was used as a template for the PCR amplification.

PCR was performed using TaKaRa Ex Taq Polymerase (Millipore) and was carried out in 0.2 ml thin walled tubes in a PCR Sprint Thermal Cycler, (Thermo Scientific). In each reaction 1x PCR buffer with 2mM $MgCl_2$ was mixed with >500ng template DNA, 200 mM of both the forward (Invitrogen) and reverse (mirCat-33 IDT) primers, 2.5mM each dNTP, 5 I.U of TaKaRa Ex Taq Polymerase and nuclease free water for a total of 50µl. The reaction conditions consisted of

1 x cycle	initial denaturation at 95^{o}C for 2 min
21 x cycles of	denaturation at 98^{o}C for 20 sec,
	annealing at 52^{o}C for 20 sec,
	extension at 68^{o}C for 20 seconds

and a final extension cycle of 5 min at 72^{o}C.

The PCR product was purified using Qiaquick MINIELUTE Columns (Qiagen) as described in section 2.1.4. Purified PCR product was then resolved on 3% MethaPhor agarose gels (Lonza) as described in section 2.1.4. PCR fragments of 70-120bp were excised from the gel. Gel purification of DNA was carried out as

described in section 2.1.6. The gel purified products were used as barcoded libraries for small scale and high throughput sequencing.

2.7.13 Small scale sequencing of gel purified PCR products

For small scale sequencing cloning of the purified cloned (section 2.1.4) into the PCR4-TOPO vector as described in section 2.1.8 and then transformed into TOP10 chemically competent cells as described in section 2.2.3. At least 12 clones per sample were picked from the LB agar plate, supplemented with ampicillin and plasmid DNA was extracted as described in section 2.2.4. Sequencing of the clones was carried out using Big Dye Terminator v3.1 Cycle Sequencing Kit (Applied Biosystems/Ambion) as described in section 2.1.9. The plasmids were sequenced by GATC Biotech, Germany. Sanger sequencing results were first analysed with Blast (http://blast.ncbi.nlm.nih.gov) to locate 3′ and 5′ linkers. Between pairs of linkers sequences of fragments (inserts) were also extracted and analysed with a second round of blast for homology with bovine or ovine RNA reference sequences (http://blast.ncbi.nlm.nih.gov).

2.7.14 High through put sequencing of gel purified PCR products and bioinformatics analysis

For high through put sequencing, the barcoded libraries (2.7.12) were pooled together and sent to ARK Genomics, The Roslin Institute, University of Edinburgh for sequencing by the Illumina Solexa (single-end sequencing, 100bp read length). Bioinformatics analysis were carried out in collaboration with Mr. Mick Watson (University of Edinburgh) and with the kind help of Dr. Finn Grey (University of

Edinburgh) (Section 4.3.1.4). Differentially enriched gene list was obtained using R (version 2.13.0) package EdgeR (Robinson, MD, and Smyth, GK., 2008) with p-<0.05 and to control for false positive predictions a 5% false discovery rate (FDR) threshold was applied the datasets (Section 4.3.2.8).

2.8 Microarray study

2.8.1 RNA processing and array hybridization

Total RNA was isolated as described in Section 2.1.10. A total 5 µg RNA per sample was sent to ARK Genomics, The Roslin Institute, University of Edinburgh. Samples were processed using Ambion GeneChip Whole Transcript Sense Target Labelling Assay and the microarray was run. Briefly total RNA of each sample was used as a template for synthesis of single stranded cDNA. Single stranded cDNA was then converted to double stranded cDNA which was then used as a template to generate antisense cRNA and amplified by *in vitro* transcription. cRNA was then purified and used for the synthesis of second cycle cDNA using random primers and the dUTP + dNTP. cRNA was degraded using RNase H leaving intact single stranded cDNA. single stranded cDNA was purified to remove enzymes, salts and unincorporated dNTPs. 5.5 µg of cDNA was then fragmented, labelled, hybridized to the Affymetrix GeneChip ovine 1.0 ST array and scanned by following the manufacturer's protocol using The Affymetrix GeneChip® Whole Transcript Terminal Labelling kit and GeneChip® Hybridization, Wash, and Stain Kit.

2.8.2 Microarray analysis

The analysis of the microarray data was performed with the help of Miss Alison Downing from ARK Genomics using Partek Genomic suite (Section 4.3.2.9). Differentially expressed genes with a statistical significance of $p<0.05$ were identified using ANOVA. A 5% false discovery rate was applied to avoid false positive predictions.

2.9 Software and programmes

2.9.1 BLAST (Basic Local Alignment Search Tool)

http://blast.ncbi.nlm.nih.gov/Blast.cgi

The nucleotide blast algorithms blastn was used to align a nucleotide query against nucleotide database available in GenBank (http://blast.ncbi.nlm.nih.gov/Blast.cgi).

2.9.2 RNAhybrid

http://bibiserv.techfak.uni-bielefeld.de/rnahybrid/welcome.html

RNAhybrid was used for miRNA target prediction. It is a tool for finding minimum free energy (mfe) hybridization of a long and short RNA.

2.9.3 UNAfold

http://eu.idtdna.com/Unafold/

UNAfold is used for nucleic acid folding and hybridization prediction. It provides multiple folding of single-stranded RNA or DNA or hybridization between two single strands at different mfe (Markham and Zuker, 2008).

2.9.4 IBM SPSS statistics 22

http://www-01.ibm.com/software/uk/analytics/spss/

SPSS statistics 22 was used to perform ANOVA and Post Hoc Tuckey's HSD multiple comparison test to find the significance difference between the groups (Section 3.3.2).

2.9.5 Ingenuity Pathway analysis (IPA)

http://www.ingenuity.com/products/ipa

IPA was used to interpret the data in the context of biological processes and canonical pathways and to analyse the involvement of different genes in different molecular and cellular functions (Section 4.3.2.12).

2.9.6 Databases

GeneCards®
http://www.genecards.org/

miRBase
http://www.mirbase.org/

Ensembl genome browser
www.ensembl.org/

National center for Biotechnology information (NCBI)
www.ncbi.nlm.nih.gov/

Chapter 3: Analysis of OvHV-2 ORFs as Ovhv2-miRs Targets

3.1 Aims

3.2 Introduction

3.3 Results

3.4 Discussion

Note: This work has been published in (Riaz *et al*., 2014) (Appendix-4).

3.1 Aim

The aim of this study was to determine if OvHV-2 miRNAs target the predicted OvHV-2 ORFs.

3.2 Introduction

The identification and validation of predicted miRNAs targets is essential to allow an understanding of miRNA functions. The most common experimental approach for the analysis of the interaction of miRNAs with their predicted mRNAs targets is a reporter gene assay. After transient transfection into a cell, a miRNA binds to its specific mRNA target site and represses the reporter protein production, thereby reducing activity/expression of the reporter gene (Kuhn *et al*., 2008). In this study the validation of viral miRNAs (ovhv2-miRs) targets within the OvHV-2 genome was performed using dual luciferase assays. OvHV-2 encodes 46 predicted miRNAs; eight of which were validated by northern blot analysis (Levy *et al*., 2012). Bioinformatic analysis predicted several possible targets for these eight miRNAs within the OvHV-2 genome. In this study six of the OvHV-2 ORFs which had predicted target sites for the ovhv2-miRs within their 5´UTR or 3´UTR, were selected for functional validation. The genes selected for the validation are predicted to be involved in virus replication/latency. These ORFs were Ov2, ORF20, ORF36, ORF49, ORF50 and ORF73. The functions of these ORFs in related gammaherpesviruses and the ovhv2-miRs which target them are described below:

3.2.1 OvHV-2 Ov2

Ov2 is one of the unique ORFs of OvHV-2 and its transcript was also highly expressed in the BJ1035 cells (Levy PhD thesis, 2012). Ov2 is homologous to A2 in AlHV-1 and is predicted to encode a protein containing a basic leucine-zipper (bZIP) motif. It is also homologous to activating transcription factor (ATF), cAMP response element binding protein (CREB) and Jun dimerization proteins (Ensser *et al*., 1997, Hart *et al*., 2007). ATF is a member of the ATF/CREB family of transcription factors and can regulate gene expression by binding to the consensus ATF/CREB *cis-regulatory* element via a bZIP domain (Wang *et al*., 2012). Martinez & Tang showed that the leucine zipper domain was required for the interaction of the KSHV bZIP protein with histone deacetylase and this interaction is important for KSHV replication (Martinez and Tang, 2012).

ovhv2-miR-4 has a predicted target site in the 3´UTR of Ov2.

3.2.2 OvHV-2 ORF20

In related herpesviruses, homologues of ORF20 (UL24 in HSV-1, UL76 in HCMV and ORF20 in KSHV and MHV-68) are involved in controlling cell cycle. MHV-68 ORF20 was characterized as being a nuclear protein which localized in the nucleus and caused cell cycle arrest at the G2/M phase of cell cycle, possibly leading to apoptosis. Its mechanism of action is to maintain Cdc2 in its phosphorylated inactive state, such that Cdc2–cyclin B complexes in cells expressing ORF20 exhibit little or no kinase activity (Nascimento *et al*., 2009, Nascimento and Parkhouse, 2007). In a

previous study in our laboratory it was shown that, like MHV-68 ORF20, OvHV-2 ORF20 also localizes to the nucleus (Levy PhD thesis, 2012).

ovhv2-miR-5, ovhv2-miR-6 and ovhv2-miR-7 have predicted target sites in the 3´UTR and ovhv2-miR-2, ovhv2-miR-4 and ovhv2-miR-5 have predicted target sites in the 5´UTR of ORF20.

3.2.3 OvHV-2 ORF36

OvHV-2 ORF36 has homology to protein kinases which are conserved among the *Herpesviridae* family (ORF36 of KSHV, UL13 of HSV, ORF47 of VZV and BGLF4 of EBV). These kinases share motifs with mammalian serine/threonine protein kinases (Kawaguchi *et al*., 2003). Herpesviruses utilise their protein kinases not only to regulate their own replicative processes but also to modify the host cellular machinery by phosphorylating target machinery (Kawaguchi and Kato, 2003). The importance of herpesvirus protein kinases for viral replication and disease has been investigated. Kinase-null mutants generated in alpha, beta, and gammaherpesviruses demonstrate decreased replication in tissue culture. Decreased virulence of HSV and VZV null mutants was also observed in a mouse model (Hamza *et al*., 2004).

ovhv2-miR-8 has a predicted target site in the 3´UTR of ORF36.

3.2.4 OvHV-2 ORF50

OvHV-2 ORF50 is a homologue of ORF50 (KSHV, RRV, MHV68 and AlHV-1) and BRLF1 of EBV (Damania *et al*., 2004, Gonzalez *et al*., 2006, Hart *et al*., 2007). ORF50 encodes a viral immediate-early transactivator protein; Rta (Section 1.3.2). In

KSHV this protein is indispensable for reactivation from latency and introduction of ORF50 into the latently infected cells alone is sufficient to initiate the viral lytic cascade (Damania *et al*., 2004) which results in viral protein production, assembly and release of virus. Rta can also initiate transcriptional activation of viral promoters, by binding in a sequence specific manner to viral DNA via Rta responsive elements, which in turn can start a cascade of lytic lifecycle (Sun *et al*., 1998). Thonur *et al* showed expression of OvHV-2 ORF50 and some other productive genes in OvHV-2 infected T cells after treating those with drug doxorubicin (Thonur *et al*., 2006). A transient peak in OvHV-2 DNA and OvHV-2 transcripts including ORF50 was also found in lungs of bison experimentally infected with OvHV-2, 9-12 days post infection, suggesting occurrence of viral replication (Cunha *et al*., 2012).

ovhv2-miR-5 has one predicted target site in the 3'UTR, ovhv2-miR-3 and ovhv2-miR-8 has one predicted target site each in the CDS and ovhv2-miR-6 has one predicted target site in the 5'UTR of ORF50.

3.2.5 OvHV-2 ORF49

In both KSHV (Gonzalez *et al*., 2006) and MHV68 (Lee *et al*., 2007) ORF49 lies adjacent and in the opposite orientation to ORF50. The protein encoded by ORF49 is expressed during the KSHV lytic cycle and shows early transcription kinetics. ORF49 is able to cooperate with ORF50 to activate several KSHV lytic promoters and could induce phosphorylation and activation of the transcription factor c-Jun, the Jun N-terminal kinase (JNK), and p38. The work suggests that ORF49 protein functions to activate the JNK and p38 pathways during the KSHV lytic cycle

(Gonzalez *et al*., 2006). The EBV homologue of ORF49 (BRRF1) has been shown to act as a transcriptional transactivator that co-operates with the BRLF1 to induce lytic replication in certain cell types (Hong *et al*., 2004). Hart *et al* predicted that OvHV-2 encodes an ORF49 homologue while AlHV-1 does not (Hart *et al*., 2007).

ovhv2-miR-6 has two predicted target sites in 3'UTR of ORF49 (Fig-6).

3.2.6 OvHV-2 ORF73

ORF73 is predicted to encode for the latency-associated nuclear antigen (LANA) in KSHV and functions to transactivate the viral latent origin of replication and tethers viral episomes to host chromosomes, thereby ensuring faithful segregation of the viral genome during cell mitosis (Grundhoff and Ganem, 2003). LANA and its functional homologue EBNA1 in EBV are consistently expressed in cells during latency and are crucial for the maintenance of viral episome in proliferating cells (Purushothaman *et al*., 2012, Sivachandran *et al*., 2012).

ovhv2-miR-6 has one predicted target site each in the 3′UTR and 5'UTR of ORF73 whereas ovhv2-miR-8 has two predicted target sites in the 5′UTR of ORF73.

There is no suitable cell culture system to propagate OvHV-2 therefore it is difficult to study the regulation of viral proteins under the influence of OvHV-2 encoded miRNAs. To confirm if the miRNAs are targeting the predicted targets in the 3′UTR or in the 5′UTR of the selected ORFs and for the functional validation of those targets sites, dual luciferase reporter assays were performed. The reduction of luciferase expression due to the targeting of miRNA target site/s upon treatment with

corresponding miRNA/s is easily measurable and expression of control luciferase gene by treatment with miRNA/s can help in normalizing the result readings.

3.3 Results

3.3.1 Investigation of OvHV-2 miRNA regulation of OvHV-2 ORFs

To investigate the effect of Ovhv2-miRs on the expression of the OvHV-2 ORFs containing predicted target sites (Section 3.2), luciferase assays were performed. The 3′UTRs of Ov2, ORF20, ORF36, ORF49, ORF50, ORF73 and the 5′UTR of ORF20 and ORF73 were selected for OvHV-2 miRNA target validation. To determine the potential regulatory effect of these miRNAs, 3′UTRs and 5′UTRs of the selected ORFs were amplified by PCR. For 3′UTRs primers were designed for the regions from the stop codon to the predicted polyA site. For the 5′UTRs primers were designed for the region from the start codon to 1000 bp upstream to allow correct expression from the natural promoter. For each ORF a separate PCR was setup and carried out using template DNA isolated from BJ1035 cells (Section 2.1.1). Successfully amplified 3′UTRs were cloned into the psiCHECK plasmid downstream of the renilla luciferase reporter gene (Rluc) and 5′UTRs were cloned into the pGL4.10 plasmid upstream of the firefly luciferase reporter gene (Fluc). BHK21 cells were co-transfected with the 3′UTRs constructs (LUC/Ov2-3', LUC/20-3',LUC/36-3',LUC/49-3',LUC/50-3'and LUC/73-3') or the 5′UTRs cloned plasmids (LUC/20-5' and LUC/73-5') with or without test or control miRNAs. Samples were harvested and luciferase levels were measured after 24 hrs (Section 2.6). The predicted targets which showed a significant knockdown in luciferase gene expression compared to their controls were then tested again by knocking out the predicted target sites using site directed mutagenesis (Section 2.5).

For site directed mutagenesis the parental luciferase constructs were used as template and a mutation was introduced in the predicted target site. Successfully mutagenized plasmids and template plasmids were used to perform luciferase assays (Section 2.6) to determine if there was a significant difference in luciferase gene expression with and without miRNA target sites.

3.3.2 Validation of OvHV-2 miRNAs targets in the 5'UTR of the selected OvHV-2 ORFs

BHK21 cells were co transfected with the LUC/20-5' or the LUC/73-5' luciferase constructs along with the PRL-TK plasmid (PRL) (Appendix-2). PRL contains a gene encoding Rluc and was used as an internal control to allow normalization of the Fluc expression. Test or control miRNAs were also transfected in two different concentrations (50 nM and 100 nM). All the transfections were carried out in 96 well plates for 24 hours. The pEGFP-N3 (Clontech) plasmid was used as a transfection control. For each region of interest three independent experiments were performed with 6 replicates for each sample. The following combinations were tested for each target:

1. No transfection (control)
2. Mock transfection (control)
3. pEGFP-N3 (transfection control)
4. Empty vector (control)
5. Empty vector + target miRNA mimics (control)
6. Target in pGL4.10 (positive control)

7. Target in pGL4.10 + each of the test miRNA mimics (Test)
8. Target in pGL4.10 + all of the test miRNAs mimics (Test)
9. Target in pGL4.10 + scramble miRNA (negative control)
10. Target in pGL4.10 + irrelevant miRNA mimic (mimics of Ovhv2-miRs that were not predicted to target the 5'UTR of the selected ORF and were used as additional negative control)

After 24 hours samples were harvested and luciferase levels were measured. The non-transfected and mock transfected sample values were used to correct for background luciferase readings. Corrected Fluc to corrected Rluc luciferase ratio values (Fluc/Rluc) were calculated. To calculate luciferase activity, luciferase level of each sample was compared with the mean luciferase level of the negative control (scramble miRNA) value. To determine if there was a significant difference between groups, a Post Hoc Tukey's HSD (honest significant difference) multiple comparison test was performed followed by a single factor analysis of variance (ANOVA). For all experiments an empty vector (lacking OvHV-2 ORF's sequence) was used to investigate off-target effects however no significant reduction in luciferase expression was observed using any of the ovhv2-miRs (Supplemental data file-3.1).

3.3.2.1 Validation of ORF73 as a predicted target of ovhv2-miR-6 and ovhv2-miR-8

No significant changes were observed in the expression of the luciferase gene tagged with the 5'UTR of ORF73 when test miRNA mimics (ovhv2-miR-6, 8 or 6+8) or irrelevant miRNA (ovhv2-miR-7) were used at 50 nM concentration [(LUC/73-

5'+miR7) p=0.999, (LUC/73-5'+miR6) p=1, (LUC/73-5'+-miR8) p=0.945, (LUC/73-5'+miR6+8) p=0.997]. While in the absence of any miRNA (test or control), the 5'UTR ORF73 showed a significantly higher luciferase expression [(LUC/73-5') p>0.001]. Following co-transfection with 100 nM of ovhv2-miR-8, ORF73 showed a significant ~50% reduction in luciferase expression in comparison to negative control [(LUC/73-5'+miR8) p=0.002]. At 100 nM ovhv2-miR-6, ovhv2-miR-6+8 and ovhv2-miR-7 showed a non-significant difference [(LUC/73-5'+miR6) p=1, (LUC/73-5'+miR6+8) p=0.479, (LUC/73-5'+miR7) p=1]. Consistent with the observations made at 50 nM, a significant enhancement of luciferase expression, over the negative control at 100 nM concentration, was seen in the absence of miRNAs (test or control) [(LUC/73-5') p>0.001] (Figure 3.1). Sequencing analysis later revealed a one bp difference in the predicted target region of ovhv2-miR-6 in the 5'UTR of ORF73 in the BJ1035 isolate used in this experiment compared to the published ORF73 sequence (Figure 3.3).

3.3.2.2 Site directed mutagenesis to remove ovhv2-miR-8 sites in the 5'UTR of ORF73

Luciferase assays showed a significant reduction in luciferase expression with the 5'UTR of ORF73 in the presence of 100 nM of ovhv2-miR-8 (Section 3.3.2.1). To analyse if the knockdown was due to specific targeting of the 5'UTR of ORF73 at the predicted ovhv2-miR-8 target sites, the sites were deleted by site directed mutagenesis (Section 2.5). The 5'UTR ORF73 was predicted to contain two ovhv2-miR-8 target sites and each site was replaced by an appropriate restriction site (Appendix-3). BHK21 cells were transfected with either ovhv2-miR-8 target site 1

deleted luciferase construct (LUC/73-5'-M1) or ovhv2-miR-8 target site 2 deleted luciferase construct (LUC/73-5'-M2). Parental template plasmid (LUC/73-5') was transfected separately as a positive control. For each luciferase assay the following combinations were tested;

1. Mutagenized or parental template constructs + ovhv2-miR-8 (test miRNA; 100 nM concentration)
2. Mutagenized or parental template constructs + negative control (scramble miRNA; 100 nM concentration)
3. Mutagenized or parental template constructs + irrelevant mimic miRNA (ovhv2-miR-7 an additional negative control; 100 nM concentration)

The Fluc and Rluc values were corrected and Fluc/Rluc ratios of each group were calculated with respect to the negative control of the same group (Section 3.3.2). The parental template construct showed a significant repression in the luciferase expression with ovhv2-miR-8 and a significantly higher expression with ovhv2-miR-7 as compared to the negative control [(LUC/73-5'+miR8) $p>0.001$, (LUC/73-5'-miR7) $p>0.001$]. Deletion of ovhv2-miR-8 sites from the 5'UTR of ORF73 restored the luciferase expression levels to that comparable to the negative control [(LUC/73-5'-M1+miR-8) $p=0.08$, (LUC/73-5'-M2+miR-8) $p=0.102$] (Figure 3.2).

These results showed that deleting either the ovhv2-miR-8 site1 or the ovhv2-miR-8 site2 from the 5'UTR of ORF73 caused a more than 20% and 50% increase in luciferase expression respectively as compared to the parental construct in the

presence of ovhv2-miR-8. This data strongly suggests that ovhv2-miR-8 can interact with the 5'UTR of ORF73 and act to down-regulate expression of that gene.

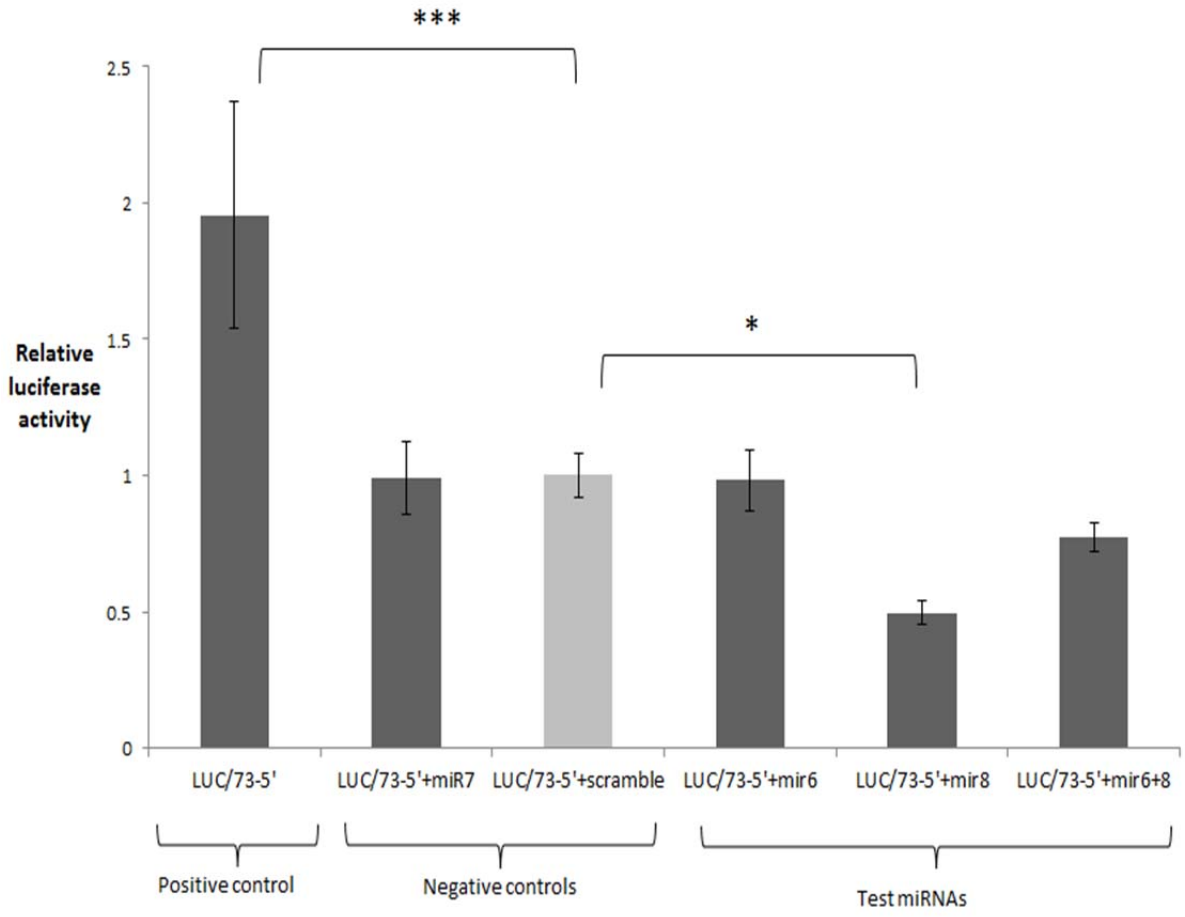

Figure 3.1: Luciferase expression levels in BHK21 cells transfected with the 5'UTR of ORF73 luciferase construct (in the pGL4.10 plasmid) in the presence/absence of target miRNA at 100 nM concentration.

Data is represented as luciferase activity with the *=$p<0.05$ and ***=$p<0.001$ relative to the respective scramble miRNA (negative control) (light grey) value at 100 nM concentration.

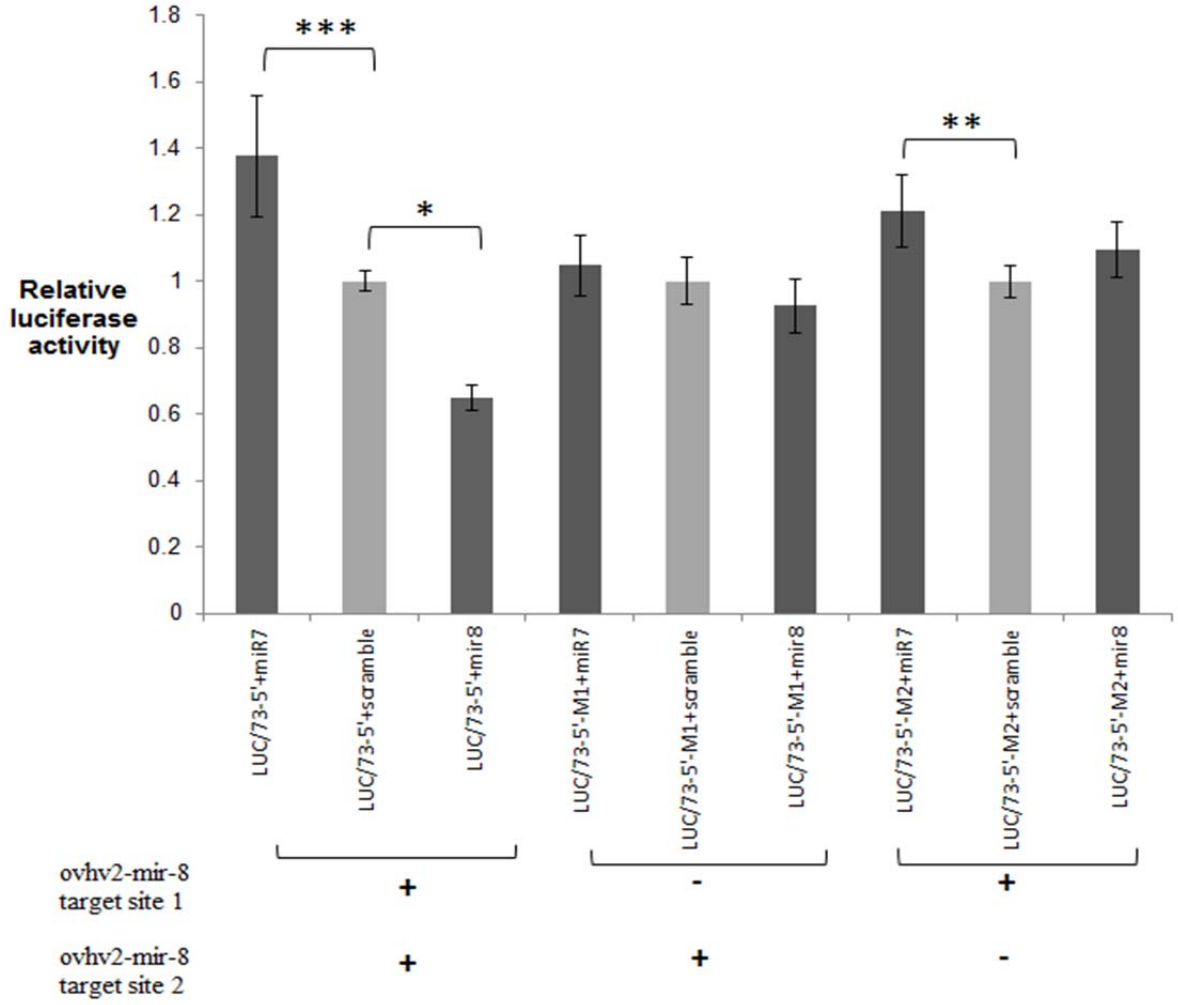

Figure 3.2: Luciferase expression levels in BHK21 cells transfected with the 5'UTR of the ORF73 luciferase constructs (in pGL4.10 plasmid) with or without deletion in the test miRNA target sites in the presence or absence of test miRNA at 100 nM concentration.

Data is represented as luciferase activity with the *=$p<0.05$, **=$p<0.01$, ***=$p<0.001$ relative to the respective scramble miRNA (negative controls) (light grey) value at 100 nM concentration. Mimic of Ovhv2-miR-8 was used as test miRNA and ovhv2-miR-7 was used as an additional negative control miRNA.

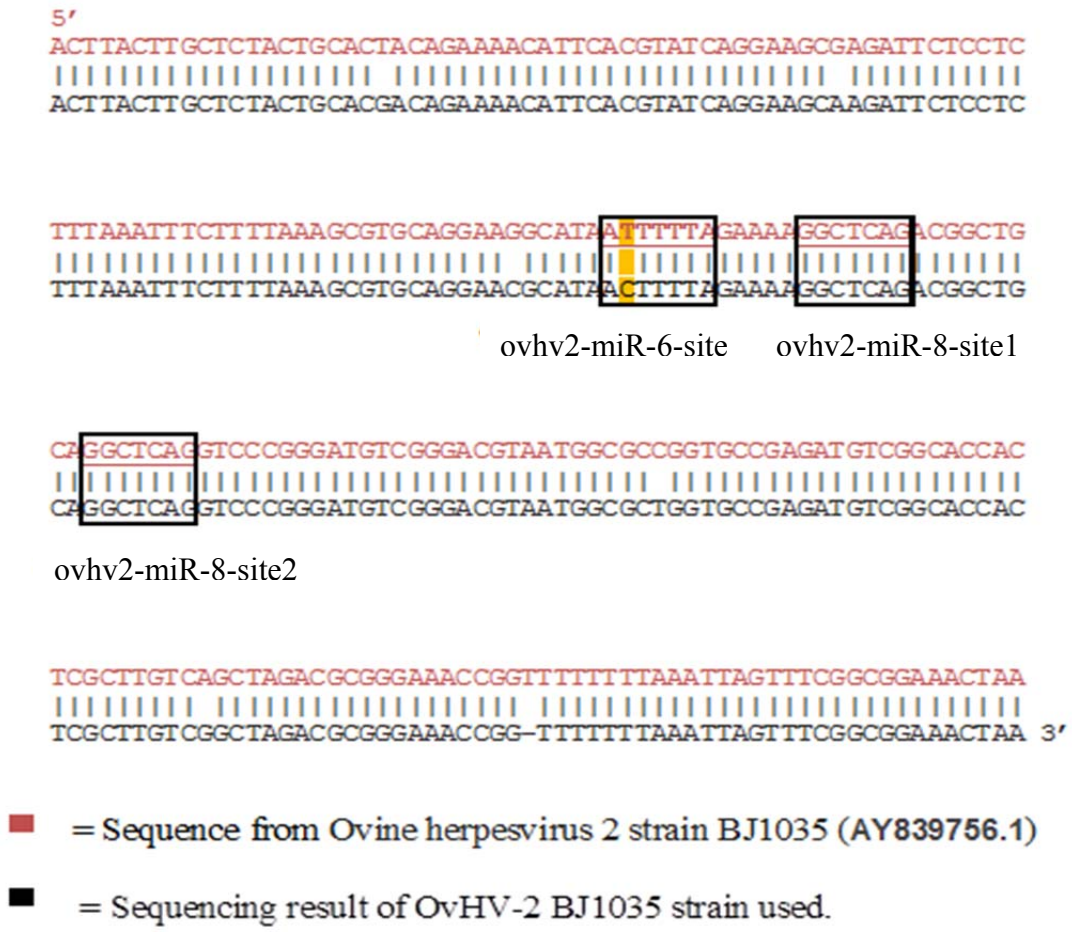

Figure 3.3: The 5'UTR of the OvHV-2 ORF73.

The 5'UTR of the OvHV-2 ORF73 (in black) amplified by polymerase chain reaction (PCR) has a one nucleotide difference in the predicted target region of ovhv2-miR-6 (highlighted in orange) from the published OvHV-2 strain BJ1035 (AY839756.1) ORF73 5'UTR sequence (in red). Black boxes show two predicted target sites of ovhv2-miR-8 and a single predicted target site of ovhv2-miR-6.

3.3.2.3 Validation of ORF20 as a predicted target of ovhv2-miR-2

Co-transfection of the luciferase construct containing the 5'UTR of ORF20 (LUC/20-5') with ovhv2-miR-2 at both 50 nM and 100 nM concentrations resulted in a significant reduction, approximately 40% and 50% in luciferase expression respectively in comparison to the negative control [(LUC/20-5'-miR2, 50 nM) $p>0.001$, (LUC/20-5'-miR2, 100 nM) $p>0.001$]. 50 nM of ovhv2-miR-5 showed a significant increase [(LUC/20-5'miR5, 50 nM) $p=0.015$] but this effect was lost at the higher concentration tested (100 nM) [(LUC/20-5'+ovhv2-miR-5, 100 nM) $p=0.064$]. The presence of ovhv2-miR-4 at 50 nM and 100 nM showed no significant effect [(LUC/20-5'+miR4, 50 nM) $p=0.434$, (LUC/20-5'+miR4, 100 nM) $p=0.982$]. All of the three test miRNAs were also used together at a final concentration of either 50 or 100 nM. At 50 nM no significant effect on luciferase expression on ORF20 was observed while at 100 nM a significant knockdown in luciferase activity was observed [(LUC/20-5'miR2-4-5, 50 nM) $p=0.939$, (LUC/20-5'+miR2-4-5, 100 nM) $p=0.021$]. The ovhv2-miR-7 at 50 nM and 100 nM showed no significant difference to negative control [(LUC/20-5'+miR7, 50 nM) $p=0.663$, (LUC/20-5'+miR7, 100 nM) $p=0.975$]. The ORF20 construct without control or test miRNAs showed a significantly higher expression in luciferase expression when compared to the negative control [(LUC/20-5', 50 nM) $p>0.001$, (LUC/20-5', 100 nM) $p>0.001$]. Figure 3.4 shows the results with 100 nM mimic concentrations.

3.3.2.4 Site directed mutagenesis to remove predicted ovhv2-miR-2 sites in the 5'UTR of ORF20

In order to confirm observed reduction in luciferase expression of LUC/20-5' (Section 3.3.2.1) with the ovhv2-miR-2 and not with the other miRNAs tested (ovhv2-miR-4 and ovhv2-miR-5), deletion of the ovhv2-miR-2 site was performed by site directed mutagenesis (Section 2.5). BHK21 cells were transfected with ovhv2-miR-2 target site deleted luciferase construct (LUC/20-5'-M). Parental template plasmid (LUC/20-5') was transfected separately as a positive control. For each luciferase assay different combinations as described in Section 3.3.2.2 were tested. The Fluc and Rluc values were corrected and Fluc/Rluc of each group were calculated as described in Section 3.3.2.

No abrogation of inhibition was observed in levels of luciferase expression when LUC/20-5'-M was co-transfected with ovhv2-miR-2 as compared to that of the parental template [(LUC/20-5'+miR2) $p>0.001$, (LUC/20-5'+miR7) $p=0.032$, (LUC/20-5'-M+miR2) $p>0.001$, (LUC/20-5'-M+miR7) $p=0.002$] (Figure 3.5). Both ORF20 constructs (parental and mutated) showed a 50 to 60% reduction in the luciferase activity as compared to that of the negative controls. These results suggest that the observed reduction of ORF20 (Figure 3.4) is not a direct result of miRNA binding to the predicted target site and may require the presence of other factors/target sites not yet identified.

Subsequently bioinformatic analysis identified at least three more target sites with G:U pairing in the seed region in the 5'UTR of OvHV-2 ORF20. The presence of

these additional putative binding sites may explain the failure to recover the inhibition in luciferase activity, using site directed mutagenesis (Figure 3.6).

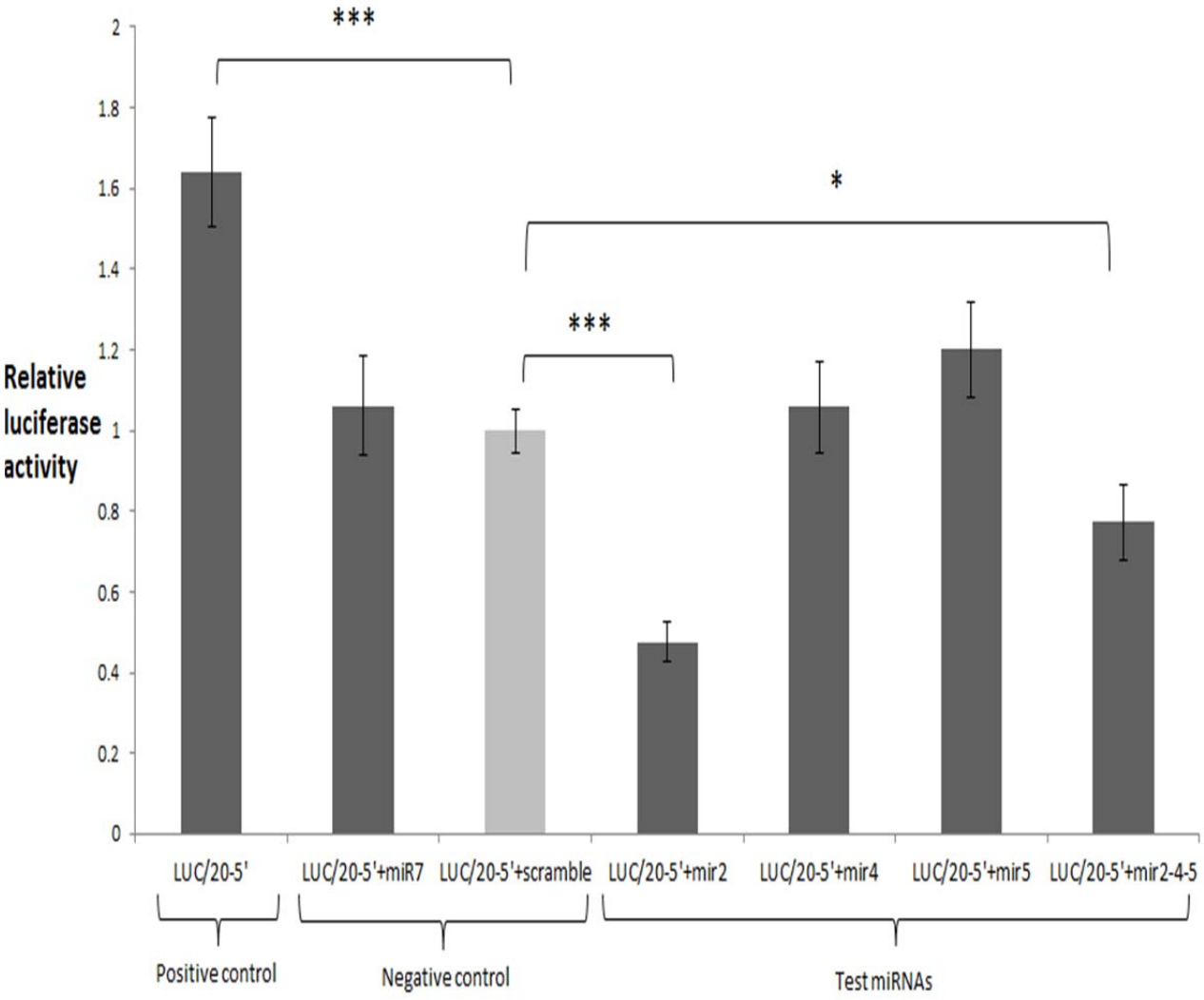

Figure 3.4: Luciferase expression levels in BHK21 cells transfected with the 5'UTR of ORF20 luciferase construct (in the pGL4.10 plasmid) in the presence/absence of target miRNA at 100 nM concentration.

Data is represented as luciferase activity with the *=$p<0.05$, **=$p<0.01$ and ***=$p<0.001$ relative to the respective scramble miRNA (negative control) (light grey) value at 100 nM concentration.

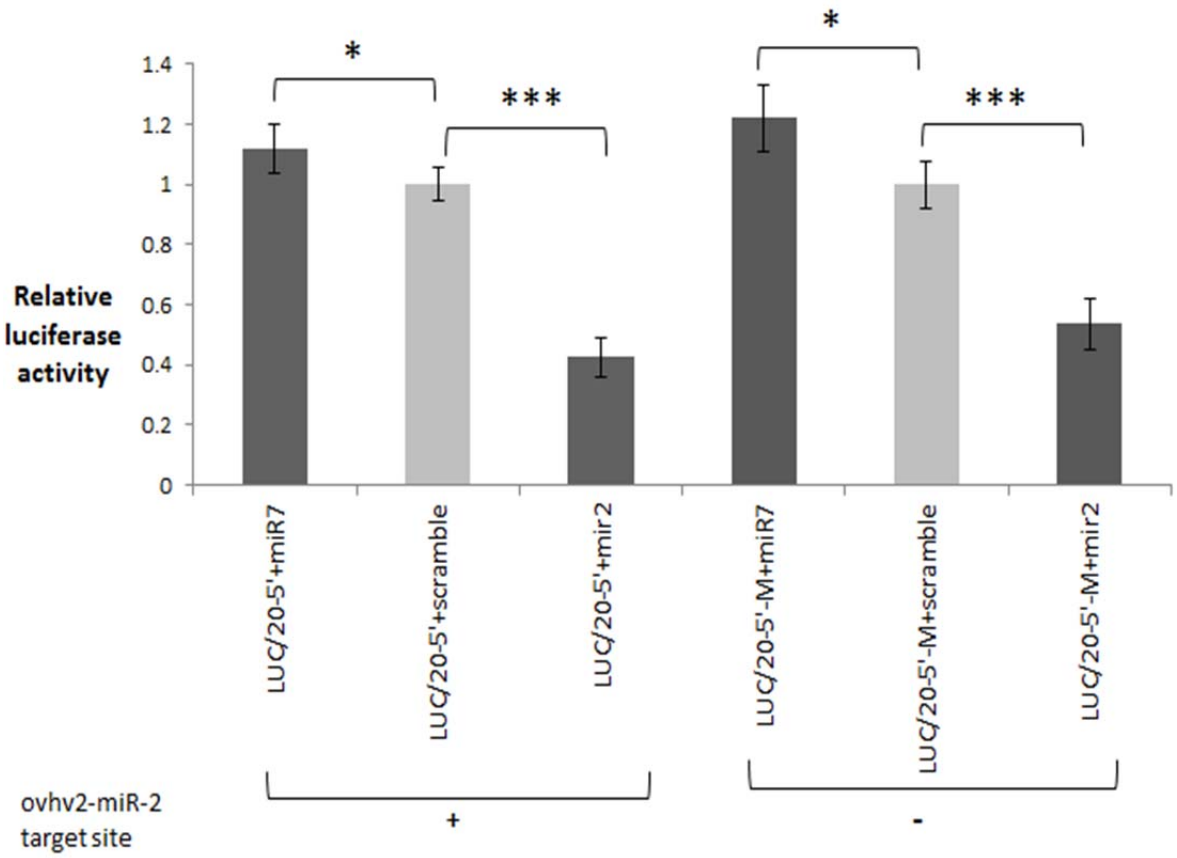

Figure 3.5: Luciferase expression levels in BHK21 cells transfected with the 5'UTR of the ORF20 luciferase constructs (in pGL4.10 plasmid) with or without deletion in the test miRNA target sites in the presence or absence of test miRNA at 100 nM concentration.

Data is represented as luciferase activity with the *=p<0.05, **=p<0.01, ***=p<0.001 being relative to the respective scramble miRNA (negative controls) (light grey) value at 100 nM concentration. Mimic of Ovhv2-miR-2 was used as test miRNA and ovhv2-miR-7 was used as an additional negative control miRNA.

```
target 5'  C     U        CCUCCUC        U 3'
           ACUG      UGU         CCAAGAU
           UGAC      ACG         GGUUCUA
miRNA  3'  GA     UGUCU    CA              5'
```

A

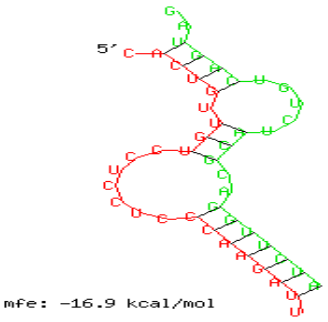


```
target 5'      A  U                G 3'
               GG CAGA     UCCAGGG
               CU GUCU     AGGUUCU
miRNA  3'  GAUGA        ACGC        A 5'
```

B

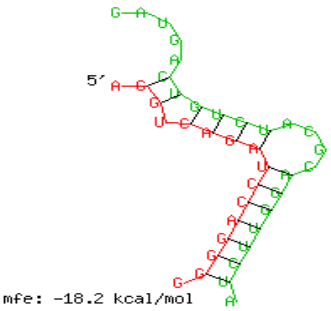


```
target 5'      A       C  G CACA        C 3'
               GACAGG UG G     UCCAGGG
               CUGUCU AC C     AGGUUCU
miRNA  3'  GAUGA           G             A 5'
```

C

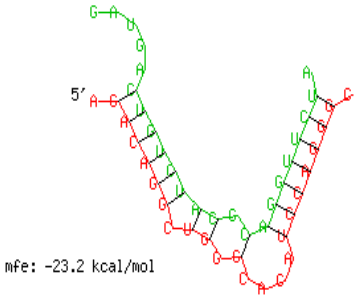


```
target 5'  C   C    GAC          UUCACGUAGCAACA        U3'
           CU CUG    ACAG UGC                   CUGAGAU
           GA GAC    UGUC ACG                   GGUUCUA
miRNA  3'     U            U    CA                    5'
```

D

Figure 3.6: Interaction between the predicted target sites and the seed region of ovhv2-miR-2 in 5'UTR of ORF20 with secondary structures predictions (right panel) using RNA hybrid programme.

A: predicted target site with perfect base pairing in the seed region.

B, C and D: predicted target sites with G:U pairing (in yellow) the seed region.

Red: Target sequence, Black: miRNA sequence

mfe: Minimum free energy

3.3.3 Validation of ovhv2-miR predicted targets located in the 3'UTRs of selected ORFs

The 3'UTRs of selected ORFs were cloned into the psiCHECK plasmid downstream of the Rluc translation stop codon (Section 2.6, Section 3.3.1). This vector also contained firefly luciferase, a second reporter gene, which acted as an internal control and allowed the normalization of Renilla luciferase expression. A positive control, psi-M23-2 (psiCHECK vector with the complementary sequence to mcmv-miR-M23-2, kindly donated by Dr. Amy Buck, University of Edinburgh) was used and transfected with or without mcmv-miR-M23-2 mimic in the same concentrations as used for the test miRNAs. The pEGFP-N3 plasmid was used as a transfection control. The following combinations were tested for each target:

1. No transfection control
2. Mock transfection control
3. pEGFP-N3 control (transfection control)
4. psi-M23-2
5. psi-M23-2 + mcmv-miR-M23-2 mimic (positive control).
6. psiCHECK (no 3'UTR control)
7. psiCHECK + target miRNA mimic/s
8. Target in psiCHECK without test or control miRNAs mimic (no miRNA control)
9. Target in psiCHECK with each of the test miRNA mimic (Test)
10. Target in psiCHECK with all of the test miRNAs mimics (Test)
11. Target in psiCHECK with scramble miRNA (negative control)

After 24 hours samples were harvested and luciferase levels were measured. The non-transfected and mock transfected samples were used to correct for background luciferase readings. Corrected Rluc/Fluc ratios were used to calculate fold difference by dividing each of the Rluc/Fluc value with the mean of the Rluc/Fluc of the negative control value. The remaining statistical analysis was performed as described in Section 3.3.2. For positive controls a one tailed independent t-test was performed.

3.3.3.1 Validation of the ORF50 as an ovhv2-miR-5 predicted target

Introduction of ovhv2-miR-5 at both concentrations led to a significant reduction of approximately 40% at 50 nM and approximately 50% at 100 nM, in the luciferase expression relative to the negative controls, [(LUC/50-3'-miR5, 50 nM) $p>0.001$, (LUC/50-3'-miR5, 100 nM) $p>0.001$] (Figure 3.7). LUC/50-3' in the absence of any miRNA showed a non-significant and a significant difference in luciferase expression from the scramble negative control at 50 nM and 100 nM concentration respectively [(LUC/50-3') $p=0.871$, (LUC/50-3', 100 nM) $p=0.002$].

The positive control psi-M23-2 co-transfected with mcmv-miR-M23-2 mimic showed a significant 80% and 90% decrease in the luciferase expression at both 50 nM and 100 nM [(psi-M23-2/miR-M23-2, 50 nM) $p>0.001$, (psi-M23-2/miR-M23-2, 100 nM) $p>0.001$] respectively (Figure 3.8). In all the other experiments positive controls (psi-M23-2 and miR-M23-2) worked in the same manner, that is the addition of miR-m23-2 caused significant knockdowns in the luciferase levels at either concentration (Luciferase readings in the Supplemental data file 3.1) and for the subsequent experiments the data is not shown.

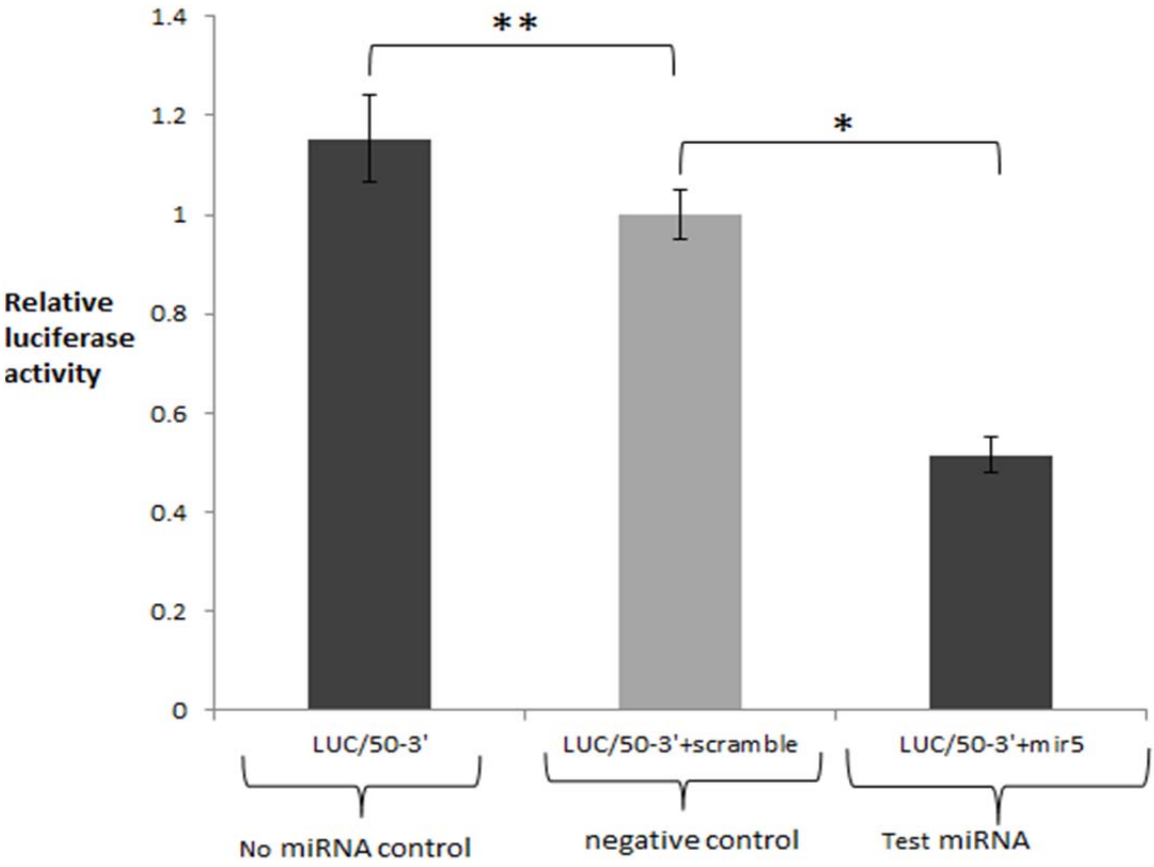

Figure 3.7: Luciferase expression levels in BHK21 cells transfected with the 3'UTR of ORF50 luciferase construct (in the psiCHECK-2 plasmid) in the presence/absence of target miRNA at 100 nM concentration.

Data is represented as luciferase activity with the *=$p<0.05$ relative to the respective scramble miRNA (negative control) (light grey) value at 100 nM concentration.

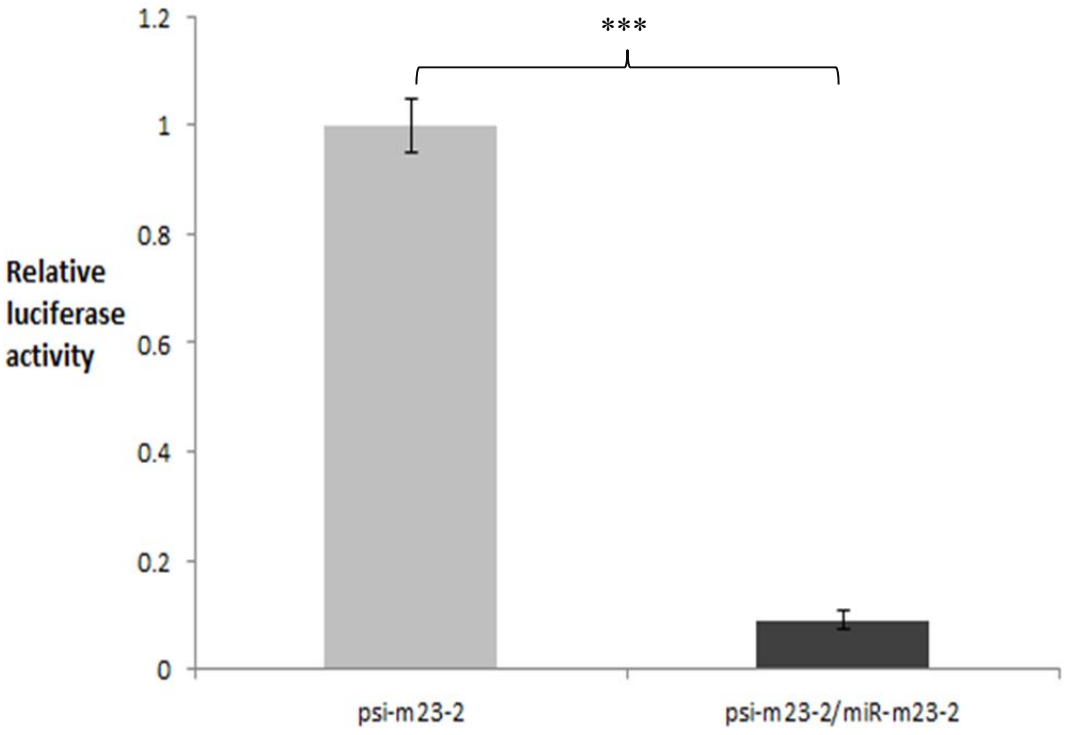

Figure 3.8: Positive control for dual luciferase assay.

Untreated samples (psi-m23-2) are shown in light grey while experimentally treated samples (with miR-m23-2) are shown in dark grey. Data is represented as luciferase activity with the ***=$p<0.001$ being relative to the psi-m23-2 value at 100 nM concentration.

3.3.3.2 Site directed mutagenesis to remove ovhv2-miR-5 sites in the 3'UTR of ORF50

To confirm if the reduction in the luciferase expression (Section 3.3.3.1) was due to the targeting by ovhv2-miR-5 at the predicted target site in the 3'UTR of ORF50, the site was deleted by site directed mutagenesis (Section 2.5). BHK21 cells were transfected with ovhv2-miR-5 target site deleted luciferase construct (LUC/50-3'-M) or template plasmid (LUC/50-3'). For each luciferase assay following combinations were tested:

1. Mutagenised or template construct + test miRNA mimic (test)
2. Mutagenised or template construct + scramble miRNA (negative control)
3. psi-M23-2 (positive control without targeting miRNA)
4. psi-M23-2 + mcmv-miR-M23-2 mimic (positive control with targeting miRNA).

The Rluc and Fluc values were corrected and Rluc/Fluc ratios of each group were calculated as described in section 3.3.3.

The parental template construct showed a significant repression in the luciferase expression with ovhv2-miR-5 as compared to the negative control [(LUC/50-3'-miR5, 100 nM) $p>0.001$)]. Deletion of the ovhv2-miR-5 target site from the 3'UTR of ORF50 restored the luciferase expression levels to that comparable to the negative control [(LUC/50-3'-M-miR5, 100 nM) $p=0.837$] (Figure 3.9).

These results indicated that the decrease in transcriptional activity was caused by the ovhv2-miR-5 site and abrogation of luciferase inhibition achieved by knocking out the target site provides evidence that the ovhv2-miR-5 site in 3'UTR of ORF50 might be a functional target site.

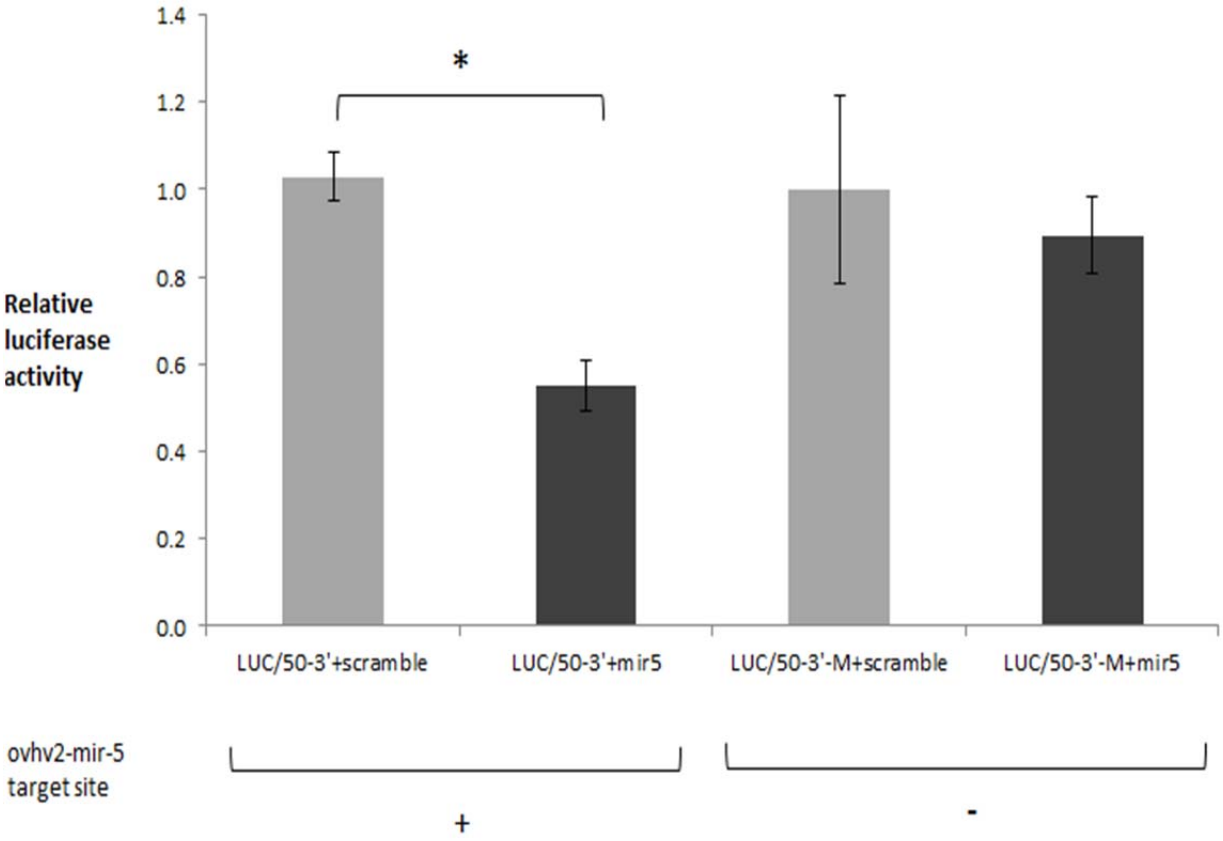

Figure 3.9: Luciferase expression levels in BHK21 cells transfected with the 3'UTR of the ORF50 luciferase constructs (in psiCHECK plasmid) with or without deletion in the test miRNA target sites in the presence or absence of test miRNA at 100 nM concentration.

Data is represented as luciferase activity with the *=$p<0.05$ relative to the respective scramble miRNA (negative controls) (light grey) value at 100 nM concentration. Mimic of ovhv2-miR-5 was used as a test miRNA.

3.3.3.3 Validation of ORF20 as predicted target for ovhv2-miR-5, 6 and 7

According to the results all the samples including the controls and tests treated with 50 nM targeting mimic showed a non-significant difference in luciferase expression from the negative control [(LUC/20-3') p=1, (LUC/20-3'-miR5-6-7, 50 nM) p=1, (LUC/20-3'-miR5, 50 nM) p=0.898, (LUC/20-3'-miR6, 50 nM) p=0.999, (LUC/20-3'-miR7, 50 nM) p=0.989]. In the absence of any miRNA, LUC/20-3'showed a significantly higher luciferase expression compared to negative control at 100 nM concentration [(LUC/20-3') p=0.001]. In contrast, psi-ORF20 co-transfected with all or either of the targeting mimic showed a non-significant increase compared to the negative control [(LUC/20-3'-miR5-6-7, 100 nM) p=0.194, (LUC/20-3'-miR5, 100 nM) p=0.625, (LUC/20-3'-miR6, 100 nM p=0.998, (LUC/20-3'-miR7, 100 nM) p=1] (Figure 3.10)

3.3.3.4 Validation of ORF36 as a predicted target of ovhv2-miR-8

LUC/36-3'in the presence or absence of the test miRNA (ovhv2-miR-8) showed no significant difference in the levels of luciferase as compared to the negative control at 50 nM or 100 nM concentration [(LUC/36-3',50 nM) p=0.421, (LUC/36-3',100 nM) p=0.107, (LUC/36-3'-miR8,50 nM) p=0.991, (LUC/36-3'-miR8,100 nM) p=0.495] (Figure 3.11).

3.3.3.5 Validation of the ORF49 as as a predicted target of ovhv2-miR-6

LUC/49-3' in the presence of test miRNA (ovhv2-miR-6) at 50 nM or 100 nM concentration showed no significant changes in luciferase activity from the negative

control miRNA when used at the similar concentrations [(LUC/49-3'-miR6, 50 nM) p=0.998, (LUC/49-3'-miR6, 100 nM) p=0.669)]. In the absence of any miRNA, LUC/49-3' showed significantly higher luciferase expression only when compared to the negative control at 100 nM but not at 50 nM concentration [(LUC/49-3', 50 nM) p=0.616, (LUC/49-3', 100 nM) p>0.001]. (Figure 3.12)

3.3.3.6 Validation of the ORF73 as a predicted target of ovhv2-miR-6

All the LUC/73-3'constructs with or without the treatment of targeting mimic (ovhv2-miR-6) at 50 nM or 100 nM concentrations, showed no significant difference from the negative control at the similar concentrations [(LUC/73-3',50 nM) p=0.124, (LUC/73-3'-miR6, 50 nM) p=0.552, (LUC/73-3', 100 nM) p=0.053, (LUC/73-3'-miR6, 100 nM) p= 0.105] (Figure 3.13).

3.3.3.7 Validation of Ov2 as as a predicted target of ovhv2-miR-4

Due to the unavailability of GloMax® 96 Luminometer, at the time the experiment was conducted, luciferase assays for LUC/Ov2-3' were performed using a Glomax 20/20 Luminometer (Promega) by manual mixing. Transfections were performed in 24 well plates for 24 hours and each sample was transfected in 3 replicates (Section 2.4.5). Two concentrations (25 nM and 50 nM) were used for mimic miRNA or scramble miRNA. Normalization of Rluc and Fluc readings and calculation of fold difference from negative control was done as described in Section 3.3.3.

No significant difference was observed in the luciferase expressions between LUC/Ov2-3' and negative control when transfected with or without 25 nm or 50 nM

of the targeting mimic; ovhv2-miR-4 [(LUC/Ov2-3', 25 nM) p=0.228, (LUC/Ov2-3', 50 nM) p=0.948, (LUC/Ov2-3'-miR4, 25 nM) p=0.260, (LUC/Ov2-3'-miR4, 50 nM) p=0.785] (3.14). Subsequent analysis later identified a one bp difference in the predicted target region of ovhv2-miR-4 in the 3'UTR of Ov2 in the BJ1035 isolate used in this experiment compared to the published Ov2 sequence (Figure 3.15). Due to the difference in the target region further experiments using 100 nM concentration of miRNA mimics were not performed.

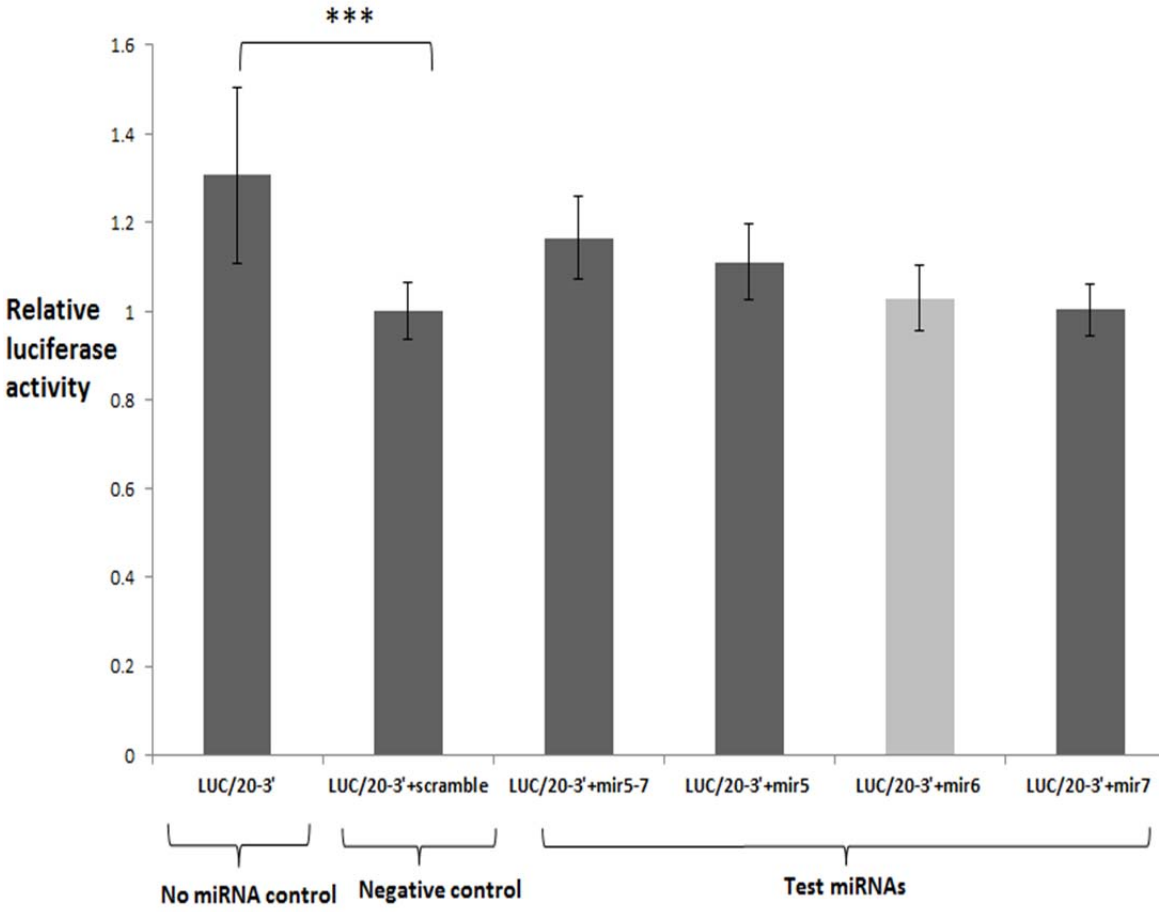

Figure 3.10: Luciferase expression levels in BHK21 cells transfected with the 3'UTR of ORF20 luciferase construct (in the psiCHECK-2 plasmid) in the presence/absence of target miRNA at 100 nM concentration.

Data is represented as luciferase activity with the ***=$p<0.001$ relative to the respective scramble miRNA (negative control) (light grey) value at 100 nM concentration.

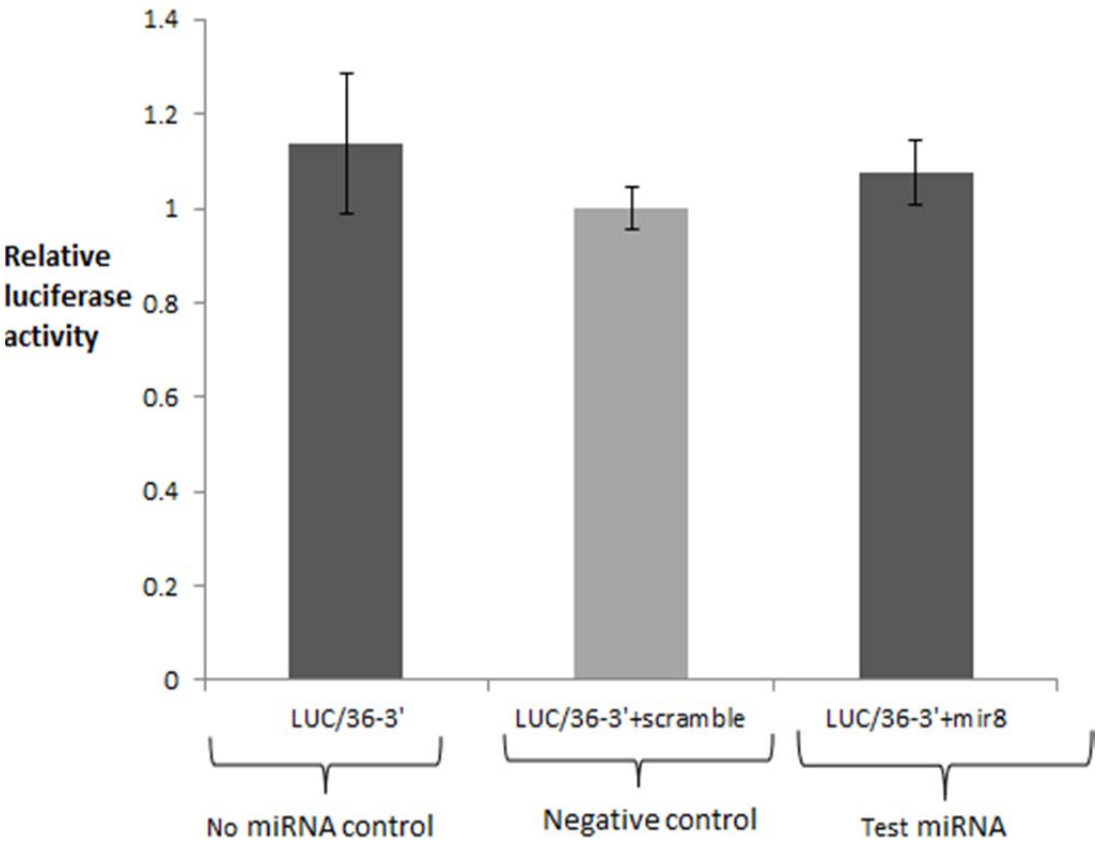

Figure 3.11: Luciferase expression levels in BHK21 cells transfected with the 3'UTR of ORF36 luciferase construct (in the psiCHECK-2 plasmid) in the presence/absence of target miRNA at 100 nM concentration.

Data is represented as luciferase activity relative to the respective scramble miRNA (negative control) (light grey) value at 100 nM concentration.

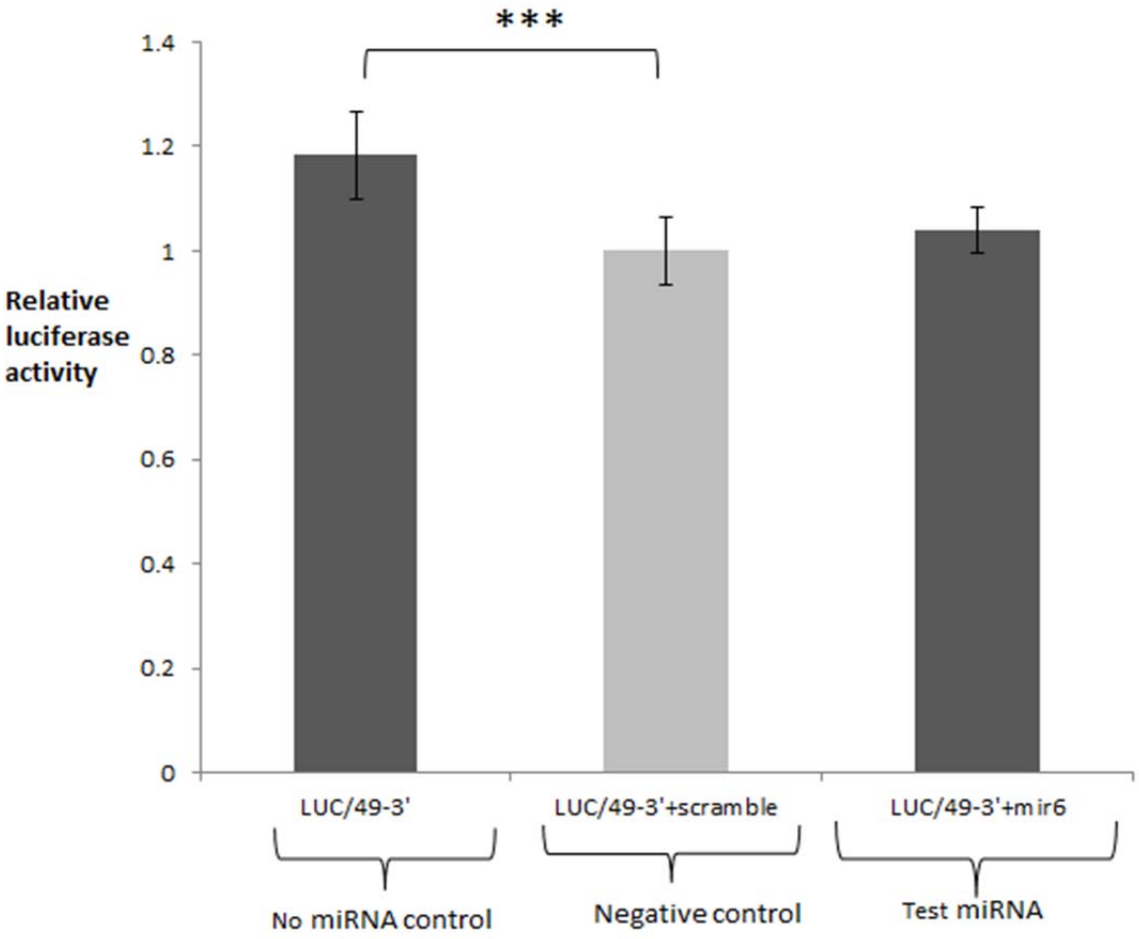

Figure 3.12: Luciferase expression levels in BHK21 cells transfected with the 3'UTR of ORF49 luciferase construct (in the psiCHECK-2 plasmid) in the presence/absence of target miRNA at 100 nM concentration.

Data is represented as luciferase activity with the *=$p<0.05$ relative to the respective scramble miRNA (negative control) (light grey) value at 100 nM concentration.

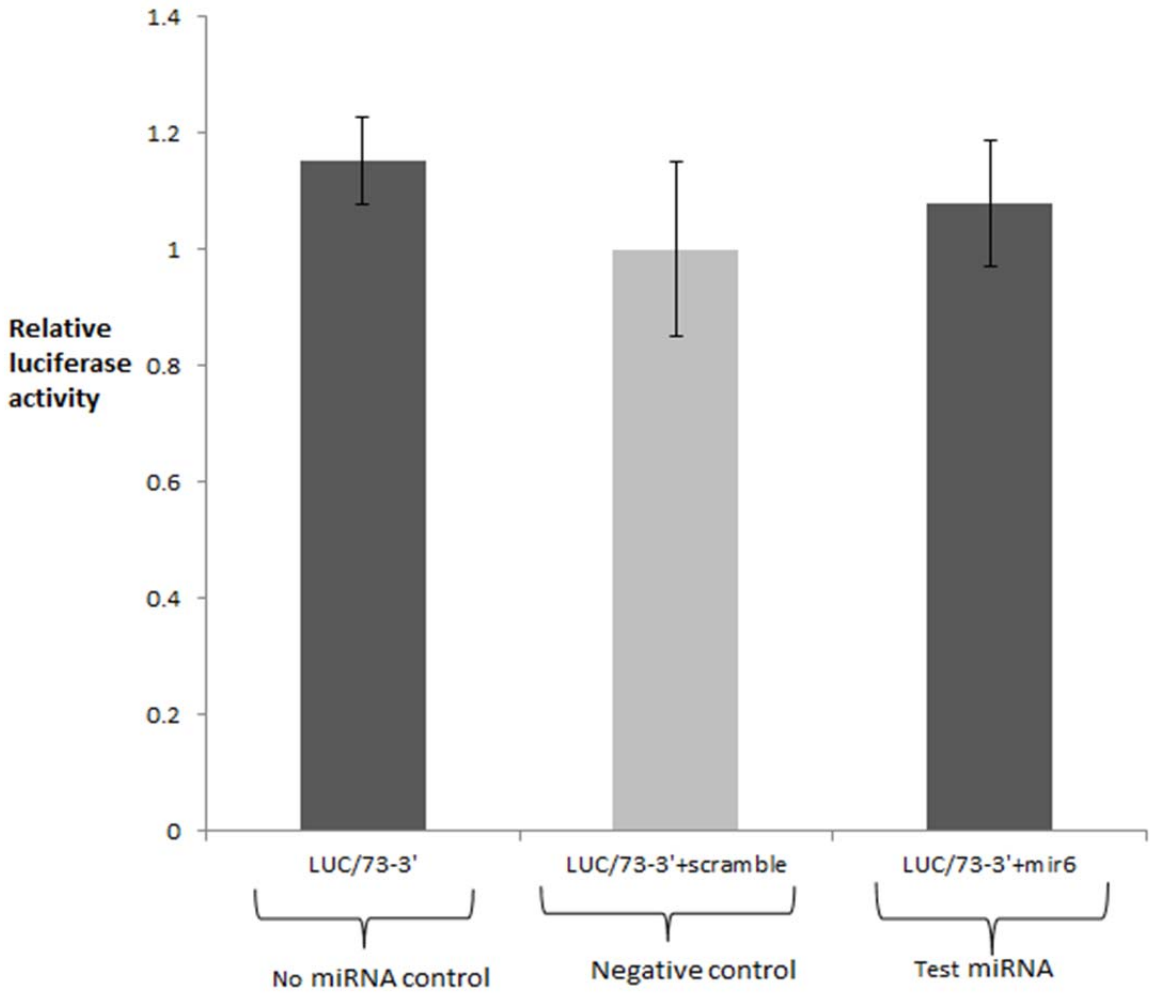

Figure 3.13: Luciferase expression levels in BHK21 cells transfected with the 3'UTR of ORF73 luciferase construct (in the psiCHECK-2 plasmid) in the presence/absence of target miRNA at 100 nM concentration.

Data is represented as luciferase activity relative to the respective scramble miRNA (negative control) (light grey) value at 100 nM concentration.

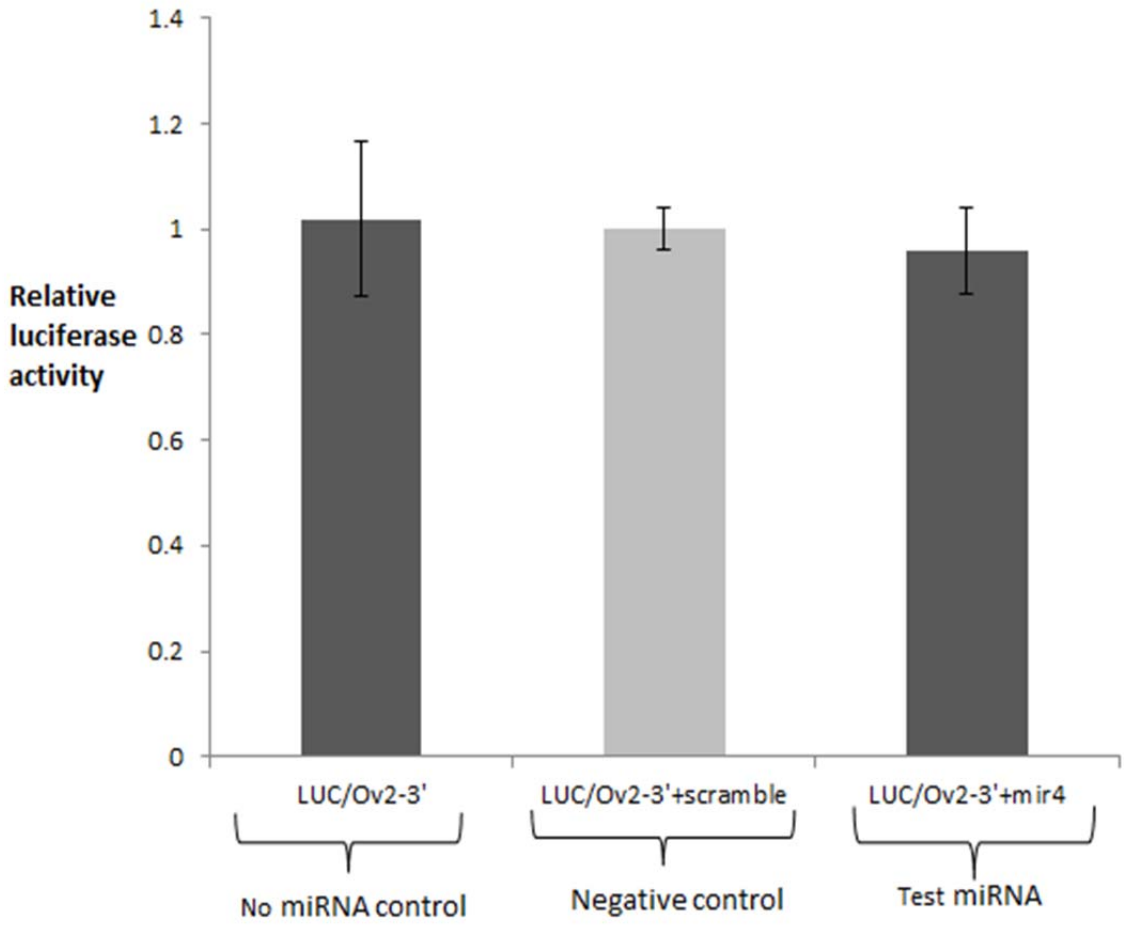

Figure 3.14: Luciferase expression levels in BHK21 cells transfected with the 3'UTR of Ov2 luciferase construct (in the psiCHECK-2 plasmid) in the presence/absence of target miRNA at 50 nM concentration.

Data is represented as luciferase activity relative to the respective scramble miRNA (negative control) (light grey) value at 100 nM concentration.

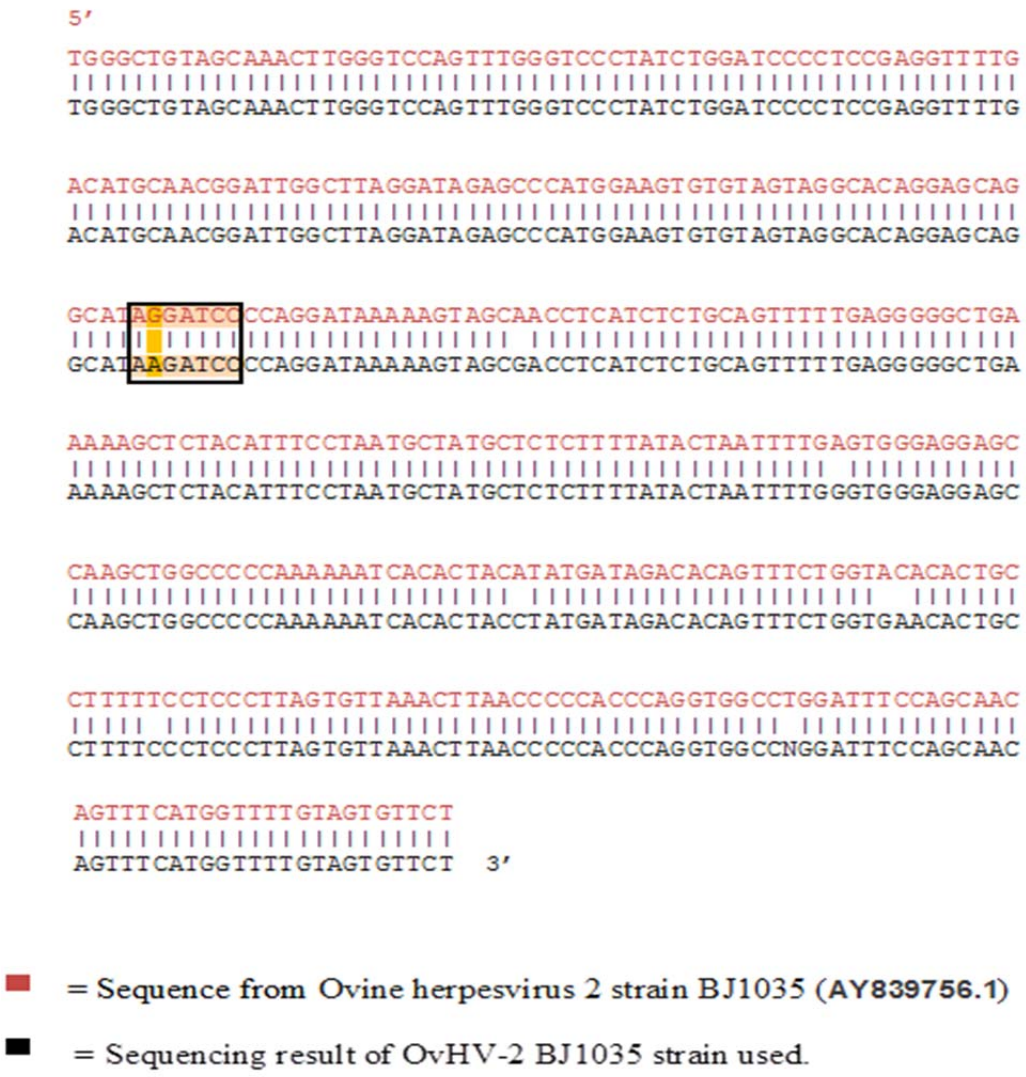

Figure 3.15: OvHV-2 Ov2-3'UTR sequence

The OvHV-2 Ov2-3'UTR sequence from BJ1035 cell line (444bp) (in black) isolated by PCR has one nucleotide difference at the predicted target site of ovhv2-miR-4 (highlighted in orange) as compared to the published OvHV-2 ORFOV2 3'UTR sequence (in red).

3.4 Discussion

All herpesviruses so far studied have been shown to encode miRNAs with the exception of VZV, however the role of those miRNAs in virus biology and pathogenesis is partly understood for only a very small number of herpesvirus miRNAs (Boss *et al*., 2009, Zhu *et al*., 2013). It has been shown that OvHV-2 encodes at least 35 miRNAs (Levy *et al*., 2012, Nightingale *et al*., 2014). The aim of this study was to experimentally validate the OvHV-2 ORFs that were predicted to be targeted by eight of the ovhv2-miRs originally validated (Levy *et al*., 2012). These ovhv2-miRs have predicted targets within cellular and viral transcripts (Levy PhD thesis, 2012). Due to the lack of a productive culture system for OvHV-2 there was no experimental means to study the virus life cycle (Reid *et al*., 1983) and hence the regulation of viral or cellular proteins under the influence of ovhv2-miRs in cell culture systems. To study the role of those miRNAs on the regulation of viral ORFs it was necessary to use a system which could determine the effects of miRNA-mRNA interactions. Dual luciferase reporter assays have been widely used to evaluate direct binding of a miRNA to its target mRNA and to validate the functionality of that interaction. Luciferase assays allow quantification of the magnitude of target silencing by miRNAs (Hansen *et al*., 2010). In this experimental model the UTR of interest is cloned downstream or upstream of a luciferase gene in a reporter plasmid. An interaction of a miRNA with the mRNA of the cloned UTR containing predicted miRNA target site, will block or inhibit the translation of the luciferase mRNA which results in a decrease in the luciferase proteins levels. The effect on the luciferase levels is easily measurable. Dual luciferase assays have the

additional benefit of co-expression of a control luciferase gene which is used as an internal control to control for discrepancies in expression readings.

In this study, luciferase assays were used to experimentally investigate six of the OvHV-2 ORFs that were predicted to contain target sites for ovhv2-miRs in their 3'UTR and/or 5'UTR. These ORFs (Ov2, ORF20, ORF36, ORF49, ORF50 and ORF73) have homologues in related herpesviruses which have functions related to virus latency, replication, cell cycle regulation or reactivation from latency (Section 3.2).

ORF73 is predicted to encode for LANA and is involved in viral episomal maintenance (Grundhoff and Ganem, 2003). An important role for KSHV miRNAs in targeting ORF73/LANA has also been reported in various studies. KSHV-miR-K-12-10a-3p and -10b-3p each can directly target two target sites in the 3'UTR of ORF73 transcripts in reporter constructs. Transfection of these miRNAs into KSHV infected cells, repressed the LANA protein levels significantly (Bai *et al*., 2014). OvHV-2 ORF73 was predicted to contain two target sites for ovhv2-miR-8 and one target site for ovhv2-miR-6 in the 5'UTR. ORF73 also has a predicted target site for ovhv2-miR-6 in the 3'UTR. The data from the luciferase assays showed that only ovhv2-miR-8 targeted the predicted target site in the ORF73 5'UTR and caused a significant reduction in the luciferase expression levels (Figure 3.1). This indicates that ovhv2-miR-6 may not interact with the target site within the mRNA and may not cause any cleavage or subsequent degradation of it. When ovhv2-miR-6 and ovhv2-miR-8 were used in combination at a 50 nM concentration of each, a <20% decrease in luciferase levels was observed and possibly that was due to only the activity of

ovhv2-miR-8. It is also worth noting that decrease in the luciferase activity at 50 nM concentration of the ovhv2-miR-8 was nearly half of the decrease when it was used at 100 nM concentration. Sequencing analysis later revealed a one bp difference in the predicted target region of ovhv2-miR-6 in the 5'UTR of ORF73 in the BJ1035 isolate used in this experiment compared to the published ORF73 sequence (accession no: AY839756.1) (Figure 3.3). It is possible that ovhv2-miR-6 might not be able to recognize the target site due to one bp change, and that there might not any contribution of ovhv2-miR-6 in this result. This sequence difference was confirmed in three separate PCR/cloning reactions.

To determine if the translational repression and decreased expression of luciferase gene was due to ovhv2-miR-8, the ovhv2-miR-8 target sites were deleted from the 5'UTR of ORF73. Results showed that disrupting each site restored the luciferase activity to a level comparable to negative control (Figure 3.2). The ovhv2-miR-8 sites in the 5'UTR overlapped each other. The seed region of the Ovhv2-mir8-site2 was located 9 nucleotides from that of the ovhv2-mir8-site1 (Figure 3.3). Further analysis of the binding of the region with in the 5'UTR of ORF73 with both target sites, using RNAhybrid programme (Kruger and Rehmsmeier, 2006) showed that site-1 can bind to the ovhv2-miR-8 with high efficiency. Site-2 lies in the region that interacts with the 3' end of the miRNA. It is therefore possible that only site-1 is functional and abrogation in the inhibition observed after the mutation in site-2 was due to the loss in non-seed sequence interactions. It is also possible that both of these sites work in a synergistically manner with each other and disruption in one affects the activity of the other. Closely spaced miRNA target sites often act synergistically

and two proximal target sites for same miRNA, individually mediate only subtle reduction, whereas both sites together can mediate more robust reduction, which was significantly cooperative (Grimson *et al*., 2007). In addition, a propensity for synergistic effect was also found for moderate distances greater than about 13 nt between seed starts and an optimal reduction was obtained when two seed sites were separated by between 13 and 35 nt (Saetrom *et al*., 2007).

ORF50 is a homologue of RTA of EBV and KSHV (Section 1.3.2; Section 3.2.4). The 3'UTR of ORF50 was predicted to be targeted by ovhv2-miR-5. Luciferase assays confirmed the interaction between predicted target site and ovhv2-miR-5. A ~50% significant reduction in the luciferase expression was observed (Figure 3.7). Deletion of the predicted target site resulted in a recovery of the luciferase levels to that seen in the intact construct (Figure 3.9). Further experiments in the lab carried out by Dr. Inga Dry have shown that the ORF50 mRNA levels can be inhibited in BJ1035 cells transfected with ovhv2-miR-5 (Riaz *et al*., 2014). The luciferase assay and inhibition assay results demonstrate that expression of ORF50 can be inhibited by a viral encoded miRNA. In other gamma herpesviruses, the expression of Rta in latently infected cells is sufficient to initiate the entire viral lytic cascade (Damania *et al*., 2004). After experimental infections of OvHV-2, ORF50 transcripts were detected in experimental animals indicating that it was related to viral transcription (Cunha *et al*., 2012). miRNAs encoded by other related gammaherpesviruses have been shown to target RTA. Bellare & Ganem showed that KSHV miR-K9 targets a region in the 3'UTR of RTA and ectopic expression of miR-K9 stabilizes the latency by attenuating the RTA accumulation (Bellare and Ganem, 2009). miR-K9 targeting

of a gene involved in triggering of lytic reactivation can be a safety mechanism for the virus to prevent RTA transcription from triggering inappropriate entry into the lytic cycle (Bellare and Ganem, 2009).

Based on the data and proposed function of ORF73 it can be speculated that a reduction in the protein levels due to ovhv2-miR-8 binding to the 5'UTR of ORF73 might suppress the expression of the latency associated antigen and thereby support the switch to lytic gene expression. In contrast specific miRNAs targeting of the 3'UTR of ORF50 shows that ovhv2-miR-5 might support the maintenance of viral episomes and stop the virus initiating the lytic lifecycle. The presence of miRNAs that cause reduction of expression of genes related to opposite functions suggests that the cultured T cells from infected cattle (BJ1035) may contain a mixture of the latent and lytically infected cells. Thonur *et al* found that cultured T cells from diseased cattle and rabbits contained both circular and linear genome conformations indicating a mixture of latent and productive cycle virus and that there was a mixture of latently- and productively-infected cells in both lines (Thonur *et al*., 2006). They also found that most of the OvHV-2 unique genes (Ov2-Ov10) were transcribed in these cells but the productive cycle genes ORF50 and ORF9 were only expressed after doxorubicin treatment (Thonur *et al*., 2006). However, sequencing analysis of OvHV-2 transcriptome in BJ1035 (Levy PhD thesis, 2012) described a different transcript profile. In the transcriptome data all the genes focused on by Thonur *et al* were expressed in BJ1035 cells, but to differing degrees and ORF50 was detectable without treatment with doxorubicin. There are a number of possible explanations regarding this difference in gene expression; First a different experiment

methodology was used in that study, Secondly, with the passage of time the cell line may develop a different ratio of latent:reactivated virus leading to an increase in reactivated virus.

Another selected target for validation was ORF20. In related viruses ORF20 is involved in controlling the cell cycle. In MHV68 ORF 20 was characterized as a nuclear protein and caused cell cycle arrest at G2/M phase of cell cycle by keeping Cdc2-cyclin B complex in an inactive form, leading to apoptosis (Nascimento *et al*., 2009). ORF20 of OvHV-2 was observed to localize in the nucleus like other related herpesviruses (Levy PhD thesis, 2012). OvHV-2 ORF 20 has predicted target sites for ovhv2-miR-5, ovhv2-miR-6 and ovhv2-miR-7 in the 3'UTR and ovhv2-miR-2, ovhv2-miR-4 and ovhv2-miR-5 in the 5'UTR. Within the 3'UTR no target site was found to be functional. No significant reduction in transcriptional activity and no synergistic effects of the three Ovhv2-miRs when transfected together, were observed (Figure 3.10). In the 5'UTR only one target site proved that it might be functional. A significant reduction in the ORF20 construct with a decrease in luciferase levels expression of 30-40% at 50 nM and 50-60% at 100 nM concentration of ovhv2-miR-2 was observed (Figures 3.4). When three ovhv2-miRs were transfected together at a final concentration of 100 nM, a significant <20% reduction was observed which might be due to the presence of ovhv2-miR-2 at 33.3nM concentration. Deletion of the ovhv2-miR-2 target site from the 5'UTR of ORF20 could not abolish the inhibition in luciferase expression (Figure 3.5) suggesting that either the target site is not a real functional site and the observed reduction was due to some other factors or that the target site is real but additional

target sites are present that are sufficient to cause a decrease in gene expression in the absence of the target site.

The interaction between ovhv2-miR-2 seed region and predicted target site, had a perfect complementarity, and no G:U pairing was allowed. If G:U base pairing was considered between the seed region and target site, three more possible target sites were found with two G:U base pairs in each interaction (Figure 3.6). More than one G:U base-pair can reduce the activity of all the target sites (Brennecke *et al*., 2005). Didiano and Hobert reported that the perfect base pairing is not generally a reliable predictor of miRNA-target interaction. They found an efficient reduction even after the introduction of several G:U wobbles at various positions of miRNA or two G:U wobbles in the seed region of a functional let-7-binding site in the lyn-41 3'UTR (Didiano and Hobert, 2006). The minimum free energy for the canonical base pairing in the seed region of ovhv2-miR-2 and target site in ORF20 was -16.9 kcal/mol while for the other target sites with G:U base pairing it was -18.2 kcal/mol, -23.2 kcal/mol and -15.4 kcal/mol. The lower the free energy of two paired RNA strands is, the more energy is needed to disrupt this duplex formation. An RNA duplex is more stable thermodynamically, which means the binding of miRNA to the mRNA is stronger, when free energy is low (Lewis *et al*., 2003, Huang *et al*., 2010). Thus one possible explanation for observing no abrogation in luciferase inhibition even after the predicted target site in the 5'UTR of ORF20 was disrupted by mutagenesis is that ovhv2-miR-2 interacted with one or more target site with G:U wobbles which have an almost as equal or as low free energy as the original interaction within 5'UTR of ORF20.

During further experiments done by Dr Inga Dry, in the lab, the existence of ORF20, ORF50 and ORF73 as transcripts including the miRNA target sites was confirmed, using an RT-qPCR strategy. The inhibition of ORF20, ORF50 and ORF73 transcripts by targeted miRNA mimics was also investigated by RT-qPCR analysis and results showed a successful reduction in the levels of ORF50 transcripts. Although, there was an apparent reduction in the levels of ORF20 transcripts it was not significant. Furthermore no reduction was observed in ORF73 transcript levels (Riaz *et al*., 2014).

Ov2 (Section 3.2.1) was also tested for the validation of predicted targets located in the 3'UTR (Figure 3.14). Ov2 is one of the unique OvHV-2 ORFs and encodes a DNA binding protein homologous to cellular transcription factors CREB and Jun (Hart *et al*., 2007). In the OvHV-2 transcriptome analysis Ov2 had a very high transcript level suggesting its importance in the pathogenesis of MCF (Levy PhD thesis, 2012). Luciferase assays showed no significant changes in expression levels when Ov2 was transfected with test miRNA ovhv2-miR-4. Further analysis identified a point mutation in the target region in the BJ1035 isolate which was used in this study (Figure 3.15), which might be the reason why ovhv2-miR-4 could not target Ov2.

ORF36, and ORF49 (Section 3.2.3 and 3.2.5) were also tested for the validation of predicted targets located in their 3'UTRs but neither of those showed any significant changes in the luciferase expression levels (Figure 3.11 ORF36 Figure 3.12 for ORF49). ORF36 is predicted to encode for a protein kinase and is conserved among the Herpesviridae family (Section 3.2.3). In most herpesviruses ORF49 is expressed

during the lytic cycle and shows early transcription kinetics. ORF49 protein is able to cooperate with RTA to activate several lytic promoters in the lytic life cycle (Section 3.2.5). These targets were predicted by bioinformatic analysis so it is possible that these are not real functional targets. However, it remains a possibility that within the 3'UTRs of ORF36 and ORF49 are real target sites and that the ovhv2-miRs do bind to the target transcript but due to other contributing factors or requirement of specific cellular factors translational repression cannot be detected in this model. Further investigation is required to exclude this possibility.

In this study eight UTRs from six OvHV-2 ORFs were functionally investigated as ovhv2-miRs targets. The selected ORFs had predicted targets located in 3'UTRs and/or 5'UTRs. miRNA mediated silencing of mRNA transcripts is regulated predominantly through binding to sequences within 3′UTRs (Farh *et al*., 2005, Gu *et al*., 2009). My results also prove that ORF50 can be regulated by ovhv2-miR-5 by targeting the complementary sequence within the 3'UTR. The other target sites located in the 3'UTRs of ORF73, ORF20, ORF36 and ORF49 were not found as miRNAs functional target sites. As these targets were identified by bioinformatics analysis it is a real possibility that these are false targets. I also tested predicted ovhv2-miRs targets located in 5'UTRs of OvHV-2 ORFs and found functional targets in the 5'UTR of ORF73 and ORF20. miRNA could associate to any position of the target mRNA and binding sites located in 5'UTRs could efficiently be repressed by miRNAs (Lytle *et al*., 2007). In another study, Grey *et al* reported the first example of a highly expressed viral (HCMV) miRNA mir-US25-1 mediated inhibition of gene expression through the novel mechanism of targeting 5'UTR

sequences. In that study the targeting of cellular transcript by miR-US25-1 has been shown using luciferase reporter assay and a recently developed biochemical approach called RISC immunoprecipitation and deletion of the identified seed sites from the 5'UTRs resulted in a loss of enrichment in the luciferase transcript measured using RT-qPCR (Grey *et al*., 2010). My results show that ovhv2-miR-8 can efficiently down-regulate ORF73 by binding its target sequence located within the 5'UTR and deletion of the target site can abrogate that reduction. Whereas ovhv2-miR-2 also can inhibit ORF20 expression by targeting complementary sequence in the 5'UTR, knocking out of that target site could not abrogate inhibition. As shown above it might be due to the presence of other target sites with G:U base pairing.

Due to technical complexity and time constraint it is beyond the scope of this project to functionally validate each of those target sites. To find out the regulation by ovhv2-miRs, identification of real targets is required and that work is in progress in the lab.

Chapter 4: Identification and characterization of cellular targets of ovhv2-miRs

4.1 Aim

To identify the cellular targets of OvHV-2 encoded miRNAs.

4.2 Introduction

OvHV-2 causes a severe lymphoproliferative disease in cattle but not in sheep (described in detail in Section 1.4). The basis of the difference in disease outcomes in two phylogenetically closely related species is unknown. We hypothesized that virus encoded miRNAs may play a role in these different disease outcomes. To test this hypothesis experiments were performed to identify the targets of OvHV-2 encoded miRNAs (ovhv2-miRs) in sheep and cattle mRNAs.

Identification of potential miRNAs targets has been one of the greatest challenges since the discovery of miRNAs. Several experimental and computational approaches (Section 1.5.5) have been used to predict targets and their interactions with their respective miRNAs. More recent approaches involve UV cross-linking and immunoprecipitation (CLIP) of the miRNA targeted mRNA within the RISC, using antibodies specific for the proteins present in the RISC, and then mapping protein-mRNA interactions using high throughput sequencing (Hafner *et al*., 2010, Skalsky *et al*., 2012). The development of CLIP has allowed the mapping of RNA interacting with a variety of proteins and can also provide useful information about protein-mRNA interacting with corresponding miRNAs. Recent CLIP related studies identified many putative miRNA binding sites, using transcriptome wide analysis of argonaute and mRNA interactions (Chi *et al*., 2009, Leung *et al*., 2011). However using these approaches it is not possible to get evidence for direct and physical mRNA-miRNA interactions. A newly developed technique, Crosslinking, Ligation

And Sequencing of Hybrids (CLASH) (previously known as crosslinking and analysis of cDNA (CRAC) allows the study of transcriptome-wide analysis of RNA-RNA interactions (Kudla *et al*., 2011). CLASH allows direct observation of nucleic acid interctomes (e.g miRNA-mRNA) as chimeras or hybrids in deep sequencing data (Kudla *et al*., 2011). CLASH has many experimental steps in common with the CLIP method, but was optimized for the recovery of RNA-RNA duplexes (Travis *et al*., 2014) and has been successfully used to find RISC-miRNA-mRNA interactions and/or miRNA-mRNA interactions in cells (Granneman et al., 2009, Helwak et al., 2013, Kudla et al., 2011, Helwak and Tollervey, 2014). CLASH is a highly sensitive technique which allows the identification of miRNA's targets or binding sites in mRNAs and also helps to understand the functions of ovhv2-miRs. The objective of the study was to use CLASH technique to identify the cellular targets of ovhv2-miRs.

4.2.1 Crosslinking, ligation and sequencing of the hybrids (CLASH)

In these studies CLASH was used to attempt to find targets in cattle transcripts for the 46 ovhv2-miRs. In addition, CLASH was also used to identify targets of three of the ovhv2-miRs (ovhv2-miR-17-1 (ovhv2-miR-8), ovhv2-miR-17-2 (ovhv2-miR-67), and ovhv2-miR-17-3 (ovhv2-miR-7) in the sheep cells. The protocol for CLASH is described in detail in Section 2.7 and an overview of the CLASH procedure is illustrated in Figure 4.1. Briefly CLASH involves using UV light (Step1; Figure 4.1) *in vivo* to crosslink the Ago2 protein (tagged with HTP (His6-TEV-ProteinA) to the miRNA-mRNA complexes within the RISC. The cross-linked proteins and miRNA-mRNA complexes were purified, under stringent condition, in two stages. The first

of these two stages involved; the binding of Protein A tag of Ago2 present in the cell lysate to IgG antibody coated magnetic beads and then isolating the bound complexes (Step2; Figure 4.1). Isolated complexes were subjected to limited RNase A and T1 digestion to remove overhanging transcripts leaving the RISC incorporated mRNA corresponding to the miRNA targets (Step3; Figure 4.1). miRNA-mRNA-RISC complexes were then eluted from the beads and loaded on Ni-NTA agarose (Ni beads). An intra-molecular ligation reaction was performed using T4 RNA ligase 1 resulting in the formation of hybrids between the miRNA and the target mRNA. 3' linker ligation using T4 RNA Ligase and radiolabelling using γ -^{32}P ATP of 5'ends of the RNAs was performed while the complexes were still immobilized on Ni beads (Step4; Figure 4.1). The radiolabelled complexes were separated and eluted from the Ni beads (Step5; Figure 4.1). The second purification step was carried out by separating the complexes by SDS polyacrylamide gel electrophoresis, and transferring to a nitrocellulose membrane. The regions containing the radiolabelled protein-RNA complexes were excised from the membrane and subjected to proteinase K treatment to digest proteins associated with the RISC complex. The released miRNA-mRNA hybrids (chimeras) were extracted with phenol-chloroform and ethanol precipitation and a 5' linker ligation was performed on each sample (Step6; Figure4.1). Addition of a 5' linker containing a known variable sequence (barcode) allowed identification of each sample through the downstream processing. Reverse transcription of RNA and PCR amplification of the cDNA libraries was carried out. PCR products were separated on a gel and then extracted from the gel (Step7; Figure4.1). Purified cDNA libraries were either cloned and Sanger sequenced or submitted to ARK Genomics for Solexa sequencing (Step8; Figure 4.1).

A

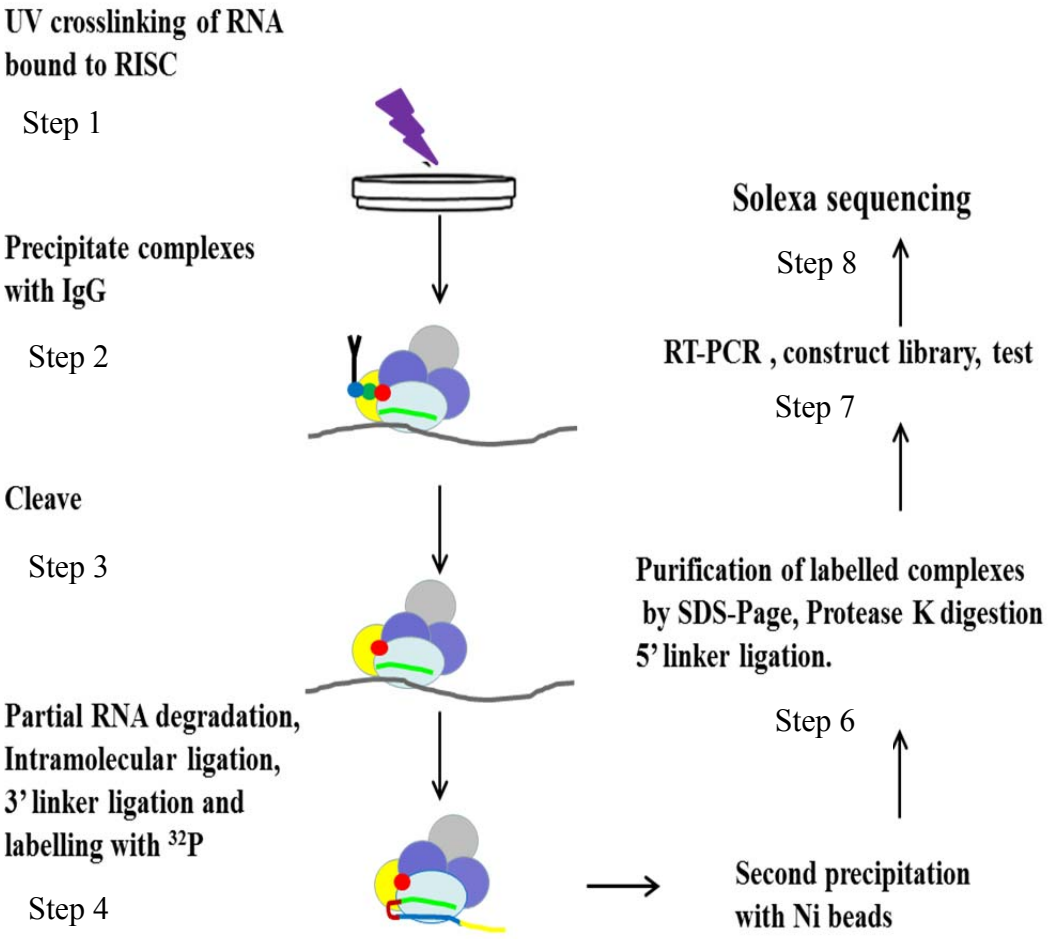

B

Figure 4.1: The CLASH technique

(A) Schematic diagram showing HTP tag fused to Argonaut 2 (Ago2) protein. (B) Outline of the different steps carried out during the CLASH experimental procedure.

4.3 Results

The CLASH approach was used to identify host cellular targets of ovhv2-miRs. The OvHV-2 infected bovine LGL cell line BJ1035 expresses all identified ovhv2-miRs and was used to identify bovine targets. Due to the unavailability of appropriate control bovine cells, only BJ1035 cells were used in this experiment and the targets for ovhv2-miRs were determined primarily by analysing CLASH hybrid data (Section 4.3.3).

To identify ovine targets for ovhv2-miRs, it was not possible to transduce and develop sheep lymphocytes expressing tagged Ago2 and ovhv2-miRs therefore sheep embryo fibroblasts (SEF) were used. For this purpose stable sheep fibroblast cell lines expressing the ovhv2-miRs and control cells were generated (Section 4.3.2).

BJ1035 and SEF expressing tagged Ago2 were generated, to allow purification of miRNA-mRNA complexes associated with the RISC.

4.3.1 CLASH for the LGL cell line BJ1035

4.3.1.1 Expression of tagged Ago2 Protein in the LGL cell line BJ1035

The pLVX-tight-puro lenti vector (pLVX-puro) (Appendix-2) into which was cloned HTP tagged human Ago2 (gift from Dr. Grey) was used to produce a tagged Ago2 expressing lentivirus in HEK293 cells. Those lentivirus particles were used for the stable transduction (section 2.4.8) and expression of tagged Ago2 in the BJ1035 cells. The amino acid sequence of bovine Ago2 is almost identical to that of the human Ago2 sequence with only two amino acids found to be different (Figure 4.2). Western blot analysis (Section 2.3.3) using anti-human Ago2 antibodies showed

successful expression of tagged Ago2 in BJ1035 cells (Figure 4.3A). Successfully transduced cells (BJ1035-AGO2) selected by Puromycin resistance (Section 2.4.7) were used to perform CLASH.

4.3.1.2 Analysis of tagged Ago2 protein Immunopreciptiation in BJ1035-AGO2 at small scale

Before carrying out CLASH experiments the efficiency of the magnetic dynabeads conjugated with purified IgG antibody (dynabeads-IgG) was tested by protein A-tag mediated immunoprecipitation (IP), to test the quality of lysate. Cell lysates were obtained by lysis of UV irradiated BJ1035-AGO2 as described in Sections 2.7.1-2.7.3. Dynabeads-IgG were used to pull down the tagged Ago-2 in the RISC. During the first washing step of IP, the flow through (FT) was also carefully collected. Enrichment of the proteins during purification was monitored by western blotting using equal quantities of cell lysates, IP samples, and the FT samples. The western blot results showed that the expression of tagged Ago2 in the cell lysate and IP samples were comparable, indicating an efficient IP. The FT sample contained very little tagged Ago2, indicating minimum loss of proteins during the washing steps (Figure 4.3B).

4.3.1.3 CLASH experiments for BJ1035-AGO2

CLASH experiments (Section 2.7.4) were performed for one sample of BJ1035 cells (BJ1035 sample for the rest of the chapter).

miRNA-mRNA complexes can be visualized at two stages during the CLASH experiment. The radio-labelled tagged Ago2 miRNA-mRNA complexes were visualized by autoradiography, after the Ni affinity purification and enzymatic

modification steps (Sections 2.7.4-2.7.8, Figure 4.1). Ago2 has a molecular weight of approximately 100 KDa and a band of this size was visible on the blot (Figure 4.3 C1). A contaminant of approximately 50 to 60 kDa was also detected (Figure 4.3 C1 asterisk*). The region associated with 100 kDa was excised from the membrane (indicated by red box in Figure 4.5A) (section 2.7.8). The RNA recovered after proteinase K treatment and 5' linker ligation was reverse transcribed and cDNA libraries were prepared (section 2.7.9 to 2.7.12). The second visualization stage of the CLASH experimental product was performed using a small quantity of the cDNA library which was amplified by PCR. A PCR product of ~150bp was detected by gel electrophoresis and excised from the gel (red squares in Figure 4.3 C2) for DNA extraction. To assess the quality of the cDNA and to confirm the successful ligation of the linkers, the sample was cloned and sequenced (section 2.7.13). An example of a typical cDNA fragment generated from CLASH experiment is illustrated in Figure 4.4. Sequencing results confirmed the presence of the 5'linker, barcodes, insert and 3'linker sequences. The size of the inserts ranged from 0-39nt in lengths. For further analysis the cDNA libraries were submitted for Solexa sequencing (Section 2.7.13).

```
Bos             MYSGAGPALAPPAPPPPPIQGYAFKPPPRPDFGTSGRTIKLQANFFEMDIPKIDIYHYEL
Homo            MYSGAGPALAPPAPPPP-IQGYAFKPPPRPDFGTSGRTIKLQANFFEMDIPKIDIYHYEL
                ***************** ****************************************

Bos             DIKPEKCPRRVNREIVEHMVQHFKTQIFGDRKPVFDGRKNLYTAMPLPIGRDKVELEVTL
Homo            DIKPEKCPRRVNREIVEHMVQHFKTQIFGDRKPVFDGRKNLYTAMPLPIGRDKVELEVTL
                ************************************************************

Bos             PGEGKDRIFKVSIKWVSCVSLQALHDALSGRLPSVPFETIQALDVVMRHLPSMRYTPVGR
Homo            PGEGKDRIFKVSIKWVSCVSLQALHDALSGRLPSVPFETIQALDVVMRHLPSMRYTPVGR
                ************************************************************

Bos             SFFTASEGCSNPLGGGREVWFGFHQSVRPSLWKMMLNIDVSATAFYKAQPVIEFVCEVLD
Homo            SFFTASEGCSNPLGGGREVWFGFHQSVRPSLWKMMLNIDVSATAFYKAQPVIEFVCEVLD
                ************************************************************

Bos             FKSIEEQQKPLTDSQRVKFTKEIKGLKVEITHCGQMKRKYRVCNVTRRPASHQTFPLQQE
Homo            FKSIEEQQKPLTDSQRVKFTKEIKGLKVEITHCGQMKRKYRVCNVTRRPASHQTFPLQQE
                ************************************************************

Bos             SGQTVECTVAQYFKDRHKLVLRYPHLPCLQVGQEQKHTYLPLEVCNIVAGQRCIKKLTDN
Homo            SGQTVECTVAQYFKDRHKLVLRYPHLPCLQVGQEQKHTYLPLEVCNIVAGQRCIKKLTDN
                ************************************************************

Bos             QTSTMIRATARSAPDRQEEISKLMRSASFNTDPYVREFGIMVKDEMTDVTGRVLQPPSIL
Homo            QTSTMIRATARSAPDRQEEISKLMRSASFNTDPYVREFGIMVKDEMTDVTGRVLQPPSIL
                ************************************************************

Bos             YGGRNKAIATPVQGVWDMRNKQFHTGIEIKVWAIACFAPQRQCTEVHLKSFTEQLRKISR
Homo            YGGRNKAIATPVQGVWDMRNKQFHTGIEIKVWAIACFAPQRQCTEVHLKSFTEQLRKISR
                ************************************************************

Bos             DAGMPIQGQPCFCKYAQGADSVEPMFRHLKNTYAGLQLVVVILPGKTPVYAEVKRVGDTV
Homo            DAGMPIQGQPCFCKYAQGADSVEPMFRHLKNTYAGLQLVVVILPGKTPVYAEVKRVGDTV
                ************************************************************

Bos             LGMATQCVQMKNVQRTTPQTLSNLWLKINVKLGGVNNILLPQGRPPVFQQPVIFLGADVT
Homo            LGMATQCVQMKNVQRTTPQTLSNLCLKINVKLGGVNNILLPQGRPPVFQQPVIFLGADVT
                ********************** ************************************

Bos             HPPAGDGKKPSIAAVVGSMDAHPNRYCATVRVQQHRQEIIQDLAAMVRELLIQFYKSTRF
Homo            HPPAGDGKKPSIAAVVGSMDAHPNRYCATVRVQQHRQEIIQDLAAMVRELLIQFYKSTRF
                ************************************************************

Bos             KPTRIIFYRDGVSEGQFQQVLHHELLAIREACIKLEKDYQPGITFIVVQKRHHTRLFCTD
Homo            KPTRIIFYRDGVSEGQFQQVLHHELLAIREACIKLEKDYQPGITFIVVQKRHHTRLFCTD
                ************************************************************

Bos             KNERVGKSGNIPAGTTVDTKITHPTEFDFYLCSHAGIQGTSRPSHYHVLWDDNRFSSDEL
Homo            KNERVGKSGNIPAGTTVDTKITHPTEFDFYLCSHAGIQGTSRPSHYHVLWDDNRFSSDEL
                ************************************************************

Bos             QILTYQLCHTYVRCTRSVSIPAPAYYAHLVAFRARYHLVDKEHDSAEGSHTSGQSNGRDH
Homo            QILTYQLCHTYVRCTRSVSIPAPAYYAHLVAFRARYHLVDKEHDSAEGSHTSGQSNGRDH
                ************************************************************
```

Figure 4.2: Sequence of Bos taurus Argonaute 2 protein

Sequence of Bos taurus Argonaute 2 protein showed two amino acids difference from Homo sapiens Argonaute 2 protein (highlighted in yellow).
Bos= Bos taurus Homo= Homo sapiens.
*= Identical amino acids in Bos taurus Argonaute2 and Homo sapiens Argonaute2 protein.

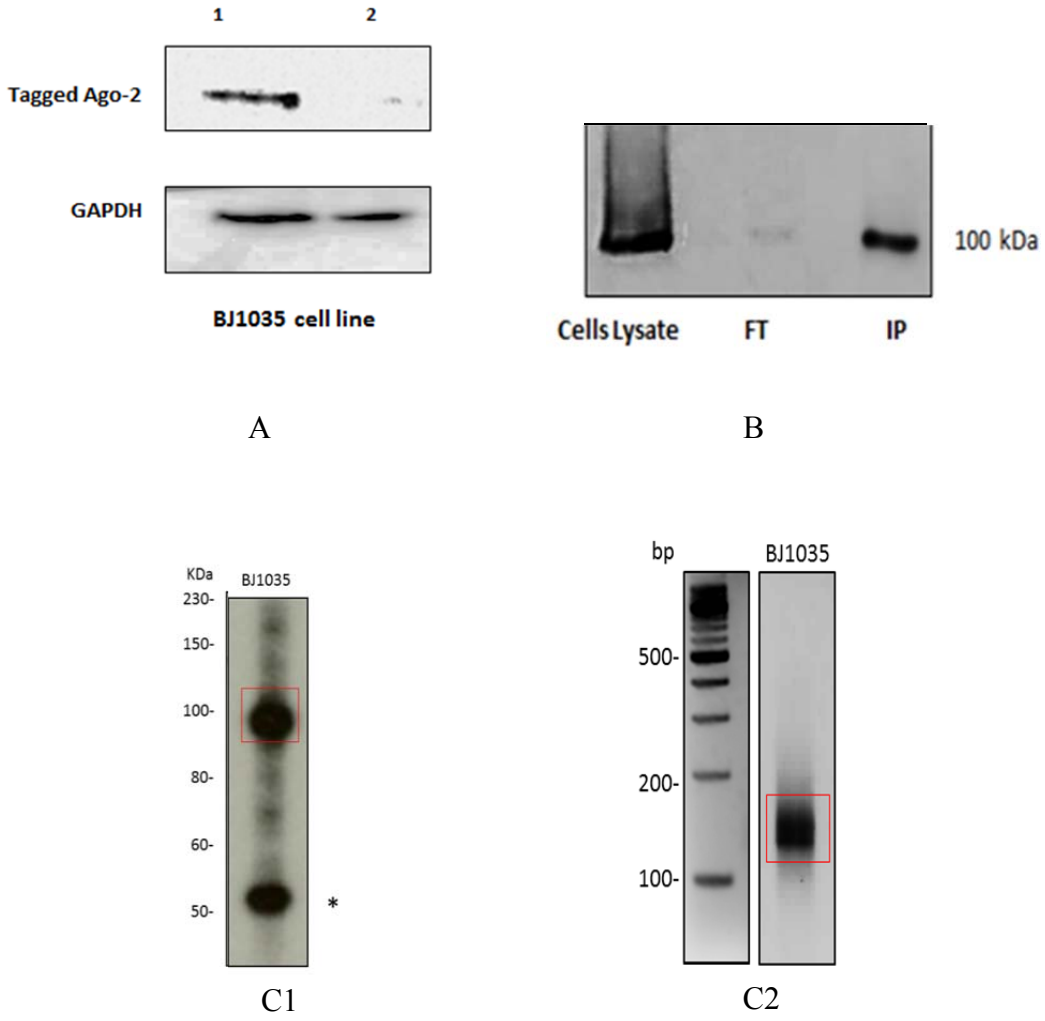

Figure 4.3: Different stages of CLASH for the visualization of CLASH experimental products.
A: Western Blot analysis with antibody against human Ago2 or GAPDH showing expression of Ago2 or GAPDH in BJ1035 cells.
Lane 1: BJ1035 transduced with HTP tagged human Ago2
Lane 2: Un-transduced BJ1035.

B: Western blot analysis to monitor the enrichment of HTP tagged Ago2 using protein A-tag mediated immuno-precipitation (IP) in the BJ1035 transduced with tagged Ago2. Cell lysate, FT and IP samples were probed with antibodies against human Ago-2 using magnetic Dyna-beads. FT: Flow through obtained during washing steps of IP.

C: Visualization of CLASH experimental product; **C1:** Autoradiograph of radiolabelled HTP tagged Ago2 with miRNA-mRNA complex after Ni-affinity purification and 3'linker ligation. Red box indicates region on the membrane that was excised and further used for miRNA-mRNA complexes and cDNA synthesis. Asterisk indicates a common contaminant of 50-60KDa. Protein size marker is indicated on the left. **C2:** MetaPhor gel electrophoresis of cDNAs library amplified by PCR. The region which was excised from the gel for DNA extraction is indicated in red box. A 100bp DNA size marker is indicated on the left.

AATGATACGGCGACCACCGAGATCTACACTCTTTCCCTACACGACGCTCTTCCGATCTAT
TGTGAGC**AGCCACCTGGGGAGTACGAACGCAAGTTTGAAACTCAAA**GGAATTCTCGG
GTGCCAAGGCCAGGAATGCCGAGACCGATCTCGTATGCCGTCTTCTGCTTG

Figure 4.4 Sequencing result of a TOPO cloned cDNA sample generated from CLASH experiment from BJ1035-AGO2.

The 5' linker, barcode and 3' linker is highlighted in cyan, grey and yellow respectively. RNA insert is shown in bold. Adapter sequences from PCR primers are shown as underlined non-highlighted areas.

4.3.1.4 High throughput sequencing of cDNA library obtained from BJ1035 sample

Bioinformatic analysis was carried out in collaboration with Mr. Mick Watson (University of Edinburgh) and with the kind help of Dr. Finn Grey (University of Edinburgh). In brief, Solexa sequencing reads of 100 bp length were selected and were separated according to the barcode associated with the BJ1035 sample. Barcode was matched with all the reads, allowing a 1bp mismatch and zero insertions or deletions. If a read matched the barcode, it was assigned to the BJ1035 sample. Approximately 21 million reads were assigned to the barcode associated with the BJ1035 sample. However a small number of reads (70,000) were found with a barcode which was not used in this study. The possible reason for this was the contamination of barcodes during synthesis and it was assumed that the dataset had some contamination of barcodes used during sequencing. The sequencing adapter was then removed from reads using Cutadapt (Martin, 2011) and the resulting reads were mapped by BLAST (NCBI), against all of the 46 ovhv2-miRs (Levy PhD thesis, 2012) and against the entire database of miRBase V19. The results were used to count the occurrence of miRNAs within each dataset. Each read in the dataset was assumed to contain 0, 1 or more miRNAs at the 5' end. Using the BLAST results, if an miRNA was found at the 5' end, it was trimmed along with the barcode; if no microRNA was found, just the barcode was trimmed. To examine the expression of targeted genes/mRNAs, the remaining parts of the reads were mapped to the predicted cattle transcripts (UMD 3.1) and the ORFs extracted from the Ovhv-2, complete genome sequence (accession AY839756.1). After applying these filters, a total of approximately 700,000 reads were obtained, for the BJ1035 sample. An

overview of this data set is described in Figure 4.5A. Finally, if a read hit both an miRNA and a mRNA, it was recorded as a chimera and the occurrence of all chimeras were counted.

4.3.1.5 CLASH data analysis for the presence of ovhv2-miRs

For the BJ1035 sample, Solexa sequencing reads were obtained as described in 4.3.1.4 and were mapped against ovhv2-miRs and cellular-miRs present in the miRBase database. A total of 468881 miRNA reads were obtained and of these 142367 (31.2%) and 313036 (68.7%) reads were matched with ovhv2-miRs and cellular miRNAs respectively (Figure 4.5B).

Ovhv2-miR-217M was the most abundant ovhv2-miRs with more than 28000 hits contributing 19.8% of all ovhv2-miRs and 6.2% of all miRNA. Ovhv2-mir-217M has seed (nucleotide 1-7 at 5'end of miRNA) sequence homology with cellular miR-216a (Figure 4.5C). However when the reads were mapped against cellular-miRs in the BJ1035 sample, no miR-216a was found. All the sequence reads recovered with ovhv2-miR-217M had full length mature ovhv2-miR-217M sequence. ovhv2-miR-57 and ovhv2-miR-53 were the next most abundant miRNAs accounting for 9.2% each, of the total ovhv2-miRs and 3% of all miRNAs abundance with more than 14000 hits each (Table 4.1). Thirty five of the previously reported 46 ovhv2-miRs (Levy PhD Thesis) were also expressed in this data in varying proportions. The number of reads for each ovhv2-miRs and their percentages as compared to total miRNA counts are shown in Table 4.1. Among those forty six ovhv2-miRs, eight were pre-validated by northern hybridization (Levy *et al*., 2012). Those eight ovhv2-miRs also showed a high abundance in this data set and collectively made 22% of the total ovhv2-miRs

read counts with 31924 hits (shown in red bars in Figure 4.6). A comparison of the reads of ovhv2-miRs obtained from the RNA seq data (Levy *et al*., 2012) and from the CLASH data set is shown in Table 4.2.

The most abundant cellular-miRs expressed in the BJ1035 sample were miR-21, miR-142-3p and miR-155 which made up 30% of the cellular-miRs identified and 19% of the total miRNA count (Table 4.3). Additionally, miR-15b-5p, miR29a, miR29b, miR-146a and miR-29a-3p were also found to be significantly (~17% of cellular-miRs) enriched in the BJ1035 sample. All the cellular-miRs with read counts of greater than 1000 in the BJ1035 sample are presented in table 4.3 and figure 4.7. A complete list of miRNAs with read counts and percentage expression is provided in the supplemental data file 4.1.

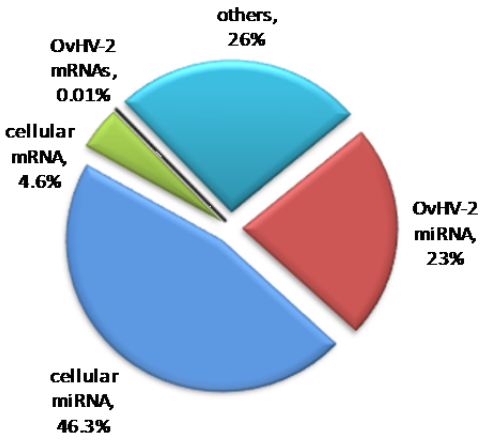

A

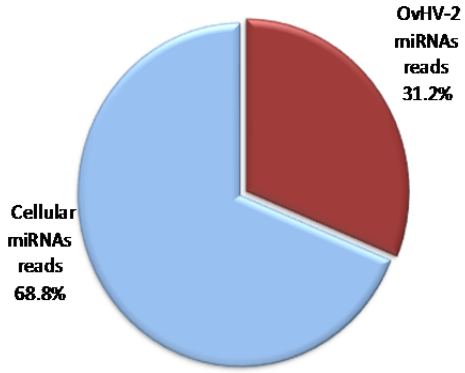

B

```
                          A      GGC  ACUGUG
miR-216a          5' UAAUCUC  GCU      A          A 3'
ovhv2-mir-217M    5' UAAUCUC  GCU      A          A 3'
                          U      CCA  UUGUAA
```

C

Figure 4.5: An overview of CLASH data

A: Data obtained from the high throughput sequencing of the cDNA library generated from LGL cell line BJ1035 expressing HTP tagged Ago2 using CLASH.

B: Proportional distribution of total of miRNA reads in CLASH data.

Pie charts indicate the proportion of mapped reads that correspond to the ovhv2-miRs (Levy PhD Thesis), cellular-miRs, OvHV-2 mRNAs, (accession AY839756.1) present in miRbase and cellular mRNA (cattle transcripts from UMD 3.1). Others indicate presence of ribosomal RNAs, pseudogenes, snRNA and snoRNA in this data set.

C: Seed sequence homology between ovhv2-miR-217M and cellular miR-216a.

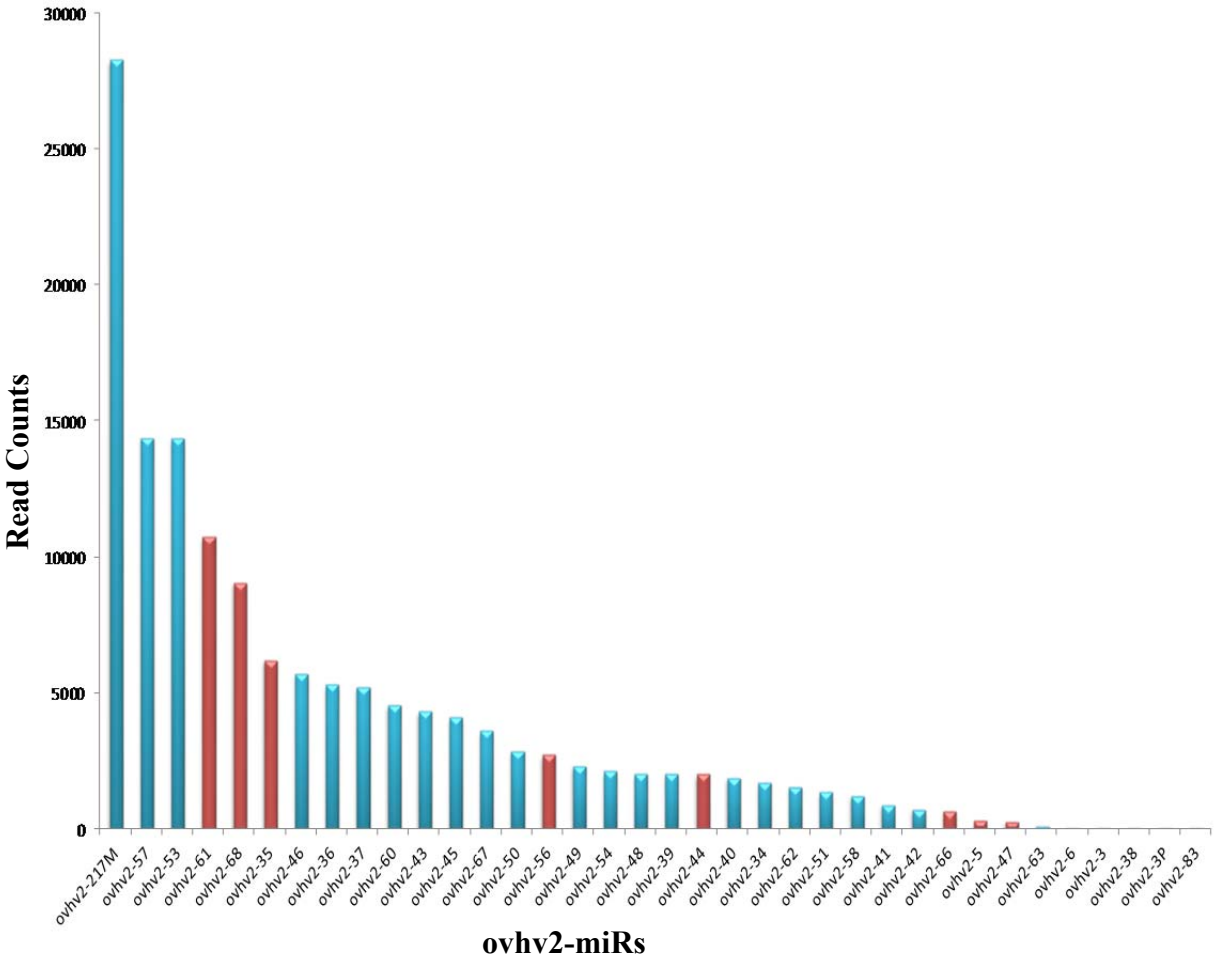

Figure 4.6: The distribution of reads that mapped to ovhv2-miRs in the CLASH dataset for BJ1035 sample.

Red bars show the ovhv2-miRs which were validated by northern hybridization (Levy *et al*., 2012).

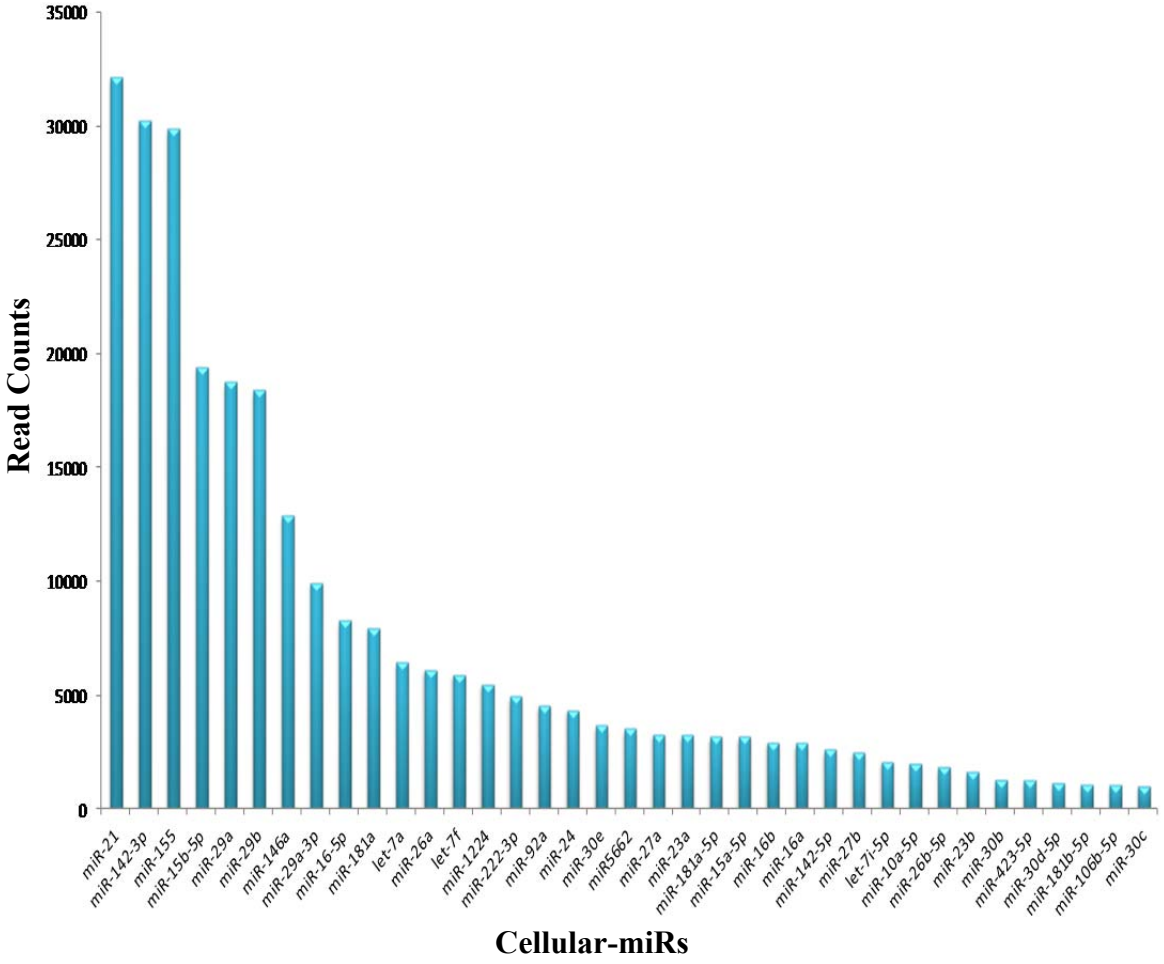

Figure 4.7: The distribution of reads that mapped to cellular-miRs present in miRBase V19 in the CLASH dataset for BJ1035 sample.

Table 4.1: Proportion of the ovhv2-miRs in the CLASH dataset.

ovhv2-miRs	Reads counts	% (as compared to the total ovhv2-miRs)	% (as compared to the total miRNAs count)
ovhv2-miR-217M	28300	19.9	6.2
ovhv2- miR-57	14386	10.1	3.2
ovhv2- miR-53	14345	10.1	3.1
ovhv2- miR-61	10737	7.5	2.3
ovhv2- miR-8	9044	6.4	2.0
ovhv2- miR-35	6210	4.4	1.4
ovhv2- miR-46	5714	4.0	1.3
ovhv2- miR-36	5296	3.7	1.2
ovhv2- miR-37	5199	3.7	1.1
ovhv2- miR-60	4542	3.2	1.0
ovhv2- miR-43	4305	3.0	0.9
ovhv2- miR-45	4071	2.9	0.9
ovhv2- miR-67	3602	2.5	0.8
ovhv2- miR-50	2837	2.0	0.6
ovhv2- miR-56	2711	2.0	0.6
ovhv2- miR-49	2298	1.6	0.5
ovhv2- miR-54	2103	1.5	0.5
ovhv2- miR-48	2029	1.4	0.4
ovhv2- miR-39	2017	1.4	0.4
ovhv2- miR-44	2005	1.4	0.4
ovhv2- miR-40	1869	1.3	0.4
ovhv2- miR-34	1686	1.2	0.4
ovhv2- miR-62	1536	1.1	0.3
ovhv2- miR-51	1350	0.9	0.3
ovhv2- miR-58	1215	0.9	0.3
ovhv2- miR-41	866	0.6	0.2
ovhv2- miR-42	703	0.5	0.2
ovhv2- miR-66	654	0.5	0.1
ovhv2- miR-5	306	0.2	0.07
ovhv2- miR-47	257	0.2	0.06
ovhv2- miR-63	116	0.1	0.03
ovhv2- miR-6	33	0.02	0.007
ovhv2- miR-3	19	0.01	0.004
ovhv2- miR-38	4	0.003	0.0009
ovhv2- miR-3P	1	0.0007	0.0002
ovhv2- miR-83	1	0.0007	0.0002

Foot notes: Percent values were calculated using read counts of each ovhv2-miR to the total read counts of ovhv2-miRs (142367) or the total read counts of ovhv2-miRs+cellular-miRs (468881).

Table 4.2: Comparative analysis of read counts of forty six ovhv2-miRs obtained from from RNA-seq study (Levy PhD thesis) and CLASH dataset.

Ovhv2-miRs	Read counts (RNA-seq)	Read counts (CLASH)	Ovhv2-miRs	Read counts (RNA-seq)	Read counts (CLASH)
ovhv2- miR-3p	25	1	ovhv2- miR-48	8095	2029
ovhv2- miR-64p	2	0	ovhv2- miR-49	2967	2298
ovhv2- miR-96p	1	0	ovhv2- miR-50	3794	2837
ovhv2- miR-1	21	0	ovhv2- miR-51	24497	1350
ovhv2- miR-3	196	19	ovhv2- miR-53	14966	14345
ovhv2- miR-4	1	0	ovhv2- miR-54	1357	2103
ovhv2- miR-1	10588	306	ovhv2- miR-5	11187	2711
ovhv2- miR-6	253	33	ovhv2- miR-57	5457	14386
ovhv2- miR-13	1	0	ovhv2- miR-58	942	1215
ovhv2- miR-34	434	1686	ovhv2- miR-60	351	4542
ovhv2- miR-2	39169	6210	ovhv2- miR-6	10378	10737
ovhv2- miR-36	6200	5296	ovhv2- miR-62	1535	1536
ovhv2- miR-37	6015	5199	ovhv2- miR-63	517	116
ovhv2- miR-38	322	4	ovhv2- miR-7	16574	654
ovhv2- miR-39	4717	2017	ovhv2- miR-67	7834	3602
ovhv2- miR-40	1014	1869	ovhv2- miR-8	46048	9044
ovhv2- miR-41	21686	866	ovhv2- miR-83	1	1
ovhv2- miR-42	740	703	ovhv2- miR-95	1	0
ovhv2- miR-43	31227	4305	ovhv2- miR-128	1	0
ovhv2- miR-3	14694	2005	ovhv2- miR-163	1	0
ovhv2- miR-45	6487	4071	ovhv2- miR-181	1	0
ovhv2- miR-46	9219	5714	ovhv2- miR-182	1	0
ovhv2- miR-4	17508	257	ovhv2-miR-217M	6064	28300

Foot notes: The eight of the ovhv2-miRs validated by northern hybridization (Levy *et al*., 2012) are indicated in blue.

Table 4.3: Proportion of the cellular-miRs in the CLASH dataset.

cellular-miRs	Reads counts	% (as compared to the total cellular-miRs)	% (as compared to the total miRNAs count)
miR-21	32163	10.3	6.9
miR-142-3p	30272	9.7	6.5
miR-155	29902	9.6	6.4
miR-15b-5p	19426	6.2	4.1
miR-29a	18763	6.0	4.0
miR-29b	18405	5.9	3.9
miR-146a	12873	4.1	2.7
miR-29a-3p	9931	3.2	2.1
miR-16-5p	8261	2.6	1.8
miR-181a	7947	2.5	1.7
let-7a	6444	2.1	1.4
miR-26a	6112	2.0	1.3
let-7f	5900	1.9	1.3
miR-1224	5463	1.7	1.2
miR-222-3p	4933	1.6	1.1
miR-92a	4548	1.5	1.0
miR-24	4349	1.4	0.9
miR-30e	3670	1.2	0.8
miR5662	3529	1.1	0.8
miR-27a	3267	1.0	0.7
miR-23a	3247	1.0	0.7
miR-181a-5p	3194	1.0	0.7
miR-15a-5p	3176	1.0	0.7
miR-16b	2947	0.9	0.6
miR-16a	2890	0.9	0.6
miR-142-5p	2624	0.8	0.6
miR-27b	2514	0.8	0.5
let-7i-5p	2091	0.7	0.4
miR-10a-5p	1997	0.6	0.4
miR-26b-5p	1845	0.6	0.4
miR-23b	1627	0.5	0.3
miR-30b	1275	0.4	0.3
miR-423-5p	1268	0.4	0.3
miR-30d-5p	1152	0.4	0.2
miR-181b-5p	1095	0.3	0.2
miR-106b-5p	1041	0.3	0.2
miR-30c	1003	0.3	0.2

Foot notes: Percent values were calculated using read counts of each cellular-miR to the total read counts of cellular-miRs (313036) or the total read counts of ovhv2-miRs+cellular-miRs (468881).

4.3.1.6 CLASH data analysis for the presence of cellular and viral mRNAs

For the BJ1035 sample a total of 206709 sequence reads from 5366 genes were obtained. A large proportion of the reads mapped to 5S ribosomal RNAs (rRNA). Due to its high abundance (168903 out of 206709), rRNA can be co-purified frequently during CLASH experiments, and in other CRAC and CLASH related studies rRNAs were also identified as common contaminants (Granneman *et al*., 2009, Hahn *et al*., 2012).

The remaining reads (34226) were associated with mRNAs (cellular and viral) and other known target classes including pseudogenes, and non-coding RNAs (Figure 4.9, Table 4.4). A total of 31269 sequence reads out of 34226 were mapped to mRNAs derived from the cattle genome and constituted nearly 15% of the total RNA reads. The three most highly targeted genes were: ankyrin repeat domain containing protein26 (Ankrd26) with 1580 reads; zinc finger MYM type-protein 3 (ZMYM3) with 1038 reads and par-3 partitioning defective 3 homolog B (PARD3B) 1004 reads. Other highly targeted genes were leucine-rich repeat-containing protein 30 (LRRC30) (537 reads), olfactory receptor family 10 subfamily K member 1 (OR10K1) (486 reads), serine racemase (SRR) (433 reads), vacuolar protein sorting-associated protein 33B (VPS33B) (368 reads), F-box/LRR-repeat protein 21 (FBXL21) (350 reads), zinc finger protein3 (ZNF3) (284 reads) and U11/U12 small nuclear ribonucleoprotein 25KDa (SNRNP25) (283 reads). mRNAs which had read counts greater than 100 in the BJ1035 sample are presented in Figure 4.9. A complete list of mRNAs with the raw read data and their percentages as a total of mRNAs, is provided in the supplemental data file 4.1.

Other classes of stable RNAs e.g small nuclear ribonucleic acid (snRNA), small nucleolar RNA (snoRNA) and tRNA were also recovered in small proportions in this dataset (Figure 4.8) 1.5% of the total reads were spliceosomal RNAs (snRNAs). Among the different classes of snRNAs (U1, U2, U4, U5, U6, U7, U12), U2 snRNA was the most enriched snRNA constituting ~68% of the total snRNA read counts. One of the OvHV-2 miR (ovhv2-miR-36) was found to form a chimera with U2 spliceosomal RNA. Details of the U2 spliceosomal RNA and ovhv2-miR-36 chimeric read are discussed in section 4.3.3. Nearly 0.7% of the total reads were mapped to the regions which were annotated as pseudogenes (Figure 4.8, Table 4.4).

A very small proportion (~0.05%) of reads mapped to the OvHV-2 predicted ORFs. ORF64 (large tegument protein), Ov8 (putative glycoprotein), ORF7 (subunit of terminase) and ORF61 (ribonucleotide reductase) were the top targeted ORFs with read counts of 16, 8, 7 and 7 respectively. (Supplemental data file 4.1 for full list of viral mRNA read counts).

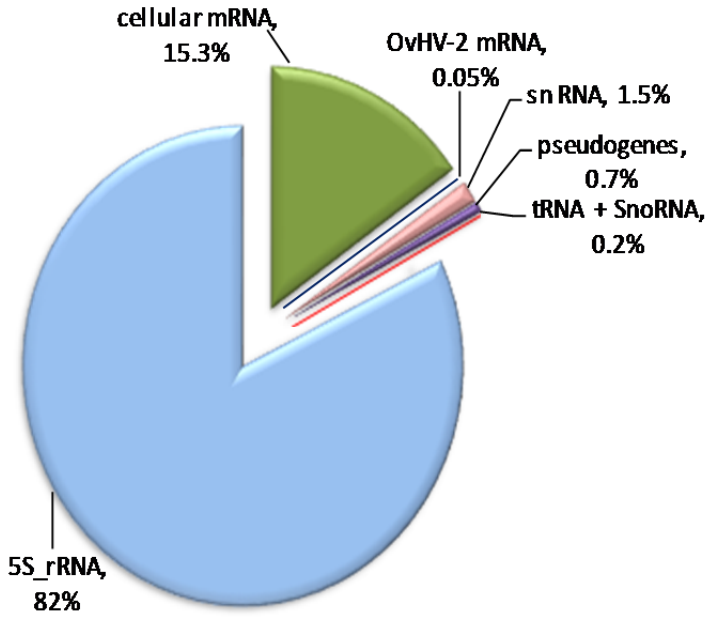

Figure 4.8: Summary of mRNAs and other RNA classes present in the CLASH dataset of BJ1035 sample.

Pie chart indicates the proportion of mapped reads that corresponds to the OvHV-2 mRNAs, cellular mRNAs, SnRNA (spliceosomal RNAs), pseudogenes, tRNAs, snoRNA (small nucleolar RNAs) and 5s_rRNA (ribosomal RNAs).

Table 4.4: Targeted classes identified in the CLASH data of BJ1035 sample.

Targeted classes in CLASH	Read counts	Percentage (%)
Cellular mRNA	31339	15.3
OvHV-2 mRNA	95	0.05
SnRNA	3083	1.5
Pseudogenes	1487	0.7
tRNA + SnoRNA	502	0.2
5S_rRNA	168903	82

Foot note: Percent values were calculated using read counts of each targeted class to the total mapped read counts (206709).
SnRNA: spliceosomal RNAs, snoRNA: small nucleolar RNAs, rRNA: ribosomal RNAs

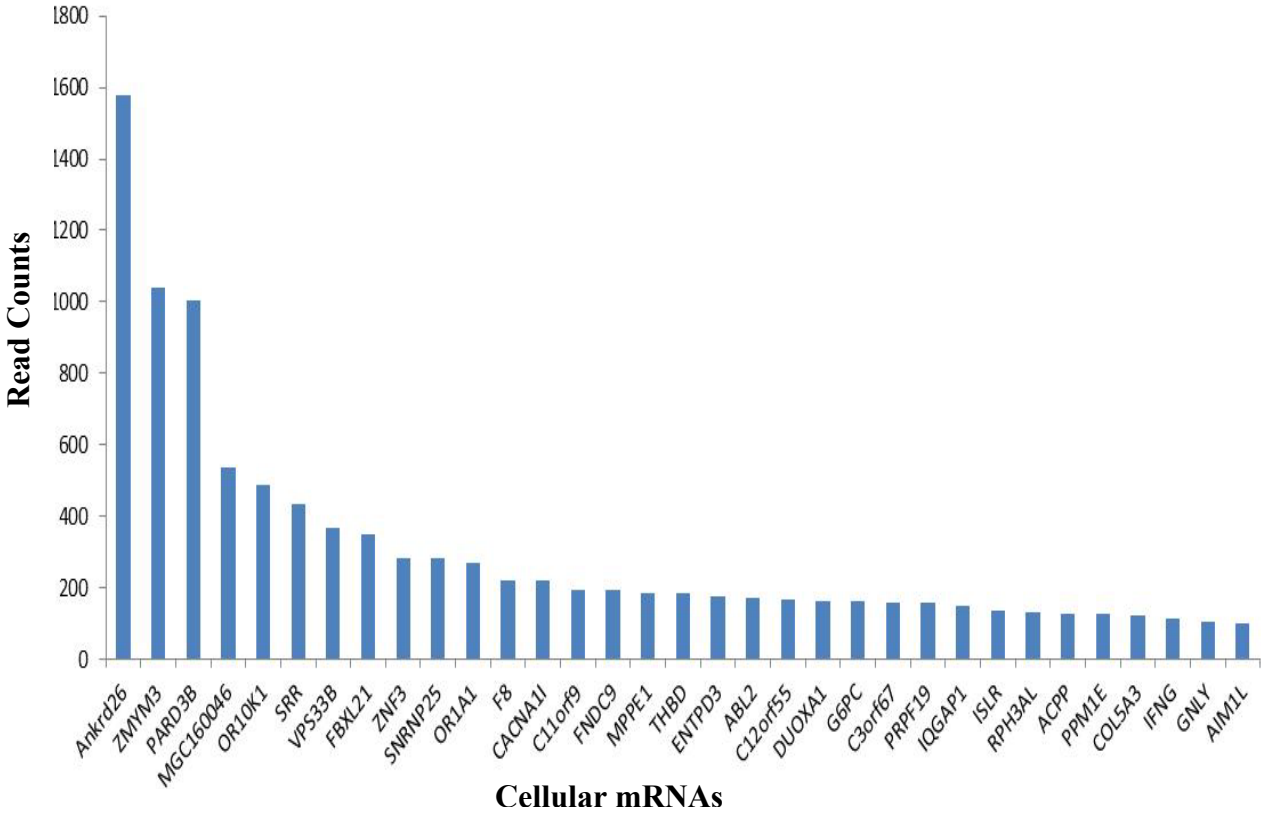

Figure 4.9: Distribution of reads that mapped to cellular mRNAs present in cattle transcripts.

Data obtained from high throughput sequencing of cDNA library generated from LGL cell line BJ1035 expressing HTP tagged Ago2.

4.3.2 CLASH for sheep embryo fibroblasts expressing ovhv2-miRs

4.3.2.1 Transient transfections of ovhv2-miRs in sheep embryo fibroblasts

Unlike BJ1035 cells sheep embryo fibroblasts (SEF) do not express ovhv2-miRs. Two regions of the OvHV-2 genome predicted to express, two clusters of ovhv2-miRs were cloned into a lentivirus vector (Section 2.1.7). Cluster-2 was 4.4kb long (coordinates: 27698-32075) and Cluster-3 was 260bp long (coordinates: 36313-36575) (Figure 1.5). Cluster-2 and Cluster-3 are predicted to encode for twenty seven and three ovhv2-miRs respectively (Levy PhD thesis, 2012). Successful amplification (Section 2.1.2) and cloning of each of the cluster region was confirmed by agarose gel electrophoresis (Section 2.1.4) and sequencing (Section 2.1.9). Transient transfections were performed and total RNA was extracted (Section 2.1.10) from the cells transfected with either pLenti-blast cloned with Cluster-2 (pLenti-Cluster-2), Cluster-3 (pLenti-Cluster-3) or empty vector (pLenti-empty). cDNA synthesis of miRNAs and RT-qPCR for cloned ovhv2-miRs expression were performed as described in section 2.1.11 and 2.1.12 respectively (Appendix-3 for RT-qPCR forward primers).

RT-qPCR analysis was used to show that SEF transduced with pLenti-Cluster-3 showed the expression of three ovhv2-miRs (ovhv2-miR-7 , ovhv2-miR-67 and ovhv2-mR-8) at levels comparable to the positive control (miR-16), a highly expressed stable cellular miRNA (Kroh *et al*., 2010). pLenti-Cluster-2 is predicted to encode for 27 ovhv2-miRs and RT-qPCRs were carried out for ovhv2-mir-43, ovhv2-mir-41, ovhv2-mir-2, ovhv2-mir-3, ovhv2-mir-62 and ovhv2-mir-63. None of

the miRNAs showed expression (data not shown). Based on these results pLenti-Cluster-3 was selected only for stable transfections of SEF for further investigations.

4.3.2.2 Transduction of SEF with lentiviruses expressing ovhv2-miRs and tagged Ago2 protein

After initial screening based on the RT-qPCR (Section 4.3.2.1), only pLenti-Cluster-3 was selected to produce lentivirus expressing ovhv2-miR-7, ovhv2-miR-67, ovhv2-miR-8 in SEF (Section 2.4.6 and 2.4.8). After transduction with lentiviruses expressing pLenti-Cluster-3 or pLenti-empty, blasticidin selection of the cells was performed (Section 2.4.7). RT-qPCRs were carried out to detect the expression of ovhv2-miRs as described in section 4.3.2.1. Results showed that each of the three miRNAs expression was comparable to the positive control (miR-16).

SEF stably expressing Cluster-3 and SEF transduced with pLenti-empty were again transduced with tagged Ago2 expressing lentivirus (section 2.4.8). Doubly transduced cells were selected by puromycin and later used to perform CLASH. Western blot analysis also indicated a successful expression of tagged Ago2 in cluster-3 expressing SEF (SEF-Cluster-3) and SEF transduced with pLenti-empty (SEF-Empty) (Figure 4.10A).

4.3.2.3 Small scale immunoprecipitation of analysis of tagged Ago2 in SEF-Cluster-3 and SEF-Empty

Before proceeding to CLASH experiments a protein A-tag mediated immunoprecipitation (IP) was performed with SEF-Cluster-3 and SEF-Empty as described in section 4.3.1.2. The western blot results showed that, the cell lysate and IP samples of SEF-Cluster-3 and SEF-Empty contained tagged Ago2, whereas the

FT sample contained very little tagged Ago2, indicating an efficient IP and no significant loss of proteins during the washing steps (Figure 4.10B and C respectively).

4.3.2.4 CLASH experiments for SEF-Cluster-3and SEF-Empty samples

CLASH experiments (section 2.8.4) were performed with three replicates each of SEF-Cluster-3 and SEF-Empty as tests (T1, T2 and T3) and negative controls (C1, C2, and C3) respectively as described in section 4.3.1.3. Bands representing the 100 KDa tagged Ago2 were identified in all the samples (Figure 4.11A). The T1 sample of SEF-Cluster-3 showed a low level of labelled radioactivity signal as compared to the other two test samples which might be due to the loss of some of the cross-linked sample during the washing steps following radiolabelling. The C3 sample of SEF-Empty showed smears above the band of desired size which might be due to presence of other RNAs. A more stringent washing during the IP and Ni affinity purification step could reduce smearing, but relevant interactions may also be lost. Common contaminants of approximately 50 to 80 Kda were detected in all samples (Figure 4.11A asterisk*). The regions associated with 100 Kda were excised from the membranes (indicated in red boxes in Figure 4.11A) as outlined in section 2.8.8. The RNA recovered after proteinase K treatment and 5' linker ligation was reverse transcribed and cDNA libraries were prepared (section 2.8.9 to 2.8.12). A small quantity of the cDNA libraries of each of the sample was amplified by PCR (PCR primers Appendix-3) and the products were visualized on the agarose gel (Figure 4.11B). In all of the samples, a PCR product of ~150bp was excised from the gel (red squares in Figure 4.11B). Sequencing results provided sufficient evidence that all the

samples have miRNAs and/or mRNA, 5'linker, barcodes and 3'linker sequences. Insert lengths observed were in the range between 0-59nt. Ovhv2-mir-67 was one of the ovhv2-miRs that were stably expressed by the transduced SEF (Section 4.3.3). Sequencing of the T2 sample identified the complete sequence of ovhv2-mir-67. This initial sequencing therefore confirmed that the viral miRNAs were being correctly processed and incorporated into the RISC complex (Figure 4.12). For further analysis the cDNA libraries were submitted for Solexa sequencing.

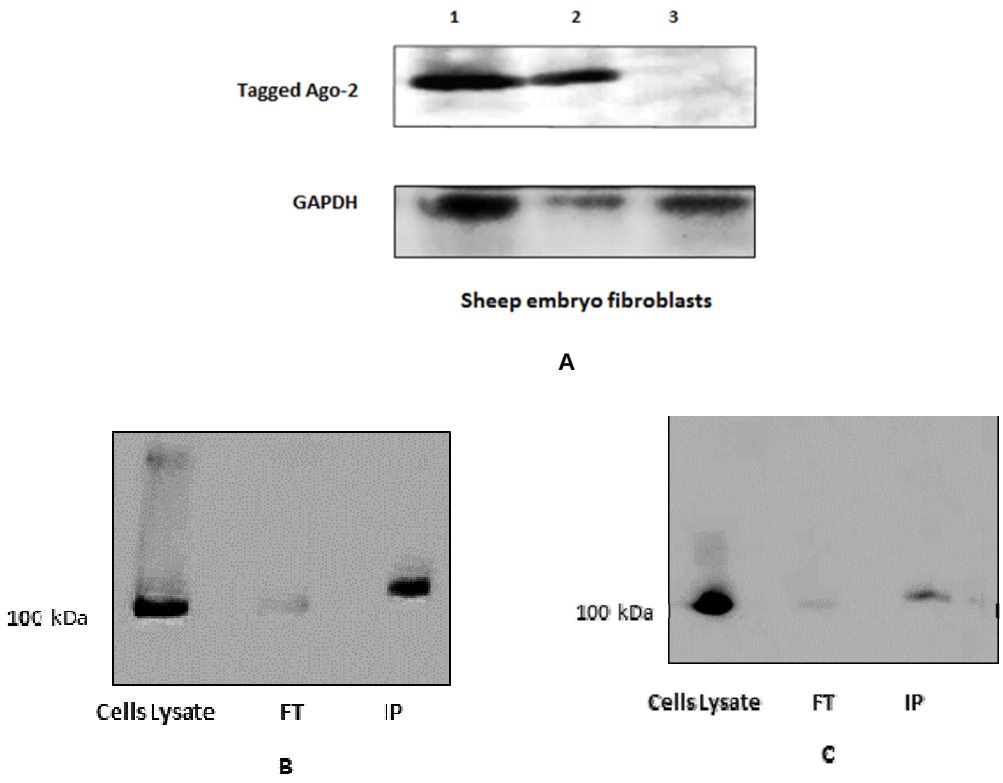

Figure 4.10: Western blot analysis to monitor tagged Ago-2 in sheep embryo fibroblasts (SEF).

A: Western blot with antibody against human Ago2 or GAPDH showing expression of tagged Ago2 in SEF.
Lane 1: SEF transduced with three ovhv2-miRs and HTP tagged Ago2
Lane 2: SEF transduced with tagged Ago2
Lane 3: Un-transduced SEF

B and **C**: Western blot analysis to monitor the enrichment of HTP tagged Ago2 using protein A-tag mediated immuno-precipitation (IP) in the SEF transduced with tagged Ago2 and/or three ovhv2-miRs. Cell lysate, FT and IP samples were probed with antibodies against human Ago-2 using magnetic Dyna-beads. FT: Flow through obtained during washing steps of IP.
B: SEF-Cluster-3: SEF transduced with three ovhv2-miRs and tagged Ago2
C: SEF-Empty: SEF transduced with tagged Ago2
FT: Flow through obtained during washing steps of IP

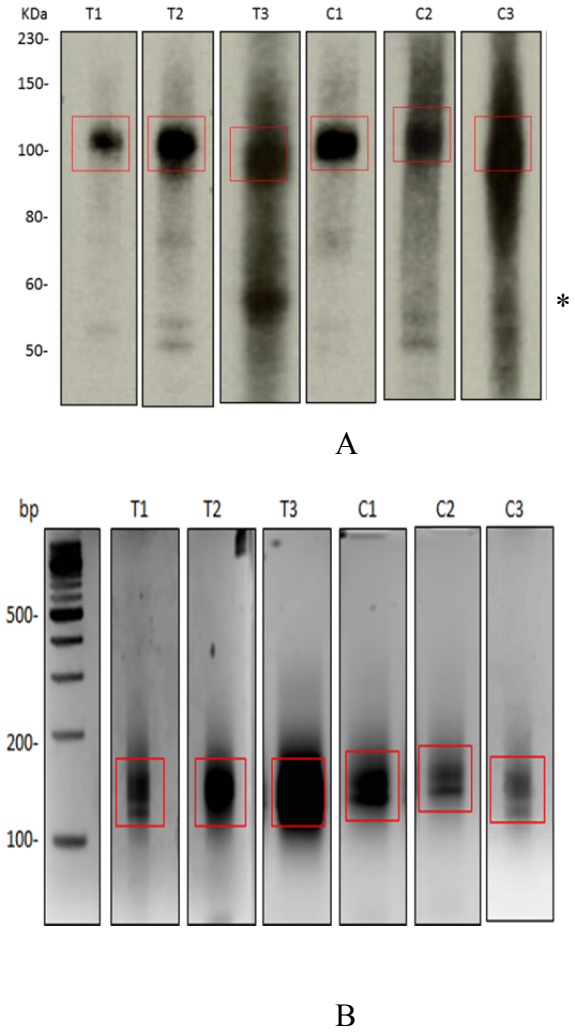

Figure 4.11: Visualization of CLASH experimental products.

(A) Autoradiograph of radiolabelled tagged Ago2 with miRNA-mRNA complex after Ni-affinity purification and 3'linker ligation. Red boxes indicate regions on the membrane that were excised and used for downstream analysis. Asterisk sign shows a common contaminant of 50-60KDa. The protein size marker is indicated on the left.

(B) MetaPhor agarose gel electrophoresis with 3% agarose and 1xTBE, of cDNAs libraries amplified by PCR. The regions which were excised from the gel for DNA extraction are indicated in red boxes. A 100bp DNA size marker (NEB) is indicated on the left.

T1, T2, T3: Three replicates of SEF-Cluster-3

C1, C2, C3: Three replicates of SEF-Empty

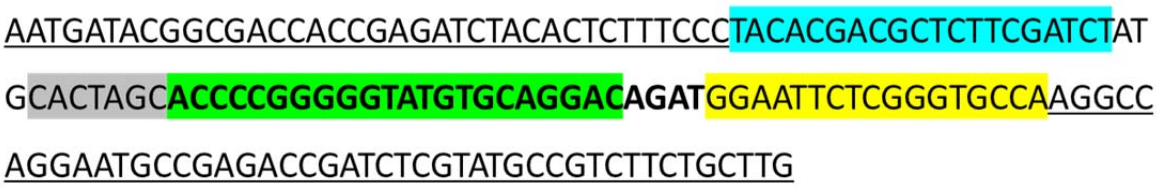

Figure 4.12: Sequencing of a cloned cDNA sample generated from the T2 sample of SEF-Cluster-3.

5' linker, barcode and 3' linker is highlighted in cyan, grey and yellow respectively. RNA insert is shown in bold. ovhv2-miR-67 sequence was also observed as a part of the insert and is shown in green. Adapter sequences from PCR primers are shown as underlined non-highlighted areas.

4.3.2.5 High Throughput sequencing of cDNA libraries obtained from SEF-Cluster-3and SEF-Empty

Bioinformatic analysis of the test and control samples were carried out as described in section 4.3.1.4. The total number of reads which could be matched with the barcodes associated with the T1, T2, T3, C1, C2 and C3 samples were 15,939,277, 14,483,617, 7,188,832, 19,151,198, 18,673,973 and 43,709,491 respectively. The resulting reads were mapped against ovhv2-miR-7, ovhv2-miR-67 and ovhv2-miR-8 and the entire database of miRBase V19 using Blast, after removing the sequencing adapter. To look for the expression of targeted genes, the reads were also mapped to the sheep genome OAR v3.1. A total of 565,833, 1,149,259 and 443,918 reads were obtained for the T1, T2 and T3 samples of SEF-Cluster-3, whereas 964,658, 237,685 and 712,257 reads were obtained from the C1, C2 and C3 samples of SEF-Empty (Table 4.5). The number of reads mapping to sheep genes and the occurrence of all chimeras were recorded.

Table 4.5: An overview of the CLASH data obtained from sheep embryo fibroblasts expressing tagged Ago2.

Samples	Total raw reads	Total mapped reads	ovhv2-miRs reads, (total ~ percent)	cellular miRs reads, (total ~ percent)	cellular mRNA reads, (total ~ percent)	other reads, (total ~ percent)	OvHV-2 Hybrid reads (total ~ percent)	Cellular hybrid reads, (total ~ percent)
T1	15939277	565833	14635, (3%)	470518, (83%)	80398, (14%)	107, (0.02%)	95, (0.02%)	80, (0.01%)
T2	14483617	1149259	96387, (8%)	1036058, (90%)	16619, (1%)	23, (0.00%)	115, (0.01%)	57, (0.00%)
T3	7188832	443918	155673, (35%)	275409, (62%)	11856, (3%)	21, (0.00%)	917 (0.21%)	42, (0.01%)
C1	19151198	964658	5606, (1%)	941923, (98%)	17000 (2%)	12, (0.00%)	0, (0.00%)	117, (0.01%)
C2	18673973	237685	4027, (2%)	208573, (88%)	24997 (11%)	35, (0.01%)	4, (0.00%)	49, (0.02%)
C3	43709491	712257	17242, (2%)	643365, (90%)	51509, (7%)	52, (0.01%)	28, (0.00%)	61, (0.01%)

Foot notes: T1, T2 and T3 are test samples expressing ovhv2-miR-7, 67 and 8.
C1, C2, C3 are control samples.
Percentage values obtained by comparing number of reads with total mapped reads (column three) of their respective group.

4.3.2.6 Analysis of ovhv2-miRs in the CLASH data from SEF-Cluster-3 and SEF-Empty

The number of reads obtained for ovhv2-miRs (ovhv2-miR-7, 67 and 8) in the test samples T1, T2 and T3 are shown in Figure 4.13. The percentages of those counts as compared to the total number of reads of their respective samples were ~3%, 8% and 35%. The presence of other ovhv2-miRs (ovhv2-miRs which were not used in this part of the study) in tests and controls was detected in a very low numbers is most likely due to the contamination of barcodes as described in the section 4.3.1.4 (Table 4.5). Sequencing results showed that ovhv2-mir-67 was the most abundant of the three ovhv2-miRs and constituted 75%, 89% and 89% of total ovhv2-miRs reads in T1, T2 and T3 samples, respectively. The abundance of ovhv2-miR-8 was 2734 (19%), 6386 (7%) and 12039 (8%) in T1, T2 and T3 samples, respectively. ovhv2-miR-7 was the least abundant of the three ovhv2-miRs with 824 (6%), 2039 (2%) and 5342 (3.4%) reads in T1, T2 and T3 respectively (Figure 4.14).

In the tests and control samples a large number of cellular-miRs was also found. The percentages of read counts for cellular-miRs as compared to the total reads counts in T1, T2 and T3 samples were 83%, 90% and 62% whereas for C1, C2 and C3 the percentages were ~98%, 87% and 90% of their total reads counts respectively (Table 4.5). It is worth noting that in test samples due to the abundance of ovhv2-miR-7, ovhv2-miR-67 and ovhv2-miR-8 the percentage of cellular-miRs is less than that of control samples.

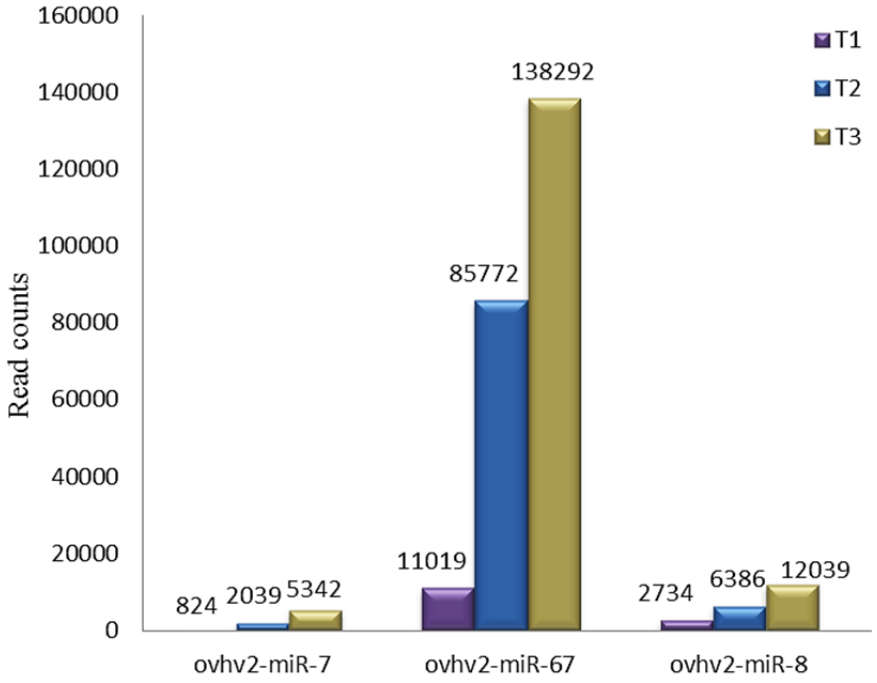

Figure 4.13: Read counts of the three ovhv2-miRs obtained from the three samples of SEF-Cluster-3.

The distribution of the ovhv2-miRs (ovhv2-miR-7, -67 and -8) in the Test samples (T1, T2, and T3) is shown.

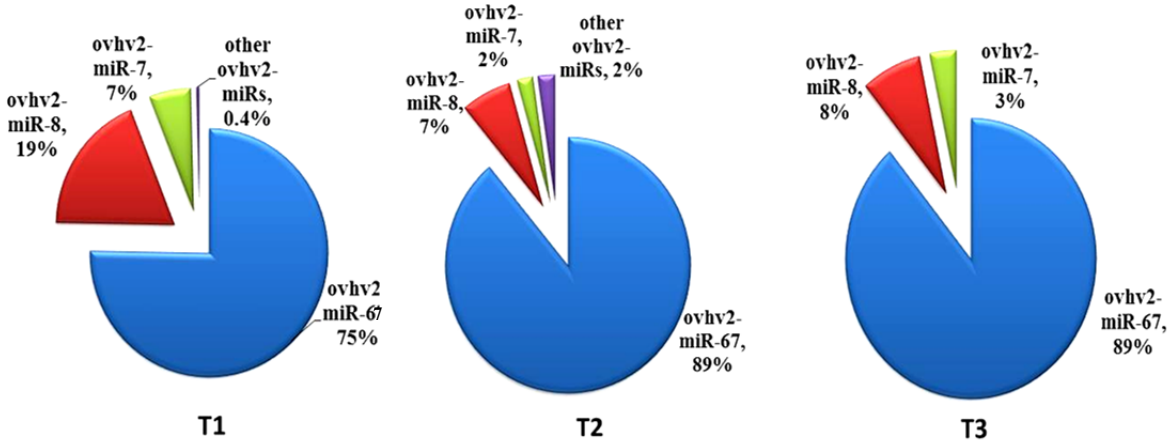

Figure 4.14: The proportion of ovhv2-miR-7, ovhv2-miR-67 and ovhv2-miR-8 in test samples (T1, T2 and T3) of SEF-Cluster-3.

Percentages of the three ovhv2-miRs as compared to the total read counts of the ovhv2-miRs, in each sample, are shown.

4.3.2.7 Analysis of sheep mRNAs in SEF-Cluster-3 and SEF-Empty

For the SEF-Cluster-3 and SEF-Empty samples Solexa sequencing reads were obtained as described in 4.3.2.5 and were mapped to predicted genes from the sheep genome. Read counts for mRNAs of tests and control samples and percentages relative to the respective samples are shown in column 5 of Table 4.5. The T1 sample showed the highest abundance of sheep mRNA reads among the three datasets of the test groups. Less than 0.02% of the total sequence reads could be matched to other RNA classes such as rRNA, tRNA, snRNA, snoRNA and transposons in each of the test and control groups (Table 4.5).

To identify the sheep genes which were differentially enriched in the test and control samples a differential gene enrichment analysis was performed.

4.3.2.8 Identification of differentially enriched sheep genes obtained in CLASH

To determine which genes showed differential enrichment in SEF-Cluster-3 samples as compared to SEF-Empty samples, the test and control sample datasets were analysed with the help of using the R (version 2.13.0) package EdgeR (Robinson *et al*., 2010). Genes with less than 100 mapped reads in the test or control groups were excluded from the analysis. P-values were obtained for all comparisons of interest. Twenty nine differentially enriched genes (DEnGs) with a p-value<0.05, between the test and control groups were identified. To control for false positive predictions a 5% false discovery rate (FDR) threshold was applied the datasets. A 5% FDR adjusted p-value (q-value≤0.05) means that 5% of significant tests will result in false positives.

At a FDR threshold for 5%, only five DEnGs out of 29 were still significant. Those genes included delta-like protein 1(DLL1) (also known LOC101117853) (q=0.03), zinc finger protein GLI2 (GLI2) (q=0.03), sec1 family domain containing 1 (SCFD1) also known as SLY1 (q=0.03), active BCR related gene (ABR) (q=0.035) and an uncharacterized protein (q=0.03) (Table 4.6). Using EdgeR positive and negative log2 fold change (logFc) values in the DEnGs was calculated. The positive logFc indicated that the number of read counts was higher in the test samples as compared to the control samples and vice versa for the negative fold change values. The five top DEnGs (shown above) were found to have positive logFc values; 6.1 (DLL1), 8.7 (GLI2), 12.7 (SCFD1), 10.4 (ABR) and 10 (uncharacterized).

The remaining 24 DEnGs with p-value<0.05 were also analysed to identify genes which could be biologically important. Eighteen of those showed a positive log fold change ranging from 3.7 to 10.6 and a q-value from 0.07 to 0.29. The remaining six genes showed a negative log fold change ranging between -9.5 to -6. These genes include translationally-controlled tumor protein TCTP also known as TPT1 (q=0.16), cold shock domain-containing protein E1 (CSDE1) (q=0.14), TBC1 domain family member 9 (TBC1D9) (q=0.082), ubinuclein-1 (UBN1) (0.13), putative RNA-binding protein Luc7-like 2 (LUC7L2) (q=0.072) and lysosomal-associated transmembrane protein 4B (LAPTM4B) (q=0.13). A complete list of the DEnGs with log fold change, p-values and q-values is shown in Table 4.6.

4.3.2.9 Identification of differentially expressed sheep genes obtained by microarray data analysis

To validate CLASH data and to identify genes whose expression changed in the presence of ovhv2-miR-7, ovhv2-miR-67 and ovhv2-miR-8, a microarray study was carried out using SEF-Cluster-3 and SEF-Empty. Total RNA from three replicates each of test and control groups were analysed using the Affymetrix ovine gene 1.0 ST array, for whole-transcript analysis using sheep genome OAR v2.0 as described in section 2.8. The analysis of the microarray data was performed with the help of Miss Alison Downing from ARK Genomics using Partek Genomic suite.

The microarray data analysis of test vs control samples showed a total of 1900 statistical significant DEG with a $p<0.05$. Out of those 1900 genes, 977 showed a negative fold change which was an indication of down regulation in the expression of those genes. The remaining 904 showed a higher expression of genes in the control as compared to the test samples (Supplemental data file 4.3). When a 5% FDR was applied to avoid false positive predictions, no DEG with $p<0.05$ could pass through the filter. Therefore another less stringent filter (fold change ≥ 1.5 or ≤ -1.5 and $p \leq 0.01$) was applied to get highly up regulated and down regulated genes. A total of 32 genes were obtained. The hierarchical clustering in the heat map showed that there was excellent intra-group agreement between test and control samples. Figure 4.16 shows the heat map for the 32 DEG identified by microarray analysis of the transduced-SEF. Twenty five of those genes are highly down-regulated and seven are highly up-regulated in the SEF-Cluster-3 as compared to SEF-Empty.

The top down-regulated genes were ferritin heavy chain (FTH1) and Ectonucleotide pyrophosphatase/phosphodiesterase family member 2 (ENPP2) also referred to Autotaxin, which showed a fold change of -2.2 and -2.03 respectively. The two top up-regulated genes were Solute carrier family 3 (neutral and basic amino acid transporter) member 1 (SLC3A1) and Desmin (DES), which showed a fold change of 2.15 and 2.25 respectively (Table 4.7).

4.3.2.10 Comparison of the DEnGs identified from CLASH and DEG from microarray data analysis

DEnGs obtained from the CLASH (Section 4.3.2.8) and DEG from microarray datasets (Section 4.3.2.9) were also compared for common sets of genes but at the defined significance levels no genes were found in common between the two data sets. There may be a number of reasons. Firstly CLASH is involved in the physical binding of the transcript to the miRs and their immuno-precipitation along with the RISC complex. In contrast microarray global analysis involves changes in the expression of genes possibly due to the downstream effects of targeting by ovhv2-miRs. Secondly miRNA induced translational repression of targeted transcripts often produces changes at a smaller level in gene expression, which may be missed by the stringent condition of CLASH and microarray data analysis. For example Endothelial PAS domain-containing protein 1 (EPAS1) was present in both data sets. In the CLASH data EPAS1 was one of the DEnGs but it could not pass the filter for differential gene expression measurement in microarray data with a p=0.038 (supplemental data file 4.2).

4.3.2.11 Identification of Ovhv2-miRs target sites within DEnGs and DEGs

In the previous sections (4.3.2.8 and 4.3.2.9) CLASH and microarray data analysis was used to identify genes which might be regulated by ovhv2-miR-7, ovhv2-miR-67 and/or ovhv2-miR-8. To proceed further it was necessary to also identify if target sequences for those ovhv2-miRs were present within the 5'UTR, CDS or 3'UTR of the DEG.

To confirm the presence of miRNA targets sites, a target prediction analysis was performed using the miRNA target prediction programe; RNAhybrid. Only those DEnGs which showed a positive fold change in CLASH data and DEG which showed a negative fold change in the microarray data were analysed using RNAhybrid. Parameters for the prediction of the miRNA target were set to identify a miRNA seed region similarity from position 1-7 or 2-8 nucleotides from the 5'end. G:U pairing was also allowed. The information on the location of the 5'UTR or 3'UTR of some of the genes was not available. In those cases the CDS was used for miRNA target site identification. Uncharacterized and non-annotated genes were also excluded from the analysis. The number of predicted target sites for ovhv2-miRs in DEnGs and DEG is shown in Table 4.8 and 4.9 respectively.

All of the DEnGs and DEG showed predicted target site/s for one or more of the three ovhv2-miRs and it is possible that the differential expression of those genes in both datasets was due to targeting of these genes by ovhv2-miRs.

Table 4.6: Differentially enriched genes (DEnGs) identified by the CLASH data analysis.

CLASH Differentially expressed genes	logFC	p-value	*q value
DLL1: Delta-like protein 1 (ligand for Notch receptors)	6.1	0.0004	0.030
Uncharacterized	10.4	0.0005	0.030
GLI2: zinc finger protein	8.7	0.0006	0.030
SCFD1; Sec1 family domain-containing protein 1	12.7	0.0007	0.030
ABR;Active breakpoint cluster region-related protein	10.0	0.001	0.035
DHX57; Putative ATP-dependent RNA helicase	8.7	0.003	0.072
POLN; DNA polymerase theta subunit	9.4	0.004	0.072
FOXRED2;FAD-dependent oxidoreductase domain-containing protein 2	7.5	0.004	0.072
LUC7L2; Putative RNA-binding protein Luc7-like 2	-6.1	0.004	0.072
C10ORF71; Uncharacterized protein	7.8	0.005	0.074
AGTPBP1; Cytosolic carboxypeptidase 1	4.4	0.007	0.102
TBC1D9; TBC1 domain family member 9	-7.0	0.007	0.082
LAPTM4B; Lysosomal-associated transmembrane protein 4B	-6.1	0.010	0.13
SLC9A5; solute carrier family 9, member 3 : SL9A5_HUMAN Sodium/hydrogen exchanger 5	10.1	0.012	0.13
UBN1; Ubinuclein-1	-6.4	0.012	0.13
CCDC88B; Coiled-coil domain-containing protein 88B	10.6	0.012	0.13
CYP4F22; Cytochrome P450 4F22	10.1	0.015	0.14
CSDE1; Cold shock domain-containing protein E1	-8.5	0.016	0.14
HIC1; Hypermethylated in cancer 1 protein	9.8	0.016	0.14
ALMS1; Alstrom syndrome protein 1	8.0	0.017	0.14
TCTP; Translationally-controlled tumor protein (TPT1)	-9.5	0.02	0.16
ADAMTSL4;ADAMTS-like protein 4	5.8	0.031	0.24
ZBTB7C; Zinc finger and BTB domain-containing protein 7C	9.5	0.032	0.24
EPAS1; Endothelial PAS domain-containing protein 1	3.7	0.034	0.24
Uncharacterized	9.4	0.039	0.26
ADAT3; tRNA-specific adenosine deaminase-like protein 3	9.4	0.041	0.27
CD177; CD177 antigen	5.3	0.044	0.27
USP19; Ubiquitin carboxyl-terminal hydrolase 19	7.1	0.046	0.29
RXFP3; Relaxin-3 receptor 1	5.6	0.047	0.29

Foot notes: $p<0.05$ for the statistical significance.
LogFC: Log2 fold change.
*: DEnGs are ranked by q-values

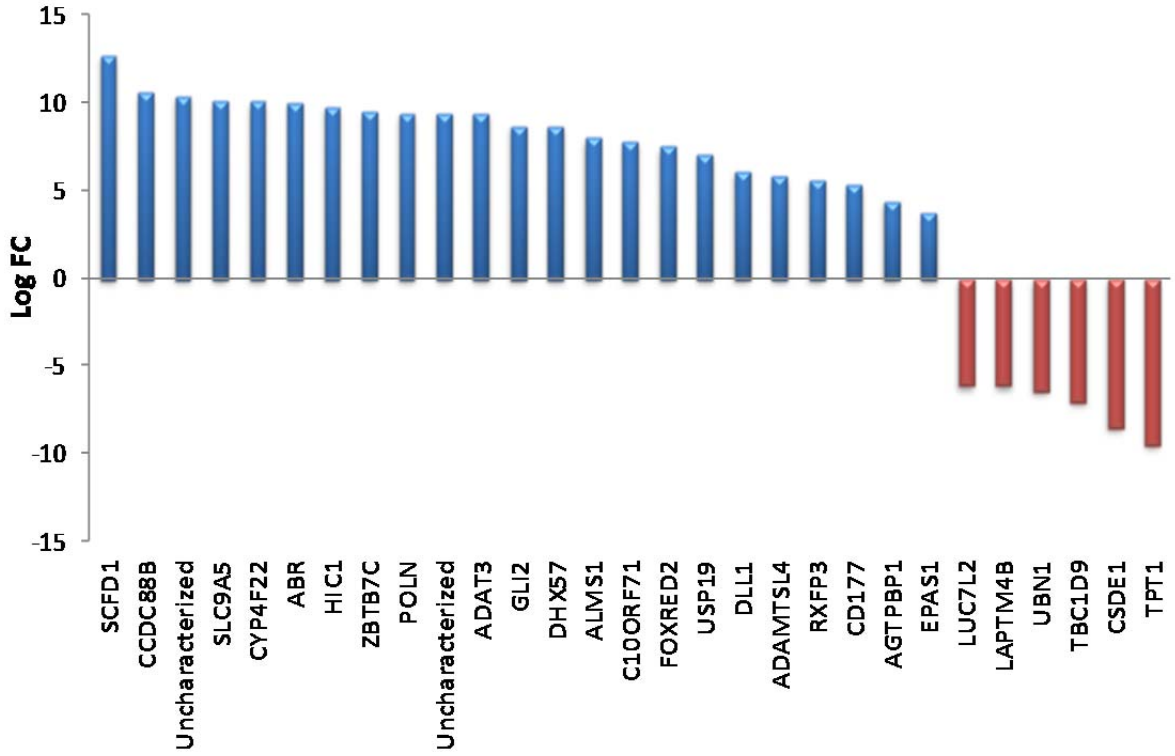

Figure 4.15: Differentially enriched genes (DEnGs) identified by the CLASH data analysis with statistical significance (adjusted p<0.05).

Blue bars show the positive fold change indicating the higher enrichment of DEnGs in test samples as compared to control samples, whereas negative fold (red bars) indicates the lower enrichment of DEnGs in test samples as compared to control samples.
LogFC: Log2 fold change.

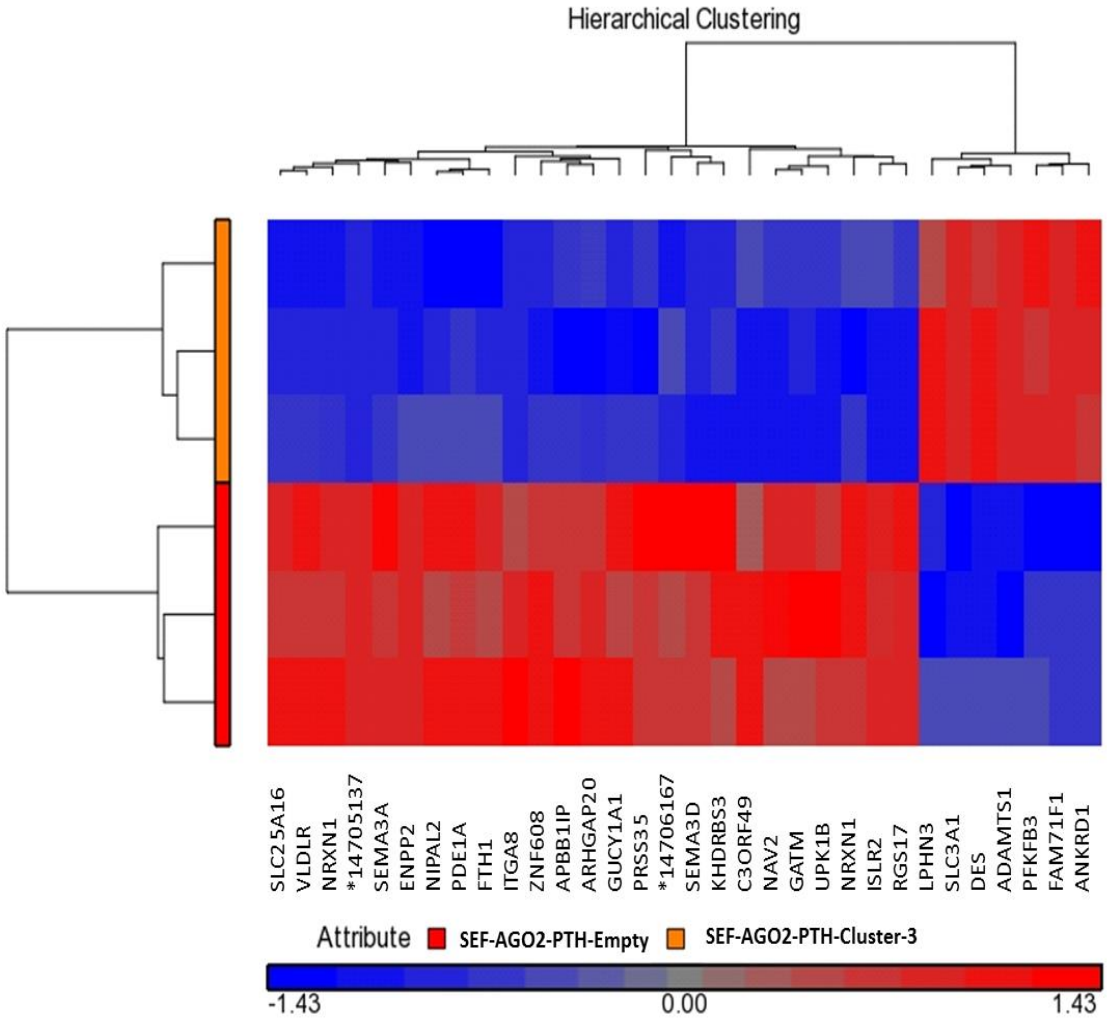

Figure 4.16: Heat map comparing differentially expressed genes obtained from microarray analysis of tests and control samples.

Shown are the genes which had p-value <0.05. The samples are represented in rows and the genes in the columns. Blue blocks indicate down regulation and red blocks indicate up-regulation while gray indicate no change.

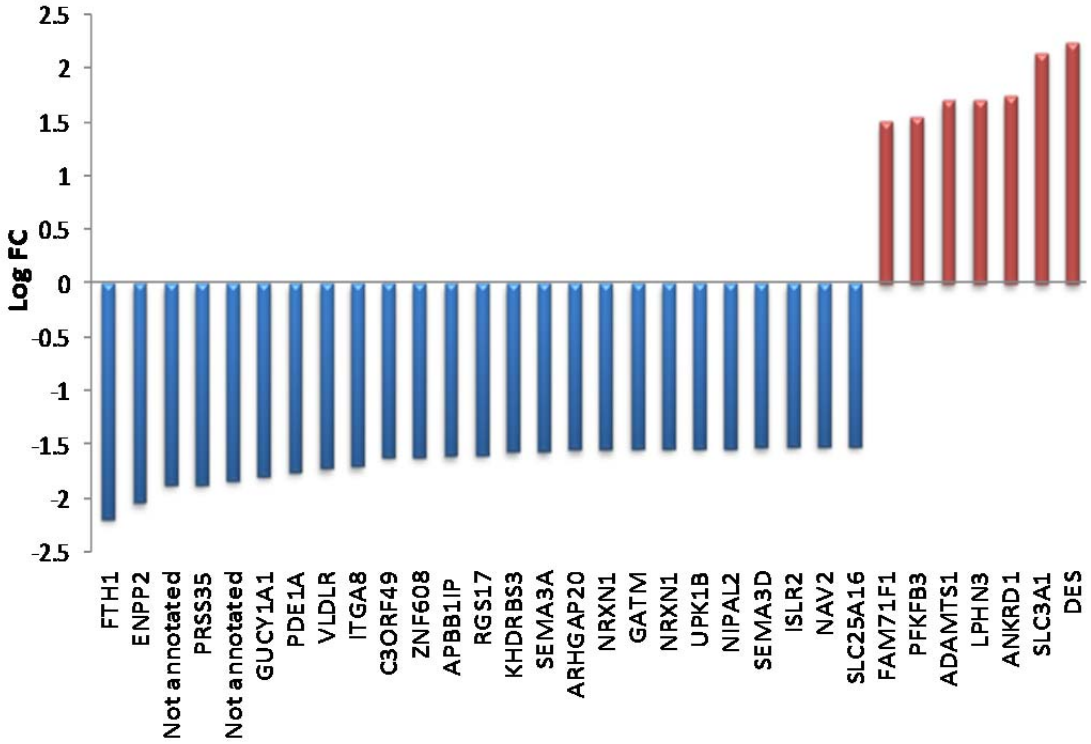

Figure 4.17: Differentially expressed genes (DEG) identified by the microarray analysis (fold change >1.5 or <-1.5 and p<0.01).

Blue bars show the negative fold change indicating the down regulation of DEG in test samples as compared to control samples, whereas negative fold (red bars) indicates the up-regulation of DEG in test samples as compared to control samples. LogFC: Log2 fold change.

Table 4.7: Differentially expressed genes (DEG) identified by microarray data analysis.

Microarray differentially expressed genes	*Log FC	p-value
FTH1; Ferritin heavy chain	-2.18	0.0057
ENPP2; Ectonucleotide pyrophosphatase/phosphodiesterase family member 2	-2.03	0.0013
Not annotated	-1.86	4.42E-07
PRSS35; Inactive serine protease 35	-1.86	0.0057
Not annotated	-1.82	0.0089
GUCY1A1; guanylate cyclase soluble subunit alpha	-1.78	0.0016
PDE1A; Calcium/calmodulin-dependent 3'; 5'-cyclic nucleotide phosphodiesterase 1A	-1.74	0.0075
VLDLR; Very low-density lipoprotein receptor	-1.71	0.0006
ITGA8; Integrin alpha-8	-1.69	0.0020
C3ORF49; uncharacterized protein	-1.61	0.0098
ZNF608; Zinc finger protein 608	-1.61	0.0007
APBB1IP; Amyloid beta A4 precursor protein-binding family B member 1-interacting protein	-1.60	0.0039
RGS17; Regulator of G-protein signaling 17	-1.59	0.0002
KHDRBS3; KH domain-containing; RNA-binding; signal transduction-associated protein 3	-1.56	0.0031
SEMA3A; Semaphorin-3A	-1.56	0.0019
ARHGAP20; Rho GTPase-activating protein 20	-1.54	0.0029
NRXN1; Neurexin-1-alpha	-1.54	0.0006
GATM; Glycine amidinotransferase; mitochondrial	-1.53	0.0015
NRXN1; Neurexin-1-alpha	-1.53	0.0053
UPK1B; Uroplakin-1b	-1.53	0.0013
NIPAL2; NIPA-like protein 2	-1.53	0.0058
SEMA3D; Semaphorin-3D	-1.52	0.0018
ISLR2; mmunoglobulin superfamily containing leucine-rich repeat protein 2	-1.51	0.0021
NAV2; Neuron navigator 2	-1.51	0.0017
SLC25A16; solute carrier family 25	-1.51	0.0004
FAM71F1; Protein FAM71F1	1.51	0.002
PFKFB3; 6-phosphofructo-2-kinase/fructose-2; 6-biphosphatase 3	1.56	0.0045
ADAMTS1; ADAM metallopeptidase with thrombospondin type 1 motif	1.7	0.0013
LPHN3; Latrophilin-3	1.71	0.0048
ANKRD1; ankyrin repeat domain 1	1.74	0.0018
SLC3A1; solute carrier family 3 (neutral and basic amino acid transporter) member 1	2.15	0.0017
DES; Desmin	2.25	0.0014

Foot notes: Statistical significance of differential expression was determined at fold change $\geq$1.5 or $\leq$-1.5 and p$\leq$0.01.

Table 4.8: Target site predictions in DEnGs obtained in the CLASH dataset

DEG in CLASH	Target in 5'UTR						Target in CDS						Target in 3'UTR					
	Perfect pairing			G:U pairing			Perfect pairing			G:U pairing			Perfect pairing			G:U pairing		
	7	67	8	7	67	8	7	67	8	7	67	8	7	67	8	7	67	8
SCFD1	-	-	-	-	1	-	-	-	-	2	-	-	-	-	-	-	-	-
GLI2	NI	NI	NI	NI	NI	NI	-	3	4	4	2	8	-	-	-	2	-	-
DLL1	NI	NI	NI	NI	NI	NI	-	1	-	3	2	3	-	2	-	-	-	1
ABR	-	-	-	-	-	-	1	-	-	2	2	3	-	-	-	-	-	-
POLN:	NI	NI	NI	NI	NI	NI	-	2	-	2	5	5	NI	NI	NI	NI	NI	NI
DHX57	NI	NI	NI	NI	NI	NI	-	-	1	2	2	3	-	-	-	2	1	-
FORED2	NI	NI	NI	NI	NI	NI	-	1	1	1	1	5	-	-	-	-	-	-
CJ071	NI	NI	NI	NI	NI	NI	-	2	3	5	-	4	NI	NI	NI	NI	NI	NI
AGTPBP1	-	-	-	-	-	-	-	-	-	1	-	2	-	-	-	-	-	1
CCDC88B	NI	NI	NI	NI	NI	NI	-	-	2	-	7	7	NI	NI	NI	NI	NI	NI
SLC9A5	NI	NI	NI	NI	NI	NI	1	1	2	3	1	5	-	-	-	2	7	5
CYP4F22	NI	NI	NI	NI	NI	NI	-	-	-	2	2	2	-	1	-	-	-	-
HIC1	NI	NI	NI	NI	NI	NI	-	-	-	1	1	1	-	-	1	-	1	1
ALMS1	NI	NI	NI	NI	NI	NI	-	-	-	9	6	8	-	-	1	-	-	-
ZBTB7C	NI	NI	NI	NI	NI	NI	-	2	1	1	2	2	-	-	-	-	-	-
ADAMTSL 4	-	-	-	-	-	3	-	1	2	3	9	9	-	-	-	1	-	1
EPAS1	NI	NI	NI	NI	NI	NI	2	1	1	-	2	4	-	-	1	-	-	-
ADAT	-	-	-	2	-	2	-	-	-	1	2	1	NI	NI	NI	NI	NI	NI
CD177	-	-	-	-	-	-	-	-	1	1	2	4	NI	NI	NI	NI	NI	NI
USP19	-	-	-	-	-	-	1	-	2	5	3	5	NI	NI	NI	NI	NI	NI
RXFP3	NI	NI	NI	NI	NI	NI	1	1	1	4	1	4	-	-	-	-	-	-

Foot notes: DEnGs were subjected to target prediction program RNAhybrid, for the prediction of targets of ovhv2-miR-7, ovhv2-miR-67 and ovhv2-miR-8.

- : No target

NI: No information of sequence available.

Table 4.9: Target site predictions in DEG obtained in microarray dataset.

DEG microarray	Target in 5'UTR						Target in CDS						Target in 3'UTR					
	Perfect pairing			G:U pairing			Perfect pairing			G:U pairing			Perfect pairing			G:U pairing		
	7	67	8	7	67	8	7	67	8	7	67	8	7	67	8	7	67	8
FTH1	-	-	-	-	-	-	-	-	-	-	-	1	-	-	-	-	-	1
ENPP2	-	-	-	-	-	-	1	1	-	4	-	4	-	-	-	1	-	-
PRSS35	-	-	-	1	-	-	-	1	1	1	2	1	-	-	-	3	1	4
GUCY1A1	-	-	-	1	1	-	1	1	3	1	1	4	-	-	-	-	1	-
PDE1A	-	-	-	2	1	1	-	-	-	1	-	-	-	-	1	6	2	1
VLDLR	NI	NI	NI	NI	NI	NI	-	-	-	-	1	5	-	-	-	-	-	-
ITGA8	-	1	-	-	-	-	-	-	-	3	1	9	-	-	-	2	-	3
C3ORF49	NI	NI	NI	NI	NI	NI	-	-	-	1	1	1	NI	NI	NI	NI	NI	NI
ZNF608	-	-	-	-	1	-	-	-	-	2	3	5	NI	NI	NI	NI	NI	NI
APBB1IP	-	-	-	-	-	-	1	1	-	2	-	2	-	-	-	1	-	-
RGS17	-	-	-	-	-	-	-	-	-	1	-	1	-	-	-	-	-	-
KHDRBS3	NI	NI	NI	NI	NI	NI	-	-	-	1	-	1	-	-	-	-	-	-
SEMA3A	-	-	1	-	-	-	-	-	-	2	2	2	-	-	-	-	-	2
ARHGAP2	NI	NI	NI	NI	NI	NI	-	-	1	2	1	7	-	-	-	1	1	3
NRXN1	-	1	-	1	-	2	-	-	1	2	2	5	-	-	-	7	1	-
GATM	-	-	-	-	-	-	-	-	1	1	-	2	-	-	-	1	1	1
UPK1B	-	-	-	-	-	-	-	-	-	2	1	2	-	-	-	1	1	1
NIPAL2	NI	NI	NI	NI	NI	NI	-	-	-	4	2	-	-	-	-	2	-	-
SEMA3D	-	-	-	1	-	-	-	-	-	1	-	3	-	-	1	2	1	5
ISLR2 2	-	-	-	-	-	-	1	3	2	2	2	2	NI	NI	NI	NI	NI	NI
NAV2	-	-	-	-	-	-	-	1	2	2	3	8	-	-	1	1	-	-
SLC25A16	NI	NI	NI	NI	NI	NI	-	-	-	1	-	1	-	-	-	1	1	-

Foot notes: DEG were subjected to target prediction program RNAhybrid, for the prediction of targets of ovhv2-miR-7, ovhv2-miR-67 and ovhv2-miR-8.

- No target

NI No information of sequence available

4.3.2.12 Biological processes and pathway analysis of the DEnGs identified from CLASH and DEG identified from microarray data

CLASH and microarray analysis enabled the identification of highly enriched and strongly down-regulated and up-regulated genes. To determine the relationship among the differential genes in the datasets (4.3.2.8 and 4.3.2.9) and their involvement in different pathways, Ingenuity Pathway Analysis (IPA) was applied. IPA can help to determine the biological relevance of the collective effects on gene expression induced by ovhv2-miRs. DEnGs and DEG and their fold change values were submitted to IPA to interpret the data in the context of biological processes and canonical pathways. Significance of the biological processes and the pathways were tested by the Fisher Exact test p-value and relationships between genes and their associated biological processes were considered statistically significant (p-value $\leq$ 0.05).

IPA analysis identified the involvement of CLASH identified DEnGs in different molecular and cellular functions, based on their roles. The top cellular processes include cell morphology, cellular development, cell to cell signaling and interaction, cellular assembly and organization, and cellular growth and proliferation (Figure 4.18). DEnGs with their associated biological processes and p-values are shown in table 4.11. GLI2, DLL1, EPAS1, HIC1, ZBTB7C and TPT1 were found to be involved in most of the IPA identified processes.

DLL1 and GLI2 were identified as the top two highly expressed DEnGs (Table 4.7). DLL1 is a part of the Notch signaling pathway. The CLASH data analysis showed that ovhv2-miR-67 formed a chimera with DLL1 (Section 4.3). GLI2 is a part of the

sonic hedgehog (SHH) signaling pathway. EPAS1 which is one of the highly expressed DEnGs in CLASH, involved in angiopoitin-Tie2 (endothelial tyrosine kinase gene) signalling pathway.

DEG identified from microarray data analysis were also analysed in IPA to identify significant biological processes involved. The top cellular processes identified were similar to those identified in the CLASH (Figure 4.18, Table 4.10). The DEG involved in most of these processes include; SEMA3A, SEMA3D, ENPP2, VLDLR, DES, NRXN1 and ITGA8.

SEMA3A and SEMA3D belong to class-3 semaphorins which are involved in semaphorin signalling pathway to regulate immune cell responses. ENPP2 is involved in the NAD (nicotinamide adenine dinucleotide) metabolism pathway. ITGA8 (integrin alpha 8) and DES (desmin) were found to be a part of the Rho pathway and Rho family GTPases pathways respectively. IPA analysis also identified the integrin pathway for ITGA8. One of the down-regulated DEG, PDE1A (Table 4.7) is a cyclic nucleotide phosphodiesterase (PDE) and is involved in G-protein coupled receptor signalling, cAMP mediated signalling and Protein kinase A signalling pathways. The most down-regulated DEG, FTH1 (Ferritin heavy chain) was also found to be the part of the NRF2 (Nuclear factor like 2)-mediated oxidative stress response pathway.

In the analysis of both data sets (CLASH and Microarray), whilst no common pathways could be found, two of the pathways (SHH and cAMP dependant PKA) are found to be related. These results indicated that many of the differential genes obtained from both data sets are involved in biological processes related to

transcription, cell growth/ proliferation, differentiation, angiogenesis and tumour related biological processes.

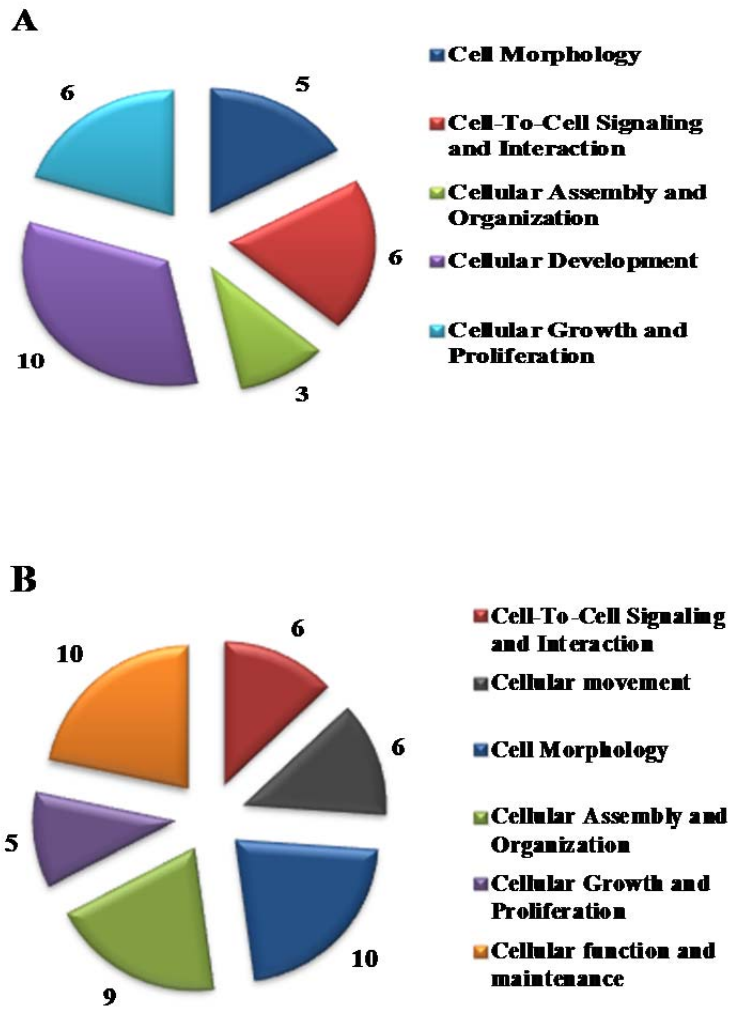

Figure 4.18: Biological processes affected by ovhv2-miRs expression in sheep embryo fibroblasts.

The pie charts represent the number of DEnGs (A) and (DEG) changing expression with known roles in biological processes, affected by three of the transduced ovhv2-miRs in sheep embryo fibroblasts. The biological processes determined by Ingenuity Pathways Analysis (IPA) of CLASH (A) and microarray (B) data sets. Correlation between genes and identified biological processes were statistically significant (p value≤0.05).

Table 4.10: Biological processes identified by Ingenuity Pathway Analysis (IPA)

Biological processes identified by Ingenuity Pathway Analysis (IPA) for the differentially expressed genes DEnGs identified in CLASH (A) and DEG identified in microarray (B) data analysis.

Biological Processes	Number of Genes involved	CLASH identified DEnGs involved in the processes	p-values
Cell Morphology	5	GLI2, ABR, TBC1D9, ALMS1, USP19	1.40E-03 - 4.52E-02
Cell-To-Cell Signaling and Interaction	6	GLI2, EPAS1,AGTPBP1, DLL1, TPT1, CD177	1.40E-03 - 4.25E-02
Cellular Assembly and Organization	3	ADAMTSL4, EPAS1, SCFD1	1.40E-03 - 3.98E-02
Cellular Development	10	GLI2, DLL1, EPAS1, ALMS1, UBN1, ZBTB7C, AGTPBP1, TPT1, USP19, HIC1	1.40E-03 - 4.65E-02
Cellular Growth and Proliferation	6	GLI2, DLL1, EPAS1, ZBTB7C, HIC1, TPT1	1.40E-03 - 3.98E-02

A

Biological Processes	Number of Genes involved	Microarray identified DEG involved in the processes	p-values
Cell-To-Cell Signaling and Interaction	6	SEMA3A, SEMA3D, VLDLR, DES, NRXN1, ITGA8	5.23E-05 - 4.92E-02
Cellular Movement	6	SEMA3A, SEMA3D, ENPP2, ADAMTS1, VLDLR	5.23E-05 - 4.60E-02
Cell Morphology	10	ENPP2, SEMA3A, SEMA3D, , NRXN1, VLDLR, ARHGAP20, ISLR2, DES, ADAMTS1, ITGA8	2.97E-04 - 4.52E-02
Cellular Assembly and Organization	9	ENPP2, NRXN1, SEMA3A, SEMA3D, VLDLR, ARHGAP20, DES, ISLR2, ITGA8	2.97E-04 - 4.92E-02
Cellular Growth and Proliferation	5	FTH1, ENPP2, ITGA8, ADAMTS1, DES	1.40E-03 - 4.92E-02
Cellular Function and Maintenance	10	ARHGAP20, ISLR2, SEMA3A, SEMA3D, VLDLR, DES, ITGA8, ADAMTS1, ENPP2, NRXN1	1.23E-03 - 4.92E-02

B

Foot notes: Significance of the biological processes were tested by the Fisher Exact test p-value and relationships between genes and their associated biological processes were statistically significant with a p-value ≤ 0.05

4.3.3 CLASH analysis of OvHV-2 miRNAs hybrids with bovine or ovine transcripts

CLASH is a method for transcriptome-wide analysis of RNA-RNA interaction duplexes bound to a protein (tagged Ago2 in this study), ligation between the two strands of RNA duplexes to form chimeric RNAs (chimeras), high throughput sequencing of resulting cDNAs and bioinformatics analysis of the resulting sequencing data to annotate chimeric reads (Travis *et al*., 2014). The chimeric reads contain, part of the 5' linker, cDNA insert (miRNA ligated to targeted mRNA/miRNA or only miRNA or only mRNA) and part or all of the 3' linker (Figure 4.1).

As described in the previous section (4.3.1 and 4.3.2) the CLASH was used to identify targets of ovhv2-miRs within bovine and ovine cells. For the identification of targets for ovhv2-miRs analysis of chimeric read data was performed. Identification of chimeric reads containing ovhv2-miRs and host mRNA/miRNA sequence would provide direct evidence of an interaction.

4.3.3.1 miRNA-mRNA Chimeras identified in BJ1035 sample

The initial bioinformatic analysis was performed as described in the section 4.3.1.4. Sequencing reads derived from CLASH experiments using BJ1035 cells (section 4.3.1.5) were analysed using stringent quality filters to identify those reads which contained two distinct fragments and could be mapped separately. Fragments from 49 genes were found to form a chimera with ovhv2-miRs. Other types of RNAs were also identified, including one spliceosomal RNA (U2) and one long non-coding RNA

(MATR3). It is worth noting that among the targeted single reads obtained from BJ1035 data set (section 4.3.1.6), U2 spliceosomal RNA was also one of the highly targeted class in CLASH results (section 4.3.1.6). In the BJ1035 dataset 0.04% of all reads were identified as chimeric reads with ovhv2-miR (Table 4.11). This is consistent with the data from related studies, which showed chimeric reads to constitute less than 1% total (Kudla *et al*., 2011).

Table 4.11: Chimeric sequencing reads associated with BJ1035 sample.

	Total reads	chimeric reads with ovhv2-miRs	chimeric reads with cellular-miRs
Number	676003	285	91
Percentage	100%	0.04%	0.01%

The predicted ovhv2-miR and mRNA interactions were analyzed using RNAhybrid; and UNAfold programes. Before analysing the chimeric reads using the programs, the lengths of mRNA fragments were adjusted by adding 25 nucleotides downstream and by extending the miRNA fragment to the full length mature miRNA (Kudla *et al*., 2011) (Supplemental data file 4.4). RNAhybrid identified miRNA-mRNA interactions within the 5'UTRs, CDS and 3'UTRs of the genes. Approximately 59% of the target sites were located in the CDS whereas 27.4% and 13.7% interactions were located in the 3'UTR and the 5'UTR respectively.

Ten percent of the miRNA-mRNA interactions were found to have perfect complementarity between the seed region of the miRNA and the target site in the mRNA. Additionally 27.5% of interactions were also found in the same region but with the presence of G:U base pairing. The remaining 63% of interactions were non-canonical and were found in the regions other than the 5'end of the miRNAs. The

binding energies for the miRNA-mRNA interactions ranged from -32 to -12.3 kcal/mol, indicating that the recovered chimeras formed stable base-paired interactions.

The top three mRNAs forming chimeras with ovhv2-miR-57, ovhv2-miR-34 and ovhv2-miR-54 were C17ORF85 (30.5%), ribosomal protein S6 kinase-like 1 (RPS6KL1) (12.3%) and WD repeat domain 60 (WDR60) (6%) respectively (Table 4.15). ovhv2-miR-53, 43, 53, 50 and 43 formed chimeras with other transcripts including active BCR-related gene (ABR) (4.2%), integrin alpha-10 precursor (ITGA10) (2.8%), melanoma antigen family A, 10-like (LOC100298021) (2.8%), MYHC-Embryonic (myosin-3) (2.6%) and PRP39 pre-mRNA processing factor 39 homolog (S. cerevisiae) (PRPF39) (2.1%), respectively (complete list in supplemental data file 4.4). ovhv2-miR-217M formed chimeras with six different transcripts including LIX1-like protein (LIX1L), polycomb protein SCMH1 (SCMH1), catsper channel auxiliary subunit beta (CATSPERB), cleavage stimulation factor subunit 3 (CSTF3), ATPase, H+ transporting, lysosomal 56/58kDa, V1 subunit B1 (ATP6V1B1) and U11/U12 small nuclear ribonucleoprotein 25 kDa protein (SNRNP25). Ovhv2-miR-53 and ovhv2-miR-5 each formed chimera/s with the fragments of five different mRNAs fragments. Ovhv2-miR-53 formed chimeras with ABR, LOC100298021, tudor domain containing 12 (TDRD12), mitogen-activated protein kinase kinase kinase 2 (MAP3K2) and myeloid/lymphoid or mixed-lineage leukemia 5 (MLL5) whereas ovhv2-miR-5 with fragments of A disintegrin and metalloproteinase with thrombospondin motifs 1 (ADAMTS1), MCF.2 cell line derived transforming sequence-like (MCF2L), sine oculis-binding protein homolog (SOBP), centrosomal

protein 152kDa (CEP152) and SEC13 homolog (SEC13). A total of 19 ovhv2-miRs out of forty six ovhv2-miRs formed chimeras with bovine transcripts (Table 4.12). The length of transcript fragments in the chimeras ranged from 12-39 nucleotides. Two of the transcripts; U2 spliceosomal RNA (U2) (20bp long fragment) and transmembrane 6 superfamily member 1 (TM6SF1) (39bp long fragment), were found to have the target sites for respective miRNA within the chimeric fragment without the addition of 25 nucleotides. Ovhv2-miR-36 and ovhv2-miR-8 formed chimeras with U2 and TM6SF1 respectively (Figure 4.19).

Table 4.12: Bovine mRNAs which formed chimeras with ovhv2-miRs.

ovhv-miR	Chimeric mRNAs	Number of chimeras	percent		ovhv-miR	Chimeric mRNAs	Number of chimeras	percent
57	C17orf85	87	30.53		61	MCOLN3	2	0.70
34	RPS6KL1	35	12.28		7	TUBA1A	2	0.70
54	WDR60	17	5.96		8	TBR1	2	0.70
56	LOC101906939	15	5.26		217M	SCMH1	2	0.70
43	ITGA10	12	4.21		217M	CATSPERB	2	0.70
53	LOC100298021	8	2.81		217M	CSTF3	2	0.70
50	myosin-3	8	2.81		217M	ATP6V1B1	2	0.70
53	ABR	7	2.46		217M	SNRNP25	2	0.70
43	PRPF39	7	2.46		36	U2	1	0.35
39	FHOD1	6	2.11		8	TM6SF1	1	0.35
39	PNPLA6	5	1.75		34	SPNS1	1	0.35
40	C9H6orf211	4	1.40		35	ATRN	1	0.35
43	TDRD7	4	1.40		35	ZFX	1	0.35
53	MLL5	3	1.05		39	SERINC1	1	0.35
58	CACNG4	3	1.05		39	ZC3H4	1	0.35
61	BAZ1A	3	1.05		53	TDRD12	1	0.35
7	CPNE9	3	1.05		53	MAP3K2	1	0.35
217M	LIX1L	3	1.05		56	CEP152	1	0.35
35	FREM3	3	1.05		56	SEC13	1	0.35
39	CA12	2	0.70		57	PDCL3	1	0.35
51	CRB2	2	0.70		58	FLVCR2	1	0.35
54	THSD1	2	0.70		61	ZNF550	1	0.35
56	ADAMTS1	2	0.70		63	MAGI3	1	0.35
56	MCF2L	2	0.70		67	LSMEM2	1	0.35
56	SOBP	2	0.70		67	LAMB2	1	0.35

A

GTGAGCACGCATCGACCTGGTATTGCTCTAGGTTGCATTTTGCTGTAGATGGAATTCTCGGGTG
145 164

B

target 5' U U 3'
AC GCA CGACCUGG
UG CGU GUUGGAUC
miRNA 3' GA U UUUAC U 5'

mfe: -17.9 kcal/mol

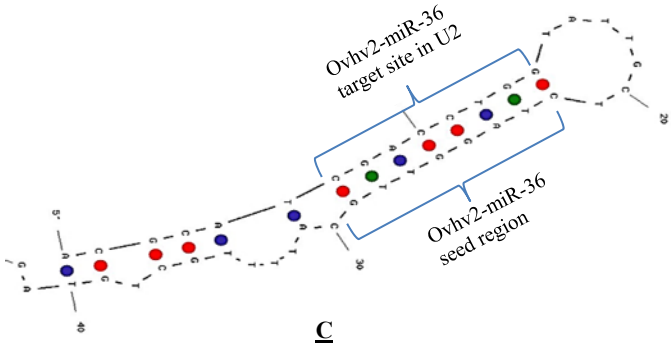

C

D

GTGAGCATATACTTGTCTTCCTGTCTGGGCTGGTTTCAGAATCTTGGCTCAGCGTGACTGCTCTTTGGAAT
1437 1474

E

target 5' U CU C U G 3'
GU UC UG CUGGGCU
CG AG GC GACUCGG
miRNA 3' UUCU UC U U 5'

mfe: -18.3 kcal/mol

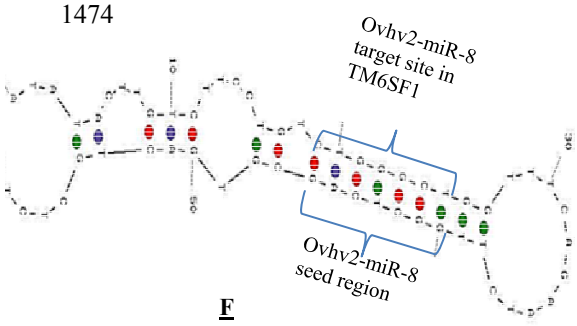

F

Figure 4.19: ovhv2-miRs formed chimeras with BJ1035 transcripts.

ovhv2-miR-36 and ovhv2-miR-8 formed chimeras with U2 spliceosomal RNA (U2) and transmembrane 6 superfamily member 1 (TM6SF1) respectively.
Sequence of U2 (**A**) and TM6SF1 (**D**) chimeric reads with their respective miRNAs. Barcode, mRNA fragment, miRNA and 3' linker are shown in blue, black, green and red respectively. miRNA target regions are shown in bold.
Figure **B** (U2) and **E** (TM6SF1) showed the results obtained from RNAhybrid software for the ovhv2-miRs target predication in the mRNA fragment of the chimeric reads.
Figure **C** (U2) and **F** (TM6SF1) showed results obtained from UNAfold software to fold chimeric reads to observe the miRNA-mRNA hybridized interactions.

4.3.3.2 Validation of ovhv2-miRs targets in BJ1035 samples identified by CLASH

Some of the bovine transcripts which were identified to form chimeras with ovhv2-miRs using the CLASH approach might be the potential targets of ovhv2-miRs and involved in MCF related pathology. To further investigate those targets a reporter gene assay (dual luciferase assay) was used to validate the predicted targets. A total of 9 transcripts were found which showed to have interactions with ovhv2-miRs in the seed regions (section 4.3.3.1). Due to time constraint it was not possible to validate all the identified targets.

Two of the targets; U2 spliceosomal RNA (U2) and transmembrane 6 superfamily member 1 (TM6SF1) were selected for validation. TM6SF1 formed a chimera with ovhv2-miR-8. TM6SF1 was chosen for further study as it was known to be a target of both the KSHV encoded miRNA miR-K-12-11 and the human oncogenic miRNA hsa-miR-155 (Skalsky *et al*., 2007). The RNAhybrid analysis also predicted an interaction between miRNAs; ovhv2-miR-36 and ovhv2-miR-8 seed regions with the target sites in U2 and TM6SF1 (Figure 4.19).

Luciferase assays were performed using constructs containing target sites from U2 or TM6SF1 cloned downstream of the renilla luciferase reporter gene of the psiCHECK2 plasmid. Luciferase constructs were created using custom oligonucleotides (section 2.6) corresponding to the regions of U2 and TM6SF1 transcripts from nucleotides 109-191 (Transcript ID: ENSBTAG00000028094) and 1455-1461 (accession number: XM_005221887.1) respectively. The target sites for ovhv2-miRs were located from nucleotide 152-158 (U2) and 1455-1461 (TM6SF1).

Luciferase constructs (LUC/U2 for U2 and LUC/TM6SF1 for TM6SF1 construct) were co-transfected with test mimic miRNAs or negative control scramble miRNA in 100 nM or 200 nM concentration, into BHK21 cells. For each region of interest each experiment was performed three times as described in the Sections 2.6 and 3.3.3, with 6 replicates in 96 well plates. For all experiments an empty vector was used to investigate off-target effects however no significant reduction in luciferase expression was observed using any of the ovhv2-miRs (Supplemental data file 4.6). In all the other experiments positive controls (psi-M23-2 and miR-M23-2) worked in the same manner as described in Section 3.3.3.1, that is the addition of miR-m23-2 caused significant reduction in the luciferase levels at either concentration (Luciferase readings in the Supplemental data file 4.6).

4.3.3.2.1 Validation of U2 as a predicted target of ovhv2-miR-36

The LUC/U2 was co-transfected with a scrambled miRNA mimic (negative control) to compare to the luciferase levels of the same plasmid co-transfected with targeting mimics. Transfection of the ovhv2-miR-36 mimic at a concentrations of 200 nM led to significant down regulation (approximately 20%) in luciferase expression relative to the negative control (LUC/U2+ovhv2-miR-36, 200 nM) $p=0.004$ (Figure 4.20). Introduction of the ovhv2-miR-36 mimic at a concentration of 100 nM showed a non-significant difference (LUC/U2+ovhv2-miR-36, 100 nM) $p=0.6$) in the luciferase expression, compared to the negative control. The LUC/U2 in the absence of any miRNA (no miRNA control), showed significant higher expression of luciferase gene as compared to negative control at both concentrations (LUC/U2, 100 nM) $p<0.001$ and LUC/U2, 200 nM) $p<0.001$ (Figure 4.20 for 200 nM).

4.3.3.2.2 Validation of TM6SF1 as a predicted target of ovhv2-miR-8

A significant increase in the luciferase expression was observed when LUC/TM6 was transfected with the ovhv2-miR-8 mimic at both concentrations (100 nM or 200 nM) as compared to the negative control (LUC/TM6+ovhv2-miR-8, 100 nM) $p<0.001$ and (LUC/TM6+ovhv2-miR-8, 200 nM) $p<0.001$. An approximately 60% and 80% increase in luciferase expression was observed at 100 and 200 nM concentrations respectively. According to the luciferase assay results, the samples transfected with LUC/TM6 also showed higher significant luciferase expression compared to the negative control at both concentrations (LUC/TM6, 100 nM) $p<0.001$ and psi- TM6, 200 nM) $p<0.001$. (Figure 4.21 for 200 nM concentration result).

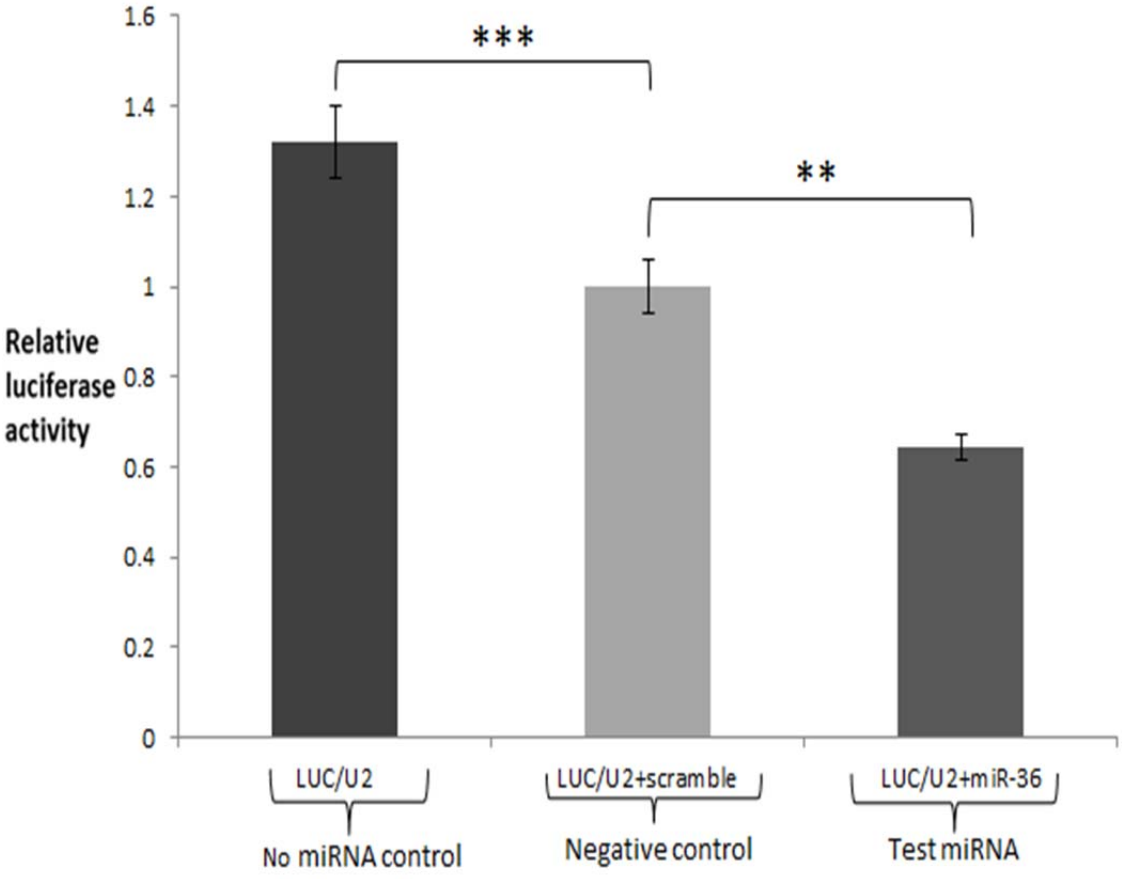

Figure 4.20: Luciferase expression levels in BHK21 cells transfected with U2 (LUC/U2) in the psiCHECK-2 plasmid in the presence/absence of target miRNA (Ovhv2-miR-36) at 200 nM concentration.

Data are represented as luciferase activity with the **=p<0.01 and ***=p<0.001 relative to negative control (light grey) value at 200 nM concentration.

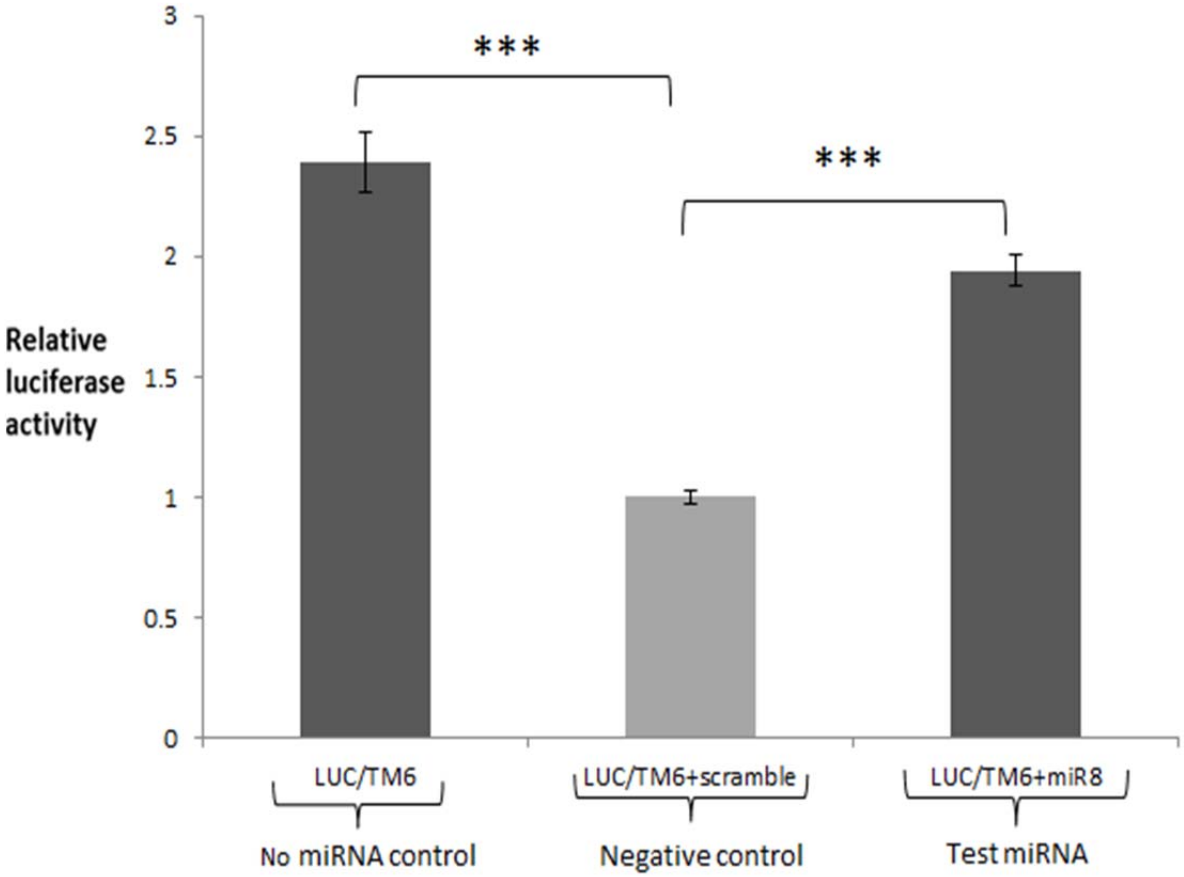

Figure 4.21: Luciferase expression levels in BHK21 cells transfected with TM6SF1 (LUC/TM6) in the psiCHECK-2 plasmid in the presence/absence of target miRNA (Ovhv2-miR-8) at 200 nM concentration.

Data are represented as luciferase activity with the ***=$p<0.001$ relative to negative control (light grey) value at 200 nM concentration.

4.3.3.3 miRNA-mRNA chimeras identified in sheep embryo fibroblasts expressing ovhv2-miRs

To identify chimeric reads and to determine the potential targets of ovhv2-miRs bioinformatics analysis was carried out on the data obtained from three replicates each of SEF-Cluster-3 (T1, T2 and T3) and SEF-Empty (C1, C2 and C3) as described in section 4.3.2.5. The total number of chimeras obtained from the T1, T2 and T3 samples were 85 (0.02%), 113 (0.01%) and 914 (0.21%) respectively. Percentages were calculated from the total mapped reads of each sample (Table 4.5). In two of the control samples; C2 and C3, 4 and 24 chimeras between ovhv2-miRs and sheep transcripts, were found respectively. The percentages of those chimeric reads were 0.002% (C2) and 0.003% (C3) as compared to the total mapped reads (Table 4.5). Two of the chimeras in the C2 sample had the sequence of ovhv2-miR217M which was not used in this experiment (Table 4.14). As no ovhv2-miR was transduced into the control samples (SEF-Empty) (4.3.2.2) and possible reason for the presence of chimeras with ovhv2-miRs may be the contamination of barcodes used during sequencing (section 4.3.1.4). In all the samples (Tests and controls) cellular miRs were also found to form chimeras with sheep mRNAs (Table 4.5).

Fragments of a total of 17, 8 and 28 mRNAs formed chimeras in the T1, T2 and T3 samples respectively (Table 4.13). ovhv2-miR-67 was the most abundant ovhv2-miR in the chimeric reads in the three test samples. In the T1 sample ovhv2-miR-67 formed chimeras with fragments of 14 different sheep mRNAs, whereas ovhv2-miR-7 and -8 formed chimeras with only 1 and 2 mRNAs, respectively. In the T2 sample ovhv2-miR-7, 67 and -8, formed chimeras with 1, 6 and 1 mRNA respectively. In the

T3 sample, ovhv2-miR-67 formed chimeras with 25 different mRNAs whereas ovhv2-miR-7 and -8 formed chimeras with only 1 and 2 mRNAs, respectively (Table 4.13).

The interactions between ovhv2-miRs and mRNAs were analysed using RNAhybrid; and UNAfold programs. RNAhybrid analysis showed most of the miRNA-mRNA interactions were in the coding regions of the transcripts (88% for T1, 75% for T2 and 82% for T3 samples). Whereas 6%, 0% and 4% interactions were found in the 5'UTR and 6%, 25% and 14% were found in the 3'UTRs of the mRNAs, in the T1, T2 and T3 samples respectively.

RNAhybrid analysis also identified approximately 18%, 38% and 29% of the miRNA-mRNA canonical interactions had perfect complementarity between the seed regions and the target site in the mRNA in the T1, T2 and T3 samples respectively, whereas 29%, 25% and 21% interactions were found in the seed regions but with the presence of G:U pairing. The remaining 53% (T1), 38% (T2) and 50% (T3) interactions were non canonical. Binding energies for the miRNA-mRNA interactions ranged from -44.4 to -17.6 kcal/mol, indicating that these chimeras formed stable base-paired interactions.

The mRNA which formed the highest number of chimeras in all the test groups was an uncharacterized protein with sequence similarity to delta-like protein 1 (DLL1). DLL1 was also found as one of the top DEnGs identified in the CLASH single reads dataset (Section 4.3.2.7 and 4.3.2.9, Table 4.7). DLL1 formed chimeras with ovhv2-miR-67 and constituted 42.4%, 80% and 84% of total chimeras in the T1, T2 and T3 samples respectively. The chimeric fragments of DLL1 mapped to two regions of the

coding sequence in the DLL1 mRNA. UNAfold and RNAhybrid analysis also identified that both of the chimeric fragments had target sites for ovhv2-miR-67 and formed canonical interactions. One target site showed perfect base pairing between the seed region (position 2 to 8) of the miRNA whereas other target site showed an interaction with position 1 to 7 of the miRNA seed region, with one G:U base pairing (Figure 4.25).

Another mRNA which was found to form chimeras with ovhv2-miR-7, in all test samples was kelch-like 2, Mayven (Drosophila) (KLHL2). KLHL2 constituted approximately 1.2%, 15% and 0.4% of the total chimeras in the T1, T2 and T3 samples respectively. The fragment of the KLHL2 in the chimeric read mapped to the 3'UTR of KLHL2 mRNA. RNAhybrid analysis identified that the KLHL2 chimeric fragment had a target site for ovhv2-miR-7 interacting with the miRNA seed region (1-7 nucleotide) with two G:U base pairings.

Multiple epidermal growth factor-like domains protein 8 (MEGF8) and Doublesex- and mab-3-related transcription factor C2 (DMRTC2) formed chimeric reads with ovhv2-miR-67 in two of the test samples; T1 and T3. MEGF8 constituted 2.4% of the total chimeric reads in T1 and 0.1% in T2. DMRTC2 constituted up 2.4% of the total chimeric reads in T1 and 3.8% in T2. The chimeric fragment of MEGF8 showed perfect base pairing between the target site present in the fragment and the seed region of ovhv2-miR-67 (nucleotides 2-8). In contrast non-canonical interactions were also found between DMRTC2 and ovhv2-miR-67 (from miRNA position 4-11). Some of the other mRNAs which formed chimeras with ovhv2-miRs include fibroblast growth factor 19 (FGF19) (1.2%) and semaphorin-5B (SEMA5B)

(1.2%) in the T1 sample, probable helicase with zinc finger domain (HELZ) (0.9%) in the T2 sample and v-crk sarcoma virus CT10 oncogene homolog (avian) (CRK) (0.8%), serine/threonine-protein kinase PAK 7 (PAK7) (0.1%) and von Willebrand factor A domain-containing protein 5B2 (VWA5B2) (0.1%) in the T3 sample. The other mRNAs forming chimeras with ovhv2-miR-7, -67 and -8 in the test samples are shown in Table 4.14. The number and overlap of the chimeric mRNAs in the test samples is shown in a Venn diagram (Figure 4.22).

Table 4.13: Number of sheep mRNAs forming chimeras with ovhv2-miRs.

Sample	Ovhv2-miR	sheep mRNAs formed chimeras	Number of Chimeras
T1	Ovhv2-miR-7	1	1
	Ovhv2-miR-67	14	81
	Ovhv2-miR-8	2	3
T2	Ovhv2-miR-7	1	17
	Ovhv2-miR-67	6	95
	Ovhv2-miR-8	1	1
T3	Ovhv2-miR-7	1	4
	Ovhv2-miR-67	25	905
	Ovhv2-miR-8	2	5
C1	Ovhv2-miR-7	0	0
	Ovhv2-miR-67	0	0
	Ovhv2-miR-8	0	0
C2	Ovhv2-miR-7	0	0
	Ovhv2-miR-67	2	2
	Ovhv2-miR-8	0	0
	ovhv2-mir-217M	1	2
C3	Ovhv2-miR-7	1	3
	Ovhv2-miR-67	4	19
	Ovhv2-miR-8	2	2

Foot notes: T1, T2 and T3: Test samples stably expressing ovhv2-miR-7, -67 and -8. C1, C2 and C3: Control samples. In control samples no ovhv2-miR was used in the experiment. Presence of ovhv2-miRs might be due to barcode contamination.

Table 4.14: Sheep mRNAs which forming chimeras with ovhv2-miR-7, -67 or -8.

ovhv-miR	Chimeric mRNAs	Number of chimeras	percent
T1			
67	DLL1	36	42.35
67	ABCA3	14	16.47
67	FAM208B	9	10.59
67	STAB1	6	7.06
67	SLC3A2	3	3.53
67	MEGF8	3	3.53
67	DMRTC2	2	2.35
67	TRANK1	2	2.35
8	TRIM27	2	2.35
67	FGF19	1	1.18
67	TIM	1	1.18
8	SGPP2	1	1.18
67	SEMA5B	1	1.18
67	IGSF3	1	1.18
67	LOC101109723	1	1.18
67	PHF17	1	1.18
7	KLHL2	1	1.18
T2			
67	DLL1	90	79.65
7	KLHL2	17	15.04
8	HELZ	1	0.88
67	COPZ2	1	0.88
67	BAHCC1	1	0.88
67	KIAA0913	1	0.88
67	RP9	1	0.88
67	HMX2	1	0.88
T3			
67	DLL1	768	84.03
67	DMRTC2	35	3.83
67	TMEM222	13	1.42
67	DMRT2	13	1.42
67	SMN1	12	1.31
67	USP24	12	1.31
67	MOGS	9	0.98
67	MARK4	9	0.98
67	CRK	7	0.77
67	PRRX2	5	0.55
67	GLTSCR1	5	0.55
7	KLHL2	4	0.44
8	BABAM1	4	0.44
67	FAM86A	3	0.33
67	UPK3BL	2	0.22
67	B3GNTL1	1	0.11
67	TLX3	1	0.11
67	WDFY4	1	0.11
67	MVP	1	0.11
67	SDK2	1	0.11
67	VWA5B2	1	0.11
67	ATG2B	1	0.11
67	NPHS1	1	0.11
67	MEGF8	1	0.11
8	PITRM1	1	0.11
67	PAK7	1	0.11
67	SLC38A4	1	0.11
67	UBE2Q2	1	0.11
C1			
-	-	0	0
C2			
217M	SCMH1	2	50
67	ABCA3	1	25
67	DLL1	1	25
C3			
67	DLL1	16	66.67
7	KLHL2	3	12.50
8	GPR137B	1	4.17
8	CRCP	1	4.17
67	MOXD2	1	4.17
67	UBE2Q2	1	4.17
67	HMGXB3	1	4.17

Foot notes: T1, T2 and T3: Test samples. C1, C2 and C3: Control samples.

Sheep mRNAs which formed chimeras in more than one samples are highlighted; DLL1: pink, KLHL2: green, DMRTC2: purple, MEGF8: orange, ABCA3: dark grey and UBE2Q2: light grey.

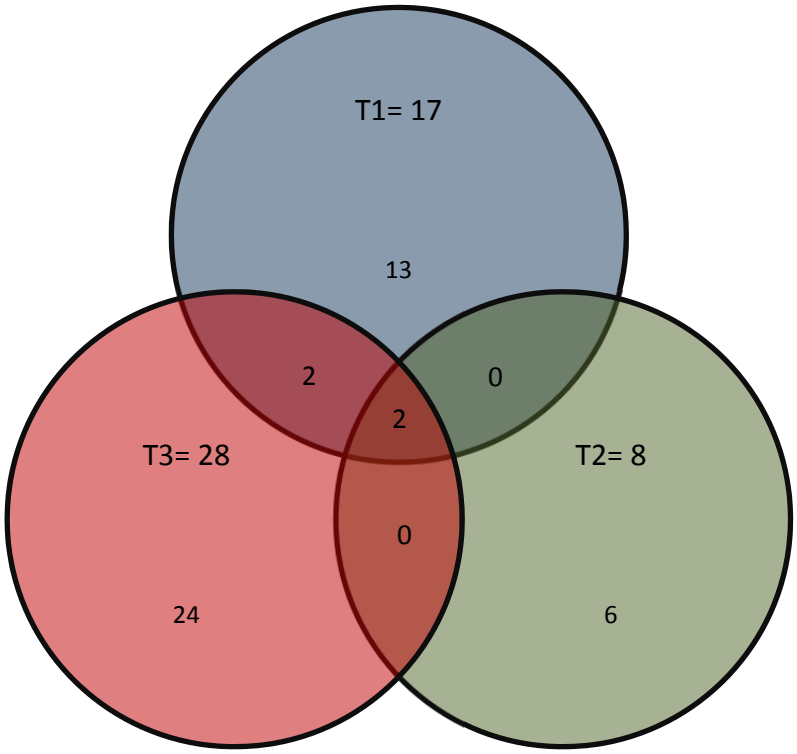

Figure 4.22: The number and overlap of the chimeric mRNAs in the sheep embryo fibroblasts expressing ovhv2-miR-7, -67 and -8 test samples.

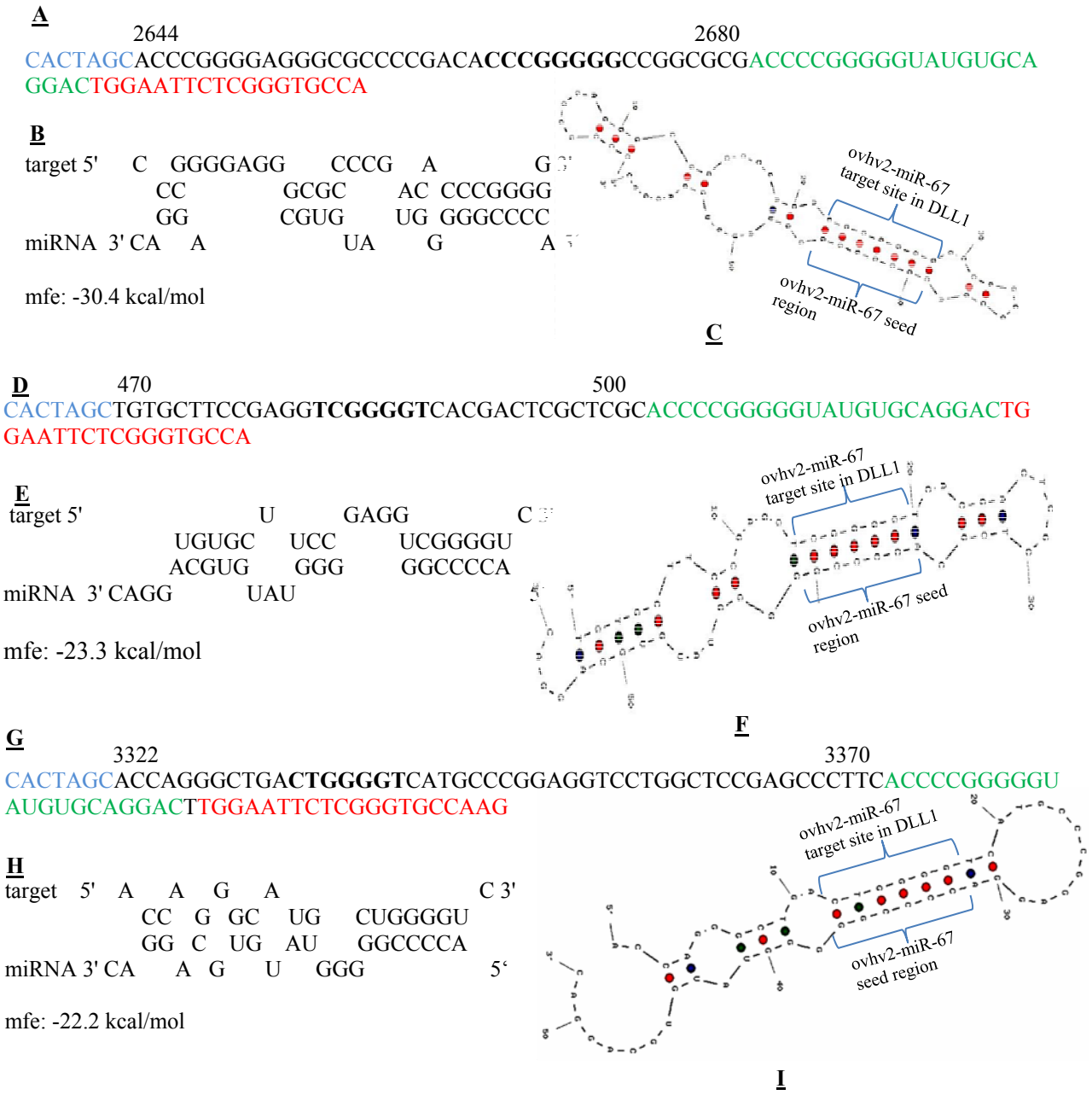

Figure 4.23: ovhv2-miR-67 formed chimeras with sheep transcripts.

ovhv2-miR-67 formed chimeras with delta like 1 (DLL1) and von Willebrand factor A domain-containing protein 5B2 (VWA5B2).
Chimeric reads of DLL1 (A and D) and VWA5B2 (G). Barcodes, mRNA fragments, miRNAs and 3' linkers are shown in blue, black, green and red respectively. miRNA target regions are shown in bold.
Figure B and E (DLL1) and H (VWA5B2) show the results obtained from RNAhybrid software for the ovhv2-miR-67 target predication in the mRNA fragment of the chimeric reads.
Figure C and F (DLL1) and I (VWA5B2) show results obtained from UNAfold software to fold chimeric reads to observe the miRNA-mRNA hybridized interactions.

4.3.3.4 Validation of ovhv2-miRs targets identified in sheep embryo fibroblasts, by CLASH

Some of the mRNAs identified in the chimera analysis (section 4.3.3.3) may be potential targets of ovhv2-miRs and may play an important role in OvHV-2 infection in sheep. To validate those targets, dual luciferase reporter assays were carried out (Section 2.6). Only those mRNAs which showed an interaction with their respective ovhv2-miRs in the seed region (nucleotides 1-7 or 2-8) were considered the further investigation. Due to the time limits it was not possible to validate all the identified targets and only two mRNAs were selected for further analysis. Of these, DLL1 was chosen as it constituted the highest number of chimeras in all of the test samples (Section 4.3.3.3) and was also the top DEnGs in the single read datasets (4.3.2.7). In addition to DLL1, VWA5B2 which formed chimera with ovhv2-miR-67 was selected for validation.

RNAhybrid analysis identified potential interactions between the miRNA seed region from position 1-7 and 2-8 with DLL1 and from position 1-7 with VWA5B2 (Figure 4.23). The target sequences were located in the coding regions of the genes. Luciferase assays were performed using plasmid constructs containing target sites from DLL1 and VWA5B2 (as described in Sections 2.6 and 4.3.3.2). Luciferase constructs were created using custom oligonucleotides (Section 2.7). For DLL1 the region of mRNA used was from nucleotide 2620 to 2706 (ovis aries chromosome 8; exon 8: 90487092-90487006). Two target sites for ovh2-miR-67 were located in the region (2644-2650 and 2665-2671). The first 52 nucleotides of the mRNA region from 2620 to 2672 (chromosome 8; exon 8: 90487092-90487006) had perfect

sequence similarity to another region (chromosome 8; 90486767-90486715) which at the time of designing the oligonucleotides and performing the luciferase assays, was shown as a part of the exon. Recent updates to the OarV3.1 annotation mapped that sequence as a part of the intron next to exon 8. Due to the presence of the sequence in the exon the primers were designed using that sequence (ovis aries chromosome 8; 90486767-90486681) and was used for the validation of ovhv2-miR-67 targets in dual luciferase assays. Fortunately the ovhv2-miR-67 target sites were located in the first 52 nucleotides of the region which showed perfect sequence homology with the DLL1 mRNA sequence. Oligonucleotides were designed for VWA5B2 corresponding to the region from 3291 to 3376 from the mRNA sequence (XM_004003830.1). The target site for the ovhv2-miR-67 was located from nucleotide 3333 to 3339.

Luciferase assays and statistical analysis of results were carried out using successfully cloned constructs (LUC/DLL1 for DLL1 and LUC/VWA for VWA5B2) as described in Section 4.3.3.2.

4.3.3.4.1 Validation of DLL1 as a predicted target of ovhv2-miR-67

Introduction of the ovhv2-miR-67 at both 100 nM and 200 nM concentrations led to a significant down regulation (approximately 50% and 60%) in luciferase expression relative to the negative controls respectively, (LUC/DLL1+ovhv2-miR-67, 100 nM) $p=0.001$, (LUC/DLL1+ovhv2-miR-67,200 nM) $p<0.001$). In the absence of any miRNA LUC/DLL1 also showed significantly higher expression of luciferase than the control (LUC/DLL1, 100 nM) $p<0.001$ and LUC/DLL1, 200 nM) $p<0.001$ (Figure 4.24 for 200 nM concentration result).

4.3.3.4.2 Validation of VWA5B2 as a predicted target of ovhv2-miR-67

In the presence of the ovhv2-miR-67 at both (100 nM and 200 nM) concentrations no significant difference was observed in the luciferase expression relative to the negative controls (LUC/VWA+ovhv2-miR-67, 100 nM) p=1.0, (LUC/VWA+ovhv2-miR-67,200 nM) p=0.42). LUC/VWA in the absence of any miRNA, showed no significant difference in expression of luciferase when compared with the control at 100 nM concentration (LUC/VWA, 100 nM) p=0.05). However a significant higher expression of luciferase was observed compared to the negative control at 200 nM concentration (LUC/VWA, 200 nM) $p<0.001$ (Figure 4.25).

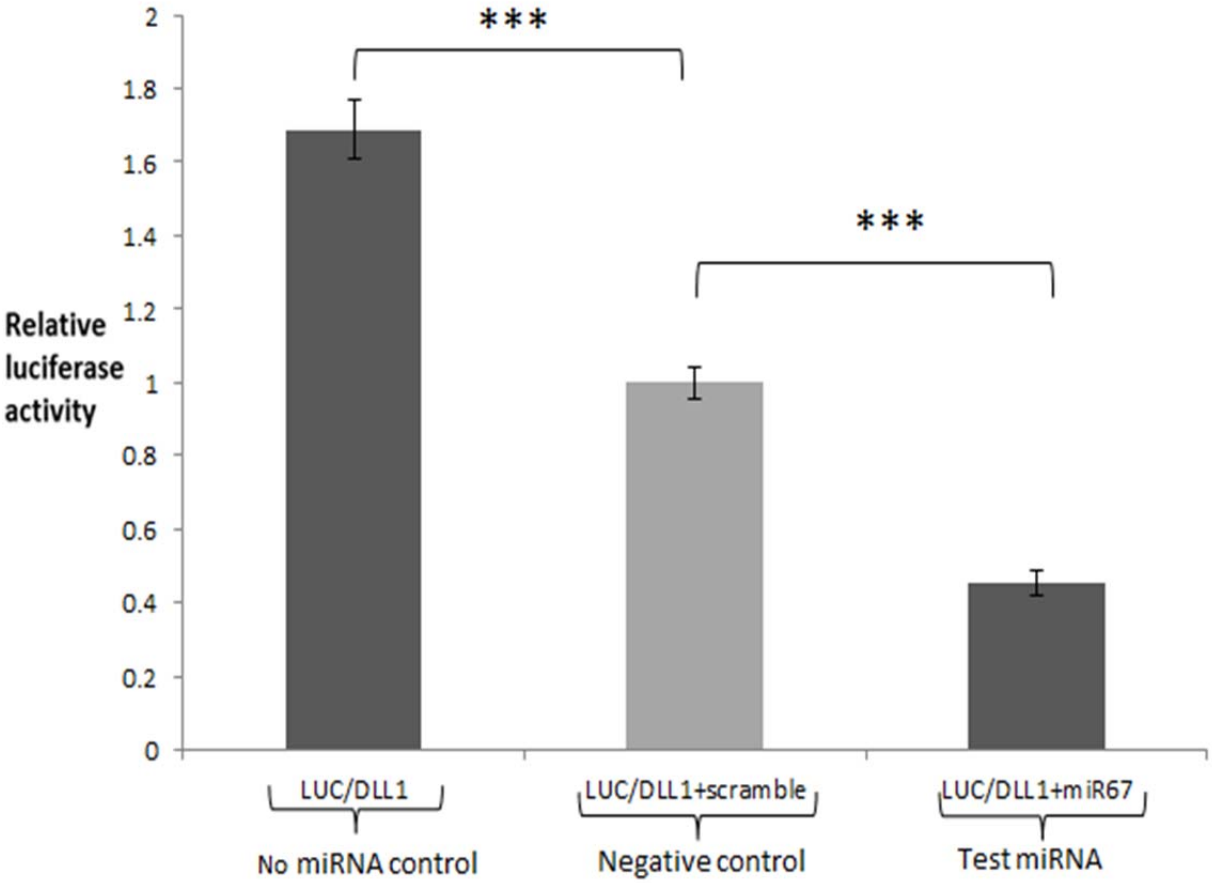

Figure 4.24: Luciferase expression levels in BHK21 cells transfected with DLL1 (LUC/DLL1) in the psiCHECK-2 plasmid in the presence/absence of target miRNA (ovhv2-miR-67) at 200 nM concentration.

Data are represented as luciferase activity with the ***=$p<0.001$ relative to negative control (light grey) value at 200 nM concentration.

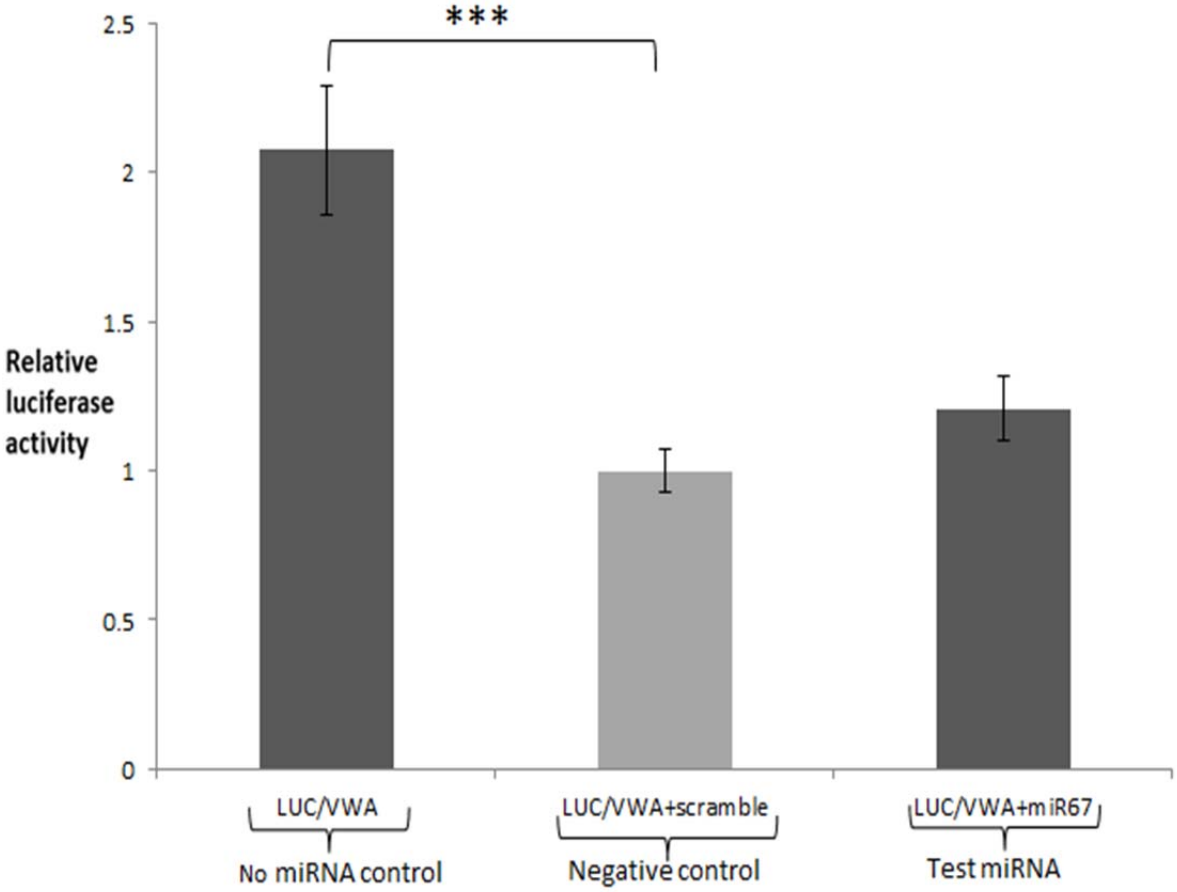

Figure 4.25: Luciferase expression levels in BHK21 cells transfected with VWA5B2 (LUC/VWA) in the psiCHECK-2 plasmid in the presence/absence of target miRNA (Ovhv2-miR-67) at 200 nM concentration.

Data are represented as luciferase activity with the ***=$p<0.001$ relative to negative control (light grey) value at 200 nM concentration.

4.4 Discussion

In order to determine the potential role of ovhv2-miRs in MCF pathogenesis, it is necessary to identify their target mRNAs. There are a number of ways to identify miRNA targets; bioinformatic analysis using the seed region sequence of miRNA to identify the complementary sites in the mRNA sequence by alignment, microarrays which determine the difference in the abundance of transcripts in the samples with/without miRNA expression, and immunoprecipitation assays to pull-down the RISC-miRNA with targeted mRNA. CLASH is a relatively new technique and is a combination of pull-down/immuno-precipitation and bioinformatics. CLASH allows direct analysis of RNA-RNA interactions in the living cells and those interactions can be recorded using high throughput sequencing. Generally, CLASH provides a reliable alternative to existing experimental and bioinformatics methods. Because crosslinking is carried out in the living cells, the dynamic state of the RNA-RNA interactions can be probed as a function of physiological conditions (Kudla *et al*., 2011). CLASH can also be used to identify miRNAs targets and their interactions with the targeted mRNAs. In this study CLASH was used to identify ovhv2-miRs targets within the transcripts of the bovine and sheep genomes.

4.4.1 CLASH identifies viral miRNA targets within LGL cell line BJ1035

The OvHV-2 infected LGL cell line BJ1035 expresses all the ovhv2-miRs and was used as a source to identify those miRs (Levy *et al*., 2012) and their targets. Due to the unavailability of appropriate control bovine cells, only BJ1035 cells were used in this study. BJ1035 cells are non-adherent cells and exhibit a doubling time of 7-8 days under appropriate conditions (Swa *et al*., 2001) and for CLASH experiments a

large number of cells (Section 2.8.1) was required. Due to the long doubling time of cells, the multi-step nature of CLASH and the time required for high throughput sequencing, it was not possible to grow BJ1035 to a sufficient density in the available timeframe and so only one BJ1035 sample was characterised. This study provides a snap shot of the miRNA interactions with bovine mRNAs. The analysis of miRNA-mRNA chimeras (Section 4.3.3.1) has enabled the identification of potential bovine mRNA targets that may, with the further study provide insight into the pathology of MCF. The CLASH single read data, showed some differences from the RNA-seq data (for the abundance of ovhv2-miRs) presented by Levy (Levy PhD thesis, 2012). This might be due the differences in the experimental procedures between the studies in the construction of the cDNA libraries. CLASH required stringent purifications of tagged protein linked with the miRNA, mRNAs or miRNA-mRNA chimera. Eight of the ovhv2-miRs validated by northern hybridization by Levy *et al* (Levy *et al*., 2012) also showed high abundance in the CLASH dataset (Table 4.2). In the CLASH data ovhv2-miR-217M was found (28300 reads) as the most abundant Ovhv2-miR whereas in the RNA-Seq data (Levy PhD thesis, 2012) ovhv2-miR-8 was found to be the most abundant (46048 reads) (Table 4.2). Thirty six of the 46 predicted ovhv2-miRs were present in CLASH data. Ten of the miRNAs which showed very low numbers in the RNA-Seq data were not present in CLASH data (Table 4.2).

The single reads data obtained in the CLASH study had a high number of cellular mRNAs (Section 4.3.1.6). Due to the absence of an uninfected control sample it was not possible to compare if those mRNAs were targeted by ovhv2-miRs. To determine the mRNA bovine targets of ovhv2-miRs, the CLASH chimera data was used.

MicroRNAs can bind to a wide variety of targets; with both canonical and non-canonical base pairing which indicates that miRNA targeting rules may be complex and flexible (Helwak *et al*., 2013). The analysis of chimeras found the presence of canonical (nucleotides 1-7 or 2-8) (approximately 37%) and non-canonical interactions (approximately 63%) between miRNAs and mRNAs. This data is in line with another CLASH related study (Helwak *et al*., 2013) where non-canonical seed interactions were approximately 1.7 fold more common than perfect base pairing.

The targets or binding sites of miRNAs can be located in the 5'UTR, CDS or 3'UTRs, with the majority of the target sites found within the CDS (Hafner *et al*., 2010, Helwak *et al*., 2013). In this study approximately 60% of miRNA target sites were found to be located in the CDS of the mRNAs which is consistent with the previous studies (approximately 50% in Hafner *et al*., 2010 and 60% in Helwak *et al*., 2013)

Among the ovhv2-miRs, ovhv2-miR-217M which was found as the most abundant miRNA in the single read dataset, was also found to form chimeras with the highest number of mRNAs (Section 4.3.3.1). Two of the mRNAs; cleavage stimulation factor subunit 3 (CSTF3) and U11/U12 small nuclear ribonuclearprotein 25 kDa protein (SNRNP25) were shown to have a canonical interaction in the seed region of ovhv2-miR-217M. The protein encoded by the CSTF3 gene is one of the three (CSTF1 and CSTF2) cleavage stimulation factors that combine to form a CSTF complex. This complex is involved in the polyadenylation and 3'end cleavage of pre-mRNAs (Takagaki and Manley, 1994). CDC73, a tumor suppressor gene, is a component of the Paf1 complex (Paf1C) and is involved in 3'end formation of polyadenylated mRNAs (Penheiter *et al*., 2005). It has been reported that CDC73 is

physically associated with CSTF and the cleavage and polyadenylation specificity factor (CPSF) and regulates transcription processing. The CDC73-CSTF-CPSF complex connects Paf1C directly with RNA for 3' end formation. CDC73 defects that predispose to tumor formation could result from alteration in the 3'mRNA processing or alteration in the chromatin structure or a combination of these events (Rozenblatt-Rosen *et al*., 2009). It is possible that ovhv2-miR-217M targets CSTF to inhibit or alter the 3'end formation of cellular mRNAs to shut off host translational machinery.

The SNRNP25 gene encodes a 25KDa protein that is a component of the U12-type spliceosome, and is involved in the pre-mRNA splicing by removing U12-type introns (Konig *et al*., 2007, Will *et al*., 2004). Both of these mRNAs have functions related to pre-mRNA splicing and polyadenylation suggesting a possible role in transcription.

Another miRNA ovhv2-miR-36 formed a chimera with U2 (Sections 4.3.1.6 and 4.3.3.2, Figure 4.19). U2 a snRNA is a component of the major (U2-dependant) spliceosome complex, and is involved in pre-mRNA splicing by catalysing the removal of U2 type introns. In eukaryotes two of the spliceosomes; U2 and U12 coexist however more than 99% of introns are the U2 type and require U2 dependent splicing events for mRNA maturation (Will and Luhrmann, 2011). ovhv2-miR217M and ovhv2-miR-36 both formed chimeras with the components of mRNA polyadenylation (CSTF3) and splicing (SNRNP25 and U2), in this study. A number of studies have reported, reciprocal functional coupling between splicing and 3′ end processing of RNA (Kyburz *et al*., 2006, Dye and Proudfoot, 1999, Niwa *et al*., 1990). In addition, *in vitro* a functional coupling and dependence was observed,

defining terminal exon and polyA site cleavage in splicing the terminal intron (Rigo and Martinson, 2008). A defect in either process has also been shown to disrupt splicing and 3′ end formation as well as the linked process of transcriptional termination (Dye and Proudfoot, 1999).

To confirm if the identified targets were real, experimental validation was required. Due to time constraints only one of the targets; U2 was chosen for target validation using dual luciferase assay (Section 4.3.3.2.1). The LUC/U2 construct contained an 82 nucleotide long U2 fragment with an ovhv2-miR-36 target site. The data from luciferase assays showed that ovhv2-miR-36 mimic could effectively knockdown the translational activity of the luciferase gene and a significant ~20% down-regulation in the expression was observed (Figure: 4.21). These results indicate that ovhv2-miR may interfere with host pre-mRNA processing. Incomplete processing may lead to non-functional mRNA formation causing shut-off of host proteins expression. As herpesviruses express numerous intronless transcripts, this may give the transcripts a competitive advantage in accessing the cellular translation machinery. The herpes simplex virus (HSV) protein ICP27 mediates the inhibition of cellular splicing. Early in infection, ICP27 interacts with several splicing factors and affects their phosphorylation. This results in the blockage of the pre-spliceosome assembly, which in turn contributes to the shut-off of host protein synthesis because of incomplete cellular pre-mRNAs processing (Bryant *et al*., 2001, Hardy and Sandri-Goldin, 1994). OvHV-2 and other related herpesviruses have a homologue of ICP27 but no such effect has been reported. ORF57 of KSHV has been reported to have roles in viral mRNA biogenesis by acting as viral splicing factor to promote splicing of KSHV transcripts (Majerciak *et al*., 2008). KSHV achieves this by recruiting

hTREX (human transcription and export complex) onto viral intronless mRNAs thereby allowing access of the viral transcripts to the cellular mRNA export proteins (Boyne *et al*., 2010) which then export the viral RNA to the cytoplasm for translation and protein production. Moreover, preventing the expression of host proteins is also an effective way for the virus to counteract the antiviral response (Mohr *et al*., 2008). Although many viruses encode proteins that specifically inactivate host cell regulatory or defence system, the small size of viral genomes limits the utility of this approach. miRNA which are smaller in size could offer an attractive alternative way for viruses to turn off specific host genes. There is a possibility that ovhv2-miR-217M and ovhv2-miR-36 inhibit cellular splicing to shutoff host genes by targeting CSTF3, SNRNP25 and U2 respectively.

Genes which involved in other cellular processes also formed chimeras with ovhv2-miRs. MCF2L, which is also called Rho specific guanine nucleotide exchange factor DBS (RhoGEFs), formed a chimera with ovhv2-miR-5. RhoGEFs catalyse the exchange of GDP to GTP on members of the Rho family of small GTPases (Whitehead *et al*., 1997). Rho GTPases are critically involved in a variety of vital cell functions such as cell proliferation, apoptosis, and gene expression and are considered to be the main regulators of the cell cytoskeleton. Increasing evidence indicates that many herpesviruses interact with cytoskeleton-regulating Rho GTPase signaling pathways during different phases of their replication cycle (Van den Broeke and Favoreel, 2011). Examples of these include Rho GTPase-mediated nuclear translocation of virus during entry to a host cell and Rho GTPase-mediated viral cell-to-cell spread during later stages of infection (Van den Broeke and Favoreel, 2011). Most Rho proteins exhibit biological activity only when these are in

the GTP-bound state and RhoGEFs are primarily thought to be Rho activators. The deregulated expression of RhoGEFs can cause tumorigenic growth and promotes the invasive potential of a variety of cell types and are often found associated with loss of contact inhibition, growth factor independence, anchorage-independent growth and tumorigenecity (Cheng *et al*., 2002, Whitehead *et al*., 1997).

ovhv2-miR-5 also formed a chimera with ADAMTS1 (also referred as METH-1). This gene encodes a member of the ADAMTS (a disintigrin and metalloproteinase with thrombospondin motif) proteins, is involved in tissue repairs processes (Krampert *et al*., 2005), anti-angiogenic activity (Obika *et al*., 2012) and inflammation (Kuno *et al*., 1997). Krampert showed ADAMTS1 may play a role in the wound-healing process, as it regulates keratinocyte differentiation as well as migration of fibroblasts and endothelial cells (Krampert *et al*., 2005).

ovhv2-miR-8 formed chimeras with two bovine mRNAs; TM6SF1 and TBR-1. TM6SF1 is a transmembrane protein and found as a differentially expressed gene in a sub set of CD8+ T cells in a study related to multiple sclerosis (Fanchiang *et al*., 2012). TM6SF1 was identified as a target of the related gamma herpesvirus KSHV encoded miRNA miR-K-12-11 and the human oncogenic miRNA has-miR-155 and in the presence of those miRs, significant inhibition of gene expression was observed using a luciferase reporter assay (Skalsky *et al*., 2007). To determine if TM6SF1 was also a real target of ovhv2-miR-8 a luciferase reporter assay was performed in this study (Section 4.3.3.2). The results indicated an increase in the luciferase expression of approximately 60 and 80% at 100 nM and 200 nM concentrations of miRNA mimics, as compared to the negative control respectively (Section 4.3.3.2.2). miRNAs generally induce translational repression by interacting with the target sites

located in mRNAs, however translational activations have also been reported (Lin *et al*., 2011a, Vasudevan *et al*., 2007, Vasudevan, 2012) (Section 1.5.3.4). Translational up-regulation by miRNAs could be achieved in two ways; activation by direct action of miRNA /miRNPs or by the relief of repression where the action of a repressive miRNA is abrogated (Vasudevan, 2012). miR-206 binds the 3'UTR and upregulates translation of KLF4 mRNA in quiescent cell lines (Lin *et al*., 2011a). The liver specific miR-122 stimulates translation of HCV RNA through direct binding to two target sites in the virus 5'UTR (Henke *et al*., 2008). miR-346 interacts with the 5'UTR of RIP140 and up-regulates translation in mouse brain tissue and p19 cells independent of AGO2 (Tsai *et al*., 2009). Binding of miR-125b to the 3'UTR of *κ*B-Ras2 mRNA and miR-466I to interleukin (IL)-10 mRNA mediates increased mRNA stability in human macrophages (Ma *et al*., 2010, Murphy *et al*., 2010). Further investigation is required to confirm if the translational activation was due to ovhv2-miR-8 interaction with TM6SF1. Experimentally a reporter assay using a miR-8 target site knockout construct could confirm if the translation activation was due to an interaction between miR-8 and TM6SF1 interactions. It is also possible that the negative control caused a non-specific effect on the knockdown experiments. Changing or adding more negative controls can also provide a better insight into the results.

TBR-1, which formed a chimera with ovhv2-miR-8, is a member of a conserved family of genes that share a common DNA-binding domain, the T-box. T-box genes encode transcription factors involved in the early cell fate decisions for differentiation and organogenesis (Wilson and Conlon, 2002).

CA12, which formed chimera with ovhv2-miR-39, belongs to the carbonic anhydrases (CAs) family. CA is a large family of zinc metalloenzymes that catalyzes the reversible hydration of carbon dioxide. CAs participate in a variety of biological processes, including respiration, calcification, acid-base balance, bone resorption, and the formation of aqueous humor, cerebrospinal fluid, saliva, and gastric acid. This gene product is a type I membrane protein that is highly expressed in normal tissues (GeneCards®). CA12 is also found to be induced by hypoxia in various tumor cells, and promotes cell survival and growth in an acidic environment through pH maintenance. Silencing of CA12 and another CA (CA9) caused a dramatic decrease in the rate of tumor growth and might act as potential candidates for anticancer treatments (Chiche *et al*., 2009). The function of this gene does not support MCF pathology. However, the OvHV-2 immortalized LGL cell line BJ1035 used in this study, is a mixed population of cells with respect to the virus life cycle; the majority of the cells are latently infected, but a small proportion express early and late virus genes (Rosbottom *et al*., 2002, Thonur *et al*., 2006). It is also possible that ovhv2-miRs may also be differentially expressed in the proportion of cells in culture in which the virus is latent.

Other mRNAs forming chimeric interactions were; LAMB2 (ovhv2-miR-67) a laminin protein belonging to a family of extracellular matrix glycoproteins, involved in cell adhesion, differentiation, migration, signalling and metastasis (Aumailley and Krieg, 1996). CPNE2 (ovhv2-miR-7), a calcium-dependent membrane-binding protein that may regulate molecular events at the interface of the cell membrane and cytoplasm (Perestenko *et al*., 2010) and THSD1 (ovhv2-miR-54) which contains a

type 1 thrombospondin domain found in a number of proteins involved in the complement pathway, as well as in extracellular matrix proteins (GeneCards®).

There were also a number of cellular mRNAs forming non-canonical chimeras with ovhv2-miRs (section 4.3.3.1). The interactions between miRNA and their targets are usually mediated by the seed region, which is a 6-8 nucleotide long fragment of miRNA at the 5'end and forms a Watson and Crick pairing with the target mRNA (Bartel, 2009). However non-canonical miRNA-mRNA interactions (interactions in the regions other than the miRNA 5'end) are also reported. Shin *et al* reported the presence of centered sites that have 11-12 contiguous Watson Crick pairs to miRNA nucleotides 4-15. Testing the perfect 11-mer matches using luciferase reporter assay starting at miRNA positions 3, 4, and 5 were each significantly associated with repression (Shin *et al*., 2010). Another study on the mapping of the human miRNA interactome by CLASH identified frequent non-canonical interactions. miR-92a was tested for experimental validation of the non-canonical interactions. Luciferase constructs with miR-92a seed region or non-seed region targets showed significant increase in expression on depletion of miR-92a (Helwak *et al*., 2013).

Some of the mRNAs identified in this study which showed non-canonical interactions with the ovhv2-miRs, have functions that could influence the control of cellular processes. ATRN (ovhv2-miR35) (also referred to DPPIV) is a normal serum glycoprotein which is rapidly expressed on the surface of activated T-cells in the initial stages of T-cell proliferation and can up-regulate antigen specific T cell responses (Duke-Cohan *et al*., 1998). ATRN positive CD4+ T cells exhibit a

memory phenotype, induce immunoglobulin synthesis in B cells and activate MHC-restricted cytotoxic T cells (Boonacker and Van Noorden, 2003).

FHOD1 (ovhv2-miR-39) interacts with Rac1 GTPases and mediates rearrangements of the actin cytoskeleton that might play a role in transcription regulation (Gasteier *et al*., 2003). ABR (ovhv2-miR-53) functions as a GTPases activating protein for Rac and CDC42 and promotes exchange of GDP to GTP (Cho *et al*., 2007). Rac is a subfamily of GTPases and is involved in the regulation of a diverse array of cellular events including cell growth, cytoskeleton reorganization and activation of protein kinase (Ridley, 2006).

MAP3K2 (ovhv2-miR-53) (also referred to MEKK2) is a member of the serine/threonine protein kinase family. This kinase preferentially activates other kinases involved in the MAP kinase signaling pathway. This kinase has been shown to directly phosphorylate and activate Ikappa B kinases, and thus plays a role in the NF-kappa B signaling pathway. This kinase has also been found to bind and activate protein kinase C-related kinase 2, which suggests its involvement in a regulated signaling process (GeneCards). MAP3K2 enhanced the lytic replication of a related gamma herpesvirus; MHV68, when overexpressed (Li *et al*., 2010).

ATP6V1B1 (ovhv2-miR-217M) is a multi-subunit enzyme and a component of a V-ATPase complex. ATP6V1B1 is associated with an ATP-dependent proton pump and mainly functions as an acidifier in the internal environment of endomembrane systems such as lysozymes and endosomes (Ohta *et al*., 1996). V-ATPases have diverse roles in normal physiological processes including endocytosis, pH homeostasis and membrane trafficking (Forgac, 2007). Acidification of intracellular

compartments has also been shown to be required for efficient MHC class II presentation (Benaroch *et al*., 1995) suggesting a role in adaptive immune system. Expression of ATP6V1B1 increases in various cancer cells and inhibitor of this protein inhibit the growth of various cells and inducing apoptosis (Manabe *et al*., 1993, Morimura *et al*., 2008). Acidic endosomal compartments also have been shown to involve in the entry of some of the enveloped viruses in to the cells (Gruenberg and van der Goot, 2006). Pavelin *et al* found that ATP6V0C, a component of the V-ATPase complex, is an essential factor for HCMV replication. ATP6V0C was also targeted by HCMV encoded miRNA US25-1. Knockdown of ATP6V0C resulted in striking inhibition of virus replication and during growth curve analysis almost no infectious virus was detected (Pavelin *et al*., 2013). They also suggested that blocking of a component of V-ATPase complex, required for efficient replication, might represent a mechanism of establishing or maintaining viral latency (Pavelin *et al*., 2013). MCF is characterized by cellular proliferation and targeting of MAP3K2 and ATP6V1B1 by ovhv2-miRs would be expected to cause an inhibitory effect on cellular growth. It is possible that targeting these mRNAs might help virus in evading the immune system or as discussed earlier that it is possibly due to the presence of cells in the BJ1035 cell line, which support latency.

PDCL3 (ovhv2-miR-57) (also known as VIAF) is an inhibitor of apoptosis (IAP) interacting factor that functions in caspase activation during apoptosis and co-regulates the apoptotic pathway (Wilkinson *et al*., 2004). MLL5 (ovhv2-miR-53) has a regulatory role in the different stages of cell cycle. Ectopically over expressed MLL5 caused G1/S phase arrest (Deng *et al*., 2004) whereas siRNA mediated knock

down of MLL5 arrested cell cycle at both G1/S and G2/M phases (Cheng *et al*., 2011).

MAGI3 (ovhv2-miR63) is involved in various cellular and signalling processes. It interacts with tumor suppressor PTEN for enhanced regulation of AKT/PKB kinase. It serves to position the PTEN to specific sub-cellular locations that are involved with the regulation of cell proliferation and survival (Wu *et al*., 2000b). Down-regulating PTEN can lead to cell proliferation, hypertrophy, and a lowered cellular response to stress (Yang *et al*., 2009). PTEN is also frequently deleted or mutated in various cancers to promote tumorigenesis. A cellular miRNA, miR-216a also targets PTEN. ovhv2-miR-217M has seed sequence homology with cellular miR-216a (Figure 4.5A) and it is possible that PTEN is also a target of ovhv2-miR-217M. To test if these mRNAs are functional targets of ovhv2-miRs and if ovhv2-miR-217M is a functional homologue of cellular miR-216a, experimental validation of those targets is required and this work is ongoing in the lab.

Chimera data analysis of BJ1035 sample therefore identified a number of cellular mRNAs which are involved in important biological processes such as transcription, cell cycle regulation, signal transduction and apoptosis. It is possible that these genes are involved in one or more features of cellular dysregulation in MCF. It is also possible that targeting of these genes by ovhv2-miRs could influence OvHV-2 persistence in the host cells. To determine how these genes are involved in MCF pathogenesis and in virus lytic or latent lifecycle, further investigation is required.

4.4.2 CLASH identifies viral and cellular miRNA targets within sheep embryo fibroblasts

To investigate ovhv2-miRs targets in the sheep transcripts, SEF were used, in the CLASH experiments. SEF were used due to two reasons; first, unavailability of OvHV-2 infected or uninfected sheep lymphocyte cell lines and second, double transductions were required which needed long antibiotic selection periods and it diminished the possibility of growing primary sheep lymphocytes in cultures. SEF were doubly transduced with lentiviruses expressing tagged Ago2 and ovhv2-miRs from Cluster-3 (Section 4.3.2.2).

The majority of ovhv2-miRs are encoded from the regions of the genome which contain no predicted protein coding ORFs (Figure 1.5). The majority of the miRNAs are localized in three clusters on the negative sense strand; Cluster-1 is located at the left-hand end of the genome, 5' of Ov2, the other two (Cluster-2 and Cluster-3) are in the 9.3 kb non-coding region between ORF11 and ORF17/17.5. Cluster-2 and Cluster-3 encode for 27 and 3 ovhv2-miRs respectively and are approximately 4.3Kb apart from each other (Figure 1.5) (Levy PhD thesis, 2012). In other gamma herpesviruses clustering of miRNAs in the regions which do not encode any ORF, was also observed (Cai *et al*., 2006a, Marshall *et al*., 2007, Samols *et al*., 2005). Cluster-2 and Cluster-3 were analysed for the expression of ovhv2-miRs by RT-qPCR. Expression of all three of the ovhv2-miRs (7, 67 and 8) located on Cluster-3 were found comparable to the positive control and that cluster was used for the CLASH experiments (Section 4.3.2.2-4.3.2.4). Illumina Solexa sequencing results of cDNA libraries from three replicates each of the test (SEF-Cluster-3) and control

(SEF-Empty) samples were analysed (4.3.2.5). The total read counts were variable between samples (Table 4.5). The protocol for performing CLASH was the same for each sample however difference in the abundance of the reads was observed (Table 4.5). One possible reason for this difference is that, the lysates for test and control samples were collected from cells with different passage number. SEF might behave differently at different passage numbers. Slight variation in the salt levels, during the experiment may also lead to differences in the total reads at the sequencing stage. Ovhv2-miR-67 was found as the most abundant among the three ovhv2-miRs. Ovhv2-miR-8 and ovhv2-miR-7 were two of the highly abundant miRs validated by northern blot anlaysis (Levy PhD thesis) but were observed to be less abundant in this dataset. CLASH experimental results are based on the immunoprecipitated/pulled down RISC-miRNA-mRA complexes whereas RNA-seq results provide a broad picture of RNAs in the cells, obtained from total RNA extracted from the cells.

To identify the targets of the three ovhv2-miRs in ovine transcripts, there were three datasets available from the test and control samples; chimeras dataset, CLASH single reads dataset and microarray dataset.

Like the chimeras obtained in the BJ1035 dataset (Section 4.3.3.1), canonical and non-canonical interactions were also found between miRNA and sheep mRNAs. Canonical interactions ranged between 47-63% in test samples (Section 4.4.3). Among the three ovhv2-miRs, miR-67 formed most of the chimeras with sheep mRNAs fragments. Some of the mRNAs forming canonical interaction with ovhv2-miRs, have functions which might be essential for cellular processes and be involved

in OvHV-2 pathology in sheep and were important to discuss. Due to time constraints only two of the chimeric mRNAs (DLL1 and VWA5B2) were selected for functional validation.

Fragments of DLL1 mRNA were found to form the highest number of chimeras. ovhv2-miR-67 was shown to interact with DLL1 in all these chimeras (Table 4.15). Among the CLASH identified DEnGs, DLL1 was also found as the highest significant gene (Table 4.7). DLL1 is a part of the Notch signaling pathway and is a ligand for Notch receptors. Notch signaling regulates differentiation of lymphocytes and blocks the differentiation of progenitor cells into the B-cell lineage while promoting the emergence of a population of cells with the characteristics of a T-cell/NK-cell precursor (Jaleco *et al*., 2001). Notch signaling is involved in various cellular processes including regulation of cell fates and cell number via effect on proliferation and survival, depending on dose, times and context of Notch signals (Maillard *et al*., 2005). Inactivation of Notch causes a complete block in the T-cell development at an early stage, before expression of T-cell lineage markers (Radtke *et al*., 1999). Activation of the Notch receptor by binding of its ligands (e.g DLL1, Jagged, or Serrate) leads to proteolytic cleavage of the receptor at the inner side of the membrane. The Notch intracellular domain (NIC) is then translocated to the nucleus, where it activates genes by interacting with the RBP-JK protein (Radtke and Raj, 2003). RBP-JK acts as a transcription repressor when not bound to NIC and a transcription activator of Notch target genes, when bound to NIC (Zimber-Strobl and Strobl, 2001). In the related gamma herpesviruses; EBV and KSHV virus transactivator proteins also interact with RBP-JK (Chang *et al*., 2005, Hayward,

2004) . EBNA2 of EBV can activate the cellular antiapoptotic bfl-1 gene (Pegman *et al*., 2006). Recombinant KSHV with deleted RBP-JK binding sites within the RTA promoter showed increased viral latency and a decreased capability for lytic replication in HEK 293 cells (Lu *et al*., 2012). EBNA2 and RTA can act as viral homologues of activated Notch receptors (Hayward, 2004). Activation of Notch signalling increases tumor cell proliferation and also maintains the cancer stem cell pool (Capaccione and Pine, 2013). Cellular miRNAs also have been shown to target Notch signalling at different levels. Tumor suppressor miRs; miR-1 and miR-34a negatively regulate DLL-1 protein levels in embryonic stem cells and down-regulate protein expression of Notch receptors in glioma and pancreatic cancer cells, respectively (Wang *et al*., 2010).

Validation of DLL1 as a real target of ovhv2-miR-67, was carried out using a dual luciferase assay (4.3.3.4.1). The detail of the fragment used is shown in Section 4.3.3.4. Luciferase assays showed a significant decrease in the expression of luciferase genes when the DLL1 constructs were treated with ovhv2-miR-67 concentrations. OvHV-2 does not cause lymphoproliferation or cytotoxicity in sheep and targeting of DLL1 by ovhv2-miR-67 might stop Notch signalling thereby stopping lymphocyte cell differentiation and maintaining viral latency. Further investigations of DLL1 as a viral target, are being carried out by Katie Nightingale. Preliminary analysis using luciferase assays showed constructs with both DLL1 predicted target sites mutated showed abrogation in the inhibition of luciferase expression compared to that of the parent construct (Katie Nightingale personal communication).

Another mRNA, VWA5B2 which formed a chimera with ovhv2-miR-67, was validated by luciferase reporter assay. VWA5B2 belongs to the von Willebrand factor (vWF) domain A containing proteins. Proteins that contain type A domains also participate in numerous biological events such as hemostasis, cell adhesion, migration, homing, pattern formation, and signal transduction and interact with a large array of ligands (Colombatti *et al*., 1993). vWF proteins are also involved in pathological processes including cell proliferation, angiogenesis, inflammation and tumor cell survival. The mitogenic effect of vWF proteins is also involved in the prompt and robust up-regulation of multiple genes associated with growth factor stimulation (Lenting *et al*., 2012). Targeting of VWA5B2 by ovhv2-miR-67 might inhibit excessive inflammation and cell proliferation produced in response to OvHV-2 infection. To determine if the VWA5B2 is a potential target of ovhv2-miR-67 luciferase analysis was carried out. The results showed no significant difference in the luciferase expression compared to that of the control, at 100 nM or 200 nM concentrations of ovhv2-miR-67 mimic (Section 4.4.4.2). There is a possibility that it is not a real target but in the absence of any further investigation, at this stage it is not possible to comment further.

KLHL2 (also referred as Mayven), was found to form chimeras with ovhv2-miR-7 in all the test samples (Table 4.15). The KLHL2 target site for ovhv2-miR-7 was located in the 3'UTR of the mRNA and the interaction between seed region and target site was canonical. KLHL2 is involved in the maintenance of the cytoskeleton. KLHL2 is also abundantly expressed in certain cancers. It activates c-Jun expression and cyclin-D1 promoter activity and promotes transcription. KLHL1 causes cell

cycle progression from G1 to S phase in cancer cells and overexpression of KLHL2 may promote tumor growth through c-Jun and cyclin D1 (Bu *et al*., 2005). KLHL2 was found in all the test samples and it is a possibility that it is a target of ovhv2-miR-7.

TRIM27 (also known as RFP transforming protein) (formed a chimera with ovhv2-miR-8 in the T1 sample) is highly expressed in various cancer cells. It can function as a transcriptional activator and repressor. TRIM27 inhibits the transcriptional activation of genes bound by tumor suppressor protein RB (Hatakeyama *et al*., 2011). On the other hand TRIM27 along with RET tyrosine kinase, a proto-oncogene increases the catalytic activity of RET which results in subsequent cell proliferation and tumorigenesis (Kato *et al*., 2000, Tezel *et al*., 2009).

FGF19 (formed a chimera with ovhv2-miR-67 in the T1 sample) when bound with its cognate receptor FGFR4 can initiate multiple signaling cascades. FGF19−FGFR4 play important roles in development and tissue repair by regulating cell proliferation, migration, chemotaxis, differentiation, morphogenesis, and angiogenesis. Dysregulation of this signaling system appears to be important for tumor development and progression (Desnoyers *et al*., 2008). The ectopic expression of FGF19 in transgenic mice led to tumor formation in the liver (Nicholes *et al*., 2002). Inhibiting the interaction of FGF19-FGFR4 can inhibit MAPK signalling and lowers the tumor growth significantly (Desnoyers *et al*., 2008).

MARK4 (formed chimera with ovhv2-miR-67 in T3 sample) protein is associated with the centrosome throughout mitosis and may be involved in cell cycle control.

Expression of this gene is a potential marker for cancer (Drewes *et al*., 1997, Trinczek *et al*., 2004).

CRK (formed a chimera with ovhv2-miR-67 in the T3 sample) is an adaptor protein and can mediate intracellular signalling related to cell motility and proliferation. CRK transmit signals from various tyrosine-phosphorylated proteins, including components of focal adhesion, growth factor receptors and signalling proteins by binding to them via its SH2 domain (Feller, 2001). In addition to its physiological functions, CRK contributes to the malignant conversion and progression of tumor cells. Overexpression of CRL has been detected in many types of human cancer cells (Rodrigues *et al*., 2005, Watanabe *et al*., 2009). PAK7 (formed a chimera with ovhv2-miR-67 in the T3 sample) is a p21 activated protein kinase that is known to be the effector of GTPases Rac and CDC42.

PAK7 can activate different pathways including c-Jun N-terminal and cell survival signalling pathway (Cotteret and Chernoff, 2006, Dan *et al*., 2002). In addition, PAK7 can inhibit the induction of apoptosis by localizing to mitochondria and phosphorylating the proapoptotic protein BAD thus blocking BAD translocation to mitochondria (Cotteret *et al*., 2003). A combined inhibition of PAK7, MAP3K7 and CK2a kinases increase apoptosis in most cancer cell lines, *in vitro* (Giroux *et al*., 2009). The genes shown above have the functions related to cell proliferation and survival, apoptosis, cell cycle, migration, signal transduction, tumour development and progression and conversion to malignancy. Targeting of these transcripts by ovhv2-miRs may help OvHV-2 to establish and maintain latency in sheep cells.

Analysis of the CLASH single read and microarray datasets also identified many DEnGs and GEG which may be important for different cellular processes and viral persistence in the host cell. Microarray was carried out to support and validate the CLASH single read results and to determine if there were any common sets of gene present in both datasets (4.3.2.8, 4.3.2.9). Those genes were identified from both datasets at a 5% false discovery rate (FDR). FDR is an expected proportion of false positives among the declared significant results (Benjamini and Hochberg, 2000), In the CLASH dataset only five genes and in microarray dataset no gene could pass the 5% FDR threshold. To provide greater insight, the analysis was extended to include the sets beyond those that met the 5% FDR criterion for two reason; Firstly, to not miss genes which could be biologically relevant and secondly, to identify genes which could be followed up in future studies. From the CLASH dataset genes with a p-value<0.05 were selected for DEnGs and in the microarray dataset genes with a fold change $\geq$ +1.5 or $\leq$ -1.5 and p<0.01 were selected as DEG.

GLI2 is a transcription factor and was found to have target sites for ovhv2-miR-7, 67 and 8 (Table 4.9) GLI2 is involved in the sonic hedgehog (SHH) signaling pathway. SHH signalling has been shown to regulate a wide range of developmental processes as well as to contribute to lymphoid cell development and differentiation. Mutation of this system has been linked to many cancers, including basal-cell carcinoma (Benson *et al*., 2004). GLI2 is suspected to be the primary activator of SHH signaling. Overexpression of GLI2 appears to be sufficient to generate and maintain the malignant process in some cancers. Active forms of GLI2 translocate to the nucleus, to induce expression of target genes such as GLI1, Ptc, Bcl-2, Bcl-X_L and

cyclinD (encoding cell cycle regulators) (Kolterud and Toftgård, 2008, Muller *et al*., 2008). In human keratinocytes GLI2 activation up-regulates a number of genes involved in cell cycle progression. GLI2 is able to induce G1–S phase progression in contact-inhibited keratinocytes which may drive tumour development (Regl *et al*., 2004). Notch signalling and SHH signalling may also be specific targets for anti-cancer drugs (Muller *et al*., 2008).

EPAS1 (also referred to hypoxia-inducible factor 2 alpha (HIF2 a)) is a transcription factor and is one of the highly expressed DEnGs in CLASH. EPAS1 has target sites for ovhv2-miR-7, -67 and -8 (Table 4.9). EPAS1 has high homology with hypoxia-inducible factor 1 α (HIF1 α) and it is reported to be involved in regulation of vascular endothelial growth factor (VEGF) transcription and in induction of oxygen related genes in response to hypoxia. EPAS1 is abundantly expressed in highly vascularized organs and was found to be involved in angiogenesis of different cell carcinomas (Maxwell, 2005, Takeda *et al*., 2004, Tian *et al*., 1997, Xia *et al*., 2001). Imtiyaz *et al* reported that mice lacking HIF 2a displayed a marked inability to mount an inflammatory response (Imtiyaz *et al*., 2010). Increased levels of HIF 2a can also upregulate the KSHV RTA promoter which results in production of RTA and lytic KSHV activation (Haque *et al*., 2003).

Some of the DEnGs identified in CLASH were found to have functions related to transcriptional repression. HIC1 (containing target sites for ovhv2-miR-7, -67 and -8 (Table 4.8) is an epigenetically regulated transcriptional repressor that cooperates with p53 to suppress cancer. The loss of HIC1 function promotes tumorigenesis via

activation of the stress-controlling protein SIRT1 and attenuates p53 function (Chen *et al*., 2005).

ZBTB7C has target sites for ovhv2-miR-7, -67 and -8 (Table 4.8) (also known as KR-POK) and is a zinc finger and BTB domain containing gene and might have a role in tumor suppression. ZBTB7C has been shown to regulate cell cycle and proliferation through the regulation of CDKN1A, a gene member of the p53 pathway. CDKN1A encodes the protein p21, which is a negative regulator of the cell cycle (Kim *et al*., 2013, Yoon *et al*., 2014). Targeting tumor suppressor genes might cause an increase in cell proliferation which is usually not observed in OvHV-2 lately infected sheep and may play a role in early infection.

TPT1, a translationally controlled tumor protein (TCTP), is a multifunctional protein, which is highly regulated during adaptation of cells to alterations in physiological conditions, such as growth induction, tumorigenesis, stress and apoptosis (Bommer *et al*., 2010). TPT1 was identified as a DEnGs in the CLASH dataset with a negative fold change indicating that the number of reads for the mRNA was higher in control samples than that of test samples. It is difficult to speculate why TPT1 expression is higher in the control samples. It has been reported that the levels of TPT1 decreases under stress conditions (Bommer *et al*., 2010, Li *et al*., 2013b). It is also possible that due to the inhibitory effect of ovhv2-miRs, cells undergo stress in test samples. It is possible that down-regulation of the expression of one transcript due to the interaction of ovhv2-miRs leads to the down-regulation of TPT1 in the test samples and this effect was not observed in control samples.

Two of the microarray-identified DEG were SEMA3A and SEMA3D which are classified as class-3 semaphorins and both have target sites for ovhv2-miR-7, -67 and -8 (Table 4.9). IPA analysis showed involvement of these genes in the semaphorin signalling pathway. Another semaphorin, SEMA5B, was found as a target of ovhv2-miR-67 in the T1 sample in the chimeras' dataset analysis (Table 4.14). Semaphorins are secreted, transmembrane proteins, defined by cysteine-rich semaphorin protein domains, that have important roles in a variety of tissues (Yazdani and Terman, 2006). Plexin are primary receptors for semaphorins and receptor ligand association leads to a cascade of events controlling cell adhesion, invasion, axon guidance, migration, angiogenesis, organogenesis and immune response. Some of the members of semaphoring including SEMA3A are also called as immune semaphorins and involve in immune cell interactions and immune cell trafficking during physiological and pathological immune responses (Takamatsu *et al*., 2010). Semaphorin signaling is deregulated in multiple cancers. Depending on the receptor complex and intracellular signal transducers, semaphorins can either promote tumorigenesis or inhibit it (Rehman and Tamagnone, 2013, Yazdani and Terman, 2006, Zhou *et al*., 2008). OvHV-2 also encodes a homologue of semaphorin gene; Ov3 (Hart *et al*., 2007). AlHV-1 A3 (AHV Sema) also has significant homology to the semaphorin gene (SEMA7A) which is a membrane-bound signalling protein found on activated lymphocytes (Ensser and Fleckenstein, 1995). So far, no precise role has been described for Ov3 and AHV Sema and these might be used to mimic certain semaphorin effects so as to evade the host immune response. RNAhybrid analysis showed the presence of target sites in the Ov3 transcript for ovhv2-miRs-7, -67 and -8. The interaction of ovhv2-miR-8 with the target site in Ov3 was canonical

(nucleotide 2-8) with perfect base pairing. It is possible that OvHV-2 regulate the expression of semaphorin using ovhv2-miRs to regulate cellular processes important for viral persistence.

One of the microarray identified DEG, PDE1A (containing target sites for ovhv2-miR-7, -67 and -8) is a cyclic nucleotide phosphodiesterase (PDE). PDE1A plays role in many signal transduction pathways and acts as one of the key regulators of physiological processes by catalysing the hydrolysis of cyclic Adenosine mono phosphate (cAMP). Canonical pathway analysis showed PDE1A was involved in three pathways; cAMP mediated signalling, G-protein coupled receptor signalling and Protein kinase A signalling. Crosstalk of these pathways is involved in many cell functions; G-protein coupled receptor signalling is involved in activation of cAMP as well as in cell proliferation, survival and motility, tumour induced angiogenesis and tumour matastasis (Dorsam and Gutkind, 2007). Protein kinase A (PKA) signalling is also dependent on cAMP for activation and is involved in phosphorylation of a large number of cellular proteins. By inhibiting PDE1A activity, the cAMP rises and causes an activation of PKA (Berridge, 2012, Houslay and Milligan, 1997).

The most down-regulated DEG in the microarray dataset, FTH1 has target sites for ovhv2-miR-8 (Table 4.9) was found to be the part of the NRF2 (Nuclear factor like 2)-mediated oxidative stress response pathway. Under oxidative stress NRF2 activates and binds to the antioxidant response element (ARE) in promoters of target genes involved in iron homeostasis and heme metabolism, such as FTH1 (Campbell *et al*., 2013). FTH1 and other ferritin heavy chain subunits are also involved in

different biological events such as cell differentiation and pathologic states such as cancer (Di Sanzo *et al*., 2011).

Other microarray identified DEG include; VLDLR (containing target sites for ovhv2-miR-67 and -8) which is a member of a family of cell surface proteins involved in receptor-mediated endocytosis of specific ligands (D'Arcangelo *et al*., 1999). ITGA8 (containing target sites for ovhv2-miR-7, -67 and -8) which belongs to a class of integrins and play roles in cell to cell and cell to extracellular matrix interactions (Schnapp *et al*., 1995).

ENPP2 (has target sites for ovhv2-miR-7, -67 and -8) which is also refered to autotaxin (ATX) is a secreted enzyme with both phosphodiesterase and phospholipase activity. ENPP2 can generate higher levels of lysophosphatidic acid (LPA) in different cancers. ENPP2 stimulates the motility of tumor cells and has angiogenic properties, and its expression is up-regulated in several kinds of carcinomas (Houben and Moolenaar, 2011, Wu *et al*., 2014). Specific down-regulation of ENPP2 reduces cell growth and viability. Baumforth *et al* reported that EBV infection of Hodgkin lymphoma (HL) cells leads to the induction of autotaxin which results in an increased generation of LPA and enhances the proliferation and survival of HL cells (Baumforth *et al*., 2005).

Taken as a whole these results indicate that many of the genes identified in three datasets (chimeras, DEnGs from CLASH single read and DEG from microarray) are involved in regulation of biological processes related to transcription, cell growth and proliferation, differentiation, angiogenesis, immune evasion and tumour related biological processes. It is a real possibility that some of these genes are true targets

of ovhv2-miRs. By targeting those genes OvHV-2 might fulfil the goal of remaining latent in the sheep cells. OvHV-2 also needs the host cell for longer to complete its lifecycle which can be achieved by helping the cell to survive longer and evade the immune system, by targeting the genes which can promote replication.

In this study CLASH was successfully used to identify OvHV-2 encoded miRNAs targets in bovine and ovine transcripts. A large number of transcripts were found as potential targets. The proteins of those transcripts have potential functions which hypothetically and theoretically relate to the involvement of those proteins in MCF pathology and virus-host interactions. However, there is no experimental evidence to prove their involvement and further investigations are required. In this study four of the CLASH identified potential targets were experimentally validated. One of the bovine targets; U2 and one of the sheep target DLL1 were successfully validated by luciferase assays. Due to time constraints it was not possible to further validate those using knockout/mutagenic experiments. Further investigation of DLL1 is being carried out, in the lab which has also shown it to be a potential target of ovhv2-miR-67. Some of the CLASH identified bovine or sheep genes in this study, might be involved in regulation of MCF pathology in bovine and sheep but before hypotheses about ovhv2-miRs regulation can be made, functional analysis is required, and that work is continuing.

Chapter 5: Conclusion

MCF occurs as a result of infection of susceptible hosts such as cattle or deer through contact with an asymptomatic carrier species, e.g sheep, that acts as a virus reservoir. Infection of susceptible species by OvHV-2, the causative agent of sheep-associated MCF, results in a fatal lymphoproliferative disease that involves marked T cell hyperplasia with infiltration of infected T cells, described as LGLs, which are virus genome positive. It has been proposed that MCF lesion development occurs not due to virus cytopathology but due to non-antigen specific, unrestricted NK like activity of virus infected LGLs (Cook and Splitter, 1988). In cattle and sheep, all virus infected lymphocytes express CD2 and variably express CD4 and CD8 (Meier-Trummer *et al*., 2010). Thus, in both cattle and sheep similar set of cells are infected by the virus but only in cattle does dysregulation of the T cells lead to development of the characteristic MCF lesions.

Analysis of the genome of OvHV-2 has shown that it encodes 35 miRNAs (Levy *et al*., 2012, Nightingale *et al*., 2014). It has been proposed that these ovhv2-miRs might interact differently with bovine and ovine genes resulting in a different disease outcome in the two closely related species. This project was designed to identify and functionally validate the targets for ovhv2-miRs in virus, cattle and sheep transcripts.

Using Blastn, a number of viral targets were predicted for eight, northern blot validated ovhv2-miRs (Levy PhD thesis, 2012). Six of the viral genes were identified as having potential targets for viral miRNAs in their 5' and 3' UTR. Based on homology with other herpesviruses, the proteins encoded by these ORFs would be expected to play a functional role in virus latency, replication, cell cycle regulation or reactivation from latency, were selected for study (Section 3.2). Three of the ORFs,

ORF20 (cell cycle control), ORF50 (reactivation) and ORF73 (viral latency), were shown to be regulated by ovhv2-miRs. To further investigate the regulation of these OvHV-2 ORFs by the ovhv2-miRs, a RT-qPCR assay was developed for the ORF20, ORF50 and ORF73 transcripts. The results show that following transfection with the relevant miRNA mimic a significant reduction in the levels of ORF50 transcripts could be observed, within the BJ1035 LGL cell-line (Riaz *et al*., 2014). Utilizing the same approach, a smaller but non-significant decrease in ORF20 mRNA levels was found, however no decrease was observed in the level of the ORF73 transcript (Riaz *et al*., 2014). A number of possible factors may address why the transfection of the BJ1035 cell-line with the mimics targeting either ORF20 or ORF73 did not reproduce the result observed *in vitro* using the luciferase- reporter gene system (Section 3.3). Firstly, BJ1035 are not a homogeneous population, so the significant variation in transcript expression between biological replicates (Dr I.Dry, Personal Communication) could overwhelm any subtle effect. Additional concerns that may also have impacted the results include the transfection efficiency of the BJ1035 cells or the concentration of miRNA mimics used.

In this study, the targets of eight validated ovhv2-miRs were analysed. It is worth to analyse remaining 25 miRNAs, using the similar approach may reveal more targets for future studies. The transfection of LGLs as an *in vitro* system has its limitations. Further work needs to be carried out to see if it can be improved as an *in vitro* biological assay for miRNA function. However it is a valuable tool in the arsenal of OvHV-2 virologists.

To identify bovine and ovine targets which formed chimeras with ovhv2-miRs, a new and highly sensitive approach, CLASH was used.

The BJ1035 cell line expresses all of the 35 ovhv2-miRs (Levy *et al*., 2012, Nightingale *et al*., 2014). The CLASH approach provided a snapshot of mRNAs targeted by ovhv2-miRs. The cellular RNAs which formed chimeras, were shown to be involved in biological pathways such as pre-mRNA splicing, cell cycle and immune system regulation (Section 4.5.1).

U2, a component of major spliceosome complex was found as a target of ovhv2-miR-36 and successfully validated using a luciferase reporter gene assay (4.3.3.2.2). Other components of the spliceosomal complex (CSTF3 and SNRNP25) were also found as predicted targets. The targeting of components of spliceosomal complex could indicate a viral strategy to interfere in pre-mRNA processing and hence shut off host protein expression or alter splicing to reduce the expression of specific transcript variants in the natural host. Herpesviruses have been shown to either interact with host cell pre-mRNA splicing (in HSV-1) or promote their own intronless mRNA splicing (in KSHV) (Bryant *et al*., 2001, Majerciak *et al*., 2008). Further investigation including luciferase assays or RT-qPCR assay using miRNA mimics to observe reduction in the levels of the luciferase or targeted transcripts respectively is necessary to understand the role of these targets in virus biology and pathology.

Recent miRNA target recognition studies have found many functional targets which interact with their targeting miRNAs in regions of the miRNAs other than seed region (Helwak *et al*., 2013, Shin *et al*., 2010). In this study, I predict that miR-217M

interacts with ATP6V1B1 non-canonically. ATP6V1B1 is a component of V-ATPase complex and mainly functions as an acidifier in internal membrane system such as lysozymes and endosomes (Ohta *et al*., 1996). V-ATPases also play important roles in other cellular processes including endocytosis, membrane trafficking, apoptosis and the immune system (Benaroch *et al*., 1995, Morimura *et al*., 2008). In HCMV, another component of the V-ATPase complex; ATP6V0C was recently shown to be a target of a HCMV encoded miRNA US25-1. Subsequent investigation showed that ATP6V0C was an essential factor in HCMV replication and control of the expression of ATP6V0C by this via viral-encoded miRNA might be important in establishing or maintaining viral latency (Pavelin *et al*., 2013).

Unlike BJ1035 cells, sheep embryo fibroblasts do not express ovhv2-miRs and so a lentivirus expressing three of the ovhv2-miRs (miR-7, miR-67, miR-8) was constructed and used. Three datasets were analysed for the identification of the targets; Chimeras obtained from test samples using CLASH, differentially enriched genes (DEnGs) obtained from test and control samples using CLASH and differentially expressed genes (DEG) obtained from the test and control samples using microarray. The CLASH and the microarray comparison did not identify any common genes (Section 4.3.2.10) possibly because CLASH involves the enrichment of genes targeted by miRNAs while microarray involves changes in the overall expression of genes, affected directly and indirectly by the targeting of the miRNAs. A number of genes were identified in the CLASH and microarray datasets. The identified genes are associated functionally in the regulation of transcription, cell

proliferation and survival, cell cycle, differentiation, apoptosis and immune evasion (Section 4.4.2).

DLL1, a part of the Notch signalling pathway, was found to be a target of miR-67 (Section 4.3.3.4.1). DLL1 is a ligand for Notch receptors and binding of these receptors to DLL1 activates Notch. The Notch signalling pathway plays a critical role in the regulation of the differentiation of lymphocytes. Notch signalling blocks the differentiation of progenitor cells into B-cell lineage and promotes the emergence of T-cells/NK cells precursors (Jaleco *et al*., 2001). OvHV-2 causes a lymphoproliferation or cytotoxicity in cattle but not in sheep. It is possible that miR-67 targets DLL1 in sheep cells and might inhibit the Notch signalling thereby stopping lymphocyte differentiation and maintaining viral latency. Work currently ongoing in the lab is focused on investigating whether the regulation of DLL1 by ovhv2-miRs differs between susceptible species and the natural host.

Three semaphorins; SEMA3A, SEMA3D and SEMA5B were identified as putative ovine targets in this study. Semaphorins are secreted, transmembrane proteins that have important roles in a variety of cell processes such as cell adhesion, cell migration. SEMA3A is among the semaphorins that are also called immune semaphorins due to their roles in immune cell interaction and movement during physiological and pathological immune responses (Takamatsu *et al*., 2010). OvHV-2 and AlHV-1 both encodes genes, Ov3 and A3 respectively which have significant homology with semaphorins (Ensser and Fleckenstein, 1995, Hart *et al*., 2007). No precise role of the viral semaphorins has been described yet. One possibility is that these viral semaphorin homologues might mimic certain functions of the cellular

semaphorins that are required for viral persistence. The encoding of a cellular homologue would thus enable the virus to use ovhv2-miRs to regulate the expression of the cellular semaphorins thereby inhibiting any anti-viral functions that they may have, without impacting the viruses own long-term persistence.

In summary, we have shown that ovhv2-miRs have targets within viral and host transcripts. Viral targets of ovhv2-miRs are involved in both in maintaining viral latency and potentially in reactivating the virus from latency. Our analysis also showed that a number of sheep and cattle genes, are targets of ovhv2-miRs. Due to time constraints it was not possible to validate all of the genes identified in the CLASH experiments. No common genes were found between the datasets of the susceptible and natural hosts, which may indicate that ovhv2-miRs might play different roles in susceptible and natural hosts. Further investigation on the role of ovhv2-miRs in the regulation of genes in susceptible and host species may increase our understanding towards the different disease outcomes and in the long-term may help develop treatments for this disease.

Appendix-1: Recipes

LB Broth	5 g yeast extract
	10g peptone from casein
	10g sodium chloride
	12g agar-agar
``	up to 1 L water.
Phosphate-buffered saline (PBS) (pH7.4)	8g NaCl
	0.2g KCl
	1.44g $Na_2H_2PO_4$
	0.24g KH_2PO_4
	Up to 1 L water
1 x TAE Buffer	40mM TRIS -acetate
	1mM EDTA (pH 8.0)
Semi Dry Transfer Buffer	3g TRIS base
	11.3g glycine
	100 ml methanol
	Up to 1L water
1 x TBS Buffer	100mM TRIS base
	0.9 % NaCl (v/v)
	pH 7.5

1 x TBST Buffer	100mM TRIS base 0.9 % NaCl (v/v) 0.1 % Tween 20 pH 7.5
0.1M Sodium Phosphate Buffer	2.62g NaH_2PO_4 14.42gm Na_2HPO_4 Up to 1 L water pH 7.4
3M Ammonium Sulfate	39.6g $(NH_4)_2SO_4$ Dissolved in 100 ml 0.1M sodium phosphate buffer
PBS+ 0.5% Triton X-100	0.5% (W/v) Triton X-100 in 100 ml of PBS
0.1M Glycin HCl	7.5g Glycin Up to 1 L water HCl to adjust pH 2.5
100mM Triethylamine	168µl of Triethylamine 11.156ml water
PBS/0.02% Sodium azide	0.1g sodium azide 500 ml PBS

CLASH Lysis Buffer	2.5ml 1M TRIS (pH 7.5)
	3ml 5M NaCl
	5ml 10% NP-40
	0.5ml 1mM EDTA
	10 ml 50% glycerol
	25µl 2-mercaptoethanol (added fresh)
	Up to 50 ml water
5 x PNK buffer	62.5ml 1M TRIS-HCl (pH 7.5)
	1.19g $MgCL_2$
	62.5ml 10% NP-40
	12.5ml 5M NaCl
	5mM 2 Mercaptoethanol (added fresh)
	Up to 250 ml water
1 x PNK_5 buffer	10 ml 5 x PNK buffer (without 2Mercaptoethanol)
	5mM 2 Mercaptoethanol (added fresh)
	Up to 40 ml water
1 x PNK_{10} buffer	10 ml 5 x PNK buffer (without 2Mercaptoethanol)
	10mM 2 Mercaptoethanol (added fresh)
	Up to 40 ml water
Ni-EB 200 buffer	0.5 ml 1M TRIS-HCl (pH7.8)

0.1 ml 5M NaCl

2ml 1M Imidazole

0.1ml 10% NP-40

5mM 2Mercaptoethanol (added fresh)

Up to 10 ml water

HS-IgG-WB buffer

2.5ml 1M TRIS-HCl (pH 7.5)

8ml 5M NaCl

1ml 0.5M $MgCl_2$

2.5ml 10% NP-40

2.5ml glycerol

5mM 2Mercaptoethanol (added fresh)

Up to 50 ml water

LS-IgG-WB buffer

2.5ml 1M TRIS-HCl (pH 7.5)

3ml 5M NaCl

0.5ml 0.5M $MgCl_2$

2.5ml 10% NP-40

2.5ml glycerol

5mM 2Mercaptoethanol (added fresh)

Up to 50 ml water

Ni-WB-I buffer

2.5ml 1M TRIS-HCl (pH7.8)

3ml 5M NaCl

0.5ml 1M Imidazole

28.66g Guanidine-HCl

0.5ml 10% NP-40

5mM 2Mercaptoethanol (added fresh)

Up to 50 ml water

Ni-WB-II buffer

2.5ml 1M TRIS-HCl (pH7.8)

3ml 5M NaCl

0.5ml 1M Imidazole

0.5ml 10% NP-40

5mM 2Mercaptoethanol (added fresh)

Up to 50 ml water

Proteinase K mix:

2.5 ml 1M Tris-HCl
0.5ml 50mM NaCl
0.5 ml 10mM imidazole
0.5 ml 0.1% NP-40

5 ml 1% SDS
0.5 ml 5mM EDTA
5mM 2Mercaptoethanol (added fresh)

Up to 50 ml water

2 x Protein Sample buffer

0.9 ml 10%SDS

0.45 ml 100% Glycerol

0.27 ml 1M Tris-HCl pH 6.8

0.05 g Bromophenol blue

0.25 ml 2-Mercaptoethanol

Up to 2ml water

1 x Protein Sample buffer	0.5 ml of 2 x Protein sample buffer
	0.5 ml water
10% Protein resolving gel	1.65 ml 30% acrylamide/0.8%bis
	1.25 ml 1.5M Tris-HCl pH 8.7
	50 µl 10% SDS
	50 µl 10% Ammonium persulfate
	5 µl TEMED
	2.01 ml water
Stacking gel	500 µl 30% acrylamide/0.8%bis
	625 µl 1M Tris-HCl pH 6.8
	50 µl 10% SDS
	25 µl 10% Ammonium persulfate
	5 µl TEMED
	3.12 ml water
10 x SDS Running buffer	30.2 g Tris-base
	180g Glycine
	10g SDS
	Up to 1L water
1 x Protein Transfer buffer	2.47g Tris-base
	11.54g Glycine
	200 ml Methanol
	Up to 1L water

1M Sodium Phosphate buffer

142g Na_2HPO_4

up to 1L water

Orthophosphoric acid to pH 7.2

Annealing buffer 10X

1 ml 1M Tris (pH 7.6)

500 µl 1M $MgCl_2$

500 µl 5M NaCl

3 ml water

Appendix-2: Vectors and Plasmids

PCR4-TOPO

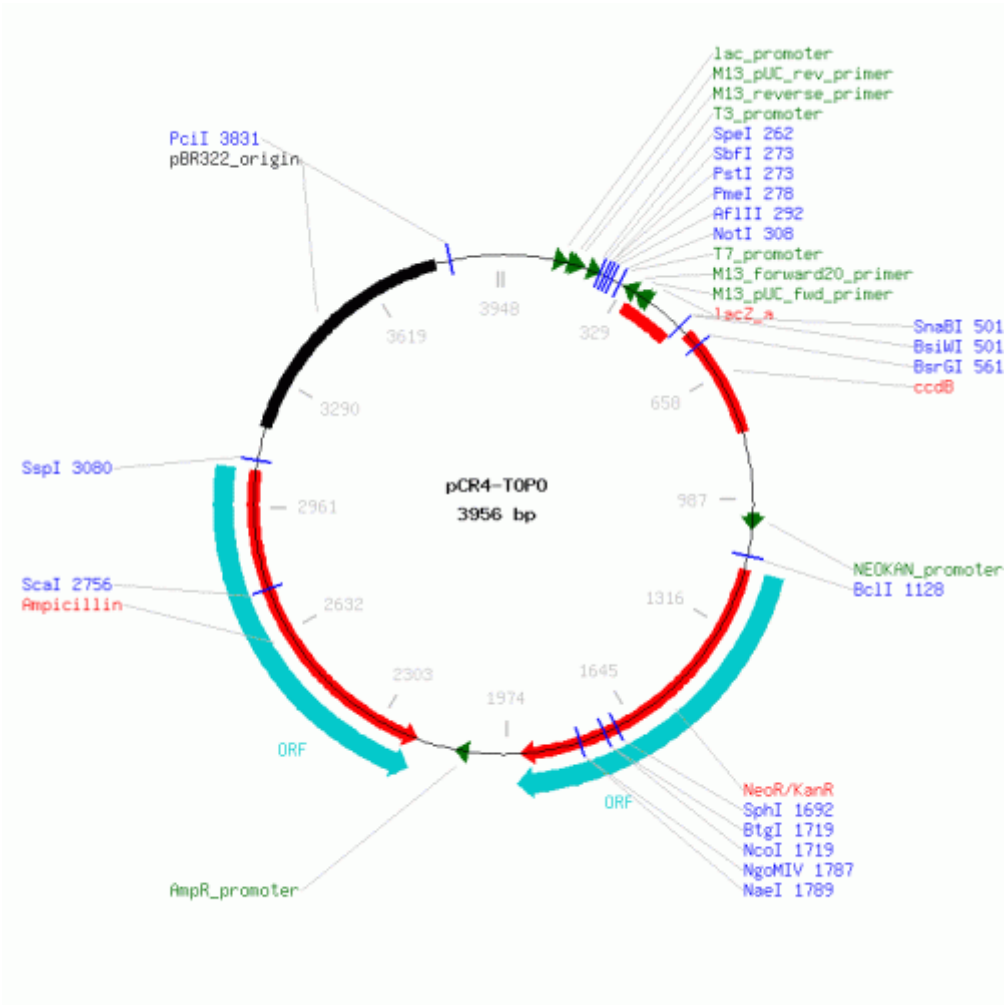

psiCHECK™-2 Vector

.

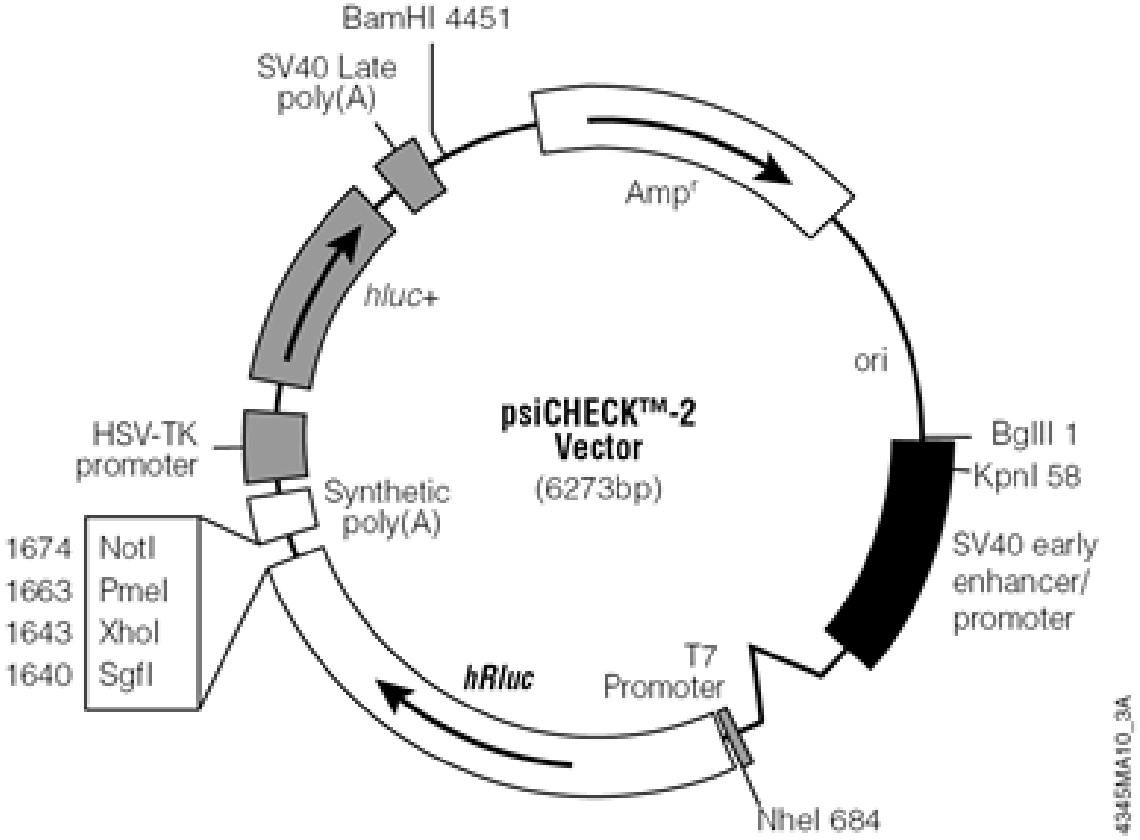

pGL4.10(luc2) vector

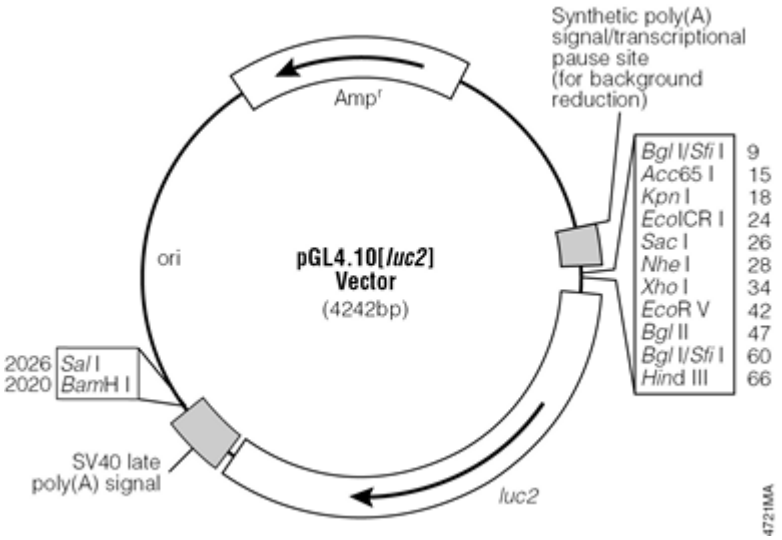

PRL-SV40 Vector

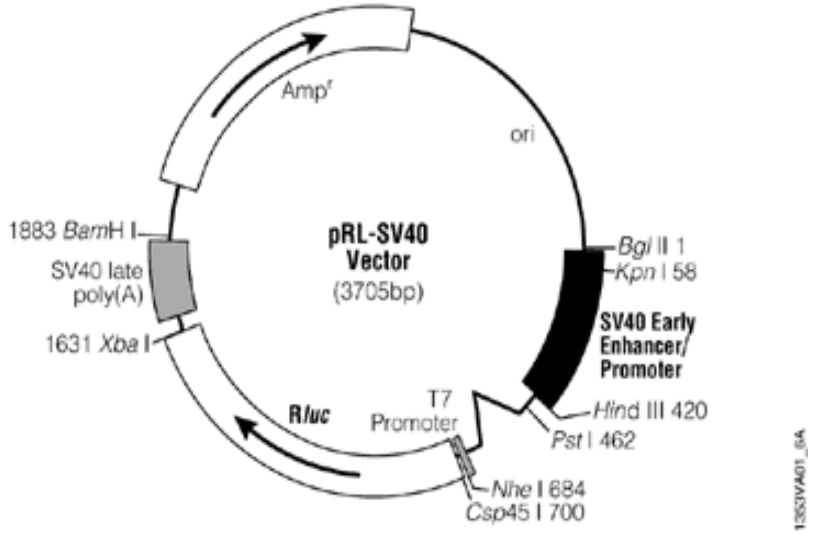

pLenti CMV Blast Empty

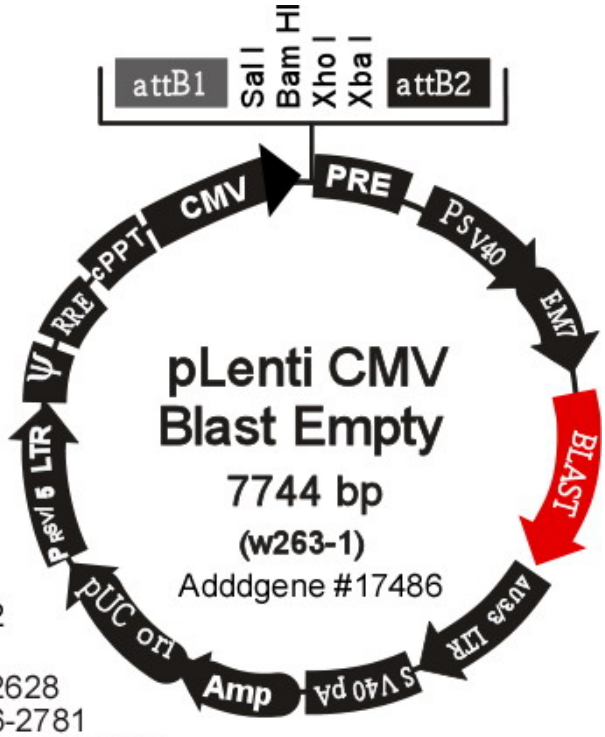

comments for pLenti CMV Blast Empty
7744 nucleotides

bla promoter: bases 32-131
ampicillin resistance gene: bases 132-982
pUC origin: bases 1138-1810
RSV/5'LTR hybrid promoter: bases 2218-2628
HIV-1 psi (ψ)packaging signal: bases 2736-2781
HIV-1 Rev response element (RRE): bases 3272-3525
3' splice acceptor: base 3862
3' splice acceptor: base 3901
Central polypurine tract (cPPT): bases 4011-4073
CMV promoter: bases 4145-4730
attB1 site: bases 4764-4788
Multiple cloning site (MCS): bases 4809-4857
*att*B2 site: bases 4857-4881
Woodchuck post-transcriptional element (PRE): bases 4911-5504
SV40 early promoter and origin: bases 5568-5930
EM7 promoter: bases 5934-5999
Blasticidin resistance gene: bases 6000-6398
ΔU3/3'LTR: bases 6486-6718
SV40 polyadenylation signal: bases 6789-6942

PLVX-Tight-Puro Vector

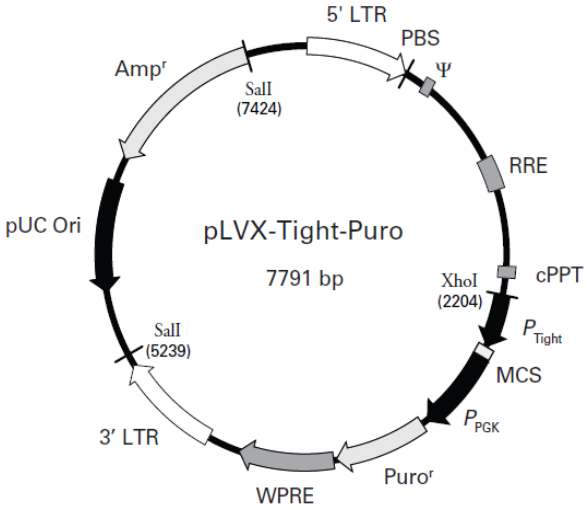

BamHI MluI
NotI XbaI* EcoRI

```
2521  TGGAGAAGGA TCCGCGGCCG CGCCGGCTCT AGATCGCGAA CGCGTGAATT CTACCGGGTA
      ACCTCTTCCT AGGCGCCGGC GCGGCCGAGA TCTAGCGCTT GCGCACTTAA GATGGCCCAT
```

Xba I site (*) is methylated in the DNA provided by Clontech Laboratories, Inc. If you wish to digest the vector with Xba I enzyme, you will need to transform the vector into a dam- host and make fresh DNA.

pLVX-Tight-Puro Vector Map and Multiple Cloning Site (MCS).

PLVX AGO2 Vector

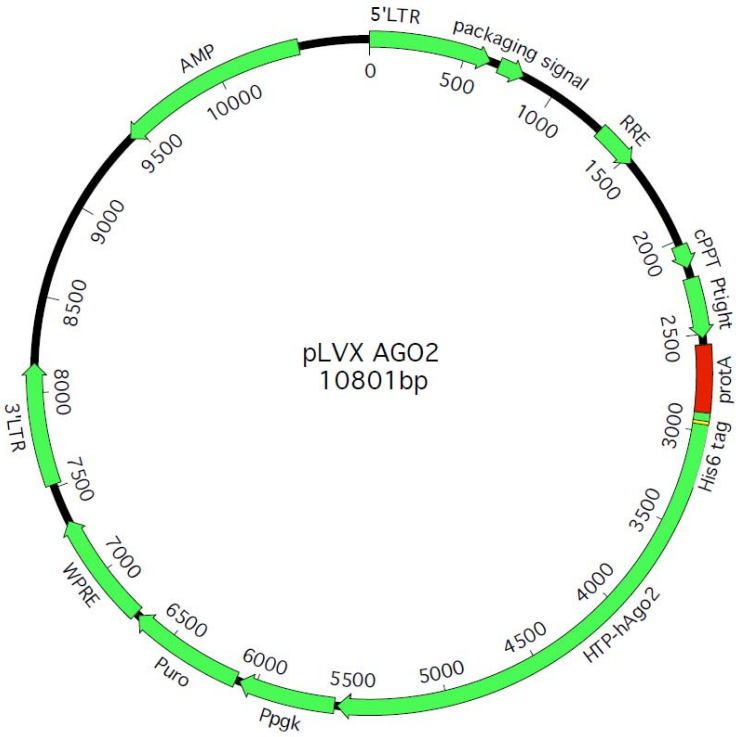

Appendix-3 Primers, miRNA mimics, Linkers and barcode sequences

PCR Primers	Sequence
LUC/3'-Ov2-Forward	5`-AACTCGAGGAGATGTGAGTTAAACCC- 3' XhoI
LUC/3'-Ov2-Reverse	5'-AAGCGGCCGCGGTAAAAGGCATGTAGTG-3' NotI
LUC/3'-20-Forward	5`-AACTCGAGACAACATAGTCCAGGCAAACA-3' XhoI
LUC/3'-20-Reverse	5`-AAGCGGCCGCCACCCCTGGCTGGACTAT-3' NotI
LUC/3'-36-Forward	5`-AACTCGAGCCTGGAGCAGACCATAAC -3' XhoI
LUC/3'-36-Reverse	5'-AAGCGGCCGCGTCTTGGGAAAATCAGCAG-3' NotI
LUC/3'-49-Forward	5'-AACTCGAGCAAACGGCAAAGCAGCTT-3' XhoI
LUC/3'-49-Reverse	5'-AAGCGGCCGCACATTCAGGGCAGGTTAC-3' NotI
LUC/3'-50-Forward	5'-AACTCGAGCTCCTCAGGGTTTCAGT-3' XhoI
LUC/3'-50-Reverse	5'-AAGCGGCCGCAGGGGGTTAAAGTGCTC-3' NotI
LUC/3'-73-Forward	5`-AACTCGAGGATACAAGCTAAGTACTGC-3` XhoI
LUC/3'-73-Reverse	5`-AAGCGGCCGCTACAGAAGCACACAGTATC-3` NotI
LUC/5'-20-Forward	5'-AACTCGAGCTGTCGCACACAACCCATC-3' XhoI
LUC/5'-20-Reverse	5'-AAAGATCTGGCCTCCAACTCTCCCTCTC- 3' BglII
LUC/5'-73- Forward	5'-AACTCGAGCTTACTCCCTTTACTCTGG-3' XhoI
LUC/5'-73-Reverse	5'-AATTCGAA TTTGTAGCTTTACTGCCTG-3' HindIII
Cluster-2-Forward	5'-AAGTCGACGACTCCAAAGAATGAATCACGC-3' SalI
Cluster-2-Reverse	5'-AAGTCGACCAGCTTTACGTGTGGCGGTC-3' SalI
Cluster-3-Forward	5'-AA CTCGAG GGTCATGACTCAGTTTGTT-3' XhoI
Cluster-3-Reverse	5'-AATCTAGACTGAAGTTCTTTGTTTGTGTC-3' XbaI
Sequencing primers	
TOPO Forward	5'-GTAAAACGACGGGCCAG-3'
TOPO Reverse	5'-CAGGAAAACAGCTATGAC-3'
psiCHECK Forward	5'-TGCTGAAGAACGAGCAGTAA-3'
psiCHECK Reverse	5'-CGAGGTCCGAAGACTCATTT-3'
pGL4-Primer Forward	5'-CTAGCAAAATAGGCTGTCCC-3'
pGL4-Primer Reverse	5'-GACGATAGTCATGCCCCGCG-3'
PLenti-Forward	5'-GCAGATATCAACAAGTTTGTAC-3'
PLenti-Reverse	5'-CACTGTGCTGGATATCAA-3'

Mutagenic primers	
LUC/3'-50-M-Forward	5'-CCCAGAAATGTGACAT GGCGCGCC CTTTTTTACTTGTGGTTTG-3' AscI
LUC/3'-50-M-Reverse	5'-CAAACCACAAGTAAAAAAG GGCGCGCC ATGTCACATTTCTGGG-3 AscI
LUC/5'-20-M-Forward	5'-CACTGTTGTCCTCCTCGTTTAAACTTGGGCACGTCGTAGTCG-3' PmeI
LUC/5'-20-M-Reverse	5'-CGACTACGACGTGCCCAAGTTTAAACGAGGAGGACAACAGTG-3' PmeI
LUC/5'-73-M1-Forward	5'CCCGACATCCCGGGACGTTTAAACGCAGCCGTCTGAGCCTTTTC 3' PmeI
LUC/5'-73-M1-Reverse	5'GAAAAGGCTCAGACGGCTGCGTTTAAACGTCCCGGGATGTCGGG 3' PmeI
LUC/5'-73-M2-Forward	5'-CCTGAGCCTGCAGCCGTGTTTAAACTTTCTAAAAATTATGCCTTC-3' PmeI
LUC/5'-73-M2--Reverse	5'-GAAGGCATAATTTTTAGAAAGTTTAAACACGGCTGCAGGCTCAGG-3' PmeI
LUC/5'-73-M1-M2-Forward	5'CGTTTAAACGCAGCCGTCCTGCAGGTTTCTAAAAGTTATGC-3' PmeI SbfI
LUC/5'-73-M1-M2-Reverese	5'-GCATAACTTTTAGAAACCTGCAGGACGGCTGCGTTTAAACG-3' SbfI PmeI
Annealing primers	
LUC/U2-Forward (XhoI and Not1)	5'CTCGAGCAGGGAGTTGGAATGGGAGCTTGCTCCGTCCACTCCACGCAT CGACCTGGTATTGCAGTACTTCCAGGAACGGTGCACCAAAGCGGCCGC-3'
LUC/U2-Reverse (NotI and XhoI)	5'GCGGCCGCTTTGGTGCACCGTTCCTGGAAGTACTGCAATACCAGGTCG ATGCGTGGAGTGGACGGAGCAAGCTCCCATTCCAACTCCCTGCTCGAG-3'
LUC/TM6SF1-Forward (XhoI and Not1)	5'CTCGAGCTGCTTTTTTCTTAAGCATACCATATACTTGTCTTCCTGTCTGG GCTGGTTTCAGAATCTATAATCAGCCATCAGAAAATTATAATTAGCGGCC GC-3'
LUC/TM6SF1-Reverse (NotI and XhoI)	5'GCGGCCGCTAATTATAATTTTCTGATGGCTGATTATAGATTCTGAAACC AGCCCAGACAGGAAGACAAGTATATGGTATGCTTAAGAAAAAAGCAGCT CGAG-3'
LUC/DLL1-Forward (XhoI and Not1)	5'CTCGAGGAGGACAGGCTGGGAAGGGGGGCCTTCCCGGGGAGGGCGCC CCGACACCCGGGGGATGGGCAGGACAGGCTGGGCAGGGGGGCCTTCCCG CGGCCGC-3'
LUC/DLL1-Reverse (NotI and XhoI)	5'GCGGCCGCGGGAAGGCCCCCCTGCCCAGCCTGTCCTGCCCATCCCCCG GGTGTCGGGGCGCCCTCCCCGGGAAGGCCCCCCTTCCCAGCCTGTCCTCC TCGAG-3'
LUC/VWA-Forward (XhoI and Not1)	5'CTCGAGCACTCTAAAGGTCATGCCCGGAGGTCCTGGCTCCGAGCCCTTC AGACAAGTAAGGTCAGCTCTGCCCCTTCTCGCTTCACCTGTCCGCGGCCG C-3'
LUC/VWA-Reverse ((NotI and XhoI)	5'GCGGCCGCGGACAGGTGAAGCGAGAAGGGGCAGAGCTGACCTTACTT

	GTCTGAAGGGCTCGGAGCCAGGACCTCCGGGCATGACCTTTAGAGTGCTCGAG-3’
RT-qPCR primers (Forward)	
Ovhv2-miR-2	5’-ATCTTGGACGCATCTGT-3’
Ovhv2-miR-41	5’-ATACACACTGAAAGA-3’
Ovhv2-miR-43	5’-AAGCACCTTGGGTGATGTC-3’
Ovhv2-miR-3	5’-TCTGTATCATAGGGGTT-3’
Ovhv2-miR-62	5’-CCTTTTTGGTGAGTTGC-3’
Ovhv2-miR-63	5’-GATTTGATAAAGCCTGC-3’
Ovhv2-miR-7	5’AAGGCGCATCATAGACAC-3’
Ovhv2-miR-67	5’-ACCCCGGGGGTATGTG-3’
Ovhv2-miR-8	5’-TGGCTCAGCGTGACTG-3’
miR-16	5’-TAGCAGCACGTAAATA-3’
Ovhv2-miR Mimic sequence	
Ovhv2-miR-2	5’-AUCUUGGACGCAUCUGUCAGUAG-3’
Ovhv2-miR-4	5’-AAGGAUCCUUAAGUGACGAACG-3’
Ovhv2-miR-5	5’-UGAAGUUACAGCUGCACCUGGAU-3’
Ovhv2-miR-6	5’-UAUUUUUAGCGGAGACCUCUAGG-3’
Ovhv2-miR-7	5’-GAAGGCGCAUCAUAGACACCACUUC-3’
Ovhv2-miR-8	5’-UGGCUCAGCGUGACUGCUCUUC-3’
Ovhv2-miR-36	5’-UCUAGGUUGCAUUUUGCUGUAG-3’
Ovhv2-miR-67	5’-ACCCCGGGGGUAUGUGCAGGAC-3’
Mir-m23-2	5’-AUGGGGGCCUCGGUCAAGCGG-3’
CLASH linkers and primers	
3’Linker (miRCat linker-33)	AppTGGAATTCTCGGGTGCCAAG/ddC/
5’Linker	invddT-ACACrGrArCrGrCrUrCrUrUrCrCr GrArUrCrUrXrXrXrXrXrArGrC (where X indicate the barcode)
Barcodes	
BJ1035-sample	NNNGTGAGC
SEF-control-1	NNNTAAGC
SEF-control-2	NNNATTAGC
SEF-control-3	NNNTCTCTAGC
SEF-Test-1	NNNGCGCAGC
SEF-Test-2	NNNAGAGC
SEF-Test-3	NNNCACTAGC
PCR primers	
miRcat-33 primer	5’-CCTTGGCACCCGAGAATT-3’
P5 Forward (library amplification)	5’AATGATACGGCGACCACCGAGATCTACACTCTTTCCCTACACGACGCTCTTCCGATCT -3’
PE-miRCat-Reverse (library amplification)	5’CAAGCAGAAGACGGCATACGAGATCGGTCTCGGCATTCCTGGCCTTGGCACCCGAGAATTCC-3’

Appendix-4: Publication

Journal of General Virology (2014), **95**, 472–480 DOI 10.1099/vir.0.059303-0

Ovine herpesvirus-2-encoded microRNAs target virus genes involved in virus latency

Aayesha Riaz, Inga Dry, Claire S. Levy,† John Hopkins, Finn Grey, Darren J. Shaw and Robert G. Dalziel

The Roslin Institute & Royal (Dick) School of Veterinary Studies, University of Edinburgh, Easter Bush Veterinary Campus, Roslin, Midlothian EH25 9RG, UK

Correspondence
Robert G. Dalziel
bob.dalziel@ed.ac.uk

Herpesviruses encode microRNAs (miRNAs) that target both virus and host genes; however, their role in herpesvirus biology is understood poorly. We identified previously eight miRNAs encoded by ovine herpesvirus-2 (OvHV-2), the causative agent of malignant catarrhal fever (MCF), and have now investigated the role of these miRNAs in regulating expression of OvHV-2 genes that play important roles in virus biology. ORF20 (cell cycle inhibition), ORF50 (reactivation) and ORF73 (latency maintenance) each contain predicted targets for several OvHV-2 miRNAs. Co-transfection of miRNA mimics with luciferase reporter constructs containing the predicted targets showed the 5′ UTRs of ORF20 and ORF73 contain functional targets for ovhv-miR-2 and ovhv2-miR-8, respectively, and the 3′ UTR of ORF50 contains a functional target for ovhv2-miR-5. Transfection of BJ1035 cells (an OvHV-2-infected bovine T-cell line) with the relevant miRNA mimic resulted in a significant decrease in ORF50 and a smaller but non-significant decrease in ORF20. However, we were unable to demonstrate a decrease in ORF73. MCF is a disease of dysregulated lymphocyte proliferation; miRNA inhibition of ORF20 expression may play a role in this aberrant lymphocyte proliferation. The proteins encoded by ORF50 and ORF73 play opposing roles in latency. It has been hypothesized that miRNA-induced inhibition of virus genes acts to ensure that fluctuations in virus mRNA levels do not result in reactivation under conditions that are unfavourable for viral replication and our data supported this hypothesis.

Received 9 September 2013
Accepted 29 October 2013

INTRODUCTION

Malignant catarrhal fever (MCF) is a fatal disease of cattle and other ruminants caused by viruses in the genus *Macavirus* of the subfamily *Gammaherpesvirinae* (Russell *et al.*, 2009). The disease occurs as a result of infection of susceptible hosts by contact with an asymptomatic carrier species that acts as a virus reservoir. Ovine herpesvirus-2 (OvHV-2) infects most sheep subclinically and is the major cause of MCF worldwide (Russell *et al.*, 2009). In both sheep and cattle, OvHV-2 infects $CD2^+$ T-lymphocytes (Meier-Trummer *et al.*, 2010; Schock *et al.*, 1998), but only in cattle does virus infection cause dysregulation of lymphoid cell function leading to uncontrolled proliferation, cytotoxicity and MCF disease. The proliferation of infected bovine T-cells is dependent on the cytokine IL-2 and immortalized T-cell lines can be cultured from affected cattle. The infected bovine T-cells do not support productive virus replication and have been described as large granular lymphocytes (LGLs) (Reid *et al.*, 1989) in part due to expression of perforin (Nelson *et al.*, 2010); unlike sheep, infected cattle cannot transmit the virus to other susceptible hosts (Russell *et al.*, 2009). The mechanism by which OvHV-2 induces MCF in cattle is unknown; virus-induced cytopathology is thought not to be involved in lesion development and it has been proposed that tissue damage arises from non-antigen-specific, MHC-unrestricted cytotoxicity of the virus-infected LGLs (Cook & Splitter, 1988).

MicroRNAs (miRNAs) are short (21–23 nt) RNAs that act as post-transcriptional inhibitors of gene expression. Cellular miRNAs expressed in the nucleus are derived from primary transcripts (pri-miRNAs) that are processed by the enzyme Drosha to form a shorter precursor miRNA (pre-miRNA). These pre-miRNAs are exported from the nucleus and once in the cytoplasm are further cleaved by the enzyme Dicer to produce a transient double-stranded precursor, where one strand is designated the miRNA or guide strand and the complementary strand is designated the miRNA* or passenger strand. The miRNA is incorporated stably into the RNA-induced silencing complex and guides it to the target mRNA, which represses translation by a number of mechanisms, including mRNA degradation and inhibition of translation. The interaction of miRNAs

†Present address: The Scripps Research Institute, 10550 North Torrey Pines Road, BCC-239, La Jolla, CA 92037, USA.

One supplementary table is available with the online version of this paper.

with target mRNAs is mediated by a seed region, nt 2–7 or 2–8 at the 5′ end of the miRNA (Bartel, 2009). Most miRNA targets identified to date are present in the 3′ UTR of mRNAs; however, some miRNAs have been reported that functionally target the 5′ UTR (Grey *et al.*, 2010; Tay *et al.*, 2008).

To date, >250 virus-encoded miRNAs have been identified, the majority from herpesviruses (Grundhoff & Sullivan, 2011). Herpesvirus-encoded miRNAs have been shown to regulate both cellular and viral gene expression, and to influence cell processes, including proliferation. In Marek's disease virus, the deletion of a single virus-encoded miRNA abrogates virus-induced cellular transformation (Zhao *et al.*, 2011), and in Epstein–Barr virus (EBV) a cluster of miRNAs has been implicated in controlling virus-induced B cell proliferation and transformation (Feederle *et al.*, 2011a, b; Seto *et al.*, 2010). We have demonstrated previously that OvHV-2 encodes at least eight miRNAs (Levy *et al.*, 2012) expressed within the immortalized bovine LGL line, BJ1035, and hypothesized that these play a critical role in MCF pathogenesis. In order to investigate the role of virus-encoded miRNAs in OvHV-2 pathogenesis it is necessary to identify their viral and cellular targets. In this study, we investigated the role of OvHV-2-encoded miRNAs in regulating selected virus gene expression. There is no *in vitro* infection system for studying OvHV-2; the only cells in which virus gene expression can be studied are immortalized LGL lines such as BJ1035 (Levy *et al.*, 2012). All cells in these LGL lines are virus genome-positive and in the majority OvHV-2 is latent; however, some lytic cycle gene expression occurs in a small proportion of the cells (Rosbottom *et al.*, 2002; Thonur *et al.*, 2006).

RESULTS

Prediction of OvHV-2-encoded miRNA targets in the OvHV-2 genome

Potential miRNA targets within the OvHV-2 genome were identified initially by scanning the entire OvHV-2 genome using BLASTN (http://blast.ncbi.nlm.nih.gov/Blast.cgi) to align the sequences complementary to the ovhv2-miRs in the OvHV-2 genome (GenBank accession no. AY839756) (Hart *et al.*, 2007). Targets were then mapped to the 5′ UTR or 3′ UTR of OvHV-2 genes. Only a small number of OvHV-2 mRNAs have been mapped previously; therefore for the majority of genes the 5′ UTRs were considered to span the region from the start codon to the predicted TATA box. For 3′ UTRs, the region from the stop codon to the predicted polyA site was used. This analysis identified potential targets in 33 OvHV-2 genes, representing all classes of virus gene, immediate early, early and late, and both structural and non-structural proteins.

For validation of predicted targets we focussed on genes/proteins predicted to play important roles in virus biology and pathogenesis. We chose to analyse targets present in the 5′ UTR or 3′ UTR of three virus genes, ORF20, ORF50 and ORF73. ORF20 has been shown to induce cell cycle arrest in other herpesviruses (Nascimento *et al.*, 2009) and the other two genes encode proteins that play contrary roles in virus latency. ORF50 is crucial for virus reactivation from latency and ORF73 is important for the maintenance of latency (Ackermann, 2006). The positions of the predicted miRNA target sites in ORF20, ORF50 and ORF73 are detailed in Table 1.

miRNAs function by targeting expressed mRNAs. ORF20 and ORF50 are only predicted ORFs from the genomic sequence, and the ORF73 transcript is only partially mapped (Coulter & Reid, 2002). In this study we confirmed the existence of these three virus ORFs as transcripts, including the miRNA target sites, using a reverse transcriptase (RT)-PCR strategy.

The annotated OvHV-2 genome predicts that ORF20 overlaps with both ORF19 and ORF21 (Fig. 1a). To allow detection of ORF20 only, cDNA synthesis was primed using a gene-specific primer located 406 bp upstream (42 530–41 549) of the ORF19 TATA box (41 106). This primer will not prime ORF21 mRNA as it is the same sense as the ORF21 transcript. Fig. 1(b) shows the 118 bp amplicon, the sequence of which was 100 % identical to the predicted ORF20 sequence (39 294–41 641) and includes the target sequence (41 617–41 635) for ovhv2-miR-2 (Fig. 1b).

The ORF50 and Ov6 transcripts are transcribed in the same direction, with the Ov6 TATA box lying 94 bp downstream of the ORF50 polyA site. ORF50 is spliced and ORF49 lies within the ORF50 intronic sequence transcribed in the opposite direction (Fig. 1a). We were unable to prime cDNA synthesis efficiently using an ORF50 gene-specific primer due to the limited number of nucleotides between the predicted target sequence and the polyA site, we therefore used both oligo (dT) and random primers to prime cDNA synthesis. PCR primers (78 080–78 099 and 79 205–79 181) were designed to generate an 1101 bp amplicon from the

Table 1. Positions of the predicted miRNA target sites in the UTRs of ORF20, ORF50 and ORF73

Gene	5′ UTR	3′ UTR	5′ UTR targets	3′ UTR targets
ORF20	41 641–41 538		ovhv2-miR-2 : 41 611–7	
ORF50		79 043–79 196		ovhv2-miR-5 : 79 161–7
ORF73	121 049–120 533		ovhv2-miR-8 : 120 824–18 : 120 840–34	

Nucleotide numbers are from GenBank accession no. AY839756 (Hart *et al.*, 2007).

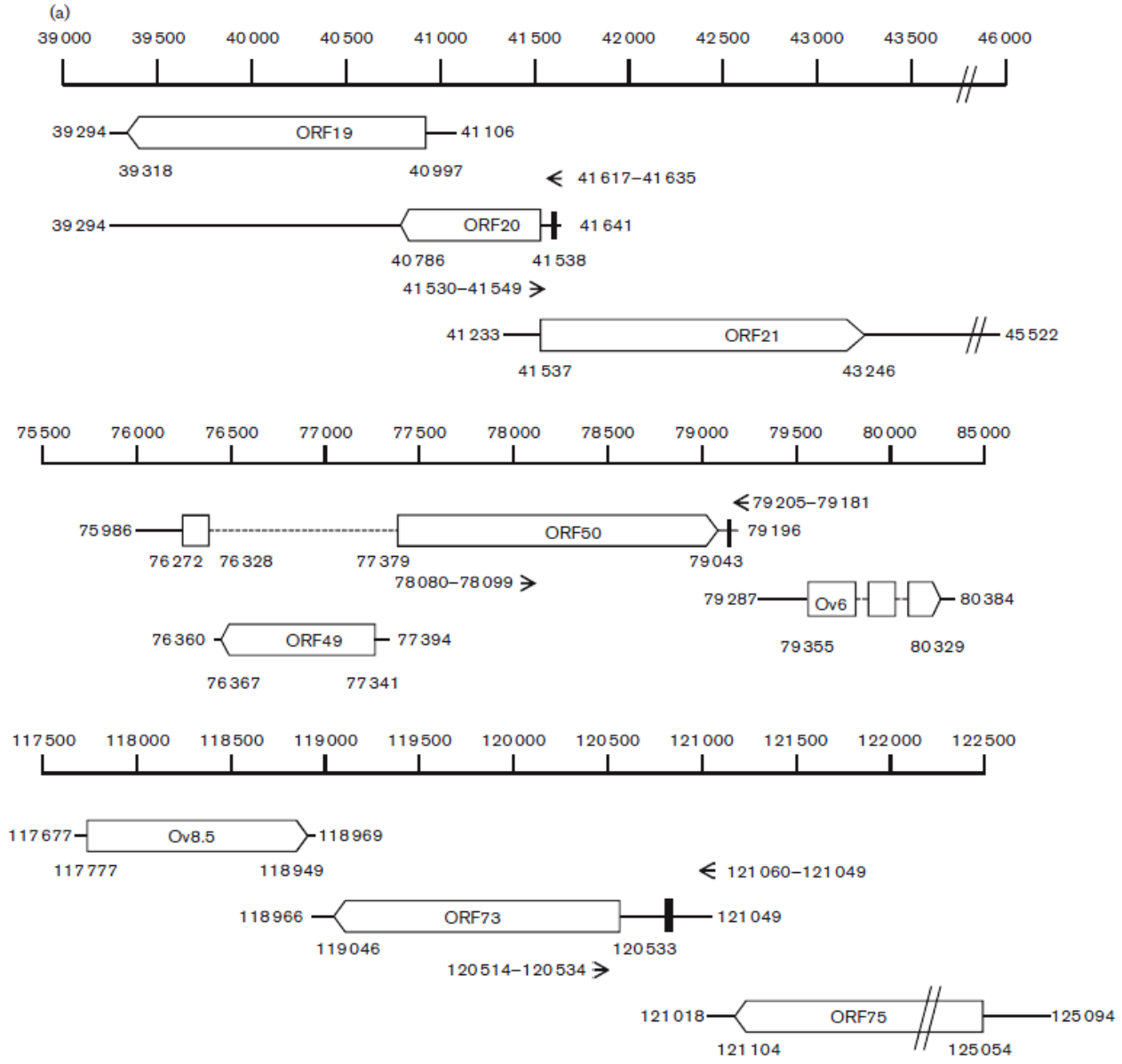

Fig. 1. (a) Genomic location of ORF20 and ORF50 relative to adjacent genes. Genes are indicated by open boxes. Arrowheads represent direction of transcription. Dotted lines represent introns. The nucleotide positions representing the location of the predicted TATA box and polyA site for each gene are indicated. The position of primers used for PCR and cDNA priming (ORF20) are indicated by arrows and nucleotide position. Predicted miRNA binding sequences are indicated by vertical bars in the respective UTRs. (b) ORF20: lane 1, no RT; lane 2, cDNA primed with 35 pM primer (250 ng); lane 3, cDNA primed with 10 pM primer (66 ng); lane 4, no template control; lane 5, DNA positive control; lane 6, marker, GeneRuler 100 bp. (c) ORF50: lane 1, no RT, lane 2, cDNA primed with oligo (dT); lane 3, cDNA primed with random primers; lane 4, no template control; lane 5, DNA positive control; lane 6, marker, GeneRuler 1 kb. (d) ORF73: lane 1, no RT, lane 2, cDNA primed with oligo dT; lane 3, cDNA primed with random primers; lane 4, no template control; lane 5, DNA positive control; lane 6, marker, GeneRuler 100 bp.

middle of the second exon of ORF50 to the polyA site. The 3′ primer (79 025–79 181) is ~1900 bp, and 82 bp upstream of ORF49 and Ov6 TATA boxes, respectively; the 5′ primer (78 080–78 099) is 118 bp upstream of the Ov6 TATA box and 2304 bp upstream of the Ov6 polyA site. Fig. 1(c) shows the 1101 bp amplicon, the sequence of which was 100 %

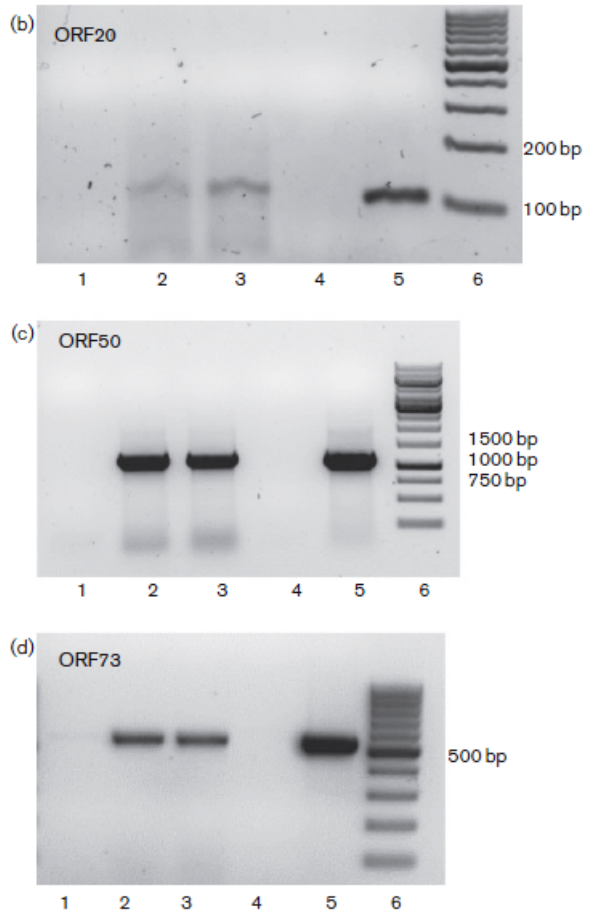

Fig. 1(b)

identical to the predicted ORF50 and included the target sequence (79 205–79 181) for ovhv2-miR-2.

ORF73 lies downstream of the ORF75 transcript and is transcribed in the same direction (Fig. 1a). The annotated OvHV-2 genome (GenBank accession no. AY839756) (Hart *et al.*, 2007) gives the 5′ terminus of the ORF73 transcript at nt 121 049, 31 bp upstream of the predicted polyA site for ORF75. We used both oligo (dT) and random primers to prime cDNA synthesis. PCR primers (120 514–120 534 and 121 060–121 041) generate a 536 bp amplicon from within the coding sequence of ORF73 to the predicted end of ORF73 mRNA. Fig. 1(d) shows this 536 bp amplicon, the sequence of which was 100 % identical to the predicted ORF73 and includes the target sequence (120 817–120 839) for ovhv2-miR-8.

Inhibition of gene expression

BJ1035 is a mixed population of cells with respect to virus life cycle; the majority are latently infected, but a small proportion express early and late virus genes (Rosbottom *et al.*, 2002; Thonur *et al.*, 2006). OvHV-2 miRNAs may be also expressed differentially in the proportion of cells in culture in which the virus is latent compared with those cells where the virus is reactivating, making analysis of inhibition of gene expression following introduction of exogenous miRNAs complex. We therefore assessed initially the ability of the ovhv2-miRs to interact with their predicted targets using a luciferase expression assay.

We have shown previously that insertion of a predicted 5′ UTR downstream of an exogenous promoter, e.g. cytomegalovirus immediate early promoter, can result in the expression of transcripts in which the start site does not reflect that of the native transcript (Grey *et al.*, 2010). In keeping with our previous studies, when analysing targets in 5′ UTRs we cloned a region ~1000 bp upstream of the AUG in an attempt to allow correct expression from the natural promoter. For all experiments a luciferase-expressing vector lacking OvHV-2 sequences was used to investigate off-target effects; no significant reduction in luciferase expression was seen using any of the ovhv2-miRs.

The 5′ UTR of ORF20 contained a predicted target site for ovhv2-miR-2 (Table 1, Fig. 3). BHK-21 cells were co-transfected with reporter constructs and miRNA mimics as described, and luciferase expression levels were measured. The combination of the ORF20 5′ UTR reporter and ovhv2-miR-2 resulted in a 57.5 (±10) % reduction ($P \leqslant 0.03$) in luciferase expression using 100 nM mimics (Fig. 2a) compared with control miRNA. The same degree of inhibition was observed using 50 nM mimics (data not shown). Ovhv2-miR-2 inhibited luciferase expression by 47.5 (±15) % ($P \leqslant 0.003$) even after the mutation of the predicted target site in the 5′ UTR (Fig. 2a), suggesting that inhibition was not due to interaction of ovhv2-miR-2 with the predicted target sequence. The 3′ UTR of ORF50 was predicted to contain a target site for ovhv2-miR-5 (Table 1, Fig. 3). The combination of ORF50 3′ UTR and ovhv2-miR-5 mimic resulted in a 45 (±10) % reduction ($P \leqslant 0.001$) in luciferase expression (Fig. 2b) compared with control miRNA. Mutation of the target site from the 3′ UTR abrogated this inhibition.

The 5′ UTR of ORF73 was predicted to contain two separate sites for ovhv2-miR-8 (Table 1, Fig. 3). The combination of the 5′ UTR of ORF73 and ovhv2-miR-8 mimic resulted in a 45(±8) % decrease ($P \leqslant 0.001$) in luciferase expression (Fig. 2c). Mutation of either of the predicted ovhv2-miR-8 target sites abolished the inhibitory effect of ovhv2-miR-8.

To further investigate inhibition of the expression of these OvHV-2 genes by the ovhv2-miRs we developed RT-quantitative PCR (qPCR) assays for ORF20, ORF50 and ORF73 transcripts. BJ1035 cells were transfected with the relevant ovhv2-miR mimics or control miRNA for 24 or 48 h, at which point cells were harvested, RNA isolated and qPCR carried out. We were able to demonstrate a 42 (±15) % reduction in levels of ORF50 transcripts

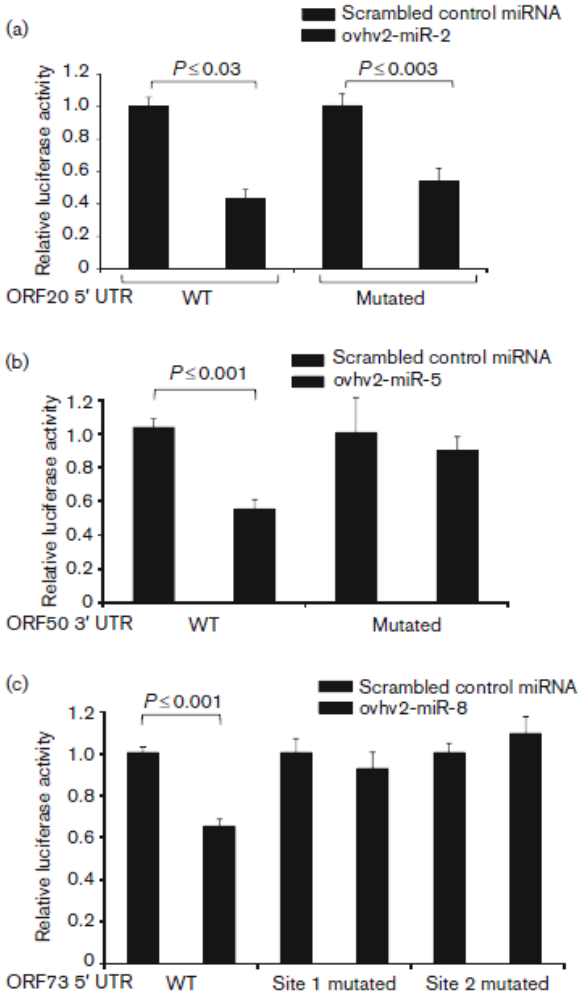

Fig. 2. BHK cells (n=6) were co-transfected with: (a) PGL-ORF20, which has the 5′ UTR of ORF20 upstream of firefly luciferase (or with a PGL-ORF20 in which the predicted ovhv2-miR-2 target site had been mutated), pRL (which expresses *Renilla* luciferase) and either an ovhv2-miR-2 mimic or a scrambled miRNA control; (b) psi-ORF50, which has the 3′ UTR of ORF50 downstream of *Renilla* luciferase (or with a psi-ORF50 in which the predicted ovhv2-miR-5 target site had been mutated) and either an ovhv2-miR-2 mimic or a scrambled miRNA control; or (c) PGL-ORF73, which has the 5′ UTR of ORF73 upstream of firefly luciferase (or with a PGL-ORF73 in which the predicted ovhv2-miR-8 target sites had been individually mutated), pRL (which expresses *Renilla* luciferase) and either an ovhv2-miR-8 mimic or a scrambled miRNA control. At 24 h post-transfection, firefly luciferase levels were measured, normalized to the *Renilla* luciferase levels, and expression in the control and test miRNA samples compared.

following transfection with ovhv2-miR-5 (Fig. 4a, P=0.042). Although there appeared to be a 12.8 (±13) % reduction in levels of ORF20 transcripts following transfection with ovhv2-miR-2 (Fig. 4b), this was not significant (P=0.532). Furthermore, we were unable to demonstrate any reduction in levels of ORF73 transcripts following transfection with ovhv2-miR-8 [+7.3 (±13.9) %] (Fig. 4c, P=0.532).

DISCUSSION

OvHV-2-induced MCF in susceptible hosts is a disease of dysregulated lymphocyte proliferation and cell function. However, these susceptible hosts cannot transmit the virus. In contrast, infection of carrier hosts is asymptomatic, but these are infectious. A previous study showed that this virus expresses at least eight miRNAs (Levy *et al.*, 2012). In this study, we investigated the control of expression of three virus genes important for control of the cell cycle (ORF20) and virus latency (ORF50 and ORF73) by virus-encoded miRNAs.

The 3′ UTR of ORF50 was predicted to be targeted by ovhv2-miR-5. This interaction was confirmed both by the luciferase assay and by inhibition of ORF50 miRNA levels in BJ1035 cells transfected with ovhv2-miR-5. Thus, we demonstrated that expression of ORF50, whose main role is to drive reactivation from latency, can be inhibited by a viral-encoded miRNA.

The 5′ UTR of ORF20 was predicted to contain one site recognized by ovhv2-miR-2. Ovhv2-miR-2 did inhibit luciferase expression; however, mutation of the predicted site did not abolish this inhibition. Thus, whilst we have demonstrated that ovhv2-miR-2 inhibits expression of a transcript containing the 5′ UTR of ORF20, we cannot definitively show that this inhibition is a consequence of its interaction with the target site predicted in the original analysis. We also investigated the ability of ovhv2-miR-2 to inhibit ORF20 expression in BJ1035 cells. We were able to demonstrate a small reduction in ORF20 mRNA levels in BJ1035 cells transfected with this ovhv2-miR-2; however, this was not statistically significant.

ORF73 was predicted to contain two sites recognized by the ovhv2-miR-8 seed sequence located nine bases apart (Fig. 3). Ovhv2-miR-8 was able to inhibit gene expression in the luciferase assay and mutation of either of these sites resulted in loss of inhibition. Further analysis of the binding of ovhv2-miR-8 to this region using the RNAhybrid tool showed that site 1 was predicted to bind the miRNA with high efficiency, but RNAhybrid did not identify site 2. Site 2 lies in the region that is likely to interact with the 3′ end of a miRNA interacting at site 1. It is therefore likely that site 1 is functional and that the loss of inhibition seen when site 2 is mutated is due to loss of non-seed sequence interactions. We were unable to demonstrate any reduction in ORF73 mRNA levels following transfection of ovhv2-miR-8 into BJ1035 cells.

The inability to demonstrate inhibition of ORF20 and ORF73 expression in BJ1035 cells may be due to a number of factors, e.g. the inherent variability within BJ1035 cells

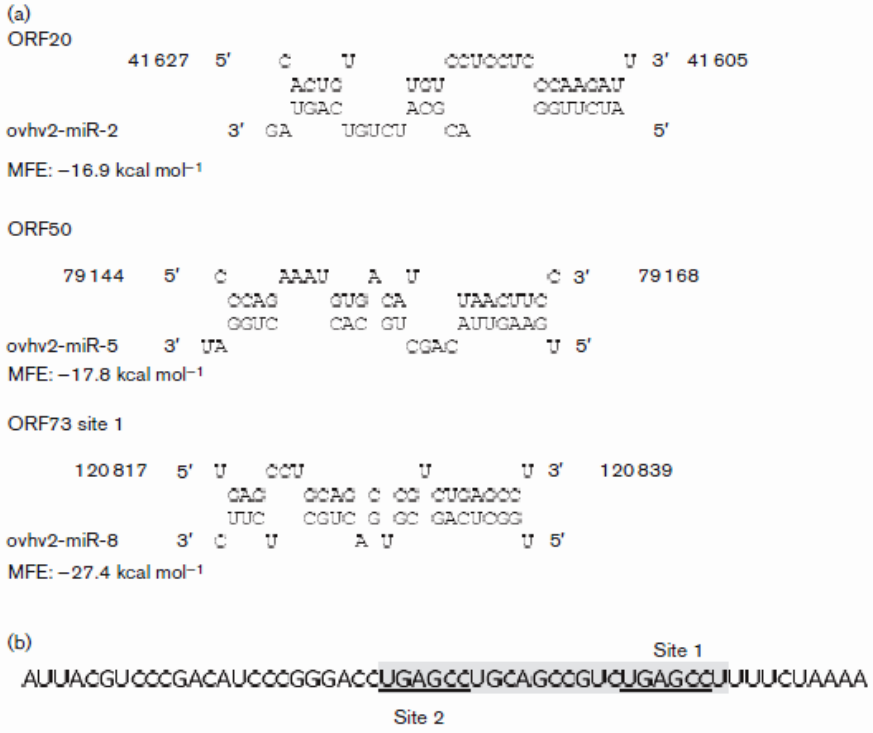

Fig. 3. (a) RNAhybrid analysis of the predicted target sites with the relevant miRNA. MFE, mean free energy. (b) Sequence of the ORF73 5′ UTR surrounding predicted sites 1 and 2 (underlined); the shaded box represents the sequence shown to interact with ovhv2-miR-8 in (a); 1 kcal=4.18 kJ.

could result in variation in baseline levels of virus gene expression or the ovhv2-miRs may inhibit translation (the luciferase assay measured protein levels) of ORF20 and ORF73 without affecting significantly mRNA levels. ORF73 is the main latency-associated protein and so will be expressed in the majority of BJ1035 cells. Our transfection efficiency for BJ1035 cells is ~40–45% (data not shown) and it is possible that the level of inhibition

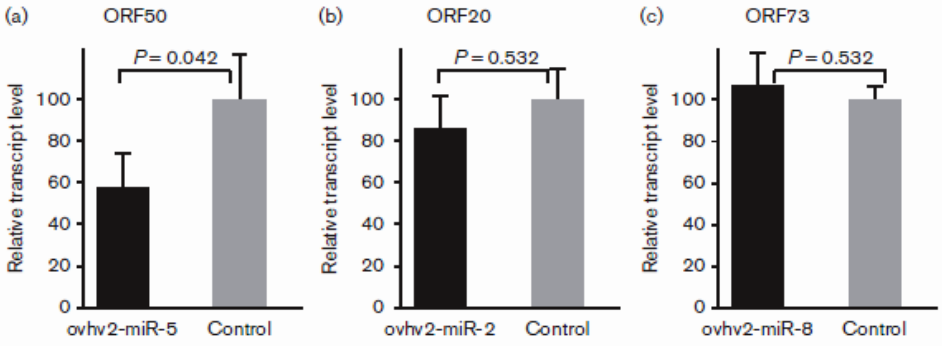

Fig. 4. BJ1035 cells (n=3) were transfected with control miRNA mimic, or (a) ovhv2-miR-5 mimic, (b) ovhv2-miR-2 mimic or (c) ovhv2-miR-8 mimic. At 24 h post-infection RNA was extracted and transcript levels of (a) ORF50, (b) ORF20 and (c) ORF73 analysed by RT-qPCR (three technical replicates per biological replicate). Levels were compared with levels in control transfected cells; error bars represent the SEM as produced by the linear mixed-effect (LME) statistical models, taking into account the technical and biological replicates.

obtained is not sufficient to be seen under these experimental conditions.

All three classes of herpesvirus, homologues of ORF20 (the UL24 family) have been shown to induce cell cycle arrest and inactivate the cyclin B/cdc2 complex (Nascimento *et al.*, 2009). The conservation of the structure and function of these proteins during herpesvirus evolution suggests strongly that they are important in herpesvirus biology (Nascimento *et al.*, 2009). Using ORF20 deletion mutants of MHV, Nascimento *et al.* (2011) also demonstrated that ORF20 is not essential for virus replication; there was a delay in virus clearance from the lungs of animals infected with the mutant virus and the mutants established latency normally. The role, if any, of ORF20 in MHV pathogenesis is therefore not clear. A recent study showed that viral cyclins play a key role in the control of latency and reactivation of the gammaherpesvirus MHV-68 (Lee *et al.*, 2012). Different mammalian cyclins could substitute for some of the functions of the MHV-68 cyclins, with different cyclins mediating persistence or reactivation (Lee *et al.*, 2012). It is possible that changes in expression of ORF20, mediated in part by ovhv2-miRs, could result in a change in the cyclin expression profile in infected cells, influencing the balance between productive and latent life cycles. A major part of MCF pathogenesis is uncontrolled proliferation of the infected LGLs, whose aberrant cytotoxic function leads to pathology. Inhibition of ORF20 expression by ovhv2-miR-2 may downregulate an ORF20-mediated block to the cell cycle, contributing to the dysregulated lymphocyte proliferation in susceptible hosts. OvHV-2 miRNAs were identified as being expressed in a bovine cell line, but their expression pattern in infected ovine cells is unknown. However, it is possible that a difference in the regulation of these miRNAs in ovine and bovine cells may result in differences in expression of ORF20, leading to the observed differences in the outcome of OvHV-2 infection in cattle and sheep.

ORF50 is a homologue of the replication and transcription activator (RTA) of EBV and Kaposi's sarcoma herpesvirus (KSHV). In KSHV, the virus-encoded miR-K5 and miR-K9 have antagonistic effects on latency: miR-K5 attenuates expression of RTA, leading to a reduction in reactivation, whilst miR-K9 targets BCLAF-1, a host transcription factor that is associated with reduced viral replication (Ziegelbauer *et al.*, 2009). Using a PARclip approach, Gottwein & Cullen (2010) reported that ORF73 of KSHV is targeted by KSHV miR-K10/miR-142-3p. Deletion of three EBV-encoded miRNAs has been shown to result in a significant increase in expression of virus latent genes (Feederle *et al.*, 2011a, b; Seto *et al.*, 2010), and Riley *et al.* (2012) showed that EBV-encoded miRNAs target virus-encoded, latency-associated genes and suggested that these miRNAs play a role in the control of EBV latency. The OvHV-2-immortalized LGL cell line, BJ1035, is a mixed population of cells with respect to virus life cycle; the majority are latently infected, but a small proportion express early and late virus genes (Rosbottom *et al.*, 2002; Thonur *et al.*, 2006). Thus, OvHV-2 miRNAs may be expressed differentially in the proportion of cells in culture in which the virus is latent compared with those cells where the virus is reactivating.

The proteins encoded by ORF50 and ORF73 play important but contrary roles in relation to latency: ORF50 is critical for virus reactivation and ORF73 is important in the maintenance of viral latency (Ackermann, 2006). Bellare & Ganem (2009) proposed that miRNA-induced inhibition of virus genes is not the sole regulator of reactivation/latency, but rather that miRNAs ensure that fluctuations in virus mRNA levels do not result in reactivation under conditions that are unfavourable for viral replication, i.e. the miRNAs act as a type of rheostat to control the levels of virus gene expression. The apparent contradiction of having miRNAs that act to both inhibit and encourage reactivation expressed in the same cell line can be explained by considering the mixed nature of the BJ1035 line. The differential expression of individual virus miRNAs in individual cells could respond to changes in the cellular environment acting to regulate virus gene expression. The factors that determine the maintenance of, or reactivation from, latency are complex; by demonstrating miRNA-mediated control of both 'pro- and anti-reactivation genes' our data add support to the hypothesis that miRNAs represent an additional layer of control exerted by the virus to control the latent state.

METHODS

Target identification. Potential miRNA targets within the OvHV-2 genome were identified using BLASTN (http://blast.ncbi.nlm.nih.gov/Blast.cgi) to align the sequences complementary to the ovhv2-miRs in the OvHV-2 genome (GenBank accession no. AY839756) (Hart *et al.*, 2007). Targets were mapped to the 5′ UTR or 3′ UTR of OvHV-2 genes. Only a small number of OvHV-2 mRNAs have been mapped previously; therefore, for the majority of genes, the 5′ UTRs were considered to span the region from the start codon to the predicted TATA box. For 3′ UTRs, the region from the stop codon to the predicted polyA site was used. Sites chosen for validation were also analysed by RNAhybrid (Rehmsmeier *et al.*, 2004) allowing no G:U pairing in the seed sequence and a helix constraint of nt 2–8.

Cell culture. Baby hamster kidney cells (BHK-21) were cultured in Glasgow's minimum essential medium (Gibco) supplemented with 10 % new born calf serum, 1 % (v/v) penicillin/streptomycin, 1 % (v/v) L-glutamine (Sigma) and 10 % (v/v) tryptose phosphate broth. BJ1035 cells were grown in suspension in Iscove's modified Dulbecco's medium (Invitrogen) (Hart *et al.*, 2007) supplemented with 10 % (v/v) FCS, 1 % (v/v) penicillin/streptomycin and 350 U proleukin (IL-2) ml^{-1} (Novartis Pharmaceutical), and cultured at 37 °C with 5 % CO_2.

Cloning of target sites. Sequences spanning the 3′ UTR and 5′ UTR of the selected genes were amplified by PCR. For 3′ UTRs, the region from the stop codon to the predicted polyA site was amplified; for 5′ UTRs, ~1000 bp upstream of the ATG was amplified. 3′ UTRs were cloned into the psiCHECK-2 Vector (Promega) downstream of a *Renilla* luciferase reporter gene (Rluc) and 5′ UTRs were cloned into the pGL4.10 vector (Promega) upstream of a firefly luciferase reporter gene (Fluc).

Transfection. BHK-21 cells (n=6) were co-transfected with reporter vectors (1.5 µg) with or without the 5′ UTR or 3′ UTR of interest and with 50 or 100 nM mimic miRNAs (miScript miRNA Mimics; Qiagen) or control miRNA (AllStars Negative Control siRNA; Qiagen) using Lipofectamine 2000 (Invitrogen) (mimic sequences: ovhv2-miR-2, 5′-AUCUUGGACGCAUCUGUCAGUAG-3′; ovhv2-miR-5, 5′-UGAAGUUACAGCUGCACCUGGAU-3′; ovhv2-miR-8, 5′-UGGCUCAGCGUGACUGCUCUUC-3′). After 24 h, samples were harvested and luciferase levels assessed using the Dual-Luciferase Reporter Assay System (Promega). For psiCheck (3′ UTR)-based vectors, Rluc (target) expression was normalized to Fluc expression from the same plasmid. For pGL4.10 (5′ UTR)-based vectors, cells were co-transfected with the pRL vector (Promega) to allow normalization of Fluc expression. BJ1035 cells were prepared for transfection by density gradient centrifugation using lymphoprep (Axis-Shield) and resuspended at a concentration of 1×10^6 cells in a final volume of 100 µl solution V (Lonza). Mimic or control miRNA (200 nM) was transfected into the prepared cells using programme X-001 of Nucleofector II (Lonza). Transfected cells (n=3) were incubated for 24 h in BJ1035 media prior to RNA extraction.

Site-directed mutagenesis. Site-directed mutagenesis was performed using the Quick Change Site-Directed Mutagenesis (Stratagene) protocol. Primers for mutagenesis (HPLC purified; Eurofins MWG Operon) were designed such that each primer was 42–45 nt in length, with a T_m>78 °C (Table S1). All mutations were confirmed by sequencing.

cDNA synthesis. RNA was isolated from BJ1035 cells using an RNeasy Kit (Qiagen). RNA (1 µg) was digested with RQ1 DNase (Promega) for 30 min at 37 °C. For analysis of ORF20, cDNA was primed with 250 or 66 ng specific primer (41 530 – CTGAAACA-TGGCCTCCAACT – −41 549). For analysis of ORF50, cDNA was primed using 250 ng oligo (dT) primer or random primers (Promega; equivalent to 0.5 µg RNA µg^{-1}). cDNA was synthesized using avian myeloblastosis virus (AMV) RT for 1 h at 42 °C (oligo (dT) and specific primer) or 37 °C (random primer).

RT-PCR analysis of transcripts. ORF20 cDNA was amplified with the primer pair TTCATAGTCACTGTTGTCC and CTGAAACA-TGGCCTCCAACT (nt 41 617–41 635 and 41 530–41 549). ORF50 cDNA was amplified with the primer pair CCCCAACAAGTCA-GCATTTT and CACTTTTATTTTAACATCACAAACC (nt 78 080–78 099 and 79 205–79 181). ORF73 cDNA was amplified with the primer pair CCACTTCGTAAAAGCACCATT and GTAATCCTG-CCCCAGCTGTA (nt 120 514–120 534 and 121 060–121 041). PCRs contained 8 pM primers, 120 µM dNTPs and 1 U HotStarTaq Plus (Qiagen) in a final reaction volume of 25 µl. Following an initial denaturation of 5 min at 95 °C, 40 cycles (30 s at 95 °C, 30 s at 58 °C and 1 min 15 s at 72 °C) were performed prior to a final extension of 5 min at 72 °C. BJ1035 DNA (100 ng) was used as a positive control for the PCR. Samples were run on a 2% agarose gel, visualized, extracted, cloned into pCR2.1-Topo (Invitrogen) and sequenced.

RT-qPCR. RNA was isolated using an RNeasy kit (Qiagen). RNA (1 µg) was digested with RQ1 DNase (Promega) for 30 min at 37 °C. cDNA was primed using 250 ng oligo (dT) primer (Promega; equivalent to 0.5 µg RNA µg^{-1}) and synthesized using AMV RT for 1 h at 42 °C. Semiquantitative PCR was performed on a Rotorgene Q machine (35 cycles of 15 s 95 °C, 30 s 58 °C and 30 s 72 °C) using the SensiFAST SYBR Hi-ROX One-Step master mix (Bioline), 2 µl diluted cDNA (1 : 10), and specific primers for glyceraldehyde 3-phosphate dehydrogenase (GAPDH) (Gossner *et al.*, 2009); ORF20 (CACTACCCAGCGCTCTTCC (41 125–41 143), TTGTACCCAACC-CCATCAAG (41 237–41 218); ORF50 (CCCCAACAAGTCAGCAT-TTT (78 080–78 099), TCAGGGGTGACTCCAATG (78 267–78 250); and ORF73 (CAGGGCAAAACGTAAAAAGC (119 367–119 348), GTGTGGAGCGTTAGGATTG (119 223–119 241) at a final concentration of 8 pM in a final reaction volume of 20 µl. Transcript levels were normalized to GAPDH and the relative expression was calculated using $2^{-\Delta\Delta C_T}$ (Livak & Schmittgen, 2001). Three technical replicates were performed for each biological replicate. Data were plotted as fold change in relation to the negative control.

Statistics. For luciferase assays, groups were compared using the single-factor ANOVA test followed by Tukey's post-hoc test. P-values represent results from the post-hoc test. To compare levels of ORF20, ORF50 or ORF73 transcripts after transfection with ovhv2-miRs, standard linear mixed-effect (LME) statistical models were used. Technical replicates were entered as random effects to account for the repeated sampling of the same cell line. Whether the data were test or control was entered as the fixed effect. For ORF50 and ORF73, three independent runs were performed and this run parameter was entered as a potential confounding fixed effect prior to control/test status. Examination of residuals demonstrated a normal distribution. The LMEs were carried out in R (version 2.15.0; http://www.r-project.org/foundation/).

ACKNOWLEDGEMENTS

This project was funded by the Biotechnology and Biological Sciences Research Council Institute Strategic Programme Grant to the Roslin Institute. A. R. is in receipt of a postgraduate scholarship from the Pakistan Higher Education Commission.

REFERENCES

Ackermann, M. (2006). Pathogenesis of gammaherpesvirus infections. *Vet Microbiol* **113**, 211–222.

Bartel, D. P. (2009). MicroRNAs: target recognition and regulatory functions. *Cell* **136**, 215–233.

Bellare, P. & Ganem, D. (2009). Regulation of KSHV lytic switch protein expression by a virus-encoded microRNA: an evolutionary adaptation that fine-tunes lytic reactivation. *Cell Host Microbe* **6**, 570–575.

Cook, C. G. & Splitter, G. A. (1988). Lytic function of bovine lymphokine-activated killer cells from a normal and a malignant catarrhal fever virus-infected animal. *Vet Immunol Immunopathol* **19**, 105–118.

Coulter, L. J. & Reid, H. W. (2002). Isolation and expression of three open reading frames from ovine herpesvirus-2. *J Gen Virol* **83**, 533–543.

Feederle, R., Linnstaedt, S. D., Bannert, H., Lips, H., Bencun, M., Cullen, B. R. & Delecluse, H.-J. (2011a). A viral microRNA cluster strongly potentiates the transforming properties of a human herpesvirus. *PLoS Pathog* **7**, e1001294.

Feederle, R., Haar, J., Bernhardt, K., Linnstaedt, S. D., Bannert, H., Lips, H., Cullen, B. R. & Delecluse, H.-J. (2011b). The members of an Epstein-Barr virus microRNA cluster cooperate to transform B lymphocytes. *J Virol* **85**, 9801–9810.

Gossner, A. G., Bennet, N., Hunter, N. & Hopkins, J. (2009). Differential expression of Prnp and Sprn in scrapie infected sheep also reveals Prnp genotype specific differences. *Biochem Biophys Res Commun* **378**, 862–866.

Gottwein, E. & Cullen, B. R. (2010). A human herpesvirus microRNA inhibits p21 expression and attenuates p21-mediated cell cycle arrest. *J Virol* **84**, 5229–5237.

Grey, F., Tirabassi, R., Meyers, H., Wu, G., McWeeney, S., Hook, L. & Nelson, J. A. (2010). A viral microRNA down-regulates multiple cell cycle genes through mRNA 5′UTRs. *PLoS Pathog* **6**, e1000967.

Grundhoff, A. & Sullivan, C. S. (2011). Virus-encoded microRNAs. *Virology* **411**, 325–343.

Hart, J., Ackermann, M., Jayawardane, G., Russell, G., Haig, D. M., Reid, H. & Stewart, J. P. (2007). Complete sequence and analysis of the ovine herpesvirus 2 genome. *J Gen Virol* **88**, 28–39.

Lee, K. S., Suarez, A. L., Claypool, D. J., Armstrong, T. K., Buckingham, E. M. & van Dyk, L. F. (2012). Viral cyclins mediate separate phases of infection by integrating functions of distinct mammalian cyclins. *PLoS Pathog* **8**, e1002496.

Levy, C. S., Hopkins, J., Russell, G. C. & Dalziel, R. G. (2012). Novel virus-encoded microRNA molecules expressed by ovine herpesvirus 2-immortalized bovine T-cells. *J Gen Virol* **93**, 150–154.

Livak, K. J. & Schmittgen, T. D. (2001). Analysis of relative gene expression data using real-time quantitative PCR and the method. *Methods* **25**, 402–408.

Meier-Trummer, C. S., Ryf, B. & Ackermann, M. (2010). Identification of peripheral blood mononuclear cells targeted by ovine herpesvirus-2 in sheep. *Vet Microbiol* **141**, 199–207.

Nascimento, R., Dias, J. D. & Parkhouse, R. M. E. (2009). The conserved UL24 family of human alpha, beta and gamma herpesviruses induces cell cycle arrest and inactivation of the cyclinB/cdc2 complex. *Arch Virol* **154**, 1143–1149.

Nascimento, R., Costa, H., Dias, J. D. & Parkhouse, R. M. E. (2011). MHV-68 Open Reading Frame 20 is a nonessential gene delaying lung viral clearance. *Arch Virol* **156**, 375–386.

Nelson, D. D., Davis, W. C., Brown, W. C., Li, H., O'Toole, D. & Oaks, J. L. (2010). $CD8^+$/perforin$^+$/$WC1^-$ gammadelta T cells, not $CD8^+$ alphabeta T cells, infiltrate vasculitis lesions of American bison (*Bison bison*) with experimental sheep-associated malignant catarrhal fever. *Vet Immunol Immunopathol* **136**, 284–291.

Rehmsmeier, M., Steffen, P., Hochsmann, M. & Giegerich, R. (2004). Fast and effective prediction of microRNA/target duplexes. *RNA* **10**, 1507–1517.

Reid, H. W., Buxton, D., Pow, I. & Finlayson, J. (1989). Isolation and characterisation of lymphoblastoid cells from cattle and deer affected with 'sheep-associated' malignant catarrhal fever. *Res Vet Sci* **47**, 90–96.

Riley, K. J., Rabinowitz, G. S., Yario, T. A., Luna, J. M., Darnell, R. B. & Steitz, J. A. (2012). EBV and human microRNAs co-target oncogenic and apoptotic viral and human genes during latency. *EMBO J* **31**, 2207–2221.

Rosbottom, J., Dalziel, R. G., Reid, H. W. & Stewart, J. P. (2002). Ovine herpesvirus 2 lytic cycle replication and capsid production. *J Gen Virol* **83**, 2999–3002.

Russell, G. C., Stewart, J. P. & Haig, D. M. (2009). Malignant catarrhal fever: a review. *Vet J* **179**, 324–335.

Schock, A., Collins, R. A. & Reid, H. W. (1998). Phenotype, growth regulation and cytokine transcription in *Ovine Herpesvirus-2* (OHV-2)-infected bovine T-cell lines. *Vet Immunol Immunopathol* **66**, 67–81.

Seto, E., Moosmann, A., Grömminger, S., Walz, N., Grundhoff, A. & Hammerschmidt, W. (2010). Micro RNAs of Epstein-Barr virus promote cell cycle progression and prevent apoptosis of primary human B cells. *PLoS Pathog* **6**, e1001063.

Tay, Y., Zhang, J. Q., Thomson, A. M., Lim, B. & Rigoutsos, I. (2008). MicroRNAs to *Nanog, Oct4* and *Sox2* coding regions modulate embryonic stem cell differentiation. *Nature* **455**, 1124–U1112.

Thonur, L., Russell, G. C., Stewart, J. P. & Haig, D. M. (2006). Differential transcription of ovine herpesvirus 2 genes in lymphocytes from reservoir and susceptible species. *Virus Genes* **32**, 27–35.

Zhao, Y., Xu, H., Yao, Y., Smith, L. P., Kgosana, L., Green, J., Petherbridge, L., Baigent, S. J. & Nair, V. (2011). Critical role of the virus-encoded microRNA-155 ortholog in the induction of Marek's disease lymphomas. *PLoS Pathog* **7**, e1001305.

Ziegelbauer, J. M., Sullivan, C. S. & Ganem, D. (2009). Tandem array-based expression screens identify host mRNA targets of virus-encoded microRNAs. *Nat Genet* **41**, 130–134.

Bibliography

ABEND, J. R., RAMALINGAM, D., KIEFFER-KWON, P., ULDRICK, T. S., YARCHOAN, R. & ZIEGELBAUER, J. M. 2012. Kaposi's sarcoma-associated herpesvirus microRNAs target IRAK1 and MYD88, two components of the toll-like receptor/interleukin-1R signaling cascade, to reduce inflammatory-cytokine expression. *Journal of Virology,* 86**,** 11663-74.

ABEND, J. R., ULDRICK, T. & ZIEGELBAUER, J. M. 2010. Regulation of tumor necrosis factor-like weak inducer of apoptosis receptor protein (TWEAKR) expression by Kaposi's sarcoma-associated herpesvirus microRNA prevents TWEAK-induced apoptosis and inflammatory cytokine expression. *Journal of Virology,* 84**,** 12139-51.

ABRAHANTE, J. E., DAUL, A. L., LI, M., VOLK, M. L., TENNESSEN, J. M., MILLER, E. A. & ROUGVIE, A. E. 2003. The Caenorhabditis elegans hunchback-like gene lin-57/hbl-1 controls developmental time and is regulated by microRNAs. *Dev Cell,* 4**,** 625-37.

ABU ELZEIN, E. M. E., HOUSAWI, F. M. T., GAMEEL, A. A., AL-AFALEQ, A. I. & EL-BASHIR, A. M. 2003. Sheep-Associated Malignant Catarrhal Fever Involving 3–5-Week-Old Calves in Saudi Arabia. *Journal of Veterinary Medicine, Series B,* 50**,** 53-59.

ACKERMANN, M. 2006. Pathogenesis of gammaherpesvirus infections. *Vet Microbiol,* 113**,** 211-22.

AHMED, M., LOCK, M., MILLER, C. G. & FRASER, N. W. 2002. Regions of the herpes simplex virus type 1 latency-associated transcript that protect cells from apoptosis in vitro and protect neuronal cells in vivo. *Journal of Virology,* 76**,** 717-29.

AJ, D., R, E., B, E., GS, H. & DJ, M. 2009. The order Herpesvirales. *Arch. Virol.,* 154**,** 171.

AKHTAR, J. & SHUKLA, D. 2009. Viral entry mechanisms: cellular and viral mediators of herpes simplex virus entry. *Febs Journal,* 276**,** 7228-7236.

ALBINI, S., ZIMMERMANN, W., NEFF, F., EHLERS, B., HANI, H., LI, H., HUSSY, D., ENGELS, M. & ACKERMANN, M. 2003. Identification and quantification of ovine gammaherpesvirus 2 DNA in fresh and stored tissues of pigs with symptoms of porcine malignant catarrhal fever. *J Clin Microbiol,* 41**,** 900-4.

ALCARAZ, A., WARREN, A., JACKSON, C., GOLD, J., MCCOY, M., CHEONG, S. H., KIMBALL, S., SELLS, S., TAUS, N. S., DIVERS, T. & LI, H. 2009. Naturally occurring sheep-associated malignant catarrhal fever in North American pigs. *J Vet Diagn Invest,* 21**,** 250-3.

ALMEIDA, A. R., LEGRAND, N., PAPIERNIK, M. & FREITAS, A. A. 2002. Homeostasis of peripheral CD4+ T cells: IL-2R alpha and IL-2 shape a population of regulatory cells that controls CD4+ T cell numbers. *J Immunol,* 169**,** 4850-60.

ALTUVIA, Y., LANDGRAF, P., LITHWICK, G., ELEFANT, N., PFEFFER, S., ARAVIN, A., BROWNSTEIN, M. J., TUSCHL, T. & MARGALIT, H. 2005. Clustering and conservation patterns of human microRNAs. *Nucleic Acids Res,* 33**,** 2697-706.

ALWINE, J. C., STEINHART, W. L. & HILL, C. W. 1974. Transcription of herpes simplex type 1 DNA in nuclei isolated from infected HEp-2 and KB cells. *Virology,* 60**,** 302-7.

AMON, W. & FARRELL, P. J. 2005. Reactivation of Epstein-Barr virus from latency. *Reviews in Medical Virology,* 15**,** 149-156.

AN, F. Q., FOLARIN, H. M., COMPITELLO, N., ROTH, J., GERSON, S. L., MCCRAE, K. R., FAKHARI, F. D., DITTMER, D. P. & RENNE, R. 2006. Long-term-infected telomerase-immortalized endothelial cells: a model for Kaposi's sarcoma-associated herpesvirus latency in vitro and in vivo. *Journal of Virology,* 80**,** 4833-46.

APARICIO, O., RAZQUIN, N., ZARATIEGUI, M., NARVAIZA, I. & FORTES, P. 2006. Adenovirus virus-associated RNA is processed to functional interfering RNAs involved in virus production. *Journal of Virology,* 80**,** 1376-84.

ARVIN, A. M. 1996. Varicella-zoster virus. *Clinical Microbiology Reviews,* 9**,** 361-&.

ASANO, Y., ITAKURA, N., KAJITA, Y., SUGA, S., YOSHIKAWA, T., YAZAKI, T., OZAKI, T., YAMANISHI, K. & TAKAHASHI, M. 1990. Severity of viremia and clinical findings in children with varicella. *J Infect Dis,* 161**,** 1095-8.

ASCHERIO, A. & MUNGER, K. L. 2010. Epstein-barr virus infection and multiple sclerosis: a review. *J Neuroimmune Pharmacol,* 5**,** 271-7.

ATANASIU, D., WHITBECK, J. C., CAIRNS, T. M., REILLY, B., COHEN, G. H. & EISENBERG, R. J. 2007. Bimolecular complementation reveals that glycoproteins gB and gH/gL of herpes simplex virus interact with each other during cell fusion. *Proc Natl Acad Sci U S A,* 104**,** 18718-23.

AUMAILLEY, M. & KRIEG, T. 1996. Laminins: a family of diverse multifunctional molecules of basement membranes. *J Invest Dermatol,* 106**,** 209-214.

BABAR, I. A., CHENG, C. J., BOOTH, C. J., LIANG, X., WEIDHAAS, J. B., SALTZMAN, W. M. & SLACK, F. J. 2012. Nanoparticle-based therapy in an in vivo microRNA-155 (miR-155)-dependent mouse model of lymphoma. *Proc Natl Acad Sci U S A,* 109**,** E1695-704.

BABCOCK, G. J., DECKER, L. L., VOLK, M. & THORLEY-LAWSON, D. A. 1998. EBV persistence in memory B cells in vivo. *Immunity,* 9**,** 395-404.

BACKOVIC, M. & JARDETZKY, T. S. 2011. Class III viral membrane fusion proteins. *Advances in experimental medicine and biology,* 714**,** 91-101.

BAEK, D., VILLEN, J., SHIN, C., CAMARGO, F. D., GYGI, S. P. & BARTEL, D. P. 2008. The impact of microRNAs on protein output. *Nature,* 455**,** 64-71.

BAI, Z., HUANG, Y., LI, W., ZHU, Y., JUNG, J. U., LU, C. & GAO, S. J. 2014. Genomewide mapping and screening of Kaposi's sarcoma-associated herpesvirus (KSHV) 3' untranslated regions identify bicistronic and polycistronic viral transcripts as frequent targets of KSHV microRNAs. *Journal of Virology,* 88**,** 377-92.

BARNARD, B. J. 1990. Epizootology of wildebeest-derived malignant catarrhal fever: possible transmission among cows and their calves in the north-western Transvaal. *Onderstepoort J Vet Res,* 57**,** 201-4.

BARTEL, D. P. 2004. MicroRNAs: genomics, biogenesis, mechanism, and function. *Cell,* 116**,** 281-97.

BARTEL, D. P. 2009. MicroRNAs: target recognition and regulatory functions. *Cell,* 136**,** 215-33.

BARTH, S., PFUHL, T., MAMIANI, A., EHSES, C., ROEMER, K., KREMMER, E., JAKER, C., HOCK, J., MEISTER, G. & GRASSER, F. A. 2008. Epstein-Barr virus-encoded microRNA miR-BART2 down-regulates the viral DNA polymerase BALF5. *Nucleic Acids Res,* 36**,** 666-75.

BATTERSON, W. & ROIZMAN, B. 1983. Characterization of the Herpes-Simplex Virion-Associated Factor Responsible for the Induction of Alpha-Genes. *Journal of Virology,* 46**,** 371-377.

BAUMFORTH, K. R., FLAVELL, J. R., REYNOLDS, G. M., DAVIES, G., PETTIT, T. R., WEI, W., MORGAN, S., STANKOVIC, T., KISHI, Y., ARAI, H., NOWAKOVA, M., PRATT, G., AOKI, J., WAKELAM, M. J., YOUNG, L. S. & MURRAY, P. G. 2005. Induction of autotaxin by the Epstein-Barr virus promotes the growth and survival of Hodgkin lymphoma cells. *Blood,* 106**,** 2138-46.

BAXTER, S. I., POW, I., BRIDGEN, A. & REID, H. W. 1993. PCR detection of the sheep-associated agent of malignant catarrhal fever. *Archives of Virology,* 132**,** 145-59.

BEDELIAN, C., NKEDIANYE, D. & HERRERO, M. 2007. Maasai perception of the impact and incidence of malignant catarrhal fever (MCF) in southern Kenya. *Prev Vet Med,* 78**,** 296-316.

BEEZHOLD, K. J., CASTRANOVA, V. & CHEN, F. 2010. Microprocessor of microRNAs: regulation and potential for therapeutic intervention. *Mol Cancer,* 9**,** 134.

BEHM-ANSMANT, I., REHWINKEL, J., DOERKS, T., STARK, A., BORK, P. & IZAURRALDE, E. 2006a. mRNA degradation by miRNAs and GW182 requires both CCR4:NOT deadenylase and DCP1:DCP2 decapping complexes. *Genes Dev,* 20**,** 1885-98.

BEHM-ANSMANT, I., REHWINKEL, J. & IZAURRALDE, E. 2006b. MicroRNAs silence gene expression by repressing protein expression and/or by promoting mRNA decay. *Cold Spring Harb Symp Quant Biol,* 71**,** 523-30.

BEITZINGER, M., PETERS, L., ZHU, J. Y., KREMMER, E. & MEISTER, G. 2007. Identification of human microRNA targets from isolated argonaute protein complexes. *RNA Biol,* 4**,** 76-84.

BELLARE, P. & GANEM, D. 2009. Regulation of KSHV lytic switch protein expression by a virus-encoded microRNA: an evolutionary adaptation that fine-tunes lytic reactivation. *Cell Host Microbe,* 6**,** 570-5.

BEN-PORAT, T., KAPLAN, A. S., STEHN, B. & RUBENSTEIN, A. S. 1976. Concatemeric forms of intracellular herpesvirus DNA. *Virology,* 69**,** 547-60.

BENAROCH, P., YILLA, M., RAPOSO, G., ITO, K., MIWA, K., GEUZE, H. J. & PLOEGH, H. L. 1995. How MHC class II molecules reach the endocytic pathway. *Embo Journal,* 14**,** 37-49.

BENJAMINI, Y. & HOCHBERG, Y. 2000. On the adaptive control of the false discovery rate in multiple testing with independent statistics. *Journal of Educational and Behavioral Statistics,* 25**,** 60-83.

BENNASSER, Y., LE, S. Y., YEUNG, M. L. & JEANG, K. T. 2004. HIV-1 encoded candidate micro-RNAs and their cellular targets. *Retrovirology,* 1**,** 43.

BENSON, R. A., LOWREY, J. A., LAMB, J. R. & HOWIE, S. E. 2004. The Notch and Sonic hedgehog signalling pathways in immunity. *Mol Immunol,* 41**,** 715-25.

BERGSTROM, T. & LYCKE, E. 1990. Neuroinvasion by herpes simplex virus. An in vitro model for characterization of neurovirulent strains. *Journal of General Virology,* 71 (Pt 2)**,** 405-10.

BERRIDGE, M. J. 2012. *Cell Signalling Biology; doi:10.1042/csb0001002*.

BHATT, K., MI, Q. S. & DONG, Z. 2011. microRNAs in kidneys: biogenesis, regulation, and pathophysiological roles. *Am J Physiol Renal Physiol,* 300**,** F602-10.

BHATTACHARYYA, S. N., HABERMACHER, R., MARTINE, U., CLOSS, E. I. & FILIPOWICZ, W. 2006. Relief of microRNA-mediated translational repression in human cells subjected to stress. *Cell,* 125**,** 1111-24.

BLASKOVIC, D., STANCEKOVA, M., SVOBODOVA, J. & MISTRIKOVA, J. 1980. Isolation of 5 Strains of Herpesviruses from 2 Species of Free-Living Small Rodents. *Acta Virologica,* 24**,** 468-468.

BOEHMER, P. E. & LEHMAN, I. R. 1997. Herpes simplex virus DNA replication. *Annu Rev Biochem,* 66**,** 347-84.

BOHNSACK, M. T., CZAPLINSKI, K. & GORLICH, D. 2004. Exportin 5 is a RanGTP-dependent dsRNA-binding protein that mediates nuclear export of pre-miRNAs. *RNA,* 10**,** 185-91.

BOMMER, U. A., HENG, C., PERRIN, A., DASH, P., LOBOV, S., ELIA, A. & CLEMENS, M. J. 2010. Roles of the translationally controlled tumour protein (TCTP) and the double-stranded RNA-dependent protein kinase, PKR, in cellular stress responses. *Oncogene,* 29**,** 763-73.

BOONACKER, E. & VAN NOORDEN, C. J. 2003. The multifunctional or moonlighting protein CD26/DPPIV. *Eur J Cell Biol,* 82**,** 53-73.

BORZA, C. M. & HUTT-FLETCHER, L. M. 2002. Alternate replication in B cells and epithelial cells switches tropism of Epstein-Barr virus. *Nature Medicine,* 8**,** 594-599.

BOSS, I. W., NADEAU, P. E., ABBOTT, J. R., YANG, Y., MERGIA, A. & RENNE, R. 2011. A Kaposi's sarcoma-associated herpesvirus-encoded ortholog of microRNA miR-155 induces human splenic B-cell expansion in NOD/LtSz-scid IL2Rgammanull mice. *Journal of Virology,* 85**,** 9877-86.

BOSS, I. W., PLAISANCE, K. B. & RENNE, R. 2009. Role of virus-encoded microRNAs in herpesvirus biology. *Trends in Microbiology,* 17**,** 544-53.

BOYNE, J. R., JACKSON, B. R., TAYLOR, A., MACNAB, S. A. & WHITEHOUSE, A. 2010. Kaposi's sarcoma-associated herpesvirus ORF57 protein interacts with PYM to enhance translation of viral intronless mRNAs. *Embo Journal,* 29**,** 1851-64.

BRAUN, J. E., HUNTZINGER, E., FAUSER, M. & IZAURRALDE, E. 2011. GW182 proteins directly recruit cytoplasmic deadenylase complexes to miRNA targets. *Mol Cell,* 44**,** 120-33.

BRENNECKE, J., STARK, A., RUSSELL, R. B. & COHEN, S. M. 2005. Principles of microRNA-target recognition. *PLoS Biol,* 3**,** e85.

BRIDGEN, A. & REID, H. W. 1991. Derivation of a DNA clone corresponding to the viral agent of sheep-associated malignant catarrhal fever. *Res Vet Sci,* 50**,** 38-44.

BRODERSEN, P., SAKVARELIDZE-ACHARD, L., BRUUN-RASMUSSEN, M., DUNOYER, P., YAMAMOTO, Y. Y., SIEBURTH, L. & VOINNET, O. 2008. Widespread translational inhibition by plant miRNAs and siRNAs. *Science,* 320**,** 1185-90.

BRYANT, H. E., WADD, S. E., LAMOND, A. I., SILVERSTEIN, S. J. & CLEMENTS, J. B. 2001. Herpes simplex virus IE63 (ICP27) protein interacts with spliceosome-associated protein 145 and inhibits splicing prior to the first catalytic step. *Journal of Virology,* 75**,** 4376-85.

BU, X., AVRAHAM, H. K., LI, X., LIM, B., JIANG, S., FU, Y., PESTELL, R. G. & AVRAHAM, S. 2005. Mayven induces c-Jun expression and cyclin D1 activation in breast cancer cells. *Oncogene,* 24**,** 2398-409.

BUCKMASTER, A. E., SCOTT, S. D., SANDERSON, M. J., BOURSNELL, M. E. G., ROSS, N. L. J. & BINNS, M. M. 1988. Gene Sequence and Mapping Data from Mareks-Disease Virus and Herpesvirus of Turkeys - Implications for Herpesvirus Classification. *Journal of General Virology,* 69**,** 2033-2042.

BUSHATI, N. & COHEN, S. M. 2007. microRNA functions. *Annu Rev Cell Dev Biol,* 23**,** 175-205.

CAI, X., HAGEDORN, C. H. & CULLEN, B. R. 2004. Human microRNAs are processed from capped, polyadenylated transcripts that can also function as mRNAs. *RNA,* 10**,** 1957-66.

CAI, X., SCHAFER, A., LU, S., BILELLO, J. P., DESROSIERS, R. C., EDWARDS, R., RAAB-TRAUB, N. & CULLEN, B. R. 2006a. Epstein-Barr virus microRNAs are evolutionarily conserved and differentially expressed. *Plos Pathogens,* 2**,** e23.

CAI, X. Z., SCHAFER, A., LU, S. H., BILELLO, J. P., DESROSIERS, R. C., EDWARDS, R., RAAB-TRAUB, N. & CULLEN, B. R. 2006b. Epstein-Barr virus MicroRNAs are evolutionarily conserved and differentially expressed. *Plos Pathogens,* 2**,** 236-247.

CALNEK, B. W., ADLDINGE.HK & KAHN, D. E. 1970. Feather Follicle Epithelium - a Source of Enveloped and Infectious Cell-Free Herpesvirus from Mareks Disease. *Avian Diseases,* 14**,** 219-&.

CAMPADELLI-FIUME, G., AMASIO, M., AVITABILE, E., CERRETANI, A., FORGHIERI, C., GIANNI, T. & MENOTTI, L. 2007. The multipartite system that mediates entry of herpes simplex virus into the cell. *Reviews in Medical Virology,* 17**,** 313-26.

CAMPBELL, M. R., KARACA, M., ADAMSKI, K. N., CHORLEY, B. N., WANG, X. & BELL, D. A. 2013. Novel hematopoietic target genes in the NRF2-mediated transcriptional pathway. *Oxid Med Cell Longev,* 2013**,** 120305.

CAPACCIONE, K. M. & PINE, S. R. 2013. The Notch signaling pathway as a mediator of tumor survival. *Carcinogenesis,* 34**,** 1420-30.

CAREL, J. C., MYONES, B. L., FRAZIER, B. & HOLERS, V. M. 1990. Structural requirements for C3d,g/Epstein-Barr virus receptor (CR2/CD21) ligand binding, internalization, and viral infection. *J Biol Chem,* 265**,** 12293-9.

CHA, T. A., TOM, E., KEMBLE, G. W., DUKE, G. M., MOCARSKI, E. S. & SPAETE, R. R. 1996. Human cytomegalovirus clinical isolates carry at least 19 genes not found in laboratory strains. *Journal of Virology,* 70**,** 78-83.

CHANG, H., DITTMER, D. P., SHIN, Y. C., HONG, Y. & JUNG, J. U. 2005. Role of Notch signal transduction in Kaposi's sarcoma-associated herpesvirus gene expression. *Journal of Virology,* 79**,** 14371-82.

CHANG, Y., CESARMAN, E., PESSIN, M. S., LEE, F., CULPEPPER, J., KNOWLES, D. M. & MOORE, P. S. 1994. Identification of herpesvirus-like DNA sequences in AIDS-associated Kaposi's sarcoma. *Science,* 266**,** 1865-9.

CHEKULAEVA, M. & FILIPOWICZ, W. 2009. Mechanisms of miRNA-mediated post-transcriptional regulation in animal cells. *Curr Opin Cell Biol,* 21**,** 452-60.

CHEN, C. Z., LI, L., LODISH, H. F. & BARTEL, D. P. 2004. MicroRNAs modulate hematopoietic lineage differentiation. *Science,* 303**,** 83-6.

CHEN, S. H., KRAMER, M. F., SCHAFFER, P. A. & COEN, D. M. 1997. A viral function represses accumulation of transcripts from productive-cycle genes in mouse ganglia latently infected with herpes simplex virus. *Journal of Virology,* 71**,** 5878-84.

CHEN, W. Y., WANG, D. H., YEN, R. C., LUO, J., GU, W. & BAYLIN, S. B. 2005. Tumor suppressor HIC1 directly regulates SIRT1 to modulate p53-dependent DNA-damage responses. *Cell,* 123**,** 437-48.

CHEN, X. P., MATA, M., KELLEY, M., GLORIOSO, J. C. & FINK, D. J. 2002. The relationship of herpes simplex virus latency associated transcript expression to genome copy number: A quantitative study using laser capture microdissection. *J Neurovirol,* 8**,** 204-210.

CHEN, Z. L., ZHAO, X. H., WANG, J. W., LI, B. Z., WANG, Z., SUN, J., TAN, F. W., DING, D. P., XU, X. H., ZHOU, F., TAN, X. G., HANG, J., SHI, S. S., FENG, X. L. & HE, J. 2011. microRNA-92a promotes lymph node metastasis of human esophageal squamous cell carcinoma via E-cadherin. *J Biol Chem,* 286**,** 10725-34.

CHENDRIMADA, T. P., FINN, K. J., JI, X., BAILLAT, D., GREGORY, R. I., LIEBHABER, S. A., PASQUINELLI, A. E. & SHIEKHATTAR, R. 2007. MicroRNA silencing through RISC recruitment of eIF6. *Nature,* 447**,** 823-8.

CHENDRIMADA, T. P., GREGORY, R. I., KUMARASWAMY, E., NORMAN, J., COOCH, N., NISHIKURA, K. & SHIEKHATTAR, R. 2005. TRBP recruits the Dicer complex to Ago2 for microRNA processing and gene silencing. *Nature,* 436**,** 740-4.

CHENG, F., LIU, J., TEH, C., CHONG, S. W., KORZH, V., JIANG, Y. J. & DENG, L. W. 2011. Camptothecin-induced downregulation of MLL5 contributes to the activation of tumor suppressor p53. *Oncogene,* 30**,** 3599-611.

CHENG, L., ROSSMAN, K. L., MAHON, G. M., WORTHYLAKE, D. K., KORUS, M., SONDEK, J. & WHITEHEAD, I. P. 2002. RhoGEF specificity mutants implicate RhoA as a target for Dbs transforming activity. *Molecular and Cellular Biology,* 22**,** 6895-905.

CHI, S. W., ZANG, J. B., MELE, A. & DARNELL, R. B. 2009. Argonaute HITS-CLIP decodes microRNA-mRNA interaction maps. *Nature,* 460**,** 479-86.

CHICHE, J., ILC, K., LAFERRIERE, J., TROTTIER, E., DAYAN, F., MAZURE, N. M., BRAHIMI-HORN, M. C. & POUYSSEGUR, J. 2009. Hypoxia-inducible carbonic anhydrase IX and XII promote tumor cell growth by counteracting acidosis through the regulation of the intracellular pH. *Cancer Research,* 69**,** 358-68.

CHO, Y. J., CUNNICK, J. M., YI, S. J., KAARTINEN, V., GROFFEN, J. & HEISTERKAMP, N. 2007. Abr and Bcr, two homologous Rac GTPase-activating proteins, control multiple cellular functions of murine macrophages. *Molecular and Cellular Biology,* 27**,** 899-911.

CHOY, E. Y., SIU, K. L., KOK, K. H., LUNG, R. W., TSANG, C. M., TO, K. F., KWONG, D. L., TSAO, S. W. & JIN, D. Y. 2008. An Epstein-Barr virus-encoded microRNA targets PUMA to promote host cell survival. *Journal of Experimental Medicine,* 205**,** 2551-60.

CIMMINO, A., CALIN, G. A., FABBRI, M., IORIO, M. V., FERRACIN, M., SHIMIZU, M., WOJCIK, S. E., AQEILAN, R. I., ZUPO, S., DONO, M., RASSENTI, L., ALDER, H., VOLINIA, S., LIU, C. G., KIPPS, T. J., NEGRINI, M. & CROCE, C. M. 2005. miR-15 and miR-16 induce apoptosis by targeting BCL2. *Proc Natl Acad Sci U S A,* 102**,** 13944-9.

CLEMENT, C., TIWARI, V., SCANLAN, P. M., VALYI-NAGY, T., YUE, B. Y. & SHUKLA, D. 2006. A novel role for phagocytosis-like uptake in herpes simplex virus entry. *The Journal of cell biology,* 174**,** 1009-21.

COLLERY, P. & FOLEY, A. 1996. An outbreak of malignant catarrhal fever in cattle in the Republic of Ireland. *Veterinary Record,* 139**,** 16-7.

COLOMBATTI, A., BONALDO, P. & DOLIANA, R. 1993. Type A modules: interacting domains found in several non-fibrillar collagens and in other extracellular matrix proteins. *Matrix,* 13**,** 297-306.

CONNOLLY, S. A., JACKSON, J. O., JARDETZKY, T. S. & LONGNECKER, R. 2011. Fusing structure and function: a structural view of the herpesvirus entry machinery. *Nature Reviews Microbiology,* 9**,** 369-381.

COOK, C. G. & SPLITTER, G. A. 1988. Lytic function of bovine lymphokine-activated killer cells from a normal and a malignant catarrhal fever virus-infected animal. *Vet Immunol Immunopathol,* 19**,** 105-18.

CORCORAN, D. L., GEORGIEV, S., MUKHERJEE, N., GOTTWEIN, E., SKALSKY, R. L., KEENE, J. D. & OHLER, U. 2011. PARalyzer: definition of RNA binding sites from PAR-CLIP short-read sequence data. *Genome Biol,* 12**,** R79.

COSTA, E. A., BOMFIM, M. R., DA FONSECA, F. G., DRUMOND, B. P., COELHO, F. M., VASCONCELOS, A. C., FURTINI, R., PAIXAO, T. A., TSOLIS, R. M., SANTOS, R. L. & RESENDE, M. 2009. Ovine herpesvirus 2 infection in Foal, Brazil. *Emerg Infect Dis,* 15**,** 844-5.

COSTA, E. A., VIOTT, A. D., MACHADO, G. D., BOMFIM, M. R. Q., COELHO, F. M., LOBATO, Z. I. P., RESENDE, M. & GUEDES, R. M. C. 2010. Transmission of Ovine Herpesvirus 2 from Asymptomatic Boars to Sows. *Emerg Infect Dis,* 16**,** 2011-2012.

COSTINEAN, S., ZANESI, N., PEKARSKY, Y., TILI, E., VOLINIA, S., HEEREMA, N. & CROCE, C. M. 2006. Pre-B cell proliferation and lymphoblastic leukemia/high-grade lymphoma in E(mu)-miR155 transgenic mice. *Proc Natl Acad Sci U S A,* 103**,** 7024-9.

COTTERET, S. & CHERNOFF, J. 2006. Nucleocytoplasmic shuttling of Pak5 regulates its antiapoptotic properties. *Molecular and Cellular Biology,* 26**,** 3215-30.

COTTERET, S., JAFFER, Z. M., BEESER, A. & CHERNOFF, J. 2003. p21-Activated kinase 5 (Pak5) localizes to mitochondria and inhibits apoptosis by phosphorylating BAD. *Molecular and Cellular Biology,* 23**,** 5526-39.

COUGOT, N., BABAJKO, S. & SERAPHIN, B. 2004. Cytoplasmic foci are sites of mRNA decay in human cells. *The Journal of cell biology,* 165**,** 31-40.

CRAWFORD, T. B., LI, H., ROSENBURG, S. R., NORHAUSEN, R. W. & GARNER, M. M. 2002. Mural folliculitis and alopecia caused by infection with goat-associated malignant catarrhal fever virus in two sika deer. *Journal of the American Veterinary Medical Association,* 221**,** 843-7, 801.

CROUGH, T. & KHANNA, R. 2009. Immunobiology of Human Cytomegalovirus: from Bench to Bedside. *Clinical Microbiology Reviews,* 22**,** 76-+.

CUI, C., GRIFFITHS, A., LI, G., SILVA, L. M., KRAMER, M. F., GAASTERLAND, T., WANG, X. J. & COEN, D. M. 2006. Prediction and identification of herpes simplex virus 1-encoded microRNAs. *Journal of Virology,* 80**,** 5499-508.

CULLEN, B. R. 2010. Five questions about viruses and microRNAs. *Plos Pathogens,* 6**,** e1000787.

CUNHA, C. W., GAILBREATH, K. L., O'TOOLE, D., KNOWLES, D. P., SCHNEIDER, D. A., WHITE, S. N., TAUS, N. S., DAVIES, C. J., DAVIS, W. C. & LI, H. 2012. Ovine herpesvirus 2 infection in American bison: virus and host dynamics in the development of sheep-associated malignant catarrhal fever. *Vet Microbiol,* 159**,** 307-19.

D'ARCANGELO, G., HOMAYOUNI, R., KESHVARA, L., RICE, D. S., SHELDON, M. & CURRAN, T. 1999. Reelin is a ligand for lipoprotein receptors. *Neuron,* 24**,** 471-9.

DAHLKE, C., MAUL, K., CHRISTALLA, T., WALZ, N., SCHULT, P., STOCKING, C. & GRUNDHOFF, A. 2012. A microRNA encoded by Kaposi sarcoma-associated herpesvirus promotes B-cell expansion in vivo. *PLoS ONE,* 7**,** e49435.

DAMANIA, B., JEONG, J. H., BOWSER, B. S., DEWIRE, S. M., STAUDT, M. R. & DITTMER, D. P. 2004. Comparison of the Rta/Orf50 transactivator proteins of gamma-2-herpesviruses. *Journal of Virology,* 78**,** 5491-9.

DAN, C., NATH, N., LIBERTO, M. & MINDEN, A. 2002. PAK5, a new brain-specific kinase, promotes neurite outgrowth in N1E-115 cells. *Molecular and Cellular Biology,* 22**,** 567-77.

DASGUPTA, A. & WILSON, D. W. 1999. ATP depletion blocks herpes simplex virus DNA packaging and capsid maturation. *Journal of Virology,* 73**,** 2006-15.

DAVID, D., DAGONI, I., GARAZI, S., PERL, S. & BRENNER, J. 2005. Two cases of the cutaneous form of sheep-associated malignant catarrhal fever in cattle. *Veterinary Record,* 156**,** 118-20.

DAVIS-DUSENBERY, B. N. & HATA, A. 2010. Mechanisms of control of microRNA biogenesis. *J Biochem,* 148**,** 381-92.

DAVIS, E., CAIMENT, F., TORDOIR, X., CAVAILLE, J., FERGUSON-SMITH, A., COCKETT, N., GEORGES, M. & CHARLIER, C. 2005. RNAi-mediated allelic trans-interaction at the imprinted Rtl1/Peg11 locus. *Curr Biol,* 15**,** 743-9.

DAVISON, A. J., EBERLE, R., EHLERS, B., HAYWARD, G. S., MCGEOCH, D. J., MINSON, A. C., PELLETT, P. E., ROIZMAN, B., STUDDERT, M. J. & THIRY, E. 2009. The order Herpesvirales. *Archives of Virology,* 154**,** 171-177.

DE YEBENES, V. G., BARTOLOME-IZQUIERDO, N. & RAMIRO, A. R. 2013. Regulation of B-cell development and function by microRNAs. *Immunol Rev,* 253**,** 25-39.

DENG, L. W., CHIU, I. & STROMINGER, J. L. 2004. MLL 5 protein forms intranuclear foci, and overexpression inhibits cell cycle progression. *Proc Natl Acad Sci U S A,* 101**,** 757-62.

DENHOLM, L. J. & WESTBURY, H. A. 1982. Malignant catarrhal fever in farmed Rusa deer (Cervus timorensis). 1. Clinico-pathological observations. *Aust Vet J,* 58**,** 81-7.

DESMECHT, D., CASSART, D., ROLLIN, F., COIGNOUL, F. & THAM, K. M. 1999. Molecular and clinicopathological diagnosis of non-wildebeest associated malignant catarrhal fever in Belgium. *Veterinary Record,* 144**,** 388.

DESNOYERS, L. R., PAI, R., FERRANDO, R. E., HOTZEL, K., LE, T., ROSS, J., CARANO, R., D'SOUZA, A., QING, J., MOHTASHEMI, I., ASHKENAZI, A. & FRENCH, D. M. 2008. Targeting FGF19 inhibits tumor growth in colon cancer xenograft and FGF19 transgenic hepatocellular carcinoma models. *Oncogene,* 27**,** 85-97.

DETTWILER, M., STAHEL, A., KRUGER, S., GERSPACH, C., BRAUN, U., ENGELS, M. & HILBE, M. 2011. A possible case of caprine-associated malignant catarrhal fever in a domestic water buffalo (Bubalus bubalis) in Switzerland. *BMC Vet Res,* 7**,** 78.

DEWALS, B., BOUDRY, C., GILLET, L., MARKINE-GORIAYNOFF, N., DE LEVAL, L., HAIG, D. M. & VANDERPLASSCHEN, A. 2006. Cloning of the genome of Alcelaphine herpesvirus 1 as an infectious and pathogenic bacterial artificial chromosome. *Journal of General Virology,* 87**,** 509-17.

DI SANZO, M., GASPARI, M., MISAGGI, R., ROMEO, F., FALBO, L., DE MARCO, C., AGOSTI, V., QUARESIMA, B., BARNI, T., VIGLIETTO, G., LARSEN, M. R., CUDA, G., COSTANZO, F. & FANIELLO, M. C. 2011. H ferritin gene silencing in a human metastatic melanoma cell line: a proteomic analysis. *J Proteome Res,* 10**,** 5444-53.

DIDIANO, D. & HOBERT, O. 2006. Perfect seed pairing is not a generally reliable predictor for miRNA-target interactions. *Nat Struct Mol Biol,* 13**,** 849-51.

DOENCH, J. G., PETERSEN, C. P. & SHARP, P. A. 2003. siRNAs can function as miRNAs. *Genes Dev,* 17**,** 438-42.

DOENCH, J. G. & SHARP, P. A. 2004. Specificity of microRNA target selection in translational repression. *Genes Dev,* 18**,** 504-11.

DONG, H., LEI, J., DING, L., WEN, Y., JU, H. & ZHANG, X. 2013. MicroRNA: function, detection, and bioanalysis. *Chem Rev,* 113**,** 6207-33.

DORSAM, R. T. & GUTKIND, J. S. 2007. G-protein-coupled receptors and cancer. *Nat Rev Cancer,* 7**,** 79-94.

DREWES, G., EBNETH, A., PREUSS, U., MANDELKOW, E. M. & MANDELKOW, E. 1997. MARK, a novel family of protein kinases that phosphorylate microtubule-associated proteins and trigger microtubule disruption. *Cell,* 89**,** 297-308.

DUKE-COHAN, J. S., GU, J., MCLAUGHLIN, D. F., XU, Y., FREEMAN, G. J. & SCHLOSSMAN, S. F. 1998. Attractin (DPPT-L), a member of the CUB family of cell adhesion and guidance proteins, is secreted by activated human T lymphocytes and modulates immune cell interactions. *Proc Natl Acad Sci U S A,* 95**,** 11336-41.

DUUS, K. M., LENTCHITSKY, V., WAGENAAR, T., GROSE, C. & WEBSTER-CYRIAQUE, J. 2004. Wild-type Kaposi's sarcoma-associated herpesvirus isolated from the oropharynx of immune-competent individuals has tropism for cultured oral epithelial cells. *Journal of Virology,* 78**,** 4074-84.

DYE, M. J. & PROUDFOOT, N. J. 1999. Terminal exon definition occurs cotranscriptionally and promotes termination of RNA polymerase II. *Mol Cell,* 3**,** 371-8.

EDINGTON, N. & PLOWRIGHT, W. 1980. The protection of rabbits against the herpesvirus of malignant catarrhal fever by inactivated vaccines. *Res Vet Sci,* 28**,** 384-6.

ELIOPOULOS, A. G., DAWSON, C. W., MOSIALOS, G., FLOETTMANN, J. E., ROWE, M., ARMITAGE, R. J., DAWSON, J., ZAPATA, J. M., KERR, D. J., WAKELAM, M. J., REED, J. C., KIEFF, E. & YOUNG, L. S. 1996. CD40-induced growth inhibition in epithelial cells is mimicked by Epstein-Barr Virus-encoded LMP1: involvement of TRAF3 as a common mediator. *Oncogene,* 13**,** 2243-54.

ENSSER, A. & FLECKENSTEIN, B. 1995. Alcelaphine herpesvirus type 1 has a semaphorin-like gene. *Journal of General Virology,* 76 (Pt 4)**,** 1063-7.

ENSSER, A., PFLANZ, R. & FLECKENSTEIN, B. 1997. Primary structure of the alcelaphine herpesvirus 1 genome. *Journal of Virology,* 71**,** 6517-25.

ESAU, C., KANG, X., PERALTA, E., HANSON, E., MARCUSSON, E. G., RAVICHANDRAN, L. V., SUN, Y., KOO, S., PERERA, R. J., JAIN, R., DEAN, N. M., FREIER, S. M., BENNETT, C. F., LOLLO, B. & GRIFFEY, R. 2004. MicroRNA-143 regulates adipocyte differentiation. *J Biol Chem,* 279**,** 52361-5.

EULALIO, A., HUNTZINGER, E., NISHIHARA, T., REHWINKEL, J., FAUSER, M. & IZAURRALDE, E. 2009. Deadenylation is a widespread effect of miRNA regulation. *RNA,* 15**,** 21-32.

EULALIO, A., REHWINKEL, J., STRICKER, M., HUNTZINGER, E., YANG, S. F., DOERKS, T., DORNER, S., BORK, P., BOUTROS, M. &

IZAURRALDE, E. 2007. Target-specific requirements for enhancers of decapping in miRNA-mediated gene silencing. *Genes Dev,* 21**,** 2558-70.

FABIAN, M. R., CIEPLAK, M. K., FRANK, F., MORITA, M., GREEN, J., SRIKUMAR, T., NAGAR, B., YAMAMOTO, T., RAUGHT, B., DUCHAINE, T. F. & SONENBERG, N. 2011. miRNA-mediated deadenylation is orchestrated by GW182 through two conserved motifs that interact with CCR4-NOT. *Nat Struct Mol Biol,* 18**,** 1211-7.

FABIAN, M. R., MATHONNET, G., SUNDERMEIER, T., MATHYS, H., ZIPPRICH, J. T., SVITKIN, Y. V., RIVAS, F., JINEK, M., WOHLSCHLEGEL, J., DOUDNA, J. A., CHEN, C. Y., SHYU, A. B., YATES, J. R., 3RD, HANNON, G. J., FILIPOWICZ, W., DUCHAINE, T. F. & SONENBERG, N. 2009. Mammalian miRNA RISC recruits CAF1 and PABP to affect PABP-dependent deadenylation. *Mol Cell,* 35**,** 868-80.

FANCHIANG, S. S., COJOCARU, R., OTHMAN, M., KHANNA, R., BROOKS, M. J., SMITH, T., TANG, X., MARICIC, I., SWAROOP, A. & KUMAR, V. 2012. Global expression profiling of peripheral Qa-1-restricted CD8alphaalpha+TCRalphabeta+ regulatory T cells reveals innate-like features: implications for immune-regulatory repertoire. *Hum Immunol,* 73**,** 214-22.

FARH, K. K., GRIMSON, A., JAN, C., LEWIS, B. P., JOHNSTON, W. K., LIM, L. P., BURGE, C. B. & BARTEL, D. P. 2005. The widespread impact of mammalian MicroRNAs on mRNA repression and evolution. *Science,* 310**,** 1817-21.

FELLER, S. M. 2001. Crk family adaptors-signalling complex formation and biological roles. *Oncogene,* 20**,** 6348-71.

FERRANTE, P., MANCUSO, R., PAGANI, E., GUERINI, F. R., CALVO, M. G., SARESELLA, M., SPECIALE, L. & CAPUTO, D. 2000. Molecular evidences for a role of HSV-1 in multiple sclerosis clinical acute attack. *J Neurovirol,* 6 Suppl 2**,** S109-14.

FICKENSCHER, H. & FLECKENSTEIN, B. 2001. Herpesvirus saimiri. *Philos Trans R Soc Lond B Biol Sci,* 356**,** 545-67.

FILIPOWICZ, W., BHATTACHARYYA, S. N. & SONENBERG, N. 2008. Mechanisms of post-transcriptional regulation by microRNAs: are the answers in sight? *Nat Rev Genet,* 9**,** 102-14.

FINGEROTH, J. D., WEIS, J. J., TEDDER, T. F., STROMINGER, J. L., BIRO, P. A. & FEARON, D. T. 1984. Epstein-Barr virus receptor of human B lymphocytes is the C3d receptor CR2. *Proc Natl Acad Sci U S A,* 81**,** 4510-4.

FISH, J. E., SANTORO, M. M., MORTON, S. U., YU, S., YEH, R. F., WYTHE, J. D., IVEY, K. N., BRUNEAU, B. G., STAINIER, D. Y. & SRIVASTAVA, D. 2008. miR-126 regulates angiogenic signaling and vascular integrity. *Dev Cell,* 15**,** 272-84.

FLANO, E., WOODLAND, D. L. & BLACKMAN, M. A. 2002. A mouse model for infectious mononucleosis. *Immunol Res,* 25**,** 201-17.

FLECKENSTEIN, B. & ENSSER, A. 2004. Herpesvirus saimiri transformation of human T lymphocytes. *Curr Protoc Immunol,* Chapter 7**,** Unit 7 21.

FORGAC, M. 2007. Vacuolar ATPases: rotary proton pumps in physiology and pathophysiology. *Nat Rev Mol Cell Biol,* 8**,** 917-29.

FOSSUM, E., FRIEDEL, C. C., RAJAGOPALA, S. V., TITZ, B., BAIKER, A., SCHMIDT, T., KRAUS, T., STELLBERGER, T., RUTENBERG, C., SUTHRAM, S., BANDYOPADHYAY, S., ROSE, D., VON BRUNN, A., UHLMANN, M., ZERETZKE, C., DONG, Y. A., BOULET, H., KOEGL, M., BAILER, S. M., KOSZINOWSKI, U., IDEKER, T., UETZ, P., ZIMMER, R. & HAAS, J. 2009. Evolutionarily conserved herpesviral protein interaction networks. *Plos Pathogens,* 5**,** e1000570.

FROLICH, K., LI, H. & MULLER-DOBLIES, U. 1998. Serosurvey for antibodies to malignant catarrhal fever-associated viruses in free-living and captive cervids in Germany. *J Wildl Dis,* 34**,** 777-82.

GANDHI, M. K., WILLS, M. R., SISSONS, J. G. P. & CARMICHAEL, A. J. 2003. Human cytomegalovirus-specific immunity following haemopoietic stem cell transplantation. *Blood Reviews,* 17**,** 259-264.

GANEM, D. 2010. KSHV and the pathogenesis of Kaposi sarcoma: listening to human biology and medicine. *J Clin Invest,* 120**,** 939-49.

GAO, F. B. 2010. Context-dependent functions of specific microRNAs in neuronal development. *Neural Dev,* 5**,** 25.

GARBER, D. A., BEVERLEY, S. M. & COEN, D. M. 1993. Demonstration of circularization of herpes simplex virus DNA following infection using pulsed field gel electrophoresis. *Virology,* 197**,** 459-62.

GARBER, D. A., SCHAFFER, P. A. & KNIPE, D. M. 1997. A LAT-associated function reduces productive-cycle gene expression during acute infection of murine sensory neurons with herpes simplex virus type 1. *Journal of Virology,* 71**,** 5885-93.

GASTEIER, J. E., MADRID, R., KRAUTKRAMER, E., SCHRODER, S., MURANYI, W., BENICHOU, S. & FACKLER, O. T. 2003. Activation of the Rac-binding partner FHOD1 induces actin stress fibers via a ROCK-dependent mechanism. *J Biol Chem,* 278**,** 38902-12.

GERAGHTY, R. J., KRUMMENACHER, C., COHEN, G. H., EISENBERG, R. J. & SPEAR, P. G. 1998. Entry of alphaherpesviruses mediated by poliovirus receptor-related protein 1 and poliovirus receptor. *Science,* 280**,** 1618-20.

GERSTER, T. & ROEDER, R. G. 1988. A Herpesvirus Trans-Activating Protein Interacts with Transcription Factor Otf-1 and Other Cellular Proteins. *Proc Natl Acad Sci U S A,* 85**,** 6347-6351.

GHILDIYAL, M., XU, J., SEITZ, H., WENG, Z. & ZAMORE, P. D. 2010. Sorting of Drosophila small silencing RNAs partitions microRNA* strands into the RNA interference pathway. *RNA,* 16**,** 43-56.

GIROUX, V., IOVANNA, J. L., GARCIA, S. & DAGORN, J. C. 2009. Combined inhibition of PAK7, MAP3K7 and CK2alpha kinases inhibits the growth of MiaPaCa2 pancreatic cancer cell xenografts. *Cancer Gene Ther,* 16**,** 731-40.

GONG, M. & KIEFF, E. 1990. Intracellular Trafficking of 2 Major Epstein-Barr-Virus Glycoproteins, Gp350/220 and Gp110. *Journal of Virology,* 64**,** 1507-1516.

GONZALEZ, C. M., WONG, E. L., BOWSER, B. S., HONG, G. K., KENNEY, S. & DAMANIA, B. 2006. Identification and characterization of the Orf49 protein of Kaposi's sarcoma-associated herpesvirus. *Journal of Virology,* 80**,** 3062-70.

GOODWIN, D. J., HALL, K. T., GILES, M. S., CALDERWOOD, M. A., MARKHAM, A. F. & WHITEHOUSE, A. 2000. The carboxy terminus of the herpesvirus saimiri ORF 57 gene contains domains that are required for transactivation and transrepression. *Journal of General Virology,* 81**,** 2253-2265.

GOODWIN, D. J., WALTERS, M. S., SMITH, P. G., THURAU, M., FICKENSCHER, H. & WHITEHOUSE, A. 2001. Herpesvirus saimiri open reading frame 50 (Rta) protein reactivates the lytic replication cycle in a persistently infected A549 cell line. *Journal of Virology,* 75**,** 4008-13.

GORDON, Y. J., JOHNSON, B., ROMANOWSKI, E. & ARAULLO-CRUZ, T. 1988. RNA complementary to herpes simplex virus type 1 ICP0 gene demonstrated in neurons of human trigeminal ganglia. *Journal of Virology,* 62**,** 1832-5.

GOTTWEIN, E., CORCORAN, D. L., MUKHERJEE, N., SKALSKY, R. L., HAFNER, M., NUSBAUM, J. D., SHAMULAILATPAM, P., LOVE, C. L., DAVE, S. S., TUSCHL, T., OHLER, U. & CULLEN, B. R. 2011. Viral microRNA targetome of KSHV-infected primary effusion lymphoma cell lines. *Cell Host Microbe,* 10**,** 515-26.

GOTTWEIN, E. & CULLEN, B. R. 2007. Protocols for expression and functional analysis of viral microRNAs. *Methods Enzymol,* 427**,** 229-43.

GOTTWEIN, E. & CULLEN, B. R. 2010. A human herpesvirus microRNA inhibits p21 expression and attenuates p21-mediated cell cycle arrest. *Journal of Virology,* 84**,** 5229-37.

GRADOVILLE, L., GERLACH, J., GROGAN, E., SHEDD, D., NIKIFOROW, S., METROKA, C. & MILLER, G. 2000. Kaposi's sarcoma-associated herpesvirus open reading frame 50/Rta protein activates the entire viral lytic cycle in the HH-B2 primary effusion lymphoma cell line. *Journal of Virology,* 74**,** 6207-12.

GRANNEMAN, S., KUDLA, G., PETFALSKI, E. & TOLLERVEY, D. 2009. Identification of protein binding sites on U3 snoRNA and pre-rRNA by UV cross-linking and high-throughput analysis of cDNAs. *Proc Natl Acad Sci U S A,* 106**,** 9613-8.

GREEN, M. L., LEISENRING, W., STACHEL, D., PERGAM, S. A., SANDMAIER, B. M., WALD, A., COREY, L. & BOECKH, M. 2012. Efficacy of a Viral Load-Based, Risk-Adapted, Preemptive Treatment Strategy for Prevention of Cytomegalovirus Disease after Hematopoietic Cell Transplantation. *Biology of Blood and Marrow Transplantation,* 18**,** 1687-1699.

GREGORY, R. I., CHENDRIMADA, T. P., COOCH, N. & SHIEKHATTAR, R. 2005. Human RISC couples microRNA biogenesis and posttranscriptional gene silencing. *Cell,* 123**,** 631-40.

GREY, F., ANTONIEWICZ, A., ALLEN, E., SAUGSTAD, J., MCSHEA, A., CARRINGTON, J. C. & NELSON, J. 2005. Identification and characterization of human cytomegalovirus-encoded microRNAs. *Journal of Virology,* 79**,** 12095-12099.

GREY, F., MEYERS, H., WHITE, E. A., SPECTOR, D. H. & NELSON, J. 2007. A human cytomegalovirus-encoded microRNA regulates expression of multiple viral genes involved in replication. *Plos Pathogens,* 3**,** e163.

GREY, F., TIRABASSI, R., MEYERS, H., WU, G., MCWEENEY, S., HOOK, L. & NELSON, J. A. 2010. A viral microRNA down-regulates multiple cell cycle genes through mRNA 5'UTRs. *Plos Pathogens,* 6**,** e1000967.

GRIFFITHS-JONES, S., GROCOCK, R. J., VAN DONGEN, S., BATEMAN, A. & ENRIGHT, A. J. 2006. miRBase: microRNA sequences, targets and gene nomenclature. *Nucleic Acids Res,* 34**,** D140-4.

GRIMSON, A., FARH, K. K., JOHNSTON, W. K., GARRETT-ENGELE, P., LIM, L. P. & BARTEL, D. P. 2007. MicroRNA targeting specificity in mammals: determinants beyond seed pairing. *Mol Cell,* 27**,** 91-105.

GRONDIN, B. & DELUCA, N. 2000. Herpes simplex virus type 1 ICP4 promotes transcription preinitiation complex formation by enhancing the binding of TFIID to DNA. *Journal of Virology,* 74**,** 11504-11510.

GRUENBERG, J. & VAN DER GOOT, F. G. 2006. Mechanisms of pathogen entry through the endosomal compartments. *Nat Rev Mol Cell Biol,* 7**,** 495-504.

GRUNDHOFF, A. & GANEM, D. 2003. The latency-associated nuclear antigen of Kaposi's sarcoma-associated herpesvirus permits replication of terminal repeat-containing plasmids. *Journal of Virology,* 77**,** 2779-83.

GRUNDHOFF, A. & SULLIVAN, C. S. 2011. Virus-encoded microRNAs. *Virology,* 411**,** 325-43.

GU, S., JIN, L., ZHANG, F., SARNOW, P. & KAY, M. A. 2009. Biological basis for restriction of microRNA targets to the 3' untranslated region in mammalian mRNAs. *Nat Struct Mol Biol,* 16**,** 144-50.

HAASCH, D., CHEN, Y. W., REILLY, R. M., CHIOU, X. G., KOTERSKI, S., SMITH, M. L., KROEGER, P., MCWEENY, K., HALBERT, D. N., MOLLISON, K. W., DJURIC, S. W. & TREVILLYAN, J. M. 2002. T cell activation induces a noncoding RNA transcript sensitive to inhibition by immunosuppressant drugs and encoded by the proto-oncogene, BIC. *Cell Immunol,* 217**,** 78-86.

HAASE, A. D., JASKIEWICZ, L., ZHANG, H., LAINE, S., SACK, R., GATIGNOL, A. & FILIPOWICZ, W. 2005. TRBP, a regulator of cellular PKR and HIV-1 virus expression, interacts with Dicer and functions in RNA silencing. *EMBO Rep,* 6**,** 961-7.

HADDAD, R. S. & HUTT-FLETCHER, L. M. 1989. Depletion of glycoprotein gp85 from virosomes made with Epstein-Barr virus proteins abolishes their ability to fuse with virus receptor-bearing cells. *Journal of Virology,* 63**,** 4998-5005.

HAECKER, I., GAY, L. A., YANG, Y., HU, J., MORSE, A. M., MCINTYRE, L. M. & RENNE, R. 2012. Ago HITS-CLIP expands understanding of Kaposi's sarcoma-associated herpesvirus miRNA function in primary effusion lymphomas. *Plos Pathogens,* 8**,** e1002884.

HAFNER, M., LANDTHALER, M., BURGER, L., KHORSHID, M., HAUSSER, J., BERNINGER, P., ROTHBALLER, A., ASCANO, M., JUNGKAMP, A. C., MUNSCHAUER, M., ULRICH, A., WARDLE, G. S., DEWELL, S., ZAVOLAN, M. & TUSCHL, T. 2010. PAR-CliP--a method to identify transcriptome-wide the binding sites of RNA binding proteins. *J Vis Exp*.

HAHN, D., KUDLA, G., TOLLERVEY, D. & BEGGS, J. D. 2012. Brr2p-mediated conformational rearrangements in the spliceosome during activation and substrate repositioning. *Genes Dev,* 26**,** 2408-21.

HAIG, D. M., GRANT, D., DEANE, D., CAMPBELL, I., THOMSON, J., JEPSON, C., BUXTON, D. & RUSSELL, G. C. 2008. An immunisation strategy for the protection of cattle against alcelaphine herpesvirus-1-induced malignant catarrhal fever. *Vaccine,* 26**,** 4461-8.

HAMZA, M. S., REYES, R. A., IZUMIYA, Y., WISDOM, R., KUNG, H. J. & LUCIW, P. A. 2004. ORF36 protein kinase of Kaposi's sarcoma herpesvirus activates the c-Jun N-terminal kinase signaling pathway. *J Biol Chem,* 279**,** 38325-30.

HANSEN, A., HENDERSON, S., LAGOS, D., NIKITENKO, L., COULTER, E., ROBERTS, S., GRATRIX, F., PLAISANCE, K., RENNE, R., BOWER, M., KELLAM, P. & BOSHOFF, C. 2010. KSHV-encoded miRNAs target MAF to induce endothelial cell reprogramming. *Genes Dev,* 24**,** 195-205.

HAQUE, M., DAVIS, D. A., WANG, V., WIDMER, I. & YARCHOAN, R. 2003. Kaposi's sarcoma-associated herpesvirus (human herpesvirus 8) contains hypoxia response elements: relevance to lytic induction by hypoxia. *Journal of Virology,* 77**,** 6761-8.

HAQUE, T., THOMAS, J. A., FALK, K. I., PARRATT, R., HUNT, B. J., YACOUB, M. & CRAWFORD, D. H. 1996. Transmission of donor Epstein-Barr virus (EBV) in transplanted organs causes lymphoproliferative disease in EBV-seronegative recipients. *Journal of General Virology,* 77 (Pt 6)**,** 1169-72.

HARDWICK, J. M., LIEBERMAN, P. M. & HAYWARD, S. D. 1988. A New Epstein-Barr Virus Transactivator, R, Induces Expression of a Cytoplasmic Early Antigen. *Journal of Virology,* 62**,** 2274-2284.

HARDY, W. R. & SANDRI-GOLDIN, R. M. 1994. Herpes simplex virus inhibits host cell splicing, and regulatory protein ICP27 is required for this effect. *Journal of Virology,* 68**,** 7790-9.

HART, J., ACKERMANN, M., JAYAWARDANE, G., RUSSELL, G., HAIG, D. M., REID, H. & STEWART, J. P. 2007. Complete sequence and analysis of the ovine herpesvirus 2 genome. *Journal of General Virology,* 88**,** 28-39.

HAYWARD, S. D. 2004. Viral interactions with the Notch pathway. *Semin Cancer Biol,* 14**,** 387-96.

HELDWEIN, E. E., LOU, H., BENDER, F. C., COHEN, G. H., EISENBERG, R. J. & HARRISON, S. C. 2006. Crystal structure of glycoprotein B from herpes simplex virus 1. *Science,* 313**,** 217-20.

HELWAK, A., KUDLA, G., DUDNAKOVA, T. & TOLLERVEY, D. 2013. Mapping the human miRNA interactome by CLASH reveals frequent noncanonical binding. *Cell,* 153**,** 654-65.

HELWAK, A. & TOLLERVEY, D. 2014. Mapping the miRNA interactome by cross-linking ligation and sequencing of hybrids (CLASH). *Nat Protoc,* 9**,** 711-28.

HENKE, J. I., GOERGEN, D., ZHENG, J., SONG, Y., SCHUTTLER, C. G., FEHR, C., JUNEMANN, C. & NIEPMANN, M. 2008. microRNA-122 stimulates translation of hepatitis C virus RNA. *Embo Journal,* 27**,** 3300-10.

HENLE, G. & HENLE, W. 1970. Observations on childhood infections with the Epstein-Barr virus. *J Infect Dis,* 121**,** 303-10.

HENLE, G., HENLE, W. & DIEHL, V. 1968. Relation of Burkitts Tumor-Associated Herpes-Type Virus to Infectious Mononucleosis. *Proc Natl Acad Sci U S A,* 59**,** 94-&.

HERBERMAN, R. B. & ORTALDO, J. R. 1981. Natural killer cells: their roles in defenses against disease. *Science,* 214**,** 24-30.

HERMEKING, H. 2010. The miR-34 family in cancer and apoptosis. *Cell Death Differ,* 17**,** 193-9.

HERROLD, R. E., MARCHINI, A., FRUEHLING, S. & LONGNECKER, R. 1996. Glycoprotein 110, the Epstein-Barr virus homolog of herpes simplex virus glycoprotein B, is essential for Epstein-Barr virus replication in vivo. *Journal of Virology,* 70**,** 2049-54.

HERTEL, J., LINDEMEYER, M., MISSAL, K., FRIED, C., TANZER, A., FLAMM, C., HOFACKER, I. L. & STADLER, P. F. 2006. The expansion of the metazoan microRNA repertoire. *BMC Genomics,* 7**,** 25.

HILL, J. M., SEDARATI, F., JAVIER, R. T., WAGNER, E. K. & STEVENS, J. G. 1990. Herpes simplex virus latent phase transcription facilitates in vivo reactivation. *Virology,* 174**,** 117-25.

HONESS, R. W. & ROIZMAN, B. 1975. Proteins specified by herpes simplex virus. XIII. Glycosylation of viral polypeptides. *Journal of Virology,* 16**,** 1308-26.

HONG, G. K., DELECLUSE, H. J., GRUFFAT, H., MORRISON, T. E., FENG, W. H., SERGEANT, A. & KENNEY, S. C. 2004. The BRRF1 early gene of Epstein-Barr virus encodes a transcription factor that enhances induction of lytic infection by BRLF1. *Journal of Virology,* 78**,** 4983-92.

HOUBEN, A. J. & MOOLENAAR, W. H. 2011. Autotaxin and LPA receptor signaling in cancer. *Cancer Metastasis Rev,* 30**,** 557-65.

HOUSLAY, M. D. & MILLIGAN, G. 1997. Tailoring cAMP-signalling responses through isoform multiplicity. *Trends Biochem Sci,* 22**,** 217-24.

HUANG, Y., ZOU, Q., SONG, H., SONG, F., WANG, L., ZHANG, G. & SHEN, X. 2010. A study of miRNAs targets prediction and experimental validation. *Protein Cell,* 1**,** 979-86.

HUMPHREYS, D. T., WESTMAN, B. J., MARTIN, D. I. & PREISS, T. 2005. MicroRNAs control translation initiation by inhibiting eukaryotic initiation factor 4E/cap and poly(A) tail function. *Proc Natl Acad Sci U S A,* 102**,** 16961-6.

HUNTZINGER, E. & IZAURRALDE, E. 2011. Gene silencing by microRNAs: contributions of translational repression and mRNA decay. *Nat Rev Genet,* 12**,** 99-110.

HUSSAIN, M. U. 2012. Micro-RNAs (miRNAs): genomic organisation, biogenesis and mode of action. *Cell and tissue research,* 349**,** 405-413.

HUTVAGNER, G. & ZAMORE, P. D. 2002. A microRNA in a multiple-turnover RNAi enzyme complex. *Science,* 297**,** 2056-60.

IMTIYAZ, H. Z., WILLIAMS, E. P., HICKEY, M. M., PATEL, S. A., DURHAM, A. C., YUAN, L. J., HAMMOND, R., GIMOTTY, P. A., KEITH, B. & SIMON, M. C. 2010. Hypoxia-inducible factor 2alpha regulates macrophage

function in mouse models of acute and tumor inflammation. *J Clin Invest,* 120**,** 2699-714.

ITO, Y., KIMURA, H., HARA, S., KIDO, S., OZAKI, T., NISHIYAMA, Y. & MORISHIMA, T. 2001. Investigation of varicella-zoster virus DNA in lymphocyte subpopulations by quantitative PCR assay. *Microbiology and Immunology,* 45**,** 267-269.

IZUMI, K. M., KAYE, K. M. & KIEFF, E. D. 1997. The Epstein-Barr virus LMP1 amino acid sequence that engages tumor necrosis factor receptor associated factors is critical for primary B lymphocyte growth transformation. *Proc Natl Acad Sci U S A,* 94**,** 1447-52.

JALECO, A. C., NEVES, H., HOOIJBERG, E., GAMEIRO, P., CLODE, N., HAURY, M., HENRIQUE, D. & PARREIRA, L. 2001. Differential effects of Notch ligands Delta-1 and Jagged-1 in human lymphoid differentiation. *Journal of Experimental Medicine,* 194**,** 991-1002.

JINEK, M. & DOUDNA, J. A. 2009. A three-dimensional view of the molecular machinery of RNA interference. *Nature,* 457**,** 405-12.

JOHN, B., ENRIGHT, A. J., ARAVIN, A., TUSCHL, T., SANDER, C. & MARKS, D. S. 2004. Human MicroRNA targets. *PLoS Biol,* 2**,** e363.

JOHNSON, D. C. & BAINES, J. D. 2011. Herpesviruses remodel host membranes for virus egress. *Nat Rev Microbiol,* 9**,** 382-94.

JOHNSTON, R. J. & HOBERT, O. 2003. A microRNA controlling left/right neuronal asymmetry in Caenorhabditis elegans. *Nature,* 426**,** 845-9.

JONES, C. 2003. Herpes simplex virus type 1 and bovine herpesvirus 1 latency. *Clinical Microbiology Reviews,* 16**,** 79-95.

JURAK, I., KRAMER, M. F., MELLOR, J. C., VAN LINT, A. L., ROTH, F. P., KNIPE, D. M. & COEN, D. M. 2010. Numerous conserved and divergent microRNAs expressed by herpes simplex viruses 1 and 2. *Journal of Virology,* 84**,** 4659-72.

KANELLOPOULOU, C., MULJO, S. A., KUNG, A. L., GANESAN, S., DRAPKIN, R., JENUWEIN, T., LIVINGSTON, D. M. & RAJEWSKY, K. 2005. Dicer-deficient mouse embryonic stem cells are defective in differentiation and centromeric silencing. *Genes Dev,* 19**,** 489-501.

KATO, M., IWASHITA, T., AKHAND, A. A., LIU, W., TAKEDA, K., TAKEUCHI, K., YOSHIHARA, M., HOSSAIN, K., WU, J., DU, J., OH, C., KAWAMOTO, Y., SUZUKI, H., TAKAHASHI, M. & NAKASHIMA, I. 2000. Molecular mechanism of activation and superactivation of Ret tyrosine kinases by ultraviolet light irradiation. *Antioxid Redox Signal,* 2**,** 841-9.

KAWAGUCHI, Y. & KATO, K. 2003. Protein kinases conserved in herpesviruses potentially share a function mimicking the cellular protein kinase cdc2. *Rev Med Virol,* 13**,** 331-40.

KAWAGUCHI, Y., KATO, K., TANAKA, M., KANAMORI, M., NISHIYAMA, Y. & YAMANASHI, Y. 2003. Conserved protein kinases encoded by herpesviruses and cellular protein kinase cdc2 target the same phosphorylation site in eukaryotic elongation factor 1delta. *J Virol,* 77**,** 2359-68.

KAYE, K. M., IZUMI, K. M. & KIEFF, E. 1993. Epstein-Barr virus latent membrane protein 1 is essential for B-lymphocyte growth transformation. *Proc Natl Acad Sci U S A,* 90**,** 9150-4.

KELLY, B. J., FRAEFEL, C., CUNNINGHAM, A. L. & DIEFENBACH, R. J. 2009. Functional roles of the tegument proteins of herpes simplex virus type 1. *Virus Research,* 145**,** 173-86.

KERTESZ, M., IOVINO, N., UNNERSTALL, U., GAUL, U. & SEGAL, E. 2007. The role of site accessibility in microRNA target recognition. *Nat Genet,* 39**,** 1278-84.

KHVOROVA, A., REYNOLDS, A. & JAYASENA, S. D. 2003. Functional siRNAs and miRNAs exhibit strand bias. *Cell,* 115**,** 209-16.

KIM, M. K., JEON, B. N., KOH, D. I., KIM, K. S., PARK, S. Y., YUN, C. O. & HUR, M. W. 2013. Regulation of the cyclin-dependent kinase inhibitor 1A gene (CDKN1A) by the repressor BOZF1 through inhibition of p53 acetylation and transcription factor Sp1 binding. *J Biol Chem,* 288**,** 7053-64.

KIM, O., LI, H. & CRAWFORD, T. B. 2003. Demonstration of sheep-associated malignant catarrhal fever virions in sheep nasal secretions. *Virus Research,* 98**,** 117-22.

KIM, V. N. 2005. MicroRNA biogenesis: coordinated cropping and dicing. *Nat Rev Mol Cell Biol,* 6**,** 376-85.

KIM, V. N., HAN, J. & SIOMI, M. C. 2009. Biogenesis of small RNAs in animals. *Nat Rev Mol Cell Biol,* 10**,** 126-39.

KINCAID, R. P., BURKE, J. M. & SULLIVAN, C. S. 2012. RNA virus microRNA that mimics a B-cell oncomiR. *Proc Natl Acad Sci U S A,* 109**,** 3077-82.

KINCAID, R. P. & SULLIVAN, C. S. 2012. Virus-encoded microRNAs: an overview and a look to the future. *Plos Pathogens,* 8**,** e1003018.

KIRIAKIDOU, M., NELSON, P. T., KOURANOV, A., FITZIEV, P., BOUYIOUKOS, C., MOURELATOS, Z. & HATZIGEORGIOU, A. 2004. A combined computational-experimental approach predicts human microRNA targets. *Genes Dev,* 18**,** 1165-78.

KLUIVER, J., POPPEMA, S., DE JONG, D., BLOKZIJL, T., HARMS, G., JACOBS, S., KROESEN, B. J. & VAN DEN BERG, A. 2005. BIC and miR-155 are highly expressed in Hodgkin, primary mediastinal and diffuse large B cell lymphomas. *Journal of Pathology,* 207**,** 243-9.

KOK, K. H., NG, M. H., CHING, Y. P. & JIN, D. Y. 2007. Human TRBP and PACT directly interact with each other and associate with dicer to facilitate the production of small interfering RNA. *J Biol Chem,* 282**,** 17649-57.

KOLTERUD, Å. & TOFTGÅRD, R. 2008. Strategies for Hedgehog inhibition and its potential role in cancer treatment. *Drug Discovery Today: Therapeutic Strategies,* 4**,** 229-235.

KONIG, H., MATTER, N., BADER, R., THIELE, W. & MULLER, F. 2007. Splicing segregation: the minor spliceosome acts outside the nucleus and controls cell proliferation. *Cell,* 131**,** 718-29.

KORALOV, S. B., MULJO, S. A., GALLER, G. R., KREK, A., CHAKRABORTY, T., KANELLOPOULOU, C., JENSEN, K., COBB, B. S., MERKENSCHLAGER, M., RAJEWSKY, N. & RAJEWSKY, K. 2008.

Dicer ablation affects antibody diversity and cell survival in the B lymphocyte lineage. *Cell,* 132**,** 860-74.

KOZOMARA, A. & GRIFFITHS-JONES, S. 2014. miRBase: annotating high confidence microRNAs using deep sequencing data. *Nucleic Acids Res,* 42**,** D68-73.

KRAMER, S., SCHIMPL, A. & HUNIG, T. 1995. Immunopathology of interleukin (IL) 2-deficient mice: thymus dependence and suppression by thymus-dependent cells with an intact IL-2 gene. *Journal of Experimental Medicine,* 182**,** 1769-76.

KRAMPERT, M., KUENZLE, S., THAI, S. N., LEE, N., IRUELA-ARISPE, M. L. & WERNER, S. 2005. ADAMTS1 proteinase is up-regulated in wounded skin and regulates migration of fibroblasts and endothelial cells. *J Biol Chem,* 280**,** 23844-52.

KRISTIE, T. M., LEBOWITZ, J. H. & SHARP, P. A. 1989. The Octamer-Binding Proteins Form Multi-Protein - DNA Complexes with the Hsv Alpha-Tif Regulatory Protein. *Embo Journal,* 8**,** 4229-4238.

KROH, E. M., PARKIN, R. K., MITCHELL, P. S. & TEWARI, M. 2010. Analysis of circulating microRNA biomarkers in plasma and serum using quantitative reverse transcription-PCR (qRT-PCR). *Methods,* 50**,** 298-301.

KRUGER, J. & REHMSMEIER, M. 2006. RNAhybrid: microRNA target prediction easy, fast and flexible. *Nucleic Acids Res,* 34**,** W451-4.

KUDLA, G., GRANNEMAN, S., HAHN, D., BEGGS, J. D. & TOLLERVEY, D. 2011. Cross-linking, ligation, and sequencing of hybrids reveals RNA-RNA interactions in yeast. *Proc Natl Acad Sci U S A,* 108**,** 10010-5.

KUHN, K., NOWAK, B., KLEIN, G., BEHNKE, A., SEIDEL, A. & LAMPEN, A. 2008. Determination of polycyclic aromatic hydrocarbons in smoked pork by effect-directed bioassay with confirmation by chemical analysis. *J Food Prot,* 71**,** 993-9.

KUNO, K., KANADA, N., NAKASHIMA, E., FUJIKI, F., ICHIMURA, F. & MATSUSHIMA, K. 1997. Molecular cloning of a gene encoding a new type of metalloproteinase-disintegrin family protein with thrombospondin motifs as an inflammation associated gene. *J Biol Chem,* 272**,** 556-62.

KYBURZ, A., FRIEDLEIN, A., LANGEN, H. & KELLER, W. 2006. Direct interactions between subunits of CPSF and the U2 snRNP contribute to the coupling of pre-mRNA 3' end processing and splicing. *Mol Cell,* 23**,** 195-205.

LALL, S., GRUN, D., KREK, A., CHEN, K., WANG, Y. L., DEWEY, C. N., SOOD, P., COLOMBO, T., BRAY, N., MACMENAMIN, P., KAO, H. L., GUNSALUS, K. C., PACHTER, L., PIANO, F. & RAJEWSKY, N. 2006. A genome-wide map of conserved microRNA targets in C. elegans. *Curr Biol,* 16**,** 460-71.

LANDTHALER, M., YALCIN, A. & TUSCHL, T. 2004. The human DiGeorge syndrome critical region gene 8 and Its D. melanogaster homolog are required for miRNA biogenesis. *Curr Biol,* 14**,** 2162-7.

LEE, I., AJAY, S. S., YOOK, J. I., KIM, H. S., HONG, S. H., KIM, N. H., DHANASEKARAN, S. M., CHINNAIYAN, A. M. & ATHEY, B. D. 2009. New class of microRNA targets containing simultaneous 5'-UTR and 3'-UTR interaction sites. *Genome Res,* 19**,** 1175-83.

LEE, R. C. & AMBROS, V. 2001. An extensive class of small RNAs in Caenorhabditis elegans. *Science,* 294**,** 862-4.

LEE, R. C., FEINBAUM, R. L. & AMBROS, V. 1993. The C. elegans heterochronic gene lin-4 encodes small RNAs with antisense complementarity to lin-14. *Cell,* 75**,** 843-54.

LEE, S., CHO, H. J., PARK, J. J., KIM, Y. S., HWANG, S., SUN, R. & SONG, M. J. 2007. The ORF49 protein of murine gammaherpesvirus 68 cooperates with RTA in regulating virus replication. *Journal of Virology,* 81**,** 9870-7.

LEE, S. H., KALEJTA, R. F., KERRY, J., SEMMES, O. J., O'CONNOR, C. M., KHAN, Z., GARCIA, B. A., SHENK, T. & MURPHY, E. 2012. BclAF1 restriction factor is neutralized by proteasomal degradation and microRNA repression during human cytomegalovirus infection. *Proc Natl Acad Sci U S A,* 109**,** 9575-80.

LEE, Y., AHN, C., HAN, J., CHOI, H., KIM, J., YIM, J., LEE, J., PROVOST, P., RADMARK, O., KIM, S. & KIM, V. N. 2003. The nuclear RNase III Drosha initiates microRNA processing. *Nature,* 425**,** 415-9.

LEE, Y., HUR, I., PARK, S. Y., KIM, Y. K., SUH, M. R. & KIM, V. N. 2006. The role of PACT in the RNA silencing pathway. *Embo Journal,* 25**,** 522-32.

LEE, Y., JEON, K., LEE, J. T., KIM, S. & KIM, V. N. 2002. MicroRNA maturation: stepwise processing and subcellular localization. *Embo Journal,* 21**,** 4663-70.

LEE, Y., KIM, M., HAN, J., YEOM, K. H., LEE, S., BAEK, S. H. & KIM, V. N. 2004a. MicroRNA genes are transcribed by RNA polymerase II. *Embo Journal,* 23**,** 4051-60.

LEE, Y. S., NAKAHARA, K., PHAM, J. W., KIM, K., HE, Z., SONTHEIMER, E. J. & CARTHEW, R. W. 2004b. Distinct roles for Drosophila Dicer-1 and Dicer-2 in the siRNA/miRNA silencing pathways. *Cell,* 117**,** 69-81.

LEHMAN, I. R. & BOEHMER, P. E. 1999. Replication of herpes simplex virus DNA. *Journal of Biological Chemistry,* 274**,** 28059-28062.

LEI, X., BAI, Z., YE, F., XIE, J., KIM, C. G., HUANG, Y. & GAO, S. J. 2010. Regulation of NF-kappaB inhibitor IkappaBalpha and viral replication by a KSHV microRNA. *Nat Cell Biol,* 12**,** 193-9.

LEIB, D. A., BOGARD, C. L., KOSZ-VNENCHAK, M., HICKS, K. A., COEN, D. M., KNIPE, D. M. & SCHAFFER, P. A. 1989. A deletion mutant of the latency-associated transcript of herpes simplex virus type 1 reactivates from the latent state with reduced frequency. *Journal of Virology,* 63**,** 2893-900.

LEISEGANG, M. S., MARTIN, R., RAMIREZ, A. S. & BOHNSACK, M. T. 2012. Exportin t and Exportin 5: tRNA and miRNA biogenesis - and beyond. *Biol Chem,* 393**,** 599-604.

LENTING, P. J., CASARI, C., CHRISTOPHE, O. D. & DENIS, C. V. 2012. von Willebrand factor: the old, the new and the unknown. *J Thromb Haemost,* 10**,** 2428-37.

LEUNG, A. K., YOUNG, A. G., BHUTKAR, A., ZHENG, G. X., BOSSON, A. D., NIELSEN, C. B. & SHARP, P. A. 2011. Genome-wide identification of Ago2 binding sites from mouse embryonic stem cells with and without mature microRNAs. *Nat Struct Mol Biol,* 18**,** 237-44.

LEVY, C. S., HOPKINS, J., RUSSELL, G. C. & DALZIEL, R. G. 2012. Novel virus-encoded microRNA molecules expressed by ovine herpesvirus 2-immortalized bovine T-cells. *Journal of General Virology,* 93**,** 150-154.

LEVY PHD THESIS. 2012. *Identification and Characterization of Ovine Herpesvirus 2 microRNAs.* PhD, University of Edinburgh.

LEWIS, B. P., BURGE, C. B. & BARTEL, D. P. 2005. Conserved seed pairing, often flanked by adenosines, indicates that thousands of human genes are microRNA targets. *Cell,* 120**,** 15-20.

LEWIS, B. P., SHIH, I. H., JONES-RHOADES, M. W., BARTEL, D. P. & BURGE, C. B. 2003. Prediction of mammalian microRNA targets. *Cell,* 115**,** 787-98.

LI, H., CUNHA, C. W., O'TOOLE, D., NICOLA, A. V., KNOWLES, D. P. & TAUS, N. S. 2013a. Development of an in vivo system to measure antibody-blocking of ovine herpesvirus 2 entry. *J Virol Methods,* 188**,** 104-7.

LI, H., CUNHA, C. W., TAUS, N. S. & KNOWLES, D. P. 2014. Malignant Catarrhal Fever: Inching Toward Understanding. *Annual Review of Animal Biosciences,* 2**,** 209-233.

LI, H., DYER, N., KELLER, J. & CRAWFORD, T. B. 2000. Newly recognized herpesvirus causing malignant catarrhal fever in white-tailed deer (Odocoileus virginianus). *J Clin Microbiol,* 38**,** 1313-8.

LI, H., GAILBREATH, K., FLACH, E. J., TAUS, N. S., COOLEY, J., KELLER, J., RUSSELL, G. C., KNOWLES, D. P., HAIG, D. M., OAKS, J. L., TRAUL, D. L. & CRAWFORD, T. B. 2005. A novel subgroup of rhadinoviruses in ruminants. *Journal of General Virology,* 86**,** 3021-6.

LI, H., KARNEY, G., O'TOOLE, D. & CRAWFORD, T. B. 2008. Long distance spread of malignant catarrhal fever virus from feedlot lambs to ranch bison. *Can Vet J,* 49**,** 183-5.

LI, H., SHEN, D. T., KNOWLES, D. P., GORHAM, J. R. & CRAWFORD, T. B. 1994. Competitive inhibition enzyme-linked immunosorbent assay for antibody in sheep and other ruminants to a conserved epitope of malignant catarrhal fever virus. *J Clin Microbiol,* 32**,** 1674-9.

LI, H., SHEN, D. T., O'TOOLE, D., KNOWLES, D. P., GORHAM, J. R. & CRAWFORD, T. B. 1995. Investigation of sheep-associated malignant catarrhal fever virus infection in ruminants by PCR and competitive inhibition enzyme-linked immunosorbent assay. *J Clin Microbiol,* 33**,** 2048-53.

LI, H., SNOWDER, G., O'TOOLE, D. & CRAWFORD, T. B. 1998. Transmission of ovine herpesvirus 2 in lambs. *J Clin Microbiol,* 36**,** 223-6.

LI, H., TAUS, N. S., JONES, C., MURPHY, B., EVERMANN, J. F. & CRAWFORD, T. B. 2006. A devastating outbreak of malignant catarrhal fever in a bison feedlot. *J Vet Diagn Invest,* 18**,** 119-23.

LI, H., TAUS, N. S., LEWIS, G. S., KIM, O., TRAUL, D. L. & CRAWFORD, T. B. 2004. Shedding of ovine herpesvirus 2 in sheep nasal secretions: the predominant mode for transmission. *J Clin Microbiol,* 42**,** 5558-64.

LI, H., WESTOVER, W. C. & CRAWFORD, T. B. 1999. Sheep-associated malignant catarrhal fever in a petting zoo. *J Zoo Wildl Med,* 30**,** 408-12.

LI, H., ZHANG, X. Y., WU, T. J., CHENG, W., LIU, X., JIANG, T. T., WEN, J., LI, J., MA, Q. L. & HUA, Z. C. 2013b. Endoplasmic reticulum stress

regulates rat mandibular cartilage thinning under compressive mechanical stress. *J Biol Chem,* 288**,** 18172-83.

LI, Q. J., CHAU, J., EBERT, P. J., SYLVESTER, G., MIN, H., LIU, G., BRAICH, R., MANOHARAN, M., SOUTSCHEK, J., SKARE, P., KLEIN, L. O., DAVIS, M. M. & CHEN, C. Z. 2007. miR-181a is an intrinsic modulator of T cell sensitivity and selection. *Cell,* 129**,** 147-61.

LI, Q. X., SPRIGGS, M. K., KOVATS, S., TURK, S. M., COMEAU, M. R., NEPOM, B. & HUTTFLETCHER, L. M. 1997. Epstein-Barr virus uses HLA class II as a cofactor for infection of B lymphocytes. *Journal of Virology,* 71**,** 4657-4662.

LI, X., FENG, J., CHEN, S., PENG, L., HE, W. W., QI, J., DENG, H. & SUN, R. 2010. Tpl2/AP-1 enhances murine gammaherpesvirus 68 lytic replication. *Journal of Virology,* 84**,** 1881-90.

LI, Y., MASAKI, T., YAMANE, D., MCGIVERN, D. R. & LEMON, S. M. 2013c. Competing and noncompeting activities of miR-122 and the 5' exonuclease Xrn1 in regulation of hepatitis C virus replication. *Proc Natl Acad Sci U S A,* 110**,** 1881-6.

LIGGITT, H. D. & DEMARTINI, J. C. 1980a. The pathomorphology of malignant catarrhal fever. I. Generalized lymphoid vasculitis. *Vet Pathol,* 17**,** 58-72.

LIGGITT, H. D. & DEMARTINI, J. C. 1980b. The pathomorphology of malignant catarrhal fever. II. Multisystemic epithelial lesions. *Vet Pathol,* 17**,** 73-83.

LIGGITT, H. D., DEMARTINI, J. C., MCCHESNEY, A. E., PIERSON, R. E. & STORZ, J. 1978. Experimental transmission of malignant catarrhal fever in cattle: gross and histopathologic changes. *American Journal of Veterinary Research,* 39**,** 1249-57.

LIM, L. P., LAU, N. C., GARRETT-ENGELE, P., GRIMSON, A., SCHELTER, J. M., CASTLE, J., BARTEL, D. P., LINSLEY, P. S. & JOHNSON, J. M. 2005. Microarray analysis shows that some microRNAs downregulate large numbers of target mRNAs. *Nature,* 433**,** 769-73.

LIN, C. C., LIU, L. Z., ADDISON, J. B., WONDERLIN, W. F., IVANOV, A. V. & RUPPERT, J. M. 2011a. A KLF4-miRNA-206 autoregulatory feedback loop can promote or inhibit protein translation depending upon cell context. *Molecular and Cellular Biology,* 31**,** 2513-27.

LIN, J. & CULLEN, B. R. 2007. Analysis of the interaction of primate retroviruses with the human RNA interference machinery. *Journal of Virology,* 81**,** 12218-26.

LIN, X., LIANG, D., HE, Z., DENG, Q., ROBERTSON, E. S. & LAN, K. 2011b. miR-K12-7-5p encoded by Kaposi's sarcoma-associated herpesvirus stabilizes the latent state by targeting viral ORF50/RTA. *PLoS ONE,* 6**,** e16224.

LINGEL, A., SIMON, B., IZAURRALDE, E. & SATTLER, M. 2003. Structure and nucleic-acid binding of the Drosophila Argonaute 2 PAZ domain. *Nature,* 426**,** 465-9.

LINGEL, A., SIMON, B., IZAURRALDE, E. & SATTLER, M. 2004. Nucleic acid 3'-end recognition by the Argonaute2 PAZ domain. *Nat Struct Mol Biol,* 11**,** 576-7.

LIU, C., MALLICK, B., LONG, D., RENNIE, W. A., WOLENC, A., CARMACK, C. S. & DING, Y. 2013. CLIP-based prediction of mammalian microRNA binding sites. *Nucleic Acids Res,* 41**,** e138.

LIU, J., CARMELL, M. A., RIVAS, F. V., MARSDEN, C. G., THOMSON, J. M., SONG, J. J., HAMMOND, S. M., JOSHUA-TOR, L. & HANNON, G. J. 2004. Argonaute2 is the catalytic engine of mammalian RNAi. *Science,* 305**,** 1437-41.

LIU, J., VALENCIA-SANCHEZ, M. A., HANNON, G. J. & PARKER, R. 2005. MicroRNA-dependent localization of targeted mRNAs to mammalian P-bodies. *Nat Cell Biol,* 7**,** 719-23.

LO, A. K. F., TO, K. F., LO, K. W., LUNG, R. W. M., HUI, J. W. Y., LIAO, G. & HAYWARD, S. D. 2007. Modulation of LMP1 protein expression by EBV-encoded microRNAs. *Proceedings of the National Academy of Sciences,* 104**,** 16164-16169.

LOKEN, T., ALEKSANDERSEN, M., REID, H. & POW, I. 1998. Malignant catarrhal fever caused by ovine herpesvirus-2 in pigs in Norway. *Veterinary Record,* 143**,** 464-7.

LOKEN, T., BOSMAN, A. M. & VAN VUUREN, M. 2009. Infection with Ovine herpesvirus 2 in Norwegian herds with a history of previous outbreaks of malignant catarrhal fever. *J Vet Diagn Invest,* 21**,** 257-61.

LONGNECKER, R. 2000. Epstein-Barr virus latency: LMP2, a regulator or means for Epstein-Barr virus persistence? *Adv Cancer Res,* 79**,** 175-200.

LU, F., STEDMAN, W., YOUSEF, M., RENNE, R. & LIEBERMAN, P. M. 2010. Epigenetic regulation of Kaposi's sarcoma-associated herpesvirus latency by virus-encoded microRNAs that target Rta and the cellular Rbl2-DNMT pathway. *Journal of Virology,* 84**,** 2697-706.

LU, J., VERMA, S. C., CAI, Q., SAHA, A., DZENG, R. K. & ROBERTSON, E. S. 2012. The RBP-Jkappa binding sites within the RTA promoter regulate KSHV latent infection and cell proliferation. *Plos Pathogens,* 8**,** e1002479.

LUKAC, D. M., KIRSHNER, J. R. & GANEM, D. 1999. Transcriptional activation by the product of open reading frame 50 of Kaposi's sarcoma-associated herpesvirus is required for lytic viral reactivation in B cells. *Journal of Virology,* 73**,** 9348-61.

LUO, Z., WEN, G., WANG, G., PU, X., YE, S., XU, Q., WANG, W. & XIAO, Q. 2013. MicroRNA-200C and -150 play an important role in endothelial cell differentiation and vasculogenesis by targeting transcription repressor ZEB1. *Stem Cells,* 31**,** 1749-62.

LYTLE, J. R., YARIO, T. A. & STEITZ, J. A. 2007. Target mRNAs are repressed as efficiently by microRNA-binding sites in the 5' UTR as in the 3' UTR. *Proc Natl Acad Sci U S A,* 104**,** 9667-72.

MA, F., LIU, X., LI, D., WANG, P., LI, N., LU, L. & CAO, X. 2010. MicroRNA-466l upregulates IL-10 expression in TLR-triggered macrophages by antagonizing RNA-binding protein tristetraprolin-mediated IL-10 mRNA degradation. *J Immunol,* 184**,** 6053-9.

MA, J. B., YE, K. & PATEL, D. J. 2004. Structural basis for overhang-specific small interfering RNA recognition by the PAZ domain. *Nature,* 429**,** 318-22.

MA, J. B., YUAN, Y. R., MEISTER, G., PEI, Y., TUSCHL, T. & PATEL, D. J. 2005. Structural basis for 5'-end-specific recognition of guide RNA by the A. fulgidus Piwi protein. *Nature,* 434**,** 666-70.

MACRAE, I. J. & DOUDNA, J. A. 2007. Ribonuclease revisited: structural insights into ribonuclease III family enzymes. *Curr Opin Struct Biol,* 17**,** 138-45.

MACRAE, I. J., MA, E., ZHOU, M., ROBINSON, C. V. & DOUDNA, J. A. 2008. In vitro reconstitution of the human RISC-loading complex. *Proc Natl Acad Sci U S A,* 105**,** 512-7.

MACRAE, I. J., ZHOU, K. & DOUDNA, J. A. 2007. Structural determinants of RNA recognition and cleavage by Dicer. *Nat Struct Mol Biol,* 14**,** 934-40.

MAILLARD, I., FANG, T. & PEAR, W. S. 2005. Regulation of lymphoid development, differentiation, and function by the Notch pathway. *Annu Rev Immunol,* 23**,** 945-74.

MAJERCIAK, V., YAMANEGI, K., ALLEMAND, E., KRUHLAK, M., KRAINER, A. R. & ZHENG, Z. M. 2008. Kaposi's sarcoma-associated herpesvirus ORF57 functions as a viral splicing factor and promotes expression of intron-containing viral lytic genes in spliceosome-mediated RNA splicing. *Journal of Virology,* 82**,** 2792-801.

MAKEYEV, E. V., ZHANG, J., CARRASCO, M. A. & MANIATIS, T. 2007. The MicroRNA miR-124 promotes neuronal differentiation by triggering brain-specific alternative pre-mRNA splicing. *Mol Cell,* 27**,** 435-48.

MANABE, T., YOSHIMORI, T., HENOMATSU, N. & TASHIRO, Y. 1993. Inhibitors of vacuolar-type H(+)-ATPase suppresses proliferation of cultured cells. *J Cell Physiol,* 157**,** 445-52.

MANIATAKI, E., DE PLANELL SAGUER, M. D. & MOURELATOS, Z. 2005. Immunoprecipitation of microRNPs and directional cloning of microRNAs. *Methods Mol Biol,* 309**,** 283-94.

MARKHAM, N. R. & ZUKER, M. 2008. UNAFold: software for nucleic acid folding and hybridization. *Methods Mol Biol,* 453**,** 3-31.

MARONEY, P. A., YU, Y. & NILSEN, T. W. 2006. MicroRNAs, mRNAs, and translation. *Cold Spring Harb Symp Quant Biol,* 71**,** 531-5.

MARSHALL, V., PARKS, T., BAGNI, R., WANG, C. D., SAMOLS, M. A., HU, J., WYVIL, K. M., ALEMAN, K., LITTLE, R. F., YARCHOAN, R., RENNE, R. & WHITBY, D. 2007. Conservation of virally encoded microRNAs in Kaposi sarcoma--associated herpesvirus in primary effusion lymphoma cell lines and in patients with Kaposi sarcoma or multicentric Castleman disease. *J Infect Dis,* 195**,** 645-59.

MARTIN, M. 2011. Cutadapt removes adapter sequences from high-throughput sequencing reads. *EMBnet. journal,* 17**,** pp. 10-12.

MARTINEZ, F. P. & TANG, Q. 2012. Leucine zipper domain is required for Kaposi sarcoma-associated herpesvirus (KSHV) K-bZIP protein to interact with histone deacetylase and is important for KSHV replication. *J Biol Chem,* 287**,** 15622-34.

MARTUCCIELLO, A., MARIANELLI, C., CAPUANO, M., ASTARITA, S., ALFANO, D. & GALIERO, G. 2006. An outbreak of malignant catarrhal fever in Mediterranean water buffalo (Bubalus bubalis). *Large Animal Review,* 12**,** 21-24.

MATHONNET, G., FABIAN, M. R., SVITKIN, Y. V., PARSYAN, A., HUCK, L., MURATA, T., BIFFO, S., MERRICK, W. C., DARZYNKIEWICZ, E., PILLAI, R. S., FILIPOWICZ, W., DUCHAINE, T. F. & SONENBERG, N. 2007. MicroRNA inhibition of translation initiation in vitro by targeting the cap-binding complex eIF4F. *Science,* 317**,** 1764-7.

MAXWELL, P. H. 2005. Hypoxia-inducible factor as a physiological regulator. *Exp Physiol,* 90**,** 791-7.

MCGEOCH, D. J. & DAVISON, A. J. 1999. The descent of human herpesvirus 8. *Semin Cancer Biol,* 9**,** 201-9.

MEIER-TRUMMER, C. S., REHRAUER, H., FRANCHINI, M., PATRIGNANI, A., WAGNER, U. & ACKERMANN, M. 2009. Malignant catarrhal fever of cattle is associated with low abundance of IL-2 transcript and a predominantly latent profile of ovine herpesvirus 2 gene expression. *PLoS ONE,* 4**,** e6265.

MEIER-TRUMMER, C. S., RYF, B. & ACKERMANN, M. 2010. Identification of peripheral blood mononuclear cells targeted by Ovine herpesvirus-2 in sheep. *Vet Microbiol,* 141**,** 199-207.

MEIJER, H. A., KONG, Y. W., LU, W. T., WILCZYNSKA, A., SPRIGGS, R. V., ROBINSON, S. W., GODFREY, J. D., WILLIS, A. E. & BUSHELL, M. 2013. Translational repression and eIF4A2 activity are critical for microRNA-mediated gene regulation. *Science,* 340**,** 82-5.

MEISTER, G., LANDTHALER, M., PATKANIOWSKA, A., DORSETT, Y., TENG, G. & TUSCHL, T. 2004. Human Argonaute2 mediates RNA cleavage targeted by miRNAs and siRNAs. *Mol Cell,* 15**,** 185-97.

MELENDEZ, L. V., DANIEL, M. D., HUNT, R. D. & GARCIA, F. G. 1968. An apparently new herpesvirus from primary kidney cultures of the squirrel monkey (Saimiri sciureus). *Lab Anim Care,* 18**,** 374-81.

METEYER, C. U., GONZALES, B. J., HEUSCHELE, W. P. & HOWARD, E. B. 1989. Epidemiologic and pathologic aspects of an epizootic of malignant catarrhal fever in exotic hoofstock. *J Wildl Dis,* 25**,** 280-6.

METTAM, R. 1924. Snotsiekte in Cattle. *9th & 10th Report, Director Veterinary Education & Research, Union South Africa 1923.***,** 395-432.

METTENLEITER, T. C. 2002. Herpesvirus assembly and egress. *Journal of Virology,* 76**,** 1537-47.

METTENLEITER, T. C., MULLER, F., GRANZOW, H. & KLUPP, B. G. 2013. The way out: what we know and do not know about herpesvirus nuclear egress. *Cellular Microbiology,* 15**,** 170-8.

METZLER, A. E. 1991. The malignant catarrhal fever complex. *Comp Immunol Microbiol Infect Dis,* 14**,** 107-24.

MILLER, N. & HUTT-FLETCHER, L. M. 1988. A monoclonal antibody to glycoprotein gp85 inhibits fusion but not attachment of Epstein-Barr virus. *Journal of Virology,* 62**,** 2366-72.

MILLER, N. & HUTT-FLETCHER, L. M. 1992. Epstein-Barr virus enters B cells and epithelial cells by different routes. *Journal of Virology,* 66**,** 3409-14.

MIRANDA, K. C., HUYNH, T., TAY, Y., ANG, Y. S., TAM, W. L., THOMSON, A. M., LIM, B. & RIGOUTSOS, I. 2006. A pattern-based method for the

identification of MicroRNA binding sites and their corresponding heteroduplexes. *Cell,* 126**,** 1203-17.

MOCARSKI, E. S. 2004. Immune escape and exploitation strategies of cytomegaloviruses: impact on and imitation of the major histocompatibility system. *Cellular Microbiology,* 6**,** 707-717.

MOHR, C. A., CICIN-SAIN, L., WAGNER, M., SACHER, T., SCHNEE, M., RUZSICS, Z. & KOSZINOWSKI, U. H. 2008. Engineering of cytomegalovirus genomes for recombinant live herpesvirus vaccines. *Int J Med Microbiol,* 298**,** 115-25.

MONTAGNER, S., ORLANDI, E. M., MERANTE, S. & MONTICELLI, S. 2013. The role of miRNAs in mast cells and other innate immune cells. *Immunol Rev,* 253**,** 12-24.

MONTEYS, A. M., SPENGLER, R. M., WAN, J., TECEDOR, L., LENNOX, K. A., XING, Y. & DAVIDSON, B. L. 2010. Structure and activity of putative intronic miRNA promoters. *RNA,* 16**,** 495-505.

MOORE, D. A., KOHRS, P., BASZLER, T., FAUX, C., SATHRE, P., WENZ, J. R., ELDRIDGE, L. & LI, H. 2010. Outbreak of malignant catarrhal fever among cattle associated with a state livestock exhibition. *Journal of the American Veterinary Medical Association,* 237**,** 87-92.

MOORE, P. S. & CHANG, Y. 2001. Molecular virology of Kaposi's sarcoma-associated herpesvirus. *Philos Trans R Soc Lond B Biol Sci,* 356**,** 499-516.

MORIMURA, T., FUJITA, K., AKITA, M., NAGASHIMA, M. & SATOMI, A. 2008. The proton pump inhibitor inhibits cell growth and induces apoptosis in human hepatoblastoma. *Pediatr Surg Int,* 24**,** 1087-94.

MORIUCHI, H., MORIUCHI, M., STRAUS, S. E. & COHEN, J. I. 1993. Varicella-zoster virus open reading frame 10 protein, the herpes simplex virus VP16 homolog, transactivates herpesvirus immediate-early gene promoters. *Journal of Virology,* 67**,** 2739-46.

MORTIMER, S. A. & DOUDNA, J. A. 2013. Unconventional miR-122 binding stabilizes the HCV genome by forming a trimolecular RNA structure. *Nucleic Acids Res,* 41**,** 4230-40.

MOURELATOS, Z., DOSTIE, J., PAUSHKIN, S., SHARMA, A., CHARROUX, B., ABEL, L., RAPPSILBER, J., MANN, M. & DREYFUSS, G. 2002. miRNPs: a novel class of ribonucleoproteins containing numerous microRNAs. *Genes Dev,* 16**,** 720-8.

MULLER-DOBLIES, U. U., EGLI, J., LI, H., BRAUN, U. & ACKERMANN, M. 2001. [Malignant catarrhal fever in Switzerland. 1.Epidemiology]. *Schweiz Arch Tierheilkd,* 143**,** 173-83.

MULLER-DOBLIES, U. U., LI, H., HAUSER, B., ADLER, H. & ACKERMANN, M. 1998. Field validation of laboratory tests for clinical diagnosis of sheep-associated malignant catarrhal fever. *J Clin Microbiol,* 36**,** 2970-2.

MULLER, J.-M., CHEVRIER, L., COCHAUD, S., MEUNIER, A.-C. & CHADENEAU, C. 2008. Hedgehog, Notch and Wnt developmental pathways as targets for anti-cancer drugs. *Drug Discovery Today: Disease Mechanisms,* 4**,** 285-291.

MURPHY, A. J., GUYRE, P. M. & PIOLI, P. A. 2010. Estradiol suppresses NF-kappa B activation through coordinated regulation of let-7a and miR-125b in primary human macrophages. *J Immunol,* 184**,** 5029-37.

MURPHY, E., VANICEK, J., ROBINS, H., SHENK, T. & LEVINE, A. J. 2008. Suppression of immediate-early viral gene expression by herpesvirus-coded microRNAs: implications for latency. *Proc Natl Acad Sci U S A,* 105**,** 5453-8.

MURPHY, E., YU, D., GRIMWOOD, J., SCHMUTZ, J., DICKSON, M., JARVIS, M. A., HAHN, G., NELSON, J. A., MYERS, R. M. & SHENK, T. E. 2003. Coding potential of laboratory and clinical strains of human cytomegalovirus. *Proc Natl Acad Sci U S A,* 100**,** 14976-81.

MUSHI, E. Z. 1980. The proliferation of malignant catarrhal fever virus in cattle and rabbits. *Bull Anim Health Prod Afr,* 28**,** 85-9.

MUSHI, E. Z., JESSETT, D. M., RURANGIRWA, F. R., ROSSITER, P. B. & KARSTAD, L. 1981. Neutralising antibodies to malignant catarrhal fever herpesvirus in wildebeest nasal secretions. *Trop Anim Health Prod,* 13**,** 55-6.

MUSHI, E. Z. & RURANGIRWA, F. R. 1981. Epidemiology of bovine malignant catarrhal fevers, a review. *Vet Res Commun,* 5**,** 127-42.

MUYLKENS, B., COUPEAU, D., DAMBRINE, G., TRAPP, S. & RASSCHAERT, D. 2010. Marek's disease virus microRNA designated Mdv1-pre-miR-M4 targets both cellular and viral genes. *Archives of Virology,* 155**,** 1823-37.

MWANGI, W. N., SMITH, L. P., BAIGENT, S. J., BEAL, R. K., NAIR, V. & SMITH, A. L. 2011. Clonal structure of rapid-onset MDV-driven CD4+ lymphomas and responding CD8+ T cells. *Plos Pathogens,* 7**,** e1001337.

NACHMANI, D., STERN-GINOSSAR, N., SARID, R. & MANDELBOIM, O. 2009. Diverse herpesvirus microRNAs target the stress-induced immune ligand MICB to escape recognition by natural killer cells. *Cell Host Microbe,* 5**,** 376-85.

NASCIMENTO, R., DIAS, J. D. & PARKHOUSE, R. M. 2009. The conserved UL24 family of human alpha, beta and gamma herpesviruses induces cell cycle arrest and inactivation of the cyclinB/cdc2 complex. *Archives of Virology,* 154**,** 1143-9.

NASCIMENTO, R. & PARKHOUSE, R. M. 2007. Murine gammaherpesvirus 68 ORF20 induces cell-cycle arrest in G2 by inhibiting the Cdc2-cyclin B complex. *Journal of General Virology,* 88**,** 1446-53.

NASH, A. A., DUTIA, B. M., STEWART, J. P. & DAVISON, A. J. 2001. Natural history of murine gamma-herpesvirus infection. *Philos Trans R Soc Lond B Biol Sci,* 356**,** 569-79.

NEIMANIS, A. S., HILL, J. E., JARDINE, C. M. & BOLLINGER, T. K. 2009. Sheep-associated malignant catarrhal fever in free-ranging moose (Alces alces) in Saskatchewan, Canada. *J Wildl Dis,* 45**,** 213-7.

NELSON, B. H. 2004. IL-2, regulatory T cells, and tolerance. *J Immunol,* 172**,** 3983-8.

NELSON, D. D., DAVIS, W. C., BROWN, W. C., LI, H., O'TOOLE, D. & OAKS, J. L. 2010. CD8(+)/perforin(+)/WC1(-) gammadelta T cells, not CD8(+) alphabeta T cells, infiltrate vasculitis lesions of American bison (Bison bison) with experimental sheep-associated malignant catarrhal fever. *Vet Immunol Immunopathol,* 136**,** 284-91.

NEVELS, M., NITZSCHE, A. & PAULUS, C. 2011. How to control an infectious bead string: nucleosome-based regulation and targeting of herpesvirus chromatin. *Reviews in Medical Virology,* 21**,** 154-180.

NICHOLAS, J., COLES, L. S., NEWMAN, C. & HONESS, R. W. 1991. Regulation of the Herpesvirus Saimiri (Hvs) Delayed-Early 110-Kilodalton Promoter by Hvs Immediate-Early Gene-Products and a Homolog of the Epstein-Barr Virus-R Trans Activator. *Journal of Virology,* 65**,** 2457-2466.

NICHOLES, K., GUILLET, S., TOMLINSON, E., HILLAN, K., WRIGHT, B., FRANTZ, G. D., PHAM, T. A., DILLARD-TELM, L., TSAI, S. P., STEPHAN, J. P., STINSON, J., STEWART, T. & FRENCH, D. M. 2002. A mouse model of hepatocellular carcinoma: ectopic expression of fibroblast growth factor 19 in skeletal muscle of transgenic mice. *American Journal of Pathology,* 160**,** 2295-307.

NICOLA, A. V., MCEVOY, A. M. & STRAUS, S. E. 2003. Roles for endocytosis and low pH in herpes simplex virus entry into HeLa and Chinese hamster ovary cells. *Journal of Virology,* 77**,** 5324-32.

NICOLA, A. V. & STRAUS, S. E. 2004. Cellular and viral requirements for rapid endocytic entry of herpes simplex virus. *Journal of Virology,* 78**,** 7508-17.

NICOLL, M. P., PROENCA, J. T., CONNOR, V. & EFSTATHIOU, S. 2012. Influence of herpes simplex virus 1 latency-associated transcripts on the establishment and maintenance of latency in the ROSA26R reporter mouse model. *Journal of Virology,* 86**,** 8848-58.

NIGHTINGALE, K., LEVY, C. S., HOPKINS, J., GREY, F., ESPER, S. & DALZIEL, R. G. 2014. Expression of ovine herpesvirus -2 encoded microRNAs in an immortalised bovine - cell line. *PLoS ONE,* 9**,** e97765.

NIWA, M., ROSE, S. D. & BERGET, S. M. 1990. In vitro polyadenylation is stimulated by the presence of an upstream intron. *Genes Dev,* 4**,** 1552-9.

NOTTROTT, S., SIMARD, M. J. & RICHTER, J. D. 2006. Human let-7a miRNA blocks protein production on actively translating polyribosomes. *Nat Struct Mol Biol,* 13**,** 1108-14.

O'CONNELL, R. M., RAO, D. S., CHAUDHURI, A. A. & BALTIMORE, D. 2010. Physiological and pathological roles for microRNAs in the immune system. *Nat Rev Immunol,* 10**,** 111-22.

O'TOOLE, D. & LI, H. 2014. The pathology of malignant catarrhal fever, with an emphasis on ovine herpesvirus 2. *Vet Pathol,* 51**,** 437-52.

O'TOOLE, D., LI, H., MILLER, D., WILLIAMS, W. R. & CRAWFORD, T. B. 1997. Chronic and recovered cases of sheep-associated malignant catarrhal fever in cattle. *Veterinary Record,* 140**,** 519-24.

O'TOOLE, D., TAUS, N. S., MONTGOMERY, D. L., OAKS, J. L., CRAWFORD, T. B. & LI, H. 2007. Intra-nasal inoculation of American bison (Bison bison) with ovine herpesvirus-2 (OvHV-2) reliably reproduces malignant catarrhal fever. *Vet Pathol,* 44**,** 655-62.

OBIKA, M., OGAWA, H., TAKAHASHI, K., LI, J., HATIPOGLU, O. F., CILEK, M. Z., MIYOSHI, T., INAGAKI, J., OHTSUKI, T., KUSACHI, S., NINOMIYA, Y. & HIROHATA, S. 2012. Tumor growth inhibitory effect of ADAMTS1 is accompanied by the inhibition of tumor angiogenesis. *Cancer Sci,* 103**,** 1889-97.

ODUMADE, O. A., HOGQUIST, K. A. & BALFOUR, H. H., JR. 2011. Progress and problems in understanding and managing primary Epstein-Barr virus infections. *Clinical Microbiology Reviews,* 24**,** 193-209.

OHTA, T., NUMATA, M., YAGISHITA, H., FUTAGAMI, F., TSUKIOKA, Y., KITAGAWA, H., KAYAHARA, M., NAGAKAWA, T., MIYAZAKI, I., YAMAMOTO, M., ISEKI, S. & OHKUMA, S. 1996. Expression of 16 kDa proteolipid of vacuolar-type H(+)-ATPase in human pancreatic cancer. *Br J Cancer,* 73**,** 1511-7.

OIE 2013. Manual of Diagnostic Tests and Vaccines for Terrestrial Animals. Chapter 2.4.15: Malignant Catarrhal Fever. OIE Terrestrial Manual.

OKAMURA, K., PHILLIPS, M. D., TYLER, D. M., DUAN, H., CHOU, Y. T. & LAI, E. C. 2008. The regulatory activity of microRNA* species has substantial influence on microRNA and 3' UTR evolution. *Nat Struct Mol Biol,* 15**,** 354-63.

OLSEN, P. H. & AMBROS, V. 1999. The lin-4 regulatory RNA controls developmental timing in Caenorhabditis elegans by blocking LIN-14 protein synthesis after the initiation of translation. *Dev Biol,* 216**,** 671-80.

OMOTO, S., ITO, M., TSUTSUMI, Y., ICHIKAWA, Y., OKUYAMA, H., BRISIBE, E. A., SAKSENA, N. K. & FUJII, Y. R. 2004. HIV-1 nef suppression by virally encoded microRNA. *Retrovirology,* 1**,** 44.

OROM, U. A., NIELSEN, F. C. & LUND, A. H. 2008. MicroRNA-10a binds the 5'UTR of ribosomal protein mRNAs and enhances their translation. *Mol Cell,* 30**,** 460-71.

PARKER, J. S., ROE, S. M. & BARFORD, D. 2005. Structural insights into mRNA recognition from a PIWI domain-siRNA guide complex. *Nature,* 434**,** 663-6.

PARKER, R. & SHETH, U. 2007. P bodies and the control of mRNA translation and degradation. *Mol Cell,* 25**,** 635-646.

PASS, R. F., FOWLER, K. B., BOPPANA, S. B., BRITT, W. J. & STAGNO, S. 2006. Congenital cytomegalovirus infection following first trimester maternal infection: Symptoms at birth and outcome. *Journal of Clinical Virology,* 35**,** 216-220.

PAULUS, C., NITZSCHE, A. & NEVELS, M. 2010. Chromatinisation of herpesvirus genomes. *Reviews in Medical Virology,* 20**,** 34-50.

PAVELIN, J., REYNOLDS, N., CHIWESHE, S., WU, G., TIRIBASSI, R. & GREY, F. 2013. Systematic microRNA analysis identifies ATP6V0C as an essential host factor for human cytomegalovirus replication. *Plos Pathogens,* 9**,** e1003820.

PEGMAN, P. M., SMITH, S. M., D'SOUZA, B. N., LOUGHRAN, S. T., MAIER, S., KEMPKES, B., CAHILL, P. A., SIMMONS, M. J., GELINAS, C. & WALLS, D. 2006. Epstein-Barr virus nuclear antigen 2 trans-activates the cellular antiapoptotic bfl-1 gene by a CBF1/RBPJ kappa-dependent pathway. *Journal of Virology,* 80**,** 8133-44.

PELLET, P. & ROIZMAN, B. 2007. Fields Virology, eds Knipe DM, Howley PM. Lippincott Williams and Wilkins, New York.

PENHEITER, K. L., WASHBURN, T. M., PORTER, S. E., HOFFMAN, M. G. & JAEHNING, J. A. 2005. A posttranscriptional role for the yeast Paf1-RNA

polymerase II complex is revealed by identification of primary targets. *Mol Cell,* 20**,** 213-23.

PENKERT, R. R. & KALEJTA, R. F. 2011. Tegument protein control of latent herpesvirus establishment and animation. *Herpesviridae,* 2**,** 3.

PERESTENKO, P. V., POOLER, A. M., NOORBAKHSHNIA, M., GRAY, A., BAUCCIO, C. & JEFFREY MCILHINNEY, R. A. 2010. Copines-1, -2, -3, -6 and -7 show different calcium-dependent intracellular membrane translocation and targeting. *Febs Journal,* 277**,** 5174-89.

PERNG, G. C. & JONES, C. 2010. Towards an understanding of the herpes simplex virus type 1 latency-reactivation cycle. *Interdiscip Perspect Infect Dis,* 2010**,** 262415.

PERNG, G. C., MAGUEN, B., JIN, L., MOTT, K. R., OSORIO, N., SLANINA, S. M., YUKHT, A., GHIASI, H., NESBURN, A. B., INMAN, M., HENDERSON, G., JONES, C. & WECHSLER, S. L. 2002. A gene capable of blocking apoptosis can substitute for the herpes simplex virus type 1 latency-associated transcript gene and restore wild-type reactivation levels. *Journal of Virology,* 76**,** 1224-35.

PERNG, G. C., SLANINA, S. M., YUKHT, A., GHIASI, H., NESBURN, A. B. & WECHSLER, S. L. 2000. The latency-associated transcript gene enhances establishment of herpes simplex virus type 1 latency in rabbits. *Journal of Virology,* 74**,** 1885-91.

PETERSEN, C. P., BORDELEAU, M. E., PELLETIER, J. & SHARP, P. A. 2006. Short RNAs repress translation after initiation in mammalian cells. *Mol Cell,* 21**,** 533-42.

PETROCCA, F., VISONE, R., ONELLI, M. R., SHAH, M. H., NICOLOSO, M. S., DE MARTINO, I., ILIOPOULOS, D., PILOZZI, E., LIU, C. G., NEGRINI, M., CAVAZZINI, L., VOLINIA, S., ALDER, H., RUCO, L. P., BALDASSARRE, G., CROCE, C. M. & VECCHIONE, A. 2008. E2F1-regulated microRNAs impair TGFbeta-dependent cell-cycle arrest and apoptosis in gastric cancer. *Cancer Cell,* 13**,** 272-86.

PFEFFER, S., SEWER, A., LAGOS-QUINTANA, M., SHERIDAN, R., SANDER, C., GRASSER, F. A., VAN DYK, L. F., HO, C. K., SHUMAN, S., CHIEN, M., RUSSO, J. J., JU, J., RANDALL, G., LINDENBACH, B. D., RICE, C. M., SIMON, V., HO, D. D., ZAVOLAN, M. & TUSCHL, T. 2005. Identification of microRNAs of the herpesvirus family. *Nat Methods,* 2**,** 269-76.

PFEFFER, S., ZAVOLAN, M., GRASSER, F. A., CHIEN, M., RUSSO, J. J., JU, J., JOHN, B., ENRIGHT, A. J., MARKS, D., SANDER, C. & TUSCHL, T. 2004. Identification of virus-encoded microRNAs. *Science,* 304**,** 734-6.

PICKERING, M. T., STADLER, B. M. & KOWALIK, T. F. 2009. miR-17 and miR-20a temper an E2F1-induced G1 checkpoint to regulate cell cycle progression. *Oncogene,* 28**,** 140-5.

PIERSON, R. E., HAMDY, F. M., DARDIRI, A. H., FERRIS, D. H. & SCHLOER, G. M. 1979. Comparison of African and American forms of malignant catarrhal fever: transmission and clinical signs. *American Journal of Veterinary Research,* 40**,** 1091-5.

PILLAI, R. S., BHATTACHARYYA, S. N., ARTUS, C. G., ZOLLER, T., COUGOT, N., BASYUK, E., BERTRAND, E. & FILIPOWICZ, W. 2005. Inhibition of translational initiation by Let-7 MicroRNA in human cells. *Science,* 309**,** 1573-6.

PLOWRIGHT, W. 1964. Studies on Malignant Catarrhal Fever of Cattle. PhD Thesis.

University of Pretoria.

PLOWRIGHT, W. 1965a. Malignant Catarrhal Fever in East Africa. I. Behaviour of the Virus in Free-Living Populations of Blue Wildebeest (Gorgon Taurinus Taurinus, Burchell). *Res Vet Sci,* 6**,** 56-68.

PLOWRIGHT, W. 1965b. Malignant Catarrhal Fever in East Africa. Ii. Observations on Wildebeest Calves at the Laboratory and Contact Transmission of the Infection to Cattle. *Res Vet Sci,* 6**,** 69-83.

PLOWRIGHT, W. 1967. Malignant catarrhal fever in East Africa 3. Neutralizing antibody in free-living wildebeest. *Res Vet Sci,* 8**,** 129-36.

PLOWRIGHT, W. 1990. Chapter 14 - Malignant Catarrhal Fever Virus. *In:* DINTER, Z. & MOREIN, B. (eds.) *Virus Infections of Ruminants*. Elsevier.

PLOWRIGHT, W., FERRIS, R. D. & SCOTT, G. R. 1960. BLUE WILDEBEEST AND THE AETIOLOGICAL AGENT OF BOVINE MALIGNANT CATARRHAL FEVER. *Nature,* 188**,** 1167-1169.

PLOWRIGHT, W., HERNIMAN, K. A., JESSETT, D. M., KALUNDA, M. & RAMPTON, C. S. 1975. Immunisation of cattle against the herpesvirus of malignant catarrhal fever: failure of inactivated culture vaccines with adjuvant. *Res Vet Sci,* 19**,** 159-66.

PURUSHOTHAMAN, P., MCDOWELL, M. E., MCGUINNESS, J., SALAS, R., RUMJAHN, S. M. & VERMA, S. C. 2012. Kaposi's sarcoma-associated herpesvirus-encoded LANA recruits topoisomerase IIbeta for latent DNA replication of the terminal repeats. *Journal of Virology,* 86**,** 9983-94.

RADTKE, F. & RAJ, K. 2003. The role of Notch in tumorigenesis: oncogene or tumour suppressor? *Nat Rev Cancer,* 3**,** 756-67.

RADTKE, F., WILSON, A., STARK, G., BAUER, M., VAN MEERWIJK, J., MACDONALD, H. R. & AGUET, M. 1999. Deficient T cell fate specification in mice with an induced inactivation of Notch1. *Immunity,* 10**,** 547-58.

RAFAILIDIS, P. I., MOURTZOUKOU, E. G., VARBOBITIS, I. C. & FALAGAS, M. E. 2008. Severe cytomegalovirus infection in apparently immunocompetent patients: a systematic review. *Virology Journal,* 5.

RAO, D. S., O'CONNELL, R. M., CHAUDHURI, A. A., GARCIA-FLORES, Y., GEIGER, T. L. & BALTIMORE, D. 2010. MicroRNA-34a perturbs B lymphocyte development by repressing the forkhead box transcription factor Foxp1. *Immunity,* 33**,** 48-59.

RAVER-SHAPIRA, N., MARCIANO, E., MEIRI, E., SPECTOR, Y., ROSENFELD, N., MOSKOVITS, N., BENTWICH, Z. & OREN, M. 2007. Transcriptional activation of miR-34a contributes to p53-mediated apoptosis. *Mol Cell,* 26**,** 731-43.

RAWSON, H., CRAMPIN, A. & NOAH, N. 2001. Deaths from chickenpox in England and Wales 1995-7: analysis of routine mortality data. *British Medical Journal,* 323**,** 1091-1093.

REGL, G., KASPER, M., SCHNIDAR, H., EICHBERGER, T., NEILL, G. W., IKRAM, M. S., QUINN, A. G., PHILPOTT, M. P., FRISCHAUF, A. M. & ABERGER, F. 2004. The zinc-finger transcription factor GLI2 antagonizes contact inhibition and differentiation of human epidermal cells. *Oncogene,* 23**,** 1263-74.

REHMAN, M. & TAMAGNONE, L. 2013. Semaphorins in cancer: biological mechanisms and therapeutic approaches. *Semin Cell Dev Biol,* 24**,** 179-89.

REHMSMEIER, M., STEFFEN, P., HOCHSMANN, M. & GIEGERICH, R. 2004. Fast and effective prediction of microRNA/target duplexes. *RNA,* 10**,** 1507-17.

REHWINKEL, J., BEHM-ANSMANT, I., GATFIELD, D. & IZAURRALDE, E. 2005. A crucial role for GW182 and the DCP1:DCP2 decapping complex in miRNA-mediated gene silencing. *RNA,* 11**,** 1640-7.

REID, H. W., BUXTON, D., BERRIE, E., POW, I. & FINLAYSON, J. 1984. Malignant catarrhal fever. *Veterinary Record,* 114**,** 581-3.

REID, H. W., BUXTON, D., CORRIGALL, W., HUNTER, A. R., MCMARTIN, D. A. & RUSHTON, R. 1979. An outbreak of malignant catarrhal fever in red deer (Cervus elephus). *Veterinary Record,* 104**,** 120-3.

REID, H. W., BUXTON, D., POW, I. & FINLAYSON, J. 1986. Malignant catarrhal fever: experimental transmission of the 'sheep-associated' form of the disease from cattle and deer to cattle, deer, rabbits and hamsters. *Res Vet Sci,* 41**,** 76-81.

REID, H. W., BUXTON, D., POW, I. & FINLAYSON, J. 1989a. Isolation and characterisation of lymphoblastoid cells from cattle and deer affected with 'sheep-associated' malignant catarrhal fever. *Res Vet Sci,* 47**,** 90-6.

REID, H. W., BUXTON, D., POW, I., FINLAYSON, J. & BERRIE, E. L. 1983. A cytotoxic T-lymphocyte line propagated from a rabbit infected with sheep associated malignant catarrhal fever. *Res Vet Sci,* 34**,** 109-13.

REID, H. W., POW, I. & BUXTON, D. 1989b. Antibody to alcelaphine herpesvirus-1 (AHV-1) in hamsters experimentally infected with AHV-1 and the 'sheep-associated' agent of malignant catarrhal fever. *Res Vet Sci,* 47**,** 383-6.

REID, S. W. & ROBINSON, B. N. 1987. Malignant catarrhal Fever in a five-month-old calf. *Can Vet J,* 28**,** 489.

REINHART, B. J., SLACK, F. J., BASSON, M., PASQUINELLI, A. E., BETTINGER, J. C., ROUGVIE, A. E., HORVITZ, H. R. & RUVKUN, G. 2000. The 21-nucleotide let-7 RNA regulates developmental timing in Caenorhabditis elegans. *Nature,* 403**,** 901-6.

RIAZ, A., DRY, I., LEVY, C. S., HOPKINS, J., GREY, F., SHAW, D. J. & DALZIEL, R. G. 2014. Ovine herpesvirus-2-encoded microRNAs target virus genes involved in virus latency. *Journal of General Virology,* 95**,** 472-80.

RICKINSON, A. & KIEFF, E. 2001. Fields virology. *Epstein-Barr Virus,* 2.

RIDLEY, A. J. 2006. Rho GTPases and actin dynamics in membrane protrusions and vesicle trafficking. *Trends Cell Biol,* 16**,** 522-9.

RIGO, F. & MARTINSON, H. G. 2008. Functional coupling of last-intron splicing and 3'-end processing to transcription in vitro: the poly(A) signal couples to splicing before committing to cleavage. *Molecular and Cellular Biology,* 28**,** 849-62.

RILEY, K. J., RABINOWITZ, G. S., YARIO, T. A., LUNA, J. M., DARNELL, R. B. & STEITZ, J. A. 2012. EBV and human microRNAs co-target oncogenic and apoptotic viral and human genes during latency. *Embo Journal,* 31**,** 2207-21.

ROBINSON, M. D., MCCARTHY, D. J. & SMYTH, G. K. 2010. edgeR: a Bioconductor package for differential expression analysis of digital gene expression data. *Bioinformatics,* 26**,** 139-40.

RODRIGUES, S. P., FATHERS, K. E., CHAN, G., ZUO, D., HALWANI, F., METERISSIAN, S. & PARK, M. 2005. CrkI and CrkII function as key signaling integrators for migration and invasion of cancer cells. *Mol Cancer Res,* 3**,** 183-94.

RODRIGUEZ, A., VIGORITO, E., CLARE, S., WARREN, M. V., COUTTET, P., SOOND, D. R., VAN DONGEN, S., GROCOCK, R. J., DAS, P. P., MISKA, E. A., VETRIE, D., OKKENHAUG, K., ENRIGHT, A. J., DOUGAN, G., TURNER, M. & BRADLEY, A. 2007. Requirement of bic/microRNA-155 for normal immune function. *Science,* 316**,** 608-11.

ROIZMAN, B. & KNIPE, D. 2001. Fields virology. *Lippincott Williams & Wilkins, Philadelphia***,** 2381-2397.

ROIZMANN, B., DESROSIERS, R. C., FLECKENSTEIN, B., LOPEZ, C., MINSON, A. C. & STUDDERT, M. J. 1992. The family Herpesviridae: an update. The Herpesvirus Study Group of the International Committee on Taxonomy of Viruses. *Archives of Virology,* 123**,** 425-49.

ROONEY, C. M., ROWE, D. T., RAGOT, T. & FARRELL, P. J. 1989. The Spliced Bzlf1 Gene of Epstein-Barr Virus (Ebv) Transactivates an Early Ebv Promoter and Induces the Virus Productive Cycle. *Journal of Virology,* 63**,** 3109-3116.

ROSBOTTOM, J., DALZIEL, R. G., REID, H. W. & STEWART, J. P. 2002. Ovine herpesvirus 2 lytic cycle replication and capsid production. *Journal of General Virology,* 83**,** 2999-3002.

ROSEWICK, N., MOMONT, M., DURKIN, K., TAKEDA, H., CAIMENT, F., CLEUTER, Y., VERNIN, C., MORTREUX, F., WATTEL, E., BURNY, A., GEORGES, M. & VAN DEN BROEKE, A. 2013. Deep sequencing reveals abundant noncanonical retroviral microRNAs in B-cell leukemia/lymphoma. *Proc Natl Acad Sci U S A,* 110**,** 2306-11.

ROSSITER, P. B. 1981. Antibodies to malignant catarrhal fever virus in sheep sera. *J Comp Pathol,* 91**,** 303-11.

ROSSITER, P. B. 1983. Antibodies to malignant catarrhal fever virus in cattle with non-wildebeest-associated malignant catarrhal fever. *J Comp Pathol,* 93**,** 93-7.

ROWE, M., LEAR, A. L., CROOM-CARTER, D., DAVIES, A. H. & RICKINSON, A. B. 1992. Three pathways of Epstein-Barr virus gene activation from EBNA1-positive latency in B lymphocytes. *Journal of Virology,* 66**,** 122-31.

ROZENBLATT-ROSEN, O., NAGAIKE, T., FRANCIS, J. M., KANEKO, S., GLATT, K. A., HUGHES, C. M., LAFRAMBOISE, T., MANLEY, J. L. & MEYERSON, M. 2009. The tumor suppressor Cdc73 functionally associates with CPSF and CstF 3' mRNA processing factors. *Proc Natl Acad Sci U S A,* 106**,** 755-60.

RUBY, J. G., STARK, A., JOHNSTON, W. K., KELLIS, M., BARTEL, D. P. & LAI, E. C. 2007. Evolution, biogenesis, expression, and target predictions of a substantially expanded set of Drosophila microRNAs. *Genome Res,* 17**,** 1850-64.

RUSSELL, G. C., BENAVIDES, J., GRANT, D., TODD, H., DEANE, D., PERCIVAL, A., THOMSON, J., CONNELLY, M. & HAIG, D. M. 2012. Duration of protective immunity and antibody responses in cattle immunised against alcelaphine herpesvirus-1-induced malignant catarrhal fever. *Vet Res,* 43**,** 51.

RUSSELL, G. C., STEWART, J. P. & HAIG, D. M. 2009. Malignant catarrhal fever: a review. *Vet J,* 179**,** 324-35.

RWEYEMAMU, M. M., KARSTAD, L., MUSHI, E. Z., OTEMA, J. C., JESSETT, D. M., ROWE, L., DREVEMO, S. & GROOTENHUIS, J. G. 1974. Malignant catarrhal fever virus in nasal secretions of wildebeest: a probable mechanism for virus transmission. *J Wildl Dis,* 10**,** 478-87.

SAETROM, P., HEALE, B. S., SNOVE, O., JR., AAGAARD, L., ALLUIN, J. & ROSSI, J. J. 2007. Distance constraints between microRNA target sites dictate efficacy and cooperativity. *Nucleic Acids Res,* 35**,** 2333-42.

SAMOLS, M. A., HU, J., SKALSKY, R. L. & RENNE, R. 2005. Cloning and identification of a microRNA cluster within the latency-associated region of Kaposi's sarcoma-associated herpesvirus. *Journal of Virology,* 79**,** 9301-5.

SAMOLS, M. A., SKALSKY, R. L., MALDONADO, A. M., RIVA, A., LOPEZ, M. C., BAKER, H. V. & RENNE, R. 2007. Identification of cellular genes targeted by KSHV-encoded microRNAs. *Plos Pathogens,* 3**,** e65.

SANFORD, S. E. & LITTLE, P. B. 1977. The gross and histopathologic lesions of maignant catarrhal fever in three captive sika deer (Cervus nippon) in southern Ontario. *J Wildl Dis,* 13**,** 29-32.

SARNOW, P., JOPLING, C. L., NORMAN, K. L., SCHUTZ, S. & WEHNER, K. A. 2006. MicroRNAs: expression, avoidance and subversion by vertebrate viruses. *Nat Rev Microbiol,* 4**,** 651-9.

SARRAS, H., ALIZADEH AZAMI, S. & MCPHERSON, J. P. 2010. In search of a function for BCLAF1. *ScientificWorldJournal,* 10**,** 1450-61.

SCHNAPP, L. M., BREUSS, J. M., RAMOS, D. M., SHEPPARD, D. & PYTELA, R. 1995. Sequence and tissue distribution of the human integrin alpha 8 subunit: a beta 1-associated alpha subunit expressed in smooth muscle cells. *Journal of Cell Science,* 108 (Pt 2)**,** 537-44.

SCHOCK, A., COLLINS, R. A. & REID, H. W. 1998. Phenotype, growth regulation and cytokine transcription in Ovine Herpesvirus-2 (OHV-2)-infected bovine T-cell lines. *Vet Immunol Immunopathol,* 66**,** 67-81.

SCHOCK, A. & REID, H. W. 1996. Characterisation of the lymphoproliferation in rabbits experimentally affected with malignant catarrhal fever. *Vet Microbiol,* 53**,** 111-9.

SCHULTHEISS, P. C., COLLINS, J. K., SPRAKER, T. R. & DEMARTINI, J. C. 2000. Epizootic malignant catarrhal fever in three bison herds: differences from cattle and association with ovine herpesvirus-2. *J Vet Diagn Invest,* 12**,** 497-502.

SCHUMACHER, D., TISCHER, B. K., TRAPP, S. & OSTERRIEDER, N. 2005. The protein encoded by the U(s)3 orthologue of Marek's disease virus is required for efficient de-envelopment of perinuclear virions and involved in actin stress fiber breakdown. *Journal of Virology,* 79**,** 3987-3997.

SELBACH, M., SCHWANHAUSSER, B., THIERFELDER, N., FANG, Z., KHANIN, R. & RAJEWSKY, N. 2008. Widespread changes in protein synthesis induced by microRNAs. *Nature,* 455**,** 58-63.

SELMAN, I. E., WISEMAN, A., MURRAY, M. & WRIGHT, N. G. 1974. A clinico-pathological study of bovine malignant catarrhal fever in Great Britain. *Veterinary Record,* 94**,** 483-90.

SHANNON-LOWE, C. D., NEUHIERL, B., BALDWIN, G., RICKINSON, A. B. & DELECLUSET, H. J. 2006. Resting B cells as a transfer vehicle for Epstein-Barr virus infection of epithelial cells. *Proc Natl Acad Sci U S A,* 103**,** 7065-7070.

SHARFE, N., DADI, H. K., SHAHAR, M. & ROIFMAN, C. M. 1997. Human immune disorder arising from mutation of the alpha chain of the interleukin-2 receptor. *Proc Natl Acad Sci U S A,* 94**,** 3168-71.

SHIEH, M. T., WUDUNN, D., MONTGOMERY, R. I., ESKO, J. D. & SPEAR, P. G. 1992. Cell surface receptors for herpes simplex virus are heparan sulfate proteoglycans. *The Journal of cell biology,* 116**,** 1273-81.

SHIN, C., NAM, J. W., FARH, K. K., CHIANG, H. R., SHKUMATAVA, A. & BARTEL, D. P. 2010. Expanding the microRNA targeting code: functional sites with centered pairing. *Mol Cell,* 38**,** 789-802.

SHUKLA, D., LIU, J., BLAIKLOCK, P., SHWORAK, N. W., BAI, X., ESKO, J. D., COHEN, G. H., EISENBERG, R. J., ROSENBERG, R. D. & SPEAR, P. G. 1999. A novel role for 3-O-sulfated heparan sulfate in herpes simplex virus 1 entry. *Cell,* 99**,** 13-22.

SIMAS, J. P. & EFSTATHIOU, S. 1998. Murine gammaherpesvirus 68: a model for the study of gammaherpesvirus pathogenesis. *Trends in Microbiology,* 6**,** 276-282.

SIMON, S., LI, H., O'TOOLE, D., CRAWFORD, T. B. & OAKS, J. L. 2003. The vascular lesions of a cow and bison with sheep-associated malignant catarrhal fever contain ovine herpesvirus 2-infected CD8+ T lymphocytes. *Journal of General Virology,* 84**,** 2009-2013.

SIVACHANDRAN, N., WANG, X. & FRAPPIER, L. 2012. Functions of the Epstein-Barr virus EBNA1 protein in viral reactivation and lytic infection. *Journal of Virology,* 86**,** 6146-58.

SKALSKY, R. L., CORCORAN, D. L., GOTTWEIN, E., FRANK, C. L., KANG, D., HAFNER, M., NUSBAUM, J. D., FEEDERLE, R., DELECLUSE, H. J., LUFTIG, M. A., TUSCHL, T., OHLER, U. & CULLEN, B. R. 2012. The viral and cellular microRNA targetome in lymphoblastoid cell lines. *Plos Pathogens,* 8**,** e1002484.

SKALSKY, R. L., SAMOLS, M. A., PLAISANCE, K. B., BOSS, I. W., RIVA, A., LOPEZ, M. C., BAKER, H. V. & RENNE, R. 2007. Kaposi's sarcoma-associated herpesvirus encodes an ortholog of miR-155. *Journal of Virology,* 81**,** 12836-45.

SMITH, B. P. 2002. *Large animal internal medicine,* St. Louis, Mo., Mosby.

SMITH, D. B. & JOHNSON, K. S. 1988. Single-step purification of polypeptides expressed in Escherichia coli as fusions with glutathione S-transferase. *Gene,* 67**,** 31-40.

SODEIK, B., EBERSOLD, M. W. & HELENIUS, A. 1997. Microtubule-mediated transport of incoming herpes simplex virus 1 capsids to the nucleus. *The Journal of cell biology,* 136**,** 1007-21.

SONG, G. & WANG, L. 2008. MiR-433 and miR-127 arise from independent overlapping primary transcripts encoded by the miR-433-127 locus. *PLoS ONE,* 3**,** e3574.

SPEAR, P. G. 2004. Herpes simplex virus: receptors and ligands for cell entry. *Cellular Microbiology,* 6**,** 401-10.

SPITZER, J., HAFNER, M., LANDTHALER, M., ASCANO, M., FARAZI, T., WARDLE, G., NUSBAUM, J., KHORSHID, M., BURGER, L., ZAVOLAN, M. & TUSCHL, T. 2014. PAR-CLIP (Photoactivatable Ribonucleoside-Enhanced Crosslinking and Immunoprecipitation): a step-by-step protocol to the transcriptome-wide identification of binding sites of RNA-binding proteins. *Methods Enzymol,* 539**,** 113-61.

STAMPFER, S. D., LOU, H., COHEN, G. H., EISENBERG, R. J. & HELDWEIN, E. E. 2010. Structural basis of local, pH-dependent conformational changes in glycoprotein B from herpes simplex virus type 1. *Journal of Virology,* 84**,** 12924-33.

STERN-GINOSSAR, N., ELEFANT, N., ZIMMERMANN, A., WOLF, D. G., SALEH, N., BITON, M., HORWITZ, E., PROKOCIMER, Z., PRICHARD, M., HAHN, G., GOLDMAN-WOHL, D., GREENFIELD, C., YAGEL, S., HENGEL, H., ALTUVIA, Y., MARGALIT, H. & MANDELBOIM, O. 2007. Host immune system gene targeting by a viral miRNA. *Science,* 317**,** 376-81.

STEVENS, J. G. 1987. Defining herpes simplex genes involved in neurovirulence and neuroinvasiveness. *Curr Eye Res,* 6**,** 63-7.

STEWART, J. P., SILVIA, O. J., ATKIN, I. M., HUGHES, D. J., EBRAHIMI, B. & ADLER, H. 2004. In vivo function of a gammaherpesvirus virion glycoprotein: influence on B-cell infection and mononucleosis. *Journal of Virology,* 78**,** 10449-59.

STRASSHEIM, S., STIK, G., RASSCHAERT, D. & LAURENT, S. 2012. mdv1-miR-M7-5p, located in the newly identified first intron of the latency-associated transcript of Marek's disease virus, targets the immediate-early genes ICP4 and ICP27. *Journal of General Virology,* 93**,** 1731-42.

STRAVER, P. J. & VAN BEKKUM, J. G. 1979. Isolation of malignant catarrhal fever virus from a European bison (Bos bonasus) in a zoological garden. *Res Vet Sci,* 26**,** 165-71.

SUBRAMANIAN, R. P. & GERAGHTY, R. J. 2007. Herpes simplex virus type 1 mediates fusion through a hemifusion intermediate by sequential activity of glycoproteins D, H, L, and B. *Proc Natl Acad Sci U S A,* 104**,** 2903-8.

SULLIVAN, C. S. 2008. New roles for large and small viral RNAs in evading host defences. *Nat Rev Genet,* 9**,** 503-7.

SUN, L. & LI, Q. 2012. The miRNAs of herpes simplex virus (HSV). *Virol Sin,* 27**,** 333-8.

SUN, R., LIN, S. F., GRADOVILLE, L., YUAN, Y., ZHU, F. & MILLER, G. 1998. A viral gene that activates lytic cycle expression of Kaposi's sarcoma-associated herpesvirus. *Proc Natl Acad Sci U S A,* 95**,** 10866-71.

SUN, R., LIN, S. F., STASKUS, K., GRADOVILLE, L., GROGAN, E., HAASE, A. & MILLER, G. 1999. Kinetics of Kaposi's sarcoma-associated herpesvirus gene expression. *Journal of Virology,* 73**,** 2232-2242.

SUNIL-CHANDRA, N. P., EFSTATHIOU, S., ARNO, J. & NASH, A. A. 1992. Virological and pathological features of mice infected with murine gamma-herpesvirus 68. *Journal of General Virology,* 73 (Pt 9)**,** 2347-56.

SWA, S., WRIGHT, H., THOMSON, J., REID, H. & HAIG, D. 2001. Constitutive activation of Lck and Fyn tyrosine kinases in large granular lymphocytes infected with the gamma-herpesvirus agents of malignant catarrhal fever. *Immunology,* 102**,** 44-52.

TAGANOV, K. D., BOLDIN, M. P., CHANG, K. J. & BALTIMORE, D. 2006. NF-kappaB-dependent induction of microRNA miR-146, an inhibitor targeted to signaling proteins of innate immune responses. *Proc Natl Acad Sci U S A,* 103**,** 12481-6.

TAKAGAKI, Y. & MANLEY, J. L. 1994. A polyadenylation factor subunit is the human homologue of the Drosophila suppressor of forked protein. *Nature,* 372**,** 471-4.

TAKAMATSU, H., OKUNO, T. & KUMANOGOH, A. 2010. Regulation of immune cell responses by semaphorins and their receptors. *Cell Mol Immunol,* 7**,** 83-8.

TAKEDA, N., MAEMURA, K., IMAI, Y., HARADA, T., KAWANAMI, D., NOJIRI, T., MANABE, I. & NAGAI, R. 2004. Endothelial PAS domain protein 1 gene promotes angiogenesis through the transactivation of both vascular endothelial growth factor and its receptor, Flt-1. *Circ Res,* 95**,** 146-53.

TAM, W. & DAHLBERG, J. E. 2006. miR-155/BIC as an oncogenic microRNA. *Genes Chromosomes Cancer,* 45**,** 211-2.

TANG, S., BERTKE, A. S., PATEL, A., WANG, K., COHEN, J. I. & KRAUSE, P. R. 2008. An acutely and latently expressed herpes simplex virus 2 viral microRNA inhibits expression of ICP34.5, a viral neurovirulence factor. *Proc Natl Acad Sci U S A,* 105**,** 10931-6.

TANG, S., PATEL, A. & KRAUSE, P. R. 2009. Novel less-abundant viral microRNAs encoded by herpes simplex virus 2 latency-associated transcript and their roles in regulating ICP34.5 and ICP0 mRNAs. *Journal of Virology,* 83**,** 1433-42.

TAUS, N. S., OAKS, J. L., GAILBREATH, K., TRAUL, D. L., O'TOOLE, D. & LI, H. 2006. Experimental aerosol infection of cattle (Bos taurus) with ovine

herpesvirus 2 using nasal secretions from infected sheep. *Vet Microbiol,* 116**,** 29-36.

TAUS, N. S., TRAUL, D. L., OAKS, J. L., CRAWFORD, T. B., LEWIS, G. S. & LI, H. 2005. Experimental infection of sheep with ovine herpesvirus 2 via aerosolization of nasal secretions. *Journal of General Virology,* 86**,** 575-9.

TEZEL, G. G., UNER, A., YILDIZ, I., GULER, G. & TAKAHASHI, M. 2009. RET finger protein expression in invasive breast carcinoma: relationship between RFP and ErbB2 expression. *Pathol Res Pract,* 205**,** 403-8.

THERMANN, R. & HENTZE, M. W. 2007. Drosophila miR2 induces pseudo-polysomes and inhibits translation initiation. *Nature,* 447**,** 875-8.

THOMPSON, M. P. & KURZROCK, R. 2004. Epstein-Barr virus and cancer. *Clin Cancer Res,* 10**,** 803-21.

THOMPSON, R. L. & SAWTELL, N. M. 1997. The herpes simplex virus type 1 latency-associated transcript gene regulates the establishment of latency. *Journal of Virology,* 71**,** 5432-40.

THOMSON, D. W., BRACKEN, C. P. & GOODALL, G. J. 2011. Experimental strategies for microRNA target identification. *Nucleic Acids Res,* 39**,** 6845-53.

THONUR, L., RUSSELL, G. C., STEWART, J. P. & HAIG, D. M. 2006. Differential transcription of ovine herpesvirus 2 genes in lymphocytes from reservoir and susceptible species. *Virus Genes,* 32**,** 27-35.

THORLEY-LAWSON, D. A. & BABCOCK, G. J. 1999. A model for persistent infection with Epstein-Barr virus: the stealth virus of human B cells. *Life Sci,* 65**,** 1433-53.

TIAN, H., MCKNIGHT, S. L. & RUSSELL, D. W. 1997. Endothelial PAS domain protein 1 (EPAS1), a transcription factor selectively expressed in endothelial cells. *Genes Dev,* 11**,** 72-82.

TILI, E., MICHAILLE, J. J., CIMINO, A., COSTINEAN, S., DUMITRU, C. D., ADAIR, B., FABBRI, M., ALDER, H., LIU, C. G., CALIN, G. A. & CROCE, C. M. 2007. Modulation of miR-155 and miR-125b levels following lipopolysaccharide/TNF-alpha stimulation and their possible roles in regulating the response to endotoxin shock. *J Immunol,* 179**,** 5082-9.

TISCHER, B. K., SCHUMACHER, D., CHABANNE-VAUTHEROT, D., ZELNIK, V., VAUTHEROT, J. F. & OSTERRIEDER, N. 2005. High-level expression of Marek's disease virus glycoprotein C is detrimental to virus growth in vitro. *Journal of Virology,* 79**,** 5889-5899.

TRAUL, D. L., ELIAS, S., TAUS, N. S., HERRMANN, L. M., OAKS, J. L. & LI, H. 2005. A real-time PCR assay for measuring alcelaphine herpesvirus-1 DNA. *J Virol Methods,* 129**,** 186-90.

TRAVIS, A. J., MOODY, J., HELWAK, A., TOLLERVEY, D. & KUDLA, G. 2014. Hyb: a bioinformatics pipeline for the analysis of CLASH (crosslinking, ligation and sequencing of hybrids) data. *Methods,* 65**,** 263-73.

TRINCZEK, B., BRAJENOVIC, M., EBNETH, A. & DREWES, G. 2004. MARK4 is a novel microtubule-associated proteins/microtubule affinity-regulating kinase that binds to the cellular microtubule network and to centrosomes. *J Biol Chem,* 279**,** 5915-23.

TROUSDALE, M. D., STEINER, I., SPIVACK, J. G., DESHMANE, S. L., BROWN, S. M., MACLEAN, A. R., SUBAK-SHARPE, J. H. & FRASER, N. W. 1991. In vivo and in vitro reactivation impairment of a herpes simplex virus type 1 latency-associated transcript variant in a rabbit eye model. *Journal of Virology,* 65**,** 6989-93.

TSAI, N. P., LIN, Y. L. & WEI, L. N. 2009. MicroRNA mir-346 targets the 5'-untranslated region of receptor-interacting protein 140 (RIP140) mRNA and up-regulates its protein expression. *Biochemical Journal,* 424**,** 411-8.

TSVITOV, M., FRAMPTON, A. R., JR., SHAH, W. A., WENDELL, S. K., OZUER, A., KAPACEE, Z., GOINS, W. F., COHEN, J. B. & GLORIOSO, J. C. 2007. Characterization of soluble glycoprotein D-mediated herpes simplex virus type 1 infection. *Virology,* 360**,** 477-91.

TUDDENHAM, L., JUNG, J. S., CHANE-WOON-MING, B., DOLKEN, L. & PFEFFER, S. 2012. Small RNA Deep Sequencing Identifies MicroRNAs and Other Small Noncoding RNAs from Human Herpesvirus 6B. *Journal of Virology,* 86**,** 1638-1649.

TUDDENHAM, L. & PFEFFER, S. 2011. Roles and regulation of microRNAs in cytomegalovirus infection. *Biochim Biophys Acta,* 1809**,** 613-22.

TUDDENHAM, L. & PFEFFER, S. 2013. Virus-Encoded microRNAs. *Encyclopedia of Molecular Cell Biology and Molecular Medicine*.

TURNER, M. L., SCHNORFEIL, F. M. & BROCKER, T. 2011. MicroRNAs regulate dendritic cell differentiation and function. *J Immunol,* 187**,** 3911-7.

UMBACH, J. L., KRAMER, M. F., JURAK, I., KARNOWSKI, H. W., COEN, D. M. & CULLEN, B. R. 2008. MicroRNAs expressed by herpes simplex virus 1 during latent infection regulate viral mRNAs. *Nature,* 454**,** 780-3.

UMBACH, J. L., WANG, K., TANG, S., KRAUSE, P. R., MONT, E. K., COHEN, J. I. & CULLEN, B. R. 2010. Identification of viral microRNAs expressed in human sacral ganglia latently infected with herpes simplex virus 2. *Journal of Virology,* 84**,** 1189-92.

UMENE, K. & SAKAOKA, H. 1999. Evolution of herpes simplex virus type 1 under herpesviral evolutionary processes. *Archives of Virology,* 144**,** 637-656.

VAN DEN BERG, A., KROESEN, B. J., KOOISTRA, K., DE JONG, D., BRIGGS, J., BLOKZIJL, T., JACOBS, S., KLUIVER, J., DIEPSTRA, A. & MAGGIO, E. 2003. High expression of B-cell receptor inducible gene BIC in all subtypes of Hodgkin lymphoma. *Genes, Chromosomes and Cancer,* 37**,** 20-28.

VAN DEN BROEKE, C. & FAVOREEL, H. W. 2011. Actin' up: herpesvirus interactions with Rho GTPase signaling. *Viruses,* 3**,** 278-92.

VASUDEVAN, S. 2012. Posttranscriptional upregulation by microRNAs. *Wiley Interdiscip Rev RNA,* 3**,** 311-30.

VASUDEVAN, S. & STEITZ, J. A. 2007. AU-rich-element-mediated upregulation of translation by FXR1 and Argonaute 2. *Cell,* 128**,** 1105-18.

VASUDEVAN, S., TONG, Y. & STEITZ, J. A. 2007. Switching from repression to activation: microRNAs can up-regulate translation. *Science,* 318**,** 1931-4.

VELLA, M. C., CHOI, E. Y., LIN, S. Y., REINERT, K. & SLACK, F. J. 2004. The C. elegans microRNA let-7 binds to imperfect let-7 complementary sites from the lin-41 3'UTR. *Genes Dev,* 18**,** 132-7.

VENTURA, A., YOUNG, A. G., WINSLOW, M. M., LINTAULT, L., MEISSNER, A., ERKELAND, S. J., NEWMAN, J., BRONSON, R. T., CROWLEY, D., STONE, J. R., JAENISCH, R., SHARP, P. A. & JACKS, T. 2008. Targeted deletion reveals essential and overlapping functions of the miR-17 through 92 family of miRNA clusters. *Cell,* 132**,** 875-86.

VINTHER, J., HEDEGAARD, M. M., GARDNER, P. P., ANDERSEN, J. S. & ARCTANDER, P. 2006. Identification of miRNA targets with stable isotope labeling by amino acids in cell culture. *Nucleic Acids Res,* 34**,** e107.

WAGNER, E. K., FLANAGAN, W. M., DEVI-RAO, G., ZHANG, Y. F., HILL, J. M., ANDERSON, K. P. & STEVENS, J. G. 1988. The herpes simplex virus latency-associated transcript is spliced during the latent phase of infection. *Journal of Virology,* 62**,** 4577-85.

WAKIYAMA, M., TAKIMOTO, K., OHARA, O. & YOKOYAMA, S. 2007. Let-7 microRNA-mediated mRNA deadenylation and translational repression in a mammalian cell-free system. *Genes Dev,* 21**,** 1857-62.

WALTERS, M. S., HALL, K. T. & WHITEHOUSE, A. 2005. The herpesvirus saimiri Rta gene autostimulates via binding to a non-consensus response element. *Journal of General Virology,* 86**,** 581-587.

WANG, H., JIANG, M., CUI, H., CHEN, M., BUTTYAN, R., HAYWARD, S. W., HAI, T., WANG, Z. & YAN, C. 2012. The stress response mediator ATF3 represses androgen signaling by binding the androgen receptor. *Molecular and Cellular Biology,* 32**,** 3190-202.

WANG, X., XU, X., MA, Z., HUO, Y., XIAO, Z., LI, Y. & WANG, Y. 2011. Dynamic mechanisms for pre-miRNA binding and export by Exportin-5. *RNA,* 17**,** 1511-28.

WANG, Z., LI, Y., KONG, D., AHMAD, A., BANERJEE, S. & SARKAR, F. H. 2010. Cross-talk between miRNA and Notch signaling pathways in tumor development and progression. *Cancer Lett,* 292**,** 141-148.

WARNER, M. S., GERAGHTY, R. J., MARTINEZ, W. M., MONTGOMERY, R. I., WHITBECK, J. C., XU, R., EISENBERG, R. J., COHEN, G. H. & SPEAR, P. G. 1998. A cell surface protein with herpesvirus entry activity (HveB) confers susceptibility to infection by mutants of herpes simplex virus type 1, herpes simplex virus type 2, and pseudorabies virus. *Virology,* 246**,** 179-89.

WATANABE, T., TSUDA, M., TANAKA, S., OHBA, Y., KAWAGUCHI, H., MAJIMA, T., SAWA, H. & MINAMI, A. 2009. Adaptor protein Crk induces Src-dependent activation of p38 MAPK in regulation of synovial sarcoma cell proliferation. *Mol Cancer Res,* 7**,** 1582-92.

WATSON, K., STEVENS, J. G., COOK, M. L. & SUBAK-SHARPE, J. H. 1980. Latency competence of thirteen HSV-1 temperature-sensitive mutants. *Journal of General Virology,* 49**,** 149-59.

WEN, W. R., IWAKIRI, D., YAMAMOTO, K., MARUO, S., KANDA, T. & TAKADA, K. 2007. Epstein-Barr virus BZLF1 gene, a switch from latency to lytic infection, is expressed as an immediate-early gene after primary infection of B lymphocytes. *Journal of Virology,* 81**,** 1037-1042.

WESTPHAL, E. M., MAUSER, A., SWENSON, J., DAVIS, M. G., TALARICO, C. L. & KENNEY, S. C. 1999. Induction of lytic Epstein-Barr virus (EBV)

infection in EBV-associated malignancies using adenovirus vectors in vitro and in vivo. *Cancer Research,* 59**,** 1485-1491.

WHITAKER, K. A., WESSELS, M. E., CAMPBELL, I. & RUSSELL, G. C. 2007. Outbreak of wildebeest-associated malignant catarrhal fever in Ankole cattle. *Veterinary Record,* 161**,** 692-5.

WHITEHEAD, I. P., CAMPBELL, S., ROSSMAN, K. L. & DER, C. J. 1997. Dbl family proteins. *Biochim Biophys Acta,* 1332**,** F1-23.

WHITEHOUSE, A., CARR, I. M., GRIFFITHS, J. C. & MEREDITH, D. M. 1997. The herpesvirus saimiri ORF50 gene, encoding a transcriptional activator homologous to the Epstein-Barr virus R protein, is transcribed from two distinct promoters of different temporal phases. *Journal of Virology,* 71**,** 2550-4.

WHITEHOUSE, A., COOPER, M. & MEREDITH, D. M. 1998. The immediate-early gene product encoded by open reading frame 57 of herpesvirus saimiri modulates gene expression at a posttranscriptional level. *Journal of Virology,* 72**,** 857-861.

WIBBELT, G., KURTH, A., YASMUM, N., BANNERT, M., NAGEL, S., NITSCHE, A. & EHLERS, B. 2007. Discovery of herpesviruses in bats. *J Gen Virol,* 88**,** 2651-5.

WIGHTMAN, B., BURGLIN, T. R., GATTO, J., ARASU, P. & RUVKUN, G. 1991. Negative regulatory sequences in the lin-14 3'-untranslated region are necessary to generate a temporal switch during Caenorhabditis elegans development. *Genes Dev,* 5**,** 1813-24.

WIGHTMAN, B., HA, I. & RUVKUN, G. 1993. Posttranscriptional regulation of the heterochronic gene lin-14 by lin-4 mediates temporal pattern formation in C. elegans. *Cell,* 75**,** 855-62.

WILKINSON, J. C., RICHTER, B. W., WILKINSON, A. S., BURSTEIN, E., RUMBLE, J. M., BALLIU, B. & DUCKETT, C. S. 2004. VIAF, a conserved inhibitor of apoptosis (IAP)-interacting factor that modulates caspase activation. *J Biol Chem,* 279**,** 51091-9.

WILL, C. L. & LUHRMANN, R. 2011. Spliceosome structure and function. *Cold Spring Harb Perspect Biol,* 3.

WILL, C. L., SCHNEIDER, C., HOSSBACH, M., URLAUB, H., RAUHUT, R., ELBASHIR, S., TUSCHL, T. & LUHRMANN, R. 2004. The human 18S U11/U12 snRNP contains a set of novel proteins not found in the U2-dependent spliceosome. *RNA,* 10**,** 929-41.

WILLIAMS, B. J. L., BOYNE, J. R., GOODWIN, D. J., ROADEN, L., HAUTBERGUE, G. M., WILSON, S. A. & WHITEHOUSE, A. 2005. The prototype gamma-2 herpesvirus nucleocytoplasmic shuttling protein, ORF 57, transports viral RNA through the cellular mRNA export pathway. *Biochemical Journal,* 387**,** 295-308.

WILSON, V. & CONLON, F. L. 2002. The T-box family. *Genome Biol,* 3**,** REVIEWS3008.

WINTER, J., JUNG, S., KELLER, S., GREGORY, R. I. & DIEDERICHS, S. 2009. Many roads to maturity: microRNA biogenesis pathways and their regulation. *Nat Cell Biol,* 11**,** 228-34.

WIYONO, A., BAXTER, S. I., SAEPULLOH, M., DAMAYANTI, R., DANIELS, P. & REID, H. W. 1994. PCR detection of ovine herpesvirus-2 DNA in Indonesian ruminants--normal sheep and clinical cases of malignant catarrhal fever. *Vet Microbiol,* 42**,** 45-52.

WU, T., KOOI, C. V., SHAH, P., CHARNIGO, R., HUANG, C., SMYTH, S. S. & MORRIS, A. J. 2014. Integrin-mediated cell surface recruitment of autotaxin promotes persistent directional cell migration. *Faseb Journal,* 28**,** 861-70.

WU, T. T., USHERWOOD, E. J., STEWART, J. P., NASH, A. A. & SUN, R. 2000a. Rta of murine gammaherpesvirus 68 reactivates the complete lytic cycle from latency. *Journal of Virology,* 74**,** 3659-67.

WU, Y., DOWBENKO, D., SPENCER, S., LAURA, R., LEE, J., GU, Q. & LASKY, L. A. 2000b. Interaction of the tumor suppressor PTEN/MMAC with a PDZ domain of MAGI3, a novel membrane-associated guanylate kinase. *J Biol Chem,* 275**,** 21477-85.

XIA, G., KAGEYAMA, Y., HAYASHI, T., KAWAKAMI, S., YOSHIDA, M. & KIHARA, K. 2001. Regulation of vascular endothelial growth factor transcription by endothelial PAS domain protein 1 (EPAS1) and possible involvement of EPAS1 in the angiogenesis of renal cell carcinoma. *Cancer,* 91**,** 1429-36.

XIA, L., ZHANG, D., DU, R., PAN, Y., ZHAO, L., SUN, S., HONG, L., LIU, J. & FAN, D. 2008a. miR-15b and miR-16 modulate multidrug resistance by targeting BCL2 in human gastric cancer cells. *Int J Cancer,* 123**,** 372-9.

XIA, T., O'HARA, A., ARAUJO, I., BARRETO, J., CARVALHO, E., SAPUCAIA, J. B., RAMOS, J. C., LUZ, E., PEDROSO, C., MANRIQUE, M., TOOMEY, N. L., BRITES, C., DITTMER, D. P. & HARRINGTON, W. J., JR. 2008b. EBV microRNAs in primary lymphomas and targeting of CXCL-11 by ebv-mir-BHRF1-3. *Cancer Research,* 68**,** 1436-42.

XIAO, P. & CAPONE, J. P. 1990. A Cellular Factor Binds to the Herpes-Simplex Virus Type-1 Transactivator Vmw65 and Is Required for Vmw65-Dependent Protein-DNA Complex Assembly with Oct-1. *Molecular and Cellular Biology,* 10**,** 4974-4977.

YAMASHITA, A., CHANG, T. C., YAMASHITA, Y., ZHU, W., ZHONG, Z., CHEN, C. Y. & SHYU, A. B. 2005. Concerted action of poly(A) nucleases and decapping enzyme in mammalian mRNA turnover. *Nat Struct Mol Biol,* 12**,** 1054-63.

YAN, K. S., YAN, S., FAROOQ, A., HAN, A., ZENG, L. & ZHOU, M. M. 2003. Structure and conserved RNA binding of the PAZ domain. *Nature,* 426**,** 469-474.

YANG, H. J., HUANG, T. J., YANG, C. F., PENG, L. X., LIU, R. Y., YANG, G. D., CHU, Q. Q., HUANG, J. L., LIU, N., HUANG, H. B., ZHU, Z. Y., QIAN, C. N. & HUANG, B. J. 2013. Comprehensive profiling of Epstein-Barr virus-encoded miRNA species associated with specific latency types in tumor cells. *Virology Journal,* 10**,** 314.

YANG, Y., ZHOU, F., FANG, Z., WANG, L., LI, Z., SUN, L., WANG, C., YAO, W., CAI, X., JIN, J. & ZHA, X. 2009. Post-transcriptional and post-translational regulation of PTEN by transforming growth factor-beta1. *J Cell Biochem,* 106**,** 1102-12.

YAZDANI, U. & TERMAN, J. R. 2006. The semaphorins. *Genome Biol,* 7**,** 211.

YI, R., POY, M. N., STOFFEL, M. & FUCHS, E. 2008. A skin microRNA promotes differentiation by repressing 'stemness'. *Nature,* 452**,** 225-9.

YOON, J. H., CHOI, W. I., JEON, B. N., KOH, D. I., KIM, M. K., KIM, M. H., KIM, J., HUR, S. S., KIM, K. S. & HUR, M. W. 2014. Human Kruppel-related 3 (HKR3) is a novel transcription activator of alternate reading frame (ARF) gene. *J Biol Chem,* 289**,** 4018-31.

YOUNG, L. S. & RICKINSON, A. B. 2004. Epstein-Barr virus: 40 years on. *Nat Rev Cancer,* 4**,** 757-68.

YU, X. K., SHAH, S., LEE, M., DAI, W., LO, P., BRITT, W., ZHU, H., LIU, F. Y. & ZHOU, Z. H. 2011. Biochemical and structural characterization of the capsid-bound tegument proteins of human cytomegalovirus. *Journal of Structural Biology,* 174**,** 451-460.

YUS, E., GUITIAN, J., DIAZ, A. & SANJUAN, M. L. 1999. Outbreak of malignant catarrhal fever in cattle in Spain. *Veterinary Record,* 145**,** 466-7.

ZALANI, S., HOLLEYGUTHRIE, E. & KENNEY, S. 1996. Epstein-Barr viral latency is disrupted by the immediate-early BRLF1 protein through a cell-specific mechanism. *Proc Natl Acad Sci U S A,* 93**,** 9194-9199.

ZEKRI, L., HUNTZINGER, E., HEIMSTADT, S. & IZAURRALDE, E. 2009. The silencing domain of GW182 interacts with PABPC1 to promote translational repression and degradation of microRNA targets and is required for target release. *Molecular and Cellular Biology,* 29**,** 6220-31.

ZENG, Y. & CULLEN, B. R. 2005. Efficient processing of primary microRNA hairpins by Drosha requires flanking nonstructured RNA sequences. *J Biol Chem,* 280**,** 27595-603.

ZENG, Y., YI, R. & CULLEN, B. R. 2005. Recognition and cleavage of primary microRNA precursors by the nuclear processing enzyme Drosha. *Embo Journal,* 24**,** 138-48.

ZHANG, H., KOLB, F. A., JASKIEWICZ, L., WESTHOF, E. & FILIPOWICZ, W. 2004. Single processing center models for human Dicer and bacterial RNase III. *Cell,* 118**,** 57-68.

ZHAO, J. L., RAO, D. S., BOLDIN, M. P., TAGANOV, K. D., O'CONNELL, R. M. & BALTIMORE, D. 2011a. NF-kappaB dysregulation in microRNA-146a-deficient mice drives the development of myeloid malignancies. *Proc Natl Acad Sci U S A,* 108**,** 9184-9.

ZHAO, Y., XU, H., YAO, Y., SMITH, L. P., KGOSANA, L., GREEN, J., PETHERBRIDGE, L., BAIGENT, S. J. & NAIR, V. 2011b. Critical role of the virus-encoded microRNA-155 ortholog in the induction of Marek's disease lymphomas. *Plos Pathogens,* 7**,** e1001305.

ZHENG, S. Q., LI, Y. X., ZHANG, Y., LI, X. & TANG, H. 2011. MiR-101 regulates HSV-1 replication by targeting ATP5B. *Antiviral Res,* 89**,** 219-26.

ZHOU, X., DUAN, X., QIAN, J. & LI, F. 2009. Abundant conserved microRNA target sites in the 5'-untranslated region and coding sequence. *Genetica,* 137**,** 159-64.

ZHOU, Y., GUNPUT, R. A. & PASTERKAMP, R. J. 2008. Semaphorin signaling: progress made and promises ahead. *Trends Biochem Sci,* 33**,** 161-70.

ZHU, Y., HAECKER, I., YANG, Y., GAO, S. J. & RENNE, R. 2013. gamma-Herpesvirus-encoded miRNAs and their roles in viral biology and pathogenesis. *Curr Opin Virol,* 3**,** 266-75.

ZIMBER-STROBL, U. & STROBL, L. J. 2001. EBNA2 and Notch signalling in Epstein-Barr virus mediated immortalization of B lymphocytes. *Semin Cancer Biol,* 11**,** 423-34.

ZISOULIS, D. G., LOVCI, M. T., WILBERT, M. L., HUTT, K. R., LIANG, T. Y., PASQUINELLI, A. E. & YEO, G. W. 2010. Comprehensive discovery of endogenous Argonaute binding sites in Caenorhabditis elegans. *Nat Struct Mol Biol,* 17**,** 173-9.